On Subspace Methods in System Identification and Sensor Array Signal Processing

Magnus Jansson

TRITA–S3–REG–9701
ISSN 0347–1071

Automatic Control
Department of Signals, Sensors and Systems
Royal Institute of Technology (KTH)
Stockholm, Sweden

Submitted to the School of Electrical Engineering, Royal Institute of Technology, in partial fulfillment of the requirements for the degree of Doctor of Philosophy.

Printed by KTH Tryck & Kopiering 1997

Abstract

The common theme of the thesis is the derivation and analysis of subspace parameter estimation methods. In particular, this thesis is concerned with the identification of linear time invariant dynamical systems and the estimation of the directions of arrival (DOAs) using sensor arrays.

The first part focuses on sensor array signal processing. The forward-backward approach has proved quite useful for improving the performance of many suboptimal array processing methods. Herein, it is shown that this approach should *not* be used with a statistically optimal method such as MODE or WSF.

A robust weighted subspace fitting method for a wide class of array perturbation models is derived. The method takes the first order errors due to finite sample effects of the noise and the model perturbation into account in an optimal way to give minimum variance estimates of the DOAs. Interestingly enough, the method reduces to the WSF (MODE) estimator if no model errors are present. On the other hand, when model errors dominate, the proposed method turns out to be equivalent to the "model-errors-only subspace fitting method". Furthermore, an alternative method known as MAPprox, is also shown to yield minimum variance estimates.

A novel subspace-based algorithm for the estimation of the DOAs of uncorrelated emitter signals is derived. The asymptotic variance of the estimates is shown to coincide with the relevant Cramér Rao lower bound. This implies that the method in certain cases has a significantly better performance than methods that do not exploit the *a priori* information about the signal correlation. Unlike previous techniques, the estimator can be implemented by making use of standard matrix operations only, if the array is uniform and linear.

The second part of the thesis deals with the analysis and interpretation of subspace methods for system identification. It is shown that sev-

eral existing subspace estimates result from a linear regression multistep-ahead prediction error minimization under certain rank constraints. Furthermore, it is found that the pole estimates obtained by two subspace system identification methods asymptotically are invariant to a row-weighting in the cost functions. The consistency of a large class of subspace estimates is analyzed. Persistence of excitation conditions on the input signal are given which guarantee consistency for systems with only measurement noise. For systems with process noise, an example where subspace methods fail to yield a consistent estimate of the transfer function is given. This failure occurs even though the input is persistently exciting. Such problems do not arise if the input is a white noise process or an ARMA process of sufficiently low order.

Acknowledgments

The years at the department of Signals, Sensors & Systems have been most enjoyable and stimulating. I would like to express my gratitude to my supervisor Professor Bo Wahlberg who convinced me to proceed the master studies towards the Ph.D. degree. Once started, I have never regretted that choice. Thank you Bo for always being positive and very encouraging.

It has been a pleasure to go to the department (almost) every morning in the last five years. Thanks to all colleagues at the department, former and present, for being who you are. I have enjoyed our discussions at lunches and coffee breaks, playing "innebandy", and ...

To all friends I apologize for often being absent minded during these years. I appreciate your support.

Many thanks to my collaborators and co-authors, the Professors Björn Ottersten, Petre Stoica, Lee Swindlehurst, Bo Wahlberg, and Tekn. Lic. Bo Göransson. The interaction has been very stimulating for me and rewarding for my work.

The financial support that made this thesis project possible is gratefully acknowledged.

Finally, I am very grateful to my family for their continuous support and encouragement. I dedicate this thesis to my family.

Contents

Chapter 1

Introduction

The subject of this thesis is so-called subspace parameter estimation methods. Two areas of application are considered. This implies that the thesis naturally divides into two main parts. Part I considers the sensor array signal processing problem and Part II is concerned with the identification of linear time-invariant dynamical systems. This chapter contains a short common introduction to these two parts.

1.1 Sensor Array Signal Processing

The basic goal of sensor array signal processing is to extract information from data obtained from multiple sensors. Consider the situation depicted in Figure 1.1. The emitters transmit energy (typically electromagnetic or acoustic) from different locations. The wavefield measured by the sensors contains information about, for example, the directions to the sources. By combining the information from the different sensors in a clever way, one may obtain accurate estimates of the directions. Applications of sensor array techniques include: radar systems, underwater surveillance by hydrophones, seismology and radio or satellite communications. Currently, there is also a large interest in using so-called smart antennas for mobile communication. The idea is to obtain diversity by making use of multiple antennas.

The research in the field of array signal processing is by now quite mature. Over the last thirty years numerous articles have been published and there are excellent reviews of the obtained results (see, e.g., [KV96,

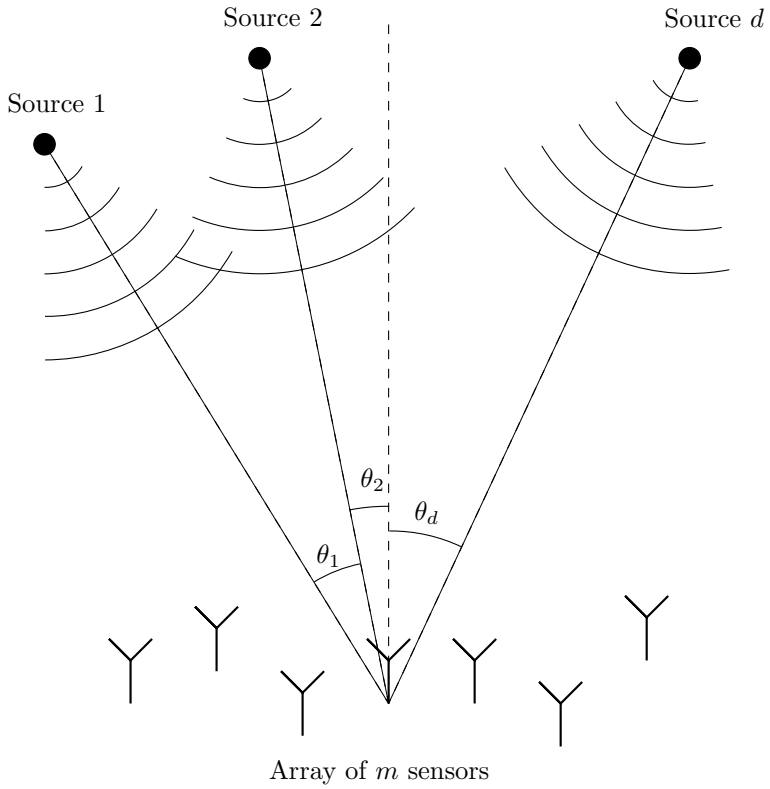

Figure 1.1: The setup for the direction estimation problem.

VB88, RA92, VDS93]). There are also several books written, including [Pil89, JD93, Hay91, SM97]. The motivation of this section is not to give a comprehensive and detailed introduction (the curious reader is referred to the cited material), but rather to give a hint on from where the research presented in the thesis starts.

1.1.1 Data Model

Consider again the situation in Figure 1.1. To develop a convenient mathematical model, one has to make several simplifications. A most important assumption made in the following is that the source signals

are narrowband. This means that the signals have bandpass characteristics around a given center or carrier frequency. Such signals are common in communications where the informative (low-frequency) signal is modulated by a high-frequency carrier before transmission. A complex representation of a narrowband signal $s(t)$ is given by

$$s(t) = \bar{s}(t)e^{j\omega_c t},$$

where ω_c is the carrier angular frequency. The narrowband assumption implies that the amplitude or the envelope $\bar{s}(t)$ varies much slower than $s(t)$. Hence, for small time delays, τ,

$$\begin{aligned} s(t-\tau) &= \bar{s}(t-\tau)e^{j\omega_c(t-\tau)} \\ &\approx \bar{s}(t)e^{j\omega_c t}e^{-j\omega_c \tau} \\ &= s(t)e^{-j\omega_c \tau}. \end{aligned}$$

That is, for narrowband signals we may model a small time delay by a phase shift.

Let $H_k(\omega, \theta)$ denote the (complex) response of the kth sensor at the frequency ω and from a wavefield in the direction θ. Furthermore, assume that $H_k(\omega, \theta) \approx H_k(\omega_c, \theta)$ over the passband around ω_c of interest. Let τ_k denote the time delay of the signal $s(t)$ at the kth sensor relative to a reference point. Then the output of sensor k can be written as

$$x_k(t) = H_k(\omega_c, \theta)s(t-\tau_k) + n_k(t) = H_k(\omega_c, \theta)s(t)e^{-j\omega_c \tau_k} + n_k(t), \tag{1.1}$$

where θ is the direction to the source emitting the signal $s(t)$. In (1.1), $n_k(t)$ is an additive noise term capturing, sensor thermal noise, background noise, model errors etc..

In essence, the narrowband assumption is used to make $\bar{s}(t)$ approximately constant during the time it takes for the wave to propagate across the array and to approximate the sensor response by a constant.

The sources are further assumed to be in the far field so that the signal wavefronts are planar when impinging on the array. This makes it possible to relate the time delay to the direction-of-arrival θ. To see this, consider the following example.

Example 1.1. A common sensor array is the uniform linear array (ULA). In the ULA configuration, the sensors are distributed along a line with equal distance between the sensor elements. Figure 1.2 illustrates the

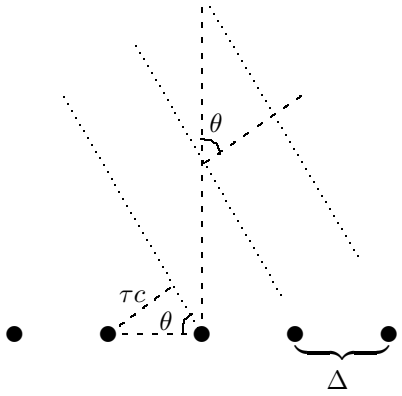

Figure 1.2: A plane wave from the direction θ impinges on a ULA of 5 sensors separated by the distance Δ. The figure illustrates geometrically the propagation delay between two adjacent sensors.

geometry when a plane wave impinges on a ULA with a separation of Δ between two adjacent sensors. Here, we consider the sensors and the sources to be in the same plane. In Figure 1.2, τ is the time it takes for the wavefront to propagate between two sensors and c is the speed of propagation. The signal impinges from the direction θ measured relative to the normal of the array. As shown in Figure 1.2, the relation between τ and θ is given by

$$c\tau = \Delta \sin(\theta) \, .$$

If there are d signals $\{s_k(t)\}_{k=1}^{d}$, then the total contribution at the ith sensor is (cf. (1.1))

$$x_i(t) = \sum_{k=1}^{d} H_i(\omega_c, \theta_k) s_k(t) e^{j\omega_c \Delta \sin(\theta_k)/c} + n_i(t),$$

where the first sensor is taken as the reference point. If the sensors are omni-directional, then $H_i(\omega_c, \theta_k)$ does not depend on θ_k. Furthermore, if the sensors are assumed to be identical, then the signal can be redefined to also include the sensor response. If the array comprises m sensors,

then the outputs can be written in a vector,

$$\begin{aligned}\mathbf{x}(t) = \begin{bmatrix}\mathbf{x}_1(t)\\ \mathbf{x}_2(t)\\ \vdots\\ \mathbf{x}_m(t)\end{bmatrix} &= \sum_{k=1}^{d} \begin{bmatrix}1\\ e^{j\omega_c \Delta \sin(\theta_k)/c}\\ \vdots\\ e^{j\omega_c \Delta (m-1)\sin(\theta_k)/c}\end{bmatrix} s_k(t) + \begin{bmatrix}n_1(t)\\ n_2(t)\\ \vdots\\ n_m(t)\end{bmatrix}\\ &= \sum_{k=1}^{d} \mathbf{a}(\theta_k) s_k(t) + \mathbf{n}(t)\\ &= \begin{bmatrix}\mathbf{a}(\theta_1) & \dots & \mathbf{a}(\theta_d)\end{bmatrix} \begin{bmatrix}s_1(t)\\ \vdots\\ s_d(t)\end{bmatrix} + \mathbf{n}(t)\\ &= \mathbf{A}(\boldsymbol{\theta})\mathbf{s}(t) + \mathbf{n}(t),\end{aligned}$$

where $\boldsymbol{\theta} = [\theta_1,\ \theta_2, \dots,\ \theta_d]^T$. The vector $\mathbf{a}(\theta)$ is often referred to as the array response or the steering vector in the direction θ, and the matrix $\mathbf{A}(\boldsymbol{\theta})$ is called the steering matrix. ■

Similar to the development in Example 1.1, the array output can in general be modeled as

$$\mathbf{x}(t) = \mathbf{A}(\boldsymbol{\theta})\mathbf{s}(t) + \mathbf{n}(t)\,. \tag{1.2}$$

The parameter vector $\boldsymbol{\theta}$ can be associated with several parameters for each signal, for example, elevation, azimuth, range, polarization and carrier frequency. Typically, we will simplify matters and only consider one parameter per signal, for example, the azimuth (the direction-of-arrival) as in the example above.

In the receiver equipment of the sensor array, the modulated signals in (1.2) are demodulated. The demodulation process extracts the (low-frequent) *baseband* signal that contains the information. By a slight abuse of notation, we still use the model (1.2) for the demodulated signals. Even though the derivation of the model above is somewhat sloppy, the idea should be clear. The interested reader is referred to [Tre71] for more details on the complex signal representation and to [Vib89, Ott89, SM97] for derivations of the array model.

Equation (1.2) constitutes one vector sample of the array output; that is, the m array outputs are sampled *simultaneously*. One vector sample or one observation of the vector process $\{\mathbf{x}(t)\}$ is sometimes called a

snapshot of the array output. Assume that N snapshots are available, the data may then be written in matrix form as

$$\mathbf{X}_N = \begin{bmatrix} \mathbf{x}(1), & \ldots, & \mathbf{x}(N) \end{bmatrix} = \mathbf{A}(\boldsymbol{\theta})\mathbf{S}_N + \mathbf{N}_N \, .$$

Here, $\mathbf{S}_N$ and $\mathbf{N}_N$ are the collection of signal and noise vectors, respectively, defined analogously to $\mathbf{X}_N$. The objective of the sensor array estimation problem can be stated as follows:

> Based on the data, $\mathbf{X}_N$, and the model for the observations, (1.2); estimate the number of signals, d, the signal parameters, $\boldsymbol{\theta}$, the signal waveforms, $\mathbf{S}_N$ (or the signal covariance matrix $\mathbf{P} = \mathrm{E}\{\mathbf{s}(t)\mathbf{s}^*(t)\}$), and the noise variance, σ^2. (See the next section for the stochastic model assumptions.)

The major concern in this thesis is the estimation of the signal parameters, $\boldsymbol{\theta}$. Once $\boldsymbol{\theta}$ is known, it is relatively straightforward to estimate the other parameters of interest (see, e.g., [Böh86, ORK89]). The number of signals, d, is assumed to be known. Literature addressing the estimation of d is, for example, [Fuc92, Wax91, VOK91b, VOK91a] and the references therein.

1.1.2 Estimation Methods

The early approaches to make use of the information obtained by the sensor array involved so-called beamforming (see [VB88]). In short, these methods form a weighted sum of the outputs of the array elements to give a measure of the received energy from different directions. This gives a spatial spectrum from which $\boldsymbol{\theta}$ can be estimated. These methods can be classified as "non-parametric" since they do not make any assumptions on the covariance of the data [SM97]. In the remainder of this section, some of the "parametric" array processing methods will be described. The methods to be presented are only those that serve as a background to the material in the thesis.

Maximum Likelihood

The maximum likelihood (ML) method is a powerful tool for parameter estimation. It allows for a systematic procedure to many estimation problems. The ML estimates have, under mild conditions, strong statistical properties. For example, if the ML estimate is consistent[1] then

[1] A parameter estimate is said to be (strongly) consistent if it converges to the true value with probability one as the number of observations tend to infinity.

it is also asymptotically statistically efficient. Here, asymptotically statistically efficient means that the ML estimator attains the Cramér-Rao lower bound (CRB) asymptotically in the number of samples. The CRB is a lower bound on the estimation error variance for any unbiased estimator [Cra46].

A common assumption on the noise, $\mathbf{n}(t)$, is that it is a zero-mean stationary complex Gaussian random process [Goo63] with second order moments

$$\mathrm{E}\{\mathbf{n}(t)\mathbf{n}^*(s)\} = \sigma^2\mathbf{I}\,\delta_{t,s}\,, \quad \mathrm{E}\{\mathbf{n}(t)\mathbf{n}^T(s)\} = \mathbf{0}\,.$$

Here, the superscript $*$ denotes complex conjugate transpose, $\delta_{t,s}$ is the Kronecker delta and $\mathbf{I}$ denotes the identity matrix. Regarding the signal waveforms, $\{\mathbf{s}(t)\}$, two common assumptions exist. Sometimes $\{\mathbf{s}(t)\}$ are treated as completely unknown complex parameters, called the deterministic approach. However, for estimator design purposes it has been shown that a stochastic model for the signals may be useful, whether or not the true signals are stochastic in nature. In what follows, the signal vector $\mathbf{s}(t)$ is assumed to be a zero-mean stationary complex Gaussian random process with second order moments

$$\mathrm{E}\{\mathbf{s}(t)\mathbf{s}^*(s)\} = \mathbf{P}\,\delta_{t,s}\,, \quad \mathrm{E}\{\mathbf{s}(t)\mathbf{s}^T(s)\} = \mathbf{0}\,.$$

Under the assumption that the noise and the emitter signals are uncorrelated, the array output is complex Gaussian with zero-mean and covariance matrix

$$\mathbf{R} = \mathrm{E}\{\mathbf{x}(t)\mathbf{x}^*(t)\} = \mathbf{A}(\boldsymbol{\theta})\mathbf{P}\mathbf{A}^*(\boldsymbol{\theta}) + \sigma^2\mathbf{I}\,. \tag{1.3}$$

The assumption of Gaussian emitter signals may be commented upon. In [OVK90, SN90] it is shown that the exact distribution is immaterial; the important quantity that determines the asymptotic properties of the signal parameter estimates is $\lim_{N\to\infty}\mathbf{S}_N\mathbf{S}_N^*/N$.

From the assumptions on the signals and noise, the array response data, $\mathbf{x}(t)$, will be complex m-variate Gaussian with zero-mean and the covariance matrix given in (1.3). The probability density function is given by [Goo63]

$$f_{\mathbf{X}}(\mathbf{x}(t)) = \frac{1}{\pi^m \det\{\mathbf{R}\}}\mathrm{e}^{-\mathbf{x}^*(t)\mathbf{R}^{-1}\mathbf{x}(t)}, \tag{1.4}$$

where $\det\{\mathbf{R}\}$ denotes the determinant of $\mathbf{R}$. The distribution depends on the unknown parameters in $\boldsymbol{\theta}$, $\mathbf{P}$ and σ^2. Introduce the parameter vector

$\mathbf{p}$ with the d^2 real-valued parameters in the Hermitian signal covariance matrix $\mathbf{P}$; that is,

$$\mathbf{p} = \big[\mathbf{P}_{11}, \quad \ldots, \quad \mathbf{P}_{dd}, \quad \bar{\mathbf{P}}_{12}, \quad \tilde{\mathbf{P}}_{12}, \quad \ldots \quad \bar{\mathbf{P}}_{(d-1)d}, \quad \tilde{\mathbf{P}}_{(d-1)d}\big]^T ,$$

where $\mathbf{P}_{ij}$ denotes the (i,j)th element of $\mathbf{P}$ and where $\bar{a} = \mathrm{Re}\{a\}$ and $\tilde{a} = \mathrm{Im}\{a\}$. Furthermore, let $\boldsymbol{\eta}$ be the vector of all unknown parameters

$$\boldsymbol{\eta} = \big[\boldsymbol{\theta}^T, \quad \mathbf{p}^T, \quad \sigma^2\big]^T .$$

The probability density function of one observation $\mathbf{x}(t)$ is given by (1.4). Since the snapshots are independent and identically distributed, the joint probability density of the N observations is

$$f(\mathbf{x}(1), \ \ldots, \ \mathbf{x}(N)|\boldsymbol{\eta}) = \prod_{t=1}^{N} \frac{1}{\pi^m \det\{\mathbf{R}\}} \mathrm{e}^{-\mathbf{x}^*(t)\mathbf{R}^{-1}\mathbf{x}(t)} . \tag{1.5}$$

Equation (1.5) is a measure of the probability that the outcome should take on the value $\mathbf{x}(1), \ \ldots, \ \mathbf{x}(N)$ given $\boldsymbol{\eta}$. When the observed values of $\mathbf{x}(t)$ are inserted in (1.5), a function of $\boldsymbol{\eta}$ is obtained. This function is called the *likelihood function* and is denoted by $f(\boldsymbol{\eta})$. The ML-estimate of $\boldsymbol{\eta}$ is given by the maximizing argument of $f(\boldsymbol{\eta})$; that is, the value that makes the likelihood of the outcome as large as possible. Maximizing $f(\boldsymbol{\eta})$ is equivalent to minimizing the negative logarithm of $f(\boldsymbol{\eta})$,

$$\begin{aligned} -\log\{f(\boldsymbol{\eta})\} &= -\sum_{t=1}^{N} \log\Big(\frac{1}{\pi^m \det\{\mathbf{R}\}} \mathrm{e}^{-\mathbf{x}^*(t)\mathbf{R}^{-1}\mathbf{x}(t)}\Big) \\ &= mN\log(\pi) + N\log(\det\{\mathbf{R}\}) + \sum_{t=1}^{N} \mathbf{x}^*(t)\mathbf{R}^{-1}\mathbf{x}(t) . \end{aligned}$$

Ignoring the constant term and normalizing by N, the criterion function is given by

$$\begin{aligned} l(\boldsymbol{\eta}) &= \log(\det\{\mathbf{R}\}) + \frac{1}{N}\sum_{t=1}^{N} \mathbf{x}^*(t)\mathbf{R}^{-1}\mathbf{x}(t) \\ &= \log(\det\{\mathbf{R}\}) + \frac{1}{N}\sum_{t=1}^{N} \mathrm{Tr}\{\mathbf{R}^{-1}\mathbf{x}(t)\mathbf{x}^*(t)\} \\ &= \log(\det\{\mathbf{R}\}) + \mathrm{Tr}\{\mathbf{R}^{-1}\hat{\mathbf{R}}\} , \end{aligned} \tag{1.6}$$

where $\mathrm{Tr}\{\cdot\}$ is the trace operator [Gra81] and $\hat{\mathbf{R}}$ is the *sample covariance matrix*,

$$\hat{\mathbf{R}} = \frac{1}{N}\sum_{t=1}^{N}\mathbf{x}(t)\mathbf{x}^*(t)\,.$$

The ML estimate is thus given by the following optimization problem

$$\hat{\boldsymbol{\eta}} = \arg\min_{\boldsymbol{\eta}}\; l(\boldsymbol{\eta})\,. \tag{1.7}$$

This is a high-dimensional nonlinear optimization problem with, at least, $d^2 + d + 1$ parameters. It is possible to decrease this dimension through a separation of the problem as shown in [Böh86, Jaf88]. Therein, Equation (1.7) is solved explicitly with respect to the signal and noise covariance parameters. For a given $\boldsymbol{\theta}$, this results in

$$\hat{\mathbf{P}}(\boldsymbol{\theta}) = \mathbf{A}^{\dagger}(\boldsymbol{\theta})\big(\hat{\mathbf{R}} - \hat{\sigma}^2(\boldsymbol{\theta})\mathbf{I}\big)\mathbf{A}^{\dagger^*}(\boldsymbol{\theta}), \tag{1.8}$$

$$\hat{\sigma}^2(\boldsymbol{\theta}) = \frac{1}{m-d}\,\mathrm{Tr}\{\boldsymbol{\Pi}^{\perp}_{\mathbf{A}}(\boldsymbol{\theta})\hat{\mathbf{R}}\}, \tag{1.9}$$

where the notations $\mathbf{A}^{\dagger} = (\mathbf{A}^*\mathbf{A})^{-1}\mathbf{A}^*$ and $\boldsymbol{\Pi}^{\perp}_{\mathbf{A}} = \mathbf{I} - \mathbf{A}\mathbf{A}^{\dagger}$ are introduced. If (1.8) and (1.9) are substituted back in (1.6), the following concentrated criterion function is obtained (after some algebra)

$$V(\boldsymbol{\theta}) = \log\Big(\det\big\{\mathbf{A}(\boldsymbol{\theta})\hat{\mathbf{P}}(\boldsymbol{\theta})\mathbf{A}^*(\boldsymbol{\theta}) + \hat{\sigma}^2(\boldsymbol{\theta})\mathbf{I}\big\}\Big)$$

and the ML-estimate of the DOAs are

$$\hat{\boldsymbol{\theta}} = \arg\min_{\boldsymbol{\theta}}\; V(\boldsymbol{\theta})\,. \tag{1.10}$$

Then, the problem is reduced to a d-dimensional non-linear search over the DOAs in the vector $\boldsymbol{\theta}$. The ML-estimates of $\mathbf{P}$ and σ^2 are obtained by inserting (1.10) in (1.8) and (1.9), respectively.

We will not further elaborate on the direct ML approach, but the presentation above serves as comparison and background to the methods used in the preceding sections. A final remark about the derivations above concerns the name ML. The presentation given here results in an ML-estimator sometimes called the stochastic or unconditional ML. There also exists a different ML-estimator called the deterministic or the conditional ML. This is due to the two different choices of model for the emitter signals mentioned above. For a discussion about the differences between these approaches, see [SN90, OVSN93].

Subspace Methods

Since the introduction of an eigenstructure technique by [Pis73] for the harmonic retrieval problem, there has been great interest in such methods in the signal processing literature. However, the major break-point came a few years later with the development of the MUSIC (multiple signal classification) algorithm by Schmidt [Sch81, Sch79] (see also [Bie79]). The eigenstructure or subspace methods try to exploit a geometrical formulation of the problem by utilizing the eigendecomposition of the array covariance matrix. Here, we just mention that the ideas of the subspace methods are closely tied to principal component and factor analysis [Hot33, Law40]. The popularity of the subspace methods is due to the fact that they have a much better resolution compared to classical beamforming techniques. That is, they have a good ability to resolve sources that are close in space (angle). The ML method presented in the previous section also has a high resolution, but it is computationally more involved than the subspace methods. Three well known subspace methods will be described below. First, a description of the eigendecomposition of the array output covariance matrix is needed.

Consider the covariance matrix

$$\mathbf{R} = \mathbf{A}(\boldsymbol{\theta})\mathbf{P}\mathbf{A}^*(\boldsymbol{\theta}) + \sigma^2\mathbf{I}\,.$$

Recall that there are m sensors and d signals. Let d' denote the rank of $\mathbf{P}$. If $d' < d$, then this indicates that some of the signals are fully correlated or coherent[2]. Let the eigendecomposition of $\mathbf{R}$ be

$$\mathbf{R} = \sum_{i=1}^{m} \lambda_i \mathbf{e}_i \mathbf{e}_i^*, \tag{1.11}$$

where the eigenvalues are assumed to be ordered as $\lambda_1 \geq \lambda_2 \geq \cdots \geq \lambda_m$. Notice that, since $\mathbf{R}$ is Hermitian, the eigenvectors can be chosen orthonormal ($\mathbf{e}_i^*\mathbf{e}_k = \delta_{i,k}$). The rank of $\mathbf{A}(\boldsymbol{\theta})\mathbf{P}\mathbf{A}^*(\boldsymbol{\theta})$ is d' which implies that there are $m - d'$ eigenvectors in its nullspace. These eigenvectors all have a corresponding eigenvalue equal to σ^2. The remaining d' eigenvalues will be larger than the noise variance. With the observations made, the relation (1.11) may be partitioned as

$$\mathbf{R} = \mathbf{E}_s\boldsymbol{\Lambda}_s\mathbf{E}_s^* + \mathbf{E}_n\boldsymbol{\Lambda}_n\mathbf{E}_n^*\,,$$

[2]Two signals are coherent if the first signal is a scaled (by a complex constant) version of the other.

where $\mathbf{\Lambda}_s = \text{diag}[\lambda_1, \ldots, \lambda_{d'}]$ and $\mathbf{\Lambda}_n = \text{diag}[\lambda_{d'+1}, \ldots, \lambda_m] = \sigma^2\mathbf{I}$. The notation diag[·] is used to denote a diagonal matrix with specified diagonal elements. The matrix $\mathbf{E}_s$ is $m \times d'$ and contains the d' "signal" eigenvectors corresponding to the eigenvalues in $\mathbf{\Lambda}_s$. Similarly, $\mathbf{E}_n$ is $m \times (m - d')$ and consists of the "noise" eigenvectors corresponding to $\mathbf{\Lambda}_n$. The following geometrical observation is at the heart of all subspace methods

$$\mathcal{R}\{\mathbf{E}_s\} \subseteq \mathcal{R}\{\mathbf{A}(\boldsymbol{\theta})\}\,, \tag{1.12}$$

where $\mathcal{R}\{\cdot\}$ denotes the range of the matrix in question. The relation (1.12) says that the subspace spanned by the columns of $\mathbf{E}_s$ is contained in or is equal to the subspace spanned by the columns of $\mathbf{A}(\boldsymbol{\theta})$. Equality in (1.12) holds if and only if there are no coherent signals ($d' = d$). If $d' = d$, then (1.12) implies that

$$\mathcal{N}\{\mathbf{E}_n^*\} = \mathcal{R}\{\mathbf{A}(\boldsymbol{\theta})\}\,, \tag{1.13}$$

where $\mathcal{N}\{\mathbf{E}_n^*\}$ denotes the null-space of $\mathbf{E}_n^*$. That is, the columns of $\mathbf{A}(\boldsymbol{\theta})$ spans the null-space of $\mathbf{E}_n^*$. This observation forms the basis of the MUSIC algorithm presented next.

MUSIC

Let $\mathbf{a}(\theta)$ denote a generic column of $\mathbf{A}(\boldsymbol{\theta})$. In view of (1.13),

$$\mathbf{a}^*(\theta)\mathbf{E}_n\mathbf{E}_n^*\mathbf{a}(\theta) = 0 \tag{1.14}$$

for $\theta = \theta_k$ ($k = 1, ..., d$), where $\{\theta_k\}$ are the true DOAs. In the MUSIC algorithm, the noise eigenvectors are estimated from the sample covariance matrix and the function

$$\frac{1}{\mathbf{a}^*(\theta)\hat{\mathbf{E}}_n\hat{\mathbf{E}}_n^*\mathbf{a}(\theta)}$$

is computed over the sector of interest. The DOAs are estimated as the d highest peaks. For uniform linear arrays,[3] MUSIC can be implemented in a "rooting" form (root-MUSIC) [Bar83]. In that case, the solutions to (1.14) are computed from the roots of a polynomial. The performance of MUSIC is in many cases excellent. However, for scenarios with strongly correlated and closely spaced emitters or for small samples it may be far from optimal.

[3] Actually, this can be easily extended to hold for all linear arrays where the distances between the sensors are rational.

ESPRIT

ESPRIT (estimation of signal parameters by rotational invariance techniques) [PRK86, RPK86, RK89] (see also [Kun81, KAB83]) exploits the geometry of a particular type of arrays. It is assumed that the array consists of two identical subarrays displaced by a known distance and in a known direction. A simple example of such an array is the ULA (see Example 1.1). Define

$$\phi_k = \omega_c \frac{\Delta}{c} \sin(\theta_k) \qquad (k = 1, ..., d), \tag{1.15}$$

$$\begin{aligned} \mathbf{A}_1 &= \begin{bmatrix} \mathbf{I}_{m-1} & \mathbf{0} \end{bmatrix} \mathbf{A}, \\ \mathbf{A}_2 &= \begin{bmatrix} \mathbf{0} & \mathbf{I}_{m-1} \end{bmatrix} \mathbf{A}, \end{aligned}$$

where $\mathbf{0}$ is an $(m-1) \times 1$ vector of zeros, and notice that

$$\mathbf{A}_2 = \mathbf{A}_1 \mathbf{\Phi}, \tag{1.16}$$

where

$$\mathbf{\Phi} = \begin{bmatrix} e^{j\phi_1} & & \mathbf{0} \\ & \ddots & \\ \mathbf{0} & & e^{j\phi_d} \end{bmatrix}.$$

Clearly, the eigenvalues of $\mathbf{\Phi}$ determine the DOAs (under some identifiability conditions not discussed here). If $d' = d$ then the relation (1.12) implies that there exists a nonsingular matrix $\mathbf{T}$ such that $\mathbf{A} = \mathbf{E}_s \mathbf{T}$. By defining

$$\begin{aligned} \mathbf{E}_{s_1} &= \begin{bmatrix} \mathbf{I}_{m-1} & \mathbf{0} \end{bmatrix} \mathbf{E}_s, \\ \mathbf{E}_{s_2} &= \begin{bmatrix} \mathbf{0} & \mathbf{I}_{m-1} \end{bmatrix} \mathbf{E}_s, \end{aligned}$$

and making use of (1.16), the following relation is obtained:

$$\mathbf{E}_{s_2} = \mathbf{E}_{s_1} \mathbf{\Psi}, \tag{1.17}$$

where $\mathbf{\Psi} = \mathbf{T}\mathbf{\Phi}\mathbf{T}^{-1}$. Observe that the matrices $\mathbf{\Phi}$ and $\mathbf{\Psi}$ have the same eigenvalues since they are related by a similarity transformation. Hence, given an estimate of $\mathbf{E}_s$, one can solve (1.17) to give an estimate of $\mathbf{\Psi}$. The directions can then be estimated through the relation between (the angles of) the eigenvalues of $\mathbf{\Psi}$ and the DOAs given above. The performance of ESPRIT is in most cases similar to the one for MUSIC.

Weighted Subspace Fitting

In [VO91], a general framework for subspace methods is presented. It is shown that many of the existing subspace-based techniques can be formulated as a subspace fitting problem. Indeed, the relation (1.12) indicates that, given an estimate of the "signal subspace", $\hat{\mathbf{E}}_s$, the parameters $\boldsymbol{\theta}$ should be chosen such that $\mathcal{R}\{\hat{\mathbf{E}}_s\}$ is contained in $\mathcal{R}\{\mathbf{A}(\boldsymbol{\theta})\}$. (It can be shown that this uniquely determines $\boldsymbol{\theta}$ under weak conditions [WZ89].) In the presence of noise, it may not be possible to find an exact solution and a measure of closeness has to be specified. The signal subspace fitting formulation relies on a criterion which gives the best weighted least squares fit of the subspaces in (1.12). Thus, consider the criterion

$$\min_{\boldsymbol{\theta},\ \mathbf{T}} \|\hat{\mathbf{E}}_s \mathbf{W}^{1/2} - \mathbf{A}(\boldsymbol{\theta})\mathbf{T}\|_F^2 \,, \tag{1.18}$$

where $\|\mathbf{A}\|_F^2 = \mathrm{Tr}\{\mathbf{A}\mathbf{A}^*\}$ denotes the square of the Frobenius matrix norm, $\hat{\mathbf{E}}_s$ is an estimate of $\mathbf{E}_s$, and $\mathbf{T}$ is an arbitrary $d \times d'$ matrix. The weighting matrix $\mathbf{W}^{1/2}$ is $d' \times d'$ and assumed to be Hermitian and positive definite. It is possible to explicitly solve (1.18) with respect to $\mathbf{T}$. The solution is given by $\hat{\mathbf{T}} = (\mathbf{A}^*\mathbf{A})^{-1}\mathbf{A}^*\hat{\mathbf{E}}_s\mathbf{W}^{1/2} = \mathbf{A}^\dagger\hat{\mathbf{E}}_s\mathbf{W}^{1/2}$ where the argument, $\boldsymbol{\theta}$, has been suppressed for notational convenience. Inserting the solution for $\mathbf{T}$ in (1.18), yields

$$\begin{aligned} V(\boldsymbol{\theta}) &= \|\hat{\mathbf{E}}_s\mathbf{W}^{1/2} - \mathbf{A}\mathbf{A}^\dagger\hat{\mathbf{E}}_s\mathbf{W}^{1/2}\|_F^2 \\ &= \|\boldsymbol{\Pi}_{\mathbf{A}}^{\perp}\hat{\mathbf{E}}_s\mathbf{W}^{1/2}\|_F^2 = \mathrm{Tr}\{\boldsymbol{\Pi}_{\mathbf{A}}^{\perp}\hat{\mathbf{E}}_s\mathbf{W}\hat{\mathbf{E}}_s^*\} \,, \end{aligned} \tag{1.19}$$

where the facts that $\boldsymbol{\Pi}_{\mathbf{A}}^{\perp}\boldsymbol{\Pi}_{\mathbf{A}}^{\perp} = \boldsymbol{\Pi}_{\mathbf{A}}^{\perp}$ and $\mathbf{W}^{1/2}\mathbf{W}^{*/2} = \mathbf{W}$ are used. The estimate of $\boldsymbol{\theta}$ is obtained as the minimizing argument of $V(\boldsymbol{\theta})$,

$$\hat{\boldsymbol{\theta}} = \arg\min_{\boldsymbol{\theta}} V(\boldsymbol{\theta}) \,. \tag{1.20}$$

As shown in [VO91], different choices of $\mathbf{W}$ lead to a whole class of estimators. It is also shown that there exists a specific weighting which minimizes the asymptotic parameter estimation error covariance matrix (in terms of matrix inequalities). The optimal weighting is given by

$$\mathbf{W}_{\mathrm{WSF}} = (\boldsymbol{\Lambda}_s - \sigma^2\mathbf{I})^2\boldsymbol{\Lambda}_s^{-1} = \tilde{\boldsymbol{\Lambda}}_s^2\boldsymbol{\Lambda}_s^{-1} \,.$$

With this specific choice of weighting, the algorithm is usually referred to as the *weighted subspace fitting* (WSF) method. Furthermore, it is shown

in [VO91] that the asymptotic covariance attains the Cramér-Rao lower bound and, hence, WSF is asymptotically statistically efficient. This implies that WSF and ML have the same asymptotic performance.

The solution of (1.20) requires a nonlinear optimization in d dimensions (if there is only one parameter associated with each signal). However, due to the form of the criterion, the implementation of WSF can be made more efficient than the implementation of ML [OVSN93].

In [SS90a], the WSF criterion (1.19) is derived in a different way than described here. In that paper, the criterion is obtained by a maximum likelihood approach based on the statistics of the sample eigenvectors, and the method is referred to as MODE (method of direction estimation).

For uniform linear arrays with identical omni-directional sensors, the minimization in (1.20) can be implemented in a very appealing manner [SS90b, SS90a]. The simplification is possible through a linear reparameterization of the nullspace of $\mathbf{A}^*$. See Section 2.4 for some more details on this.

1.1.3 Discussion

In this section, the different topics of the thesis are related to the background material presented above.

Chapter 2 concerns the application of different DOA estimators to the forward-backward (FB) sample covariance matrix of the output from a ULA. For the current discussion, it suffices to say that the FB approach uses the reflectional symmetry of the ULA to, in principle, "decorrelate" the signals (see Chapter 2 for a more detailed description). By this operation, it is expected that estimation methods that work well in scenarios with low signal correlation should improve their performance when applied to the FB preprocessed covariance matrix. To show that this indeed may be the case, consider the following example.

Example 1.2. Consider a ULA consisting of six omni-directional and identical sensors separated by half of the carrier's wavelength. The two signals impinge on the array from $\theta_1 = -7.5^\circ$ and $\theta_2 = 7.5^\circ$ relative to broadside. The signal covariance is

$$\mathbf{P} = \begin{bmatrix} 1 & 0.8e^{i\pi/4} \\ 0.8e^{-i\pi/4} & 1 \end{bmatrix}.$$

The noise variance is fixed to $\sigma^2 = 1$. The DOAs are estimated in four different ways; by applying the root-MUSIC and ESPRIT methods to either the standard sample covariance matrix, or to the forward-backward

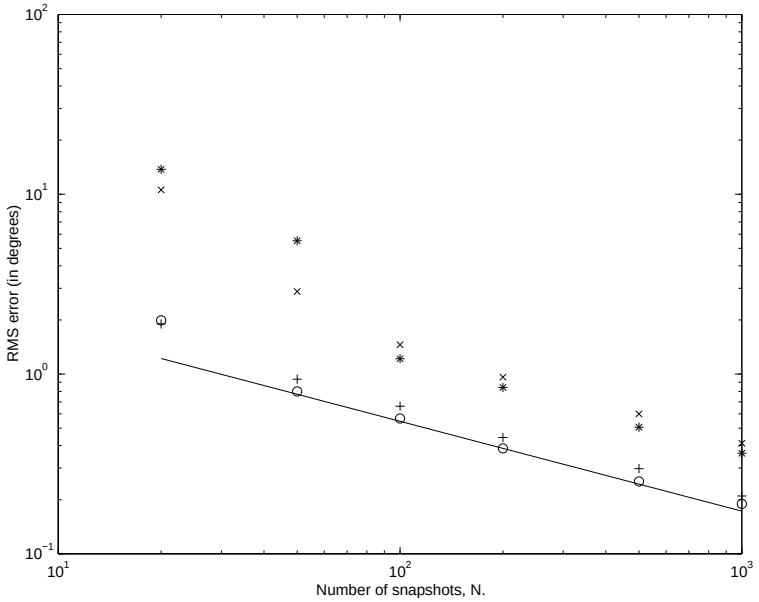

Figure 1.3: Root-mean-square errors for θ_1 (in degrees) for root-MUSIC (*), FB-MUSIC (o), ESPRIT (x) and FB-ESPRIT (+) versus the number of snapshots N. The solid line represents the CRB.

sample covariance. The acronyms FB-MUSIC and FB-ESPRIT will be used when root-MUSIC and, respectively, ESPRIT are applied to the eigenvectors of the FB sample covariance matrix. The root-mean-square (RMS) errors for the estimates obtained by the four methods are compared for different sample lengths in Figure 2.1. (Only the RMS values for θ_1 are shown; the plot corresponding to θ_2 is similar.) The sample RMS values are based on 500 independent trials. From the figure, it can be seen that the FB approach gives a significant improvement in performance for both MUSIC and ESPRIT. ■

While the performance of MUSIC and ESPRIT can be enhanced by using the FB approach, it is shown in Chapter 2 that this is not true for WSF, or equivalently, MODE. On the contrary, in general the performance of WSF/MODE degrades when applied to the FB sample covariance. Hence, the conclusion of Chapter 2 is that the FB approach should

not be used with a statistically efficient method such as WSF/MODE.

A number of idealizations and assumptions were made when deriving the array model. In practice these may be more or less invalid. For example, the array model depends on the exact knowledge of the sensor positions, the gain and phase of the independent sensors etc.. Sometimes the array response is obtained by so-called array calibration. This simply consists of measuring the response of the array when it is excited by signals in known locations. Needless to say, this does not give a perfect error-free model. In Chapter 3, a method that takes small model errors into account when estimating the directions of arrival is proposed. By compensating for the model errors in the estimator, a more robust method is obtained.

It is well known that the MUSIC estimator performs well when the emitter signals are uncorrelated. Often it is even considered to be close to optimal in that case. However, it seems meaningful to ask: What is the best possible performance that can be obtained if it is *a priori* known that the signals are uncorrelated? In Chapter 4, the corresponding CRB is derived. As expected, that CRB is a *lower* bound than the bound given by the "standard" CRB, where the signal correlation is considered to be arbitrary. This implies that if one can derive a method that optimally exploits the *a priori* knowledge that the emitter signals are uncorrelated, then it will perform better than, for example, MUSIC and WSF. One efficient method is maximum likelihood (ML). The ML estimate for the current problem is obtained by minimizing the criterion in (1.6) under the constraint that the signal covariance is diagonal. However, this seems to be a quite complicated minimization problem of high dimension (since the unknowns are the DOAs, the diagonal elements of $\mathbf{P}$ and σ^2). A second alternative is to use the generalized least squares (GLS) method (also known as the method of moments or the covariance matching method) in which the sample and the model covariance are matched in a weighted least squares sense. The GLS method is known to be asymptotically statistically efficient for the case under study (see [And84] and the references therein). Using the GLS method on the problem at hand, it is possible to separate the criterion so that the direction estimates can be obtained as the result of a d-dimensional non-linear minimization. Hence, compared to ML, this leads to a less complicated optimization problem. In Chapter 4, we propose a novel method for direction estimation in cases when it is *a priori* known that the emitter signals are uncorrelated. The method is shown to be asymptotically statistically efficient. Furthermore, the method allows for a relatively simple implementation when the array is

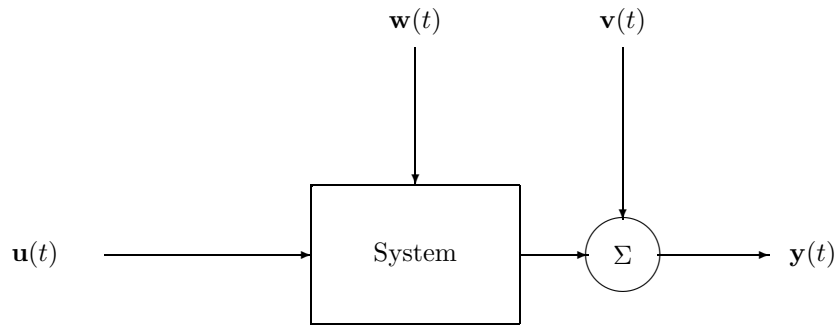

Figure 1.4: Linear finite dimensional time-invariant dynamic system.

uniform and linear. Then, the estimates are obtained by using standard matrix operations (like an eigendecomposition) only. Hence, there is no need for an iterative search procedure.

More precise descriptions of the contributions of the thesis are given in Section 1.3.

1.2 System Identification

The second part of this thesis concerns subspace system identification. System identification deals with the topic of obtaining mathematical models of dynamic systems from measured data. The applications of system identification techniques are widespread in almost all engineering disciplines. The theory is firmly established and covered in several books including [Boh91, Eyk74, GP77, HD88, Joh93, Lju87, SS89].

1.2.1 Background

Consider the situation in Figure 1.4. In the figure, $\mathbf{u}(t)$ and $\mathbf{y}(t)$ are observed input and output signals, respectively. The signals $\mathbf{w}(t)$ and $\mathbf{v}(t)$ represent unknown inputs to the system. All signals may very well be vector valued. Assume that the system is linear and time-invariant and, hence, that the observed output can be described as

$$\mathbf{y}(t) = \mathbf{G}(q)\mathbf{u}(t) + \mathbf{H}(q)\mathbf{e}(t). \tag{1.21}$$

In (1.21), the transfer operators or the *transfer functions* $\mathbf{H}(q)$ and $\mathbf{G}(q)$ are functions of the forward shift operator q ($q\mathbf{u}(t) = \mathbf{u}(t+1)$). Moreover, $\mathbf{H}(q)$ is monic, which means that its first impulse response coefficient is the identity, $\mathbf{I}$. The part $\mathbf{H}(q)\mathbf{e}(t)$, where $\{\mathbf{e}(t)\}$ is a white noise process, encompasses the effect of both $\mathbf{w}(t)$ and $\mathbf{v}(t)$ in Figure 1.4.

System identification aims at estimating the transfer functions $\mathbf{H}(q)$ and $\mathbf{G}(q)$ from measurements of $\mathbf{u}(t)$ and $\mathbf{y}(t)$ at the time instances $t = 1, 2, ..., N$. A very general approach which has proved successful is the prediction error method (PEM). The idea of PEM is to minimize the difference between the measured output $\mathbf{y}(t)$ and the prediction of $\mathbf{y}(t)$ based on past data. The best linear one-step ahead predictor is given by [Lju87]

$$\hat{\mathbf{y}}(t, \boldsymbol{\theta}) = \mathbf{H}^{-1}(q, \boldsymbol{\theta})\mathbf{G}(q, \boldsymbol{\theta})\mathbf{u}(t) + \left[\mathbf{I} - \mathbf{H}^{-1}(q, \boldsymbol{\theta})\right]\mathbf{y}(t),$$

where $\mathbf{G}(q, \boldsymbol{\theta})$ and $\mathbf{H}(q, \boldsymbol{\theta})$ are parameterized models of $\mathbf{G}(q)$ and $\mathbf{H}(q)$, respectively. The PEM estimate of $\boldsymbol{\theta}$ is defined by

$$\hat{\boldsymbol{\theta}} = \arg\min_{\boldsymbol{\theta}} V(\boldsymbol{\theta}),$$

where a typical choice of the criterion is

$$V(\boldsymbol{\theta}) = \frac{1}{N}\sum_{t=1}^{N}[\mathbf{y}(t) - \hat{\mathbf{y}}(t, \boldsymbol{\theta})]^T\mathbf{W}[\mathbf{y}(t) - \hat{\mathbf{y}}(t, \boldsymbol{\theta})]$$

for a positive definite weighting matrix $\mathbf{W}$.

It should be remarked that the use of PEM is not limited to the case where there exists a "true system" represented by (1.21). The system can be of higher dimension than the model and it can be non-linear. The identified model will then be an approximation of the system with certain properties [Lju87, SS89].

In general, the minimization of the prediction errors requires a non-linear iterative search. The success of such procedures depends heavily on if there exists a sufficiently good initial estimate. It is also important to have a numerically reliable (canonical) parameterization of $\mathbf{G}(q, \boldsymbol{\theta})$ and $\mathbf{H}(q, \boldsymbol{\theta})$. This is an issue that is most difficult for multi-variable systems (see, for example, [VL82, Lju87, GW84, GW74]).

The subspace identification methods have in many cases shown to give accurate models. Those models can either be used as they are, or they may serve as an initial estimate for PEM to give a refined model. There exists alternative methods to provide initial model estimates, such

as, instrumental variable and two-stage least-squares methods [Lju87, SS89]. One reason for the interest in the subspace methods is due to computational aspects. Many subspace methods can be implemented in a very effective way by making use of numerical linear algebra tools such as QR-factorization and singular value decomposition [CXK94, CK95, VD91, VD96].

1.2.2 Subspace Methods

Subspace methods for system identification have their origin in the realization theory (see, for example, [HK66, Aka74a, Aka74b, Fau76]). The deterministic realization algorithm of Ho and Kalman [HK66] was turned into an identification algorithm in [ZM74, Kun78] where the singular value decomposition (SVD) was used as a tool to suppress the effects of noise. Later extensions include [Bay92, KDS88, LS91, Lju91, JP85]. These approaches are based on impulse response data. Often it is difficult to get accurate estimates of the impulse response coefficients from data. The subspace methods considered here directly utilize the measured time domain data. Some basic approaches include [Gop69, De 88, DVVM88, MDVV89, Ver91]. More general methods are presented in [Lar83, VD94b, Ver94, PSD96]. These methods consider combined deterministic-stochastic systems where the output is due to both observed and unobserved inputs. There are also subspace methods for the pure time series case [Aka75, Aok87, AK90, VD93, Lar83, DPS95] and for the errors-in-variables problem [SCE95, CS96]. However, the main interest in what follows is on the combined methods. We refer to the survey papers [Vib95, RA92, VDS93] and the book [VD96] for a more comprehensive presentation of (the history of) the subspace identification methods.

In the following, a brief introduction to the basic ideas that underlie the subspace identification methods is given. A linear time-invariant discrete-time system of order n can be described by the state-space equations

$$\mathbf{x}(t+1) = \mathbf{A}\mathbf{x}(t) + \mathbf{B}\mathbf{u}(t) + \mathbf{w}(t), \tag{1.22a}$$

$$\mathbf{y}(t) = \mathbf{C}\mathbf{x}(t) + \mathbf{D}\mathbf{u}(t) + \mathbf{v}(t). \tag{1.22b}$$

Here, $\mathbf{u}(t) \in \mathbb{R}^m$ and $\mathbf{y}(t) \in \mathbb{R}^l$ represent the observed input and output data, respectively. The state-vector $\mathbf{x}(t) \in \mathbb{R}^n$ is an internal variable. The state equation is perturbed by the *process* noise $\mathbf{w}(t) \in \mathbb{R}^n$, and the

output equation contains the *measurement* noise $\mathbf{v}(t) \in \mathbb{R}^l$. Both $\mathbf{w}(t)$ and $\mathbf{v}(t)$ are white noise processes. We assume that the description is minimal. That is, there is no other state-space description with lower state-dimension than n. Observe that, if the state-sequence $\{\mathbf{x}(t)\}$ were known, then it would be straightforward to estimate the state-space matrices $\{\mathbf{A}, \mathbf{B}, \mathbf{C}, \mathbf{D}\}$ in (1.22) by linear regression. The question is how to estimate the state from the measured data $\{\mathbf{u}(t), \mathbf{y}(t)\}$.

Before presenting the data-model that is used for state estimation, we need to define the following block matrices:

$$\mathbf{\Gamma}_\alpha = \begin{bmatrix} \mathbf{C} \\ \mathbf{CA} \\ \vdots \\ \mathbf{CA}^{\alpha-1} \end{bmatrix},$$

$$\mathbf{\Phi}_\alpha = \begin{bmatrix} \mathbf{D} & \mathbf{0} & \cdots & \mathbf{0} \\ \mathbf{CB} & \mathbf{D} & \ddots & \mathbf{0} \\ \vdots & \ddots & \ddots & \vdots \\ \mathbf{CA}^{\alpha-2}\mathbf{B} & \mathbf{CA}^{\alpha-3}\mathbf{B} & \cdots & \mathbf{D} \end{bmatrix},$$

$$\mathbf{\Psi}_\alpha = \begin{bmatrix} \mathbf{0} & \cdots & \mathbf{0} & \mathbf{0} \\ \mathbf{C} & \ddots & \mathbf{0} & \mathbf{0} \\ \vdots & \ddots & \vdots & \vdots \\ \mathbf{CA}^{\alpha-2} & \cdots & \mathbf{C} & \mathbf{0} \end{bmatrix}.$$

Notice that $\mathbf{\Gamma}_\alpha$ is the *extended* observability matrix if $\alpha > n$ and it is full column rank since the system is minimal. Introduce the notation

$$\mathbf{y}_\alpha(t) = \begin{bmatrix} \mathbf{y}^T(t) & \mathbf{y}^T(t+1) & \ldots & \mathbf{y}^T(t+\alpha-1) \end{bmatrix}^T, \tag{1.23}$$

which is of dimension αl. Similarly, define the vectors $\mathbf{u}_\alpha(t)$, $\mathbf{w}_\alpha(t)$, and $\mathbf{v}_\alpha(t)$ made from inputs, process and measurement noises, respectively.

We are now ready to give the basic data model that is used in the subspace identification methods. From the state-space equations (1.22), it is easily seen that

$$\mathbf{y}_\alpha(t) = \mathbf{\Gamma}_\alpha \mathbf{x}(t) + \mathbf{\Phi}_\alpha \mathbf{u}_\alpha(t) + \mathbf{n}_\alpha(t), \tag{1.24}$$

where

$$\mathbf{n}_\alpha(t) = \mathbf{\Psi}_\alpha \mathbf{w}_\alpha(t) + \mathbf{v}_\alpha(t).$$

Observe that the vectors $\mathbf{y}_\alpha(t)$, $\mathbf{u}_\alpha(t)$, and $\mathbf{n}_\alpha(t)$ contain data from time t and onwards. The state $\mathbf{x}(t)$ contains the information about the past necessary to predict the future behavior of the system. In fact,

$$\hat{\mathbf{y}}_\alpha(t) = \mathbf{\Gamma}_\alpha \mathbf{x}(t)$$

is the optimal (in the mean-square sense) prediction of $\mathbf{y}_\alpha(t)$ given data up to time t. Assume for the moment that $\hat{\mathbf{y}}_\alpha(t)$ is known for $t = 1, 2, \ldots, N$. Define the matrices

$$\hat{\mathbf{Y}}_\alpha = \begin{bmatrix} \hat{\mathbf{y}}_\alpha(1) & \hat{\mathbf{y}}_\alpha(2) & \ldots & \hat{\mathbf{y}}_\alpha(N) \end{bmatrix}, \tag{1.25}$$

$$\mathbf{X} = \begin{bmatrix} \mathbf{x}(1) & \mathbf{x}(2) & \ldots & \mathbf{x}(N) \end{bmatrix}. \tag{1.26}$$

Clearly,

$$\hat{\mathbf{Y}}_\alpha = \mathbf{\Gamma}_\alpha \mathbf{X} \tag{1.27}$$

and it is of dimension $\alpha l \times N$. If $N > n$ and $\alpha l > n$, then[4]

$$\text{rank}\{\hat{\mathbf{Y}}_\alpha\} = n \tag{1.28}$$

and, hence, $\hat{\mathbf{Y}}_\alpha$ is *low-rank*. The factorization in (1.27) is not unique since $\mathbf{\Gamma}_\alpha \mathbf{T} \mathbf{T}^{-1} \mathbf{X} = \mathbf{\Gamma}_\alpha \mathbf{X}$ for any non-singular matrix $\mathbf{T}$. This non-uniqueness corresponds to a change of state-space basis ($\mathbf{x}(t) \to \mathbf{T}^{-1}\mathbf{x}(t)$) and changes only the internal structure of the system description. The input-output relation does not change. This implies that if $\hat{\mathbf{Y}}_\alpha$ is known, then $\mathbf{\Gamma}_\alpha$ and $\mathbf{X}$ (in some state-space basis) can be obtained by a low-rank factorization of $\hat{\mathbf{Y}}_\alpha$.

It remains to show how to estimate $\hat{\mathbf{Y}}_\alpha$, and how to factorize that estimate. Recall the relation (1.24) and observe that the state-vector $\mathbf{x}(t)$ contains the past information. In other words, $\mathbf{x}(t)$ can be written as a linear combination of the past data $\{\mathbf{u}(t-k), \mathbf{y}(t-k)\}$ for $k = 1, 2, \ldots, \infty$. From (1.24), we can write

$$\begin{aligned} \mathbf{y}_\alpha(t) &= \mathbf{\Gamma}_\alpha \mathbf{x}(t) + \mathbf{\Phi}_\alpha \mathbf{u}_\alpha(t) + \mathbf{n}_\alpha(t) \\ &\approx \mathbf{\Gamma}_\alpha \left(\mathbf{K}_1 \mathbf{y}_\beta(t-\beta) + \mathbf{K}_2 \mathbf{u}_\beta(t-\beta) \right) + \mathbf{\Phi}_\alpha \mathbf{u}_\alpha(t) + \mathbf{n}_\alpha(t), \\ &\triangleq \mathbf{L}_1 \mathbf{y}_\beta(t-\beta) + \mathbf{L}_2 \mathbf{u}_\beta(t-\beta) + \mathbf{\Phi}_\alpha \mathbf{u}_\alpha(t) + \mathbf{n}_\alpha(t), \end{aligned} \tag{1.29}$$

[4] Here, we assume that $\mathbf{X}$ is full row-rank ($= n$), which is generically true for large N if the inputs are sufficiently exciting. This is actually at the basis of the realization theory presented in [Aka74a, Aka74b, HK66].

where the notation $\mathbf{u}_\beta(t-\beta)$ and $\mathbf{y}_\beta(t-\beta)$ is analogous to (1.23):

$$\mathbf{u}_\beta(t-\beta) = \begin{bmatrix}\mathbf{u}^T(t-\beta) & \mathbf{u}^T(t-\beta+1) & \dots & \mathbf{u}^T(t-1)\end{bmatrix}^T,$$
$$\mathbf{y}_\beta(t-\beta) = \begin{bmatrix}\mathbf{y}^T(t-\beta) & \mathbf{y}^T(t-\beta+1) & \dots & \mathbf{y}^T(t-1)\end{bmatrix}^T.$$

In (1.29), $\mathbf{L}_1 = \mathbf{\Gamma}_\alpha \mathbf{K}_1$ and $\mathbf{L}_2 = \mathbf{\Gamma}_\alpha \mathbf{K}_2$ are two unknown matrices. The approximation in (1.29) is due to the fact that the amount of past input-output data is truncated. Only β past samples are used to estimate $\mathbf{x}(t)$.[5] Since $\mathbf{\Gamma}_\alpha$ is unknown, it is actually $\mathbf{\Gamma}_\alpha \mathbf{x}(t)$ that is estimated from the past data in (1.29). The idea is to use (1.29) to estimate $\hat{\mathbf{y}}_\alpha(t)$ as

$$\hat{\mathbf{y}}_\alpha(t) \approx \mathbf{L}_1 \mathbf{y}_\beta(t-\beta) + \mathbf{L}_2 \mathbf{u}_\beta(t-\beta).$$

If $\mathbf{\Phi}_\alpha$ was known, then $\mathbf{L}_1$ and $\mathbf{L}_2$ could be estimated by linear regression. However, since $\mathbf{\Phi}_\alpha$ is unknown, it is estimated as well. Let $\hat{\mathbf{L}}_1$, $\hat{\mathbf{L}}_2$ and $\hat{\mathbf{\Phi}}_\alpha$ denote the estimates of the respective quantity obtained by linear regression in (1.29). An estimate of the prediction matrix $\hat{\mathbf{Y}}_\alpha$ in (1.25) is then

$$\hat{\hat{\mathbf{Y}}}_\alpha = \hat{\mathbf{L}}_1 \begin{bmatrix}\mathbf{y}_\beta(1) & \dots & \mathbf{y}_\beta(N)\end{bmatrix} + \hat{\mathbf{L}}_2 \begin{bmatrix}\mathbf{u}_\beta(1) & \dots & \mathbf{u}_\beta(N)\end{bmatrix}.$$

For finite data (finite N), $\hat{\hat{\mathbf{Y}}}_\alpha$ typically has full rank. Since the rank of $\hat{\mathbf{Y}}_\alpha$ is equal to n, it is sensible to somehow reduce the rank of $\hat{\hat{\mathbf{Y}}}_\alpha$. The singular value decomposition (SVD) is a powerful tool in numerical linear algebra. One of its strong properties is that it provides the best (in spectral or Frobenius norm) low-rank approximation of a full rank matrix [GV96]. Let

$$\hat{\hat{\mathbf{Y}}}_\alpha = \hat{\mathbf{Q}}\hat{\mathbf{S}}\hat{\mathbf{V}}^T = \begin{bmatrix}\hat{\mathbf{Q}}_s & \hat{\mathbf{Q}}_n\end{bmatrix} \begin{bmatrix}\hat{\mathbf{S}}_s & \mathbf{0} \\ \mathbf{0} & \hat{\mathbf{S}}_n\end{bmatrix} \begin{bmatrix}\hat{\mathbf{V}}_s^T \\ \hat{\mathbf{V}}_n^T\end{bmatrix} \tag{1.30}$$

be the SVD of $\hat{\hat{\mathbf{Y}}}_\alpha$. In (1.30), $\hat{\mathbf{Q}}$ and $\hat{\mathbf{V}}$ are orthonormal matrices and $\hat{\mathbf{S}}$ is a diagonal matrix having the singular values arranged in non-increasing order along the diagonal. The partitioning in (1.30) is made so that $\hat{\mathbf{S}}_s$ is $n \times n$ and $\hat{\mathbf{S}}_n$ contains the remaining (small) singular values. Notice

[5] For simplicity, we have taken the same number, β, of past inputs and outputs. Of course, it is possible to take different numbers for the input and the output, respectively.

that $\hat{\mathbf{S}}_n = \mathbf{0}$ in the ideal case ($N \to \infty$). Retaining the part of the SVD corresponding to the n largest singular values gives

$$\hat{\hat{\mathbf{Y}}}_\alpha \approx \hat{\mathbf{Q}}_s \hat{\mathbf{S}}_s \hat{\mathbf{V}}_s^T, \tag{1.31}$$

which is the desired rank n approximation of $\hat{\hat{\mathbf{Y}}}_\alpha$. In view of (1.27) and (1.31), we obtain the following estimates of the extended observability matrix and the state-sequence:

$$\begin{aligned} \hat{\mathbf{\Gamma}}_\alpha &= \hat{\mathbf{Q}}_s \hat{\mathbf{S}}_s^{1/2} \mathbf{T}, \\ \hat{\mathbf{X}} &= \mathbf{T}^{-1} \hat{\mathbf{S}}_s^{1/2} \hat{\mathbf{V}}_s^T. \end{aligned}$$

Here, $\hat{\mathbf{S}}_s^{1/2}$ denotes the square root of $\hat{\mathbf{S}}_s$, and $\mathbf{T}$ is an arbitrary non-singular $n \times n$ matrix. Recall that $\mathbf{T}$ merely determines the state-space basis of the realization and does not affect the input-output relation. We may, for example, choose $\mathbf{T} = \mathbf{I}$. Thus, by the manipulations above, we have an estimate of $\mathbf{X}$ which can be used to estimate the system matrices by linear regression in the state-space equations (1.22) as mentioned before. Furthermore, the sample covariance of the residuals in the regression gives an estimate of the covariance of the noise process $\begin{bmatrix} \mathbf{w}^T(t) & \mathbf{v}^T(t) \end{bmatrix}^T$.

The procedure presented above summarizes the general ideas that, more or less explicitly, are used in the subspace system identification methods. Clearly, the crucial step is how to estimate the states. The approximations made above are the truncation of past data (β), and the estimation of $\hat{\hat{\mathbf{Y}}}_\alpha$ by linear regression. It can be shown [PSD96] that the state estimate derived above is consistent if $\beta \to \infty$. The existing subspace methods contain several modifications of the above procedure. One of the reasons why these modifications are made is that it is possible to get consistent estimates of the system matrices for a finite β.

Conceptually, the idea of first estimating the state and then the system matrices by linear regression is very appealing. However, as mentioned above, it is complicated to obtain a consistent estimate of the state. A common approach to estimate $\mathbf{A}$ and $\mathbf{C}$ is instead to use the shift-invariance structure in $\mathbf{\Gamma}_\alpha$ as in the classical realization algorithm by Ho and Kalman [HK66] (see Section 5.5). Recall that an estimate of $\mathbf{\Gamma}_\alpha$ is obtained from the factorization of $\hat{\hat{\mathbf{Y}}}_\alpha$ in (1.30). An advantage with methods based on $\hat{\mathbf{\Gamma}}_\alpha$ is that it is much easier to obtain a consistent estimate of $\mathbf{\Gamma}_\alpha$ than it is to estimate the states (see Chapter 6). Given estimates of $\mathbf{A}$ and $\mathbf{C}$, the $\mathbf{B}$ and $\mathbf{D}$ matrices can be estimated by linear

regression since the transfer function from $\mathbf{u}(t)$ to $\mathbf{y}(t)$ is linear in $\mathbf{B}$ and $\mathbf{D}$. (There are also other possibilities [VD96, Ver94].)

Another approach is presented by Van Overschee and De Moor [VD94b]. In [VD94b], it is shown that the state estimate obtained for fixed β can be interpreted as being the output of a bank of non-steady state Kalman filters. This observation is used to rewrite the state-space equations into a slightly modified linear regression from which the system matrices $\{\mathbf{A}, \mathbf{B}, \mathbf{C}, \mathbf{D}\}$ can be estimated by least-squares.

1.2.3 Discussion

Many of the subspace system identification methods have been derived in an algebraic framework involving orthogonal and oblique projections on the data. Traditionally, such operations are in the system identification literature rather described in terms of cross-correlations. The subspace methods also make extensive use of tools from numerical linear algebra, which is beneficial at the implementation level, but it complicates the understanding of the underlying ideas. Among other facts, this has somewhat obscured the relation between classical methods (like PEM and instrumental variable methods) and the 4SID methods. It is still a topic of research to bring these two approaches closer. One of the aims of Chapter 5 is to point to similarities and differences by formulating the subspace estimation problem in a linear regression framework. (By subspace estimation we mean the estimation of the extended observability matrix $\mathbf{\Gamma}_\alpha$.) This formulation is similar to the one in the previous section and gives some further insights into the relation between the different subspace estimates that have been proposed in the literature. The linear regression formulation unifies the subspace estimation step of most existing methods. Weighting matrices that appear rather ad hoc in many previous derivations fall naturally into the formulation of the subspace estimation in terms of a linear regression cost function minimization. As seen above, there are a number of truncation parameters that are to be chosen by the user (α and β). Some effects due to different choices of these parameters are in Chapter 5 studied by means of asymptotic variance expressions for the pole estimates. It can be shown that most of the common choices of subspace estimates lead to the same asymptotic variance of the poles when the observed input is white noise. For colored inputs, there are differences though. This is illustrated in a numerical example.

The subspace identification methods rely on the fact that a certain

cross-correlation matrix ($\hat{\mathbf{Y}}_\alpha$) is low-rank. The rank should be equal to the system order to guarantee identifiability. Given the "true" system and the signal properties, it is of course possible to check this condition. If only the system order n is known, it is also possible to test if the data quantity is "sufficiently" close to a rank n matrix by, for example, a hypothesis test. If the rank is to small, then this indicates that the data are not informative enough, and the experiment should be re-designed. In Chapter 6, excitation conditions on the data to ensure consistency are discussed. For more or less restrictive assumptions on the system, explicit persistence of excitation conditions on the observed input signal are given. An interesting observation made in Chapter 6 is the fact that a persistence of excitation condition on the input does not in general guarantee consistency. Indeed, there exists examples for which the aforementioned rank condition does not hold. This means that, in such cases, the subspace methods under consideration do not give a consistent estimate of the true system. One should, however, remember that such counterexamples are rather "pathological" and generically the rank condition holds for the persistence of excitation conditions given in the thesis. The importance of this result maybe is more relevant from a performance point of view. It is expected that the accuracy of the estimated model is poor if the identification conditions are close to a "counterexample".

1.3 Outline and Contributions

This section gives a chapter by chapter description of the contributions made in the thesis. This also serves as a brief overview of what will follow.

Chapter 2

The chapter studies the application of the MODE (method of direction estimation) or the weighted subspace fitting (WSF) principle to the principal (signal) eigenvectors of the forward-backward (FB) sample covariance matrix. The MODE principle consists of matching the signal eigenvectors to the array model in a statistically sound way. Somewhat surprisingly, it turns out that the best one can do is to apply the standard MODE estimator to the eigenelements of the FB-covariance. It is shown that the accuracy of the so-obtained estimates in general is inferior to the standard MODE estimate. The FB approach has shown to be beneficial for

other (suboptimal) array processing algorithms such as MUSIC and ESPRIT. However, in view of the abovementioned result, forward-backward averaging is not recommended to be used in conjunction with MODE or WSF.

An article version of this chapter has been accepted for publication as

> Petre Stoica and Magnus Jansson, "On Forward-Backward MODE for Array Signal Processing", *Digital Signal Processing – A Review Journal*, Aug. 1997.

This work is also related to the material presented in

> Magnus Jansson and Björn Ottersten, "Covariance Preprocessing in Weighted Subspace Fitting", In *Proc. IEEE/IEE workshop on signal processing methods in multipath environments*, pp. 23-32, Glasgow, Scotland, Apr. 1995.

That paper analyzes the performance of MODE and WSF when the sample covariance matrix is linearly preprocessed before the estimator is applied. The forward-backward preprocessing is a special case for which that analysis holds.

Chapter 3

In many cases it is not the errors due to noise that is the limiting factor when high resolution direction estimators is applied in real situations. The performance limitations may rather be due to errors in the array model. The problem of obtaining a robust direction of arrival estimator is considered in this chapter. The robustness refers to insensitivity to errors in the array model. A signal subspace fitting approach is taken and a weighting that accounts for both the finite sample effects of the noise and the model errors is derived. It is shown that the weighting can be written as the sum of two terms. The first, is nothing but the standard WSF weighting that is optimal in the case with no model errors. The second term compensates for the first order effects of the errors in the array model. The asymptotic performance is shown to coincide with the CRB for the problem under study. There exists other methods (MAPprox and MAP-NSF) that have the same asymptotic optimality properties, but the proposed method (GWSF) has some important advantages. Compared to MAP-NSF, GWSF has a much better small sample performance when the sources are closely spaced and/or when they are highly correlated.

The GWSF formulation also allows for a relatively simple and efficient implementation compared to both MAPprox and MAP-NSF. The chapter also contains a performance analysis of MAPprox which establishes the asymptotic optimality of the method that has been observed in simulations.

The results presented in Chapter 3 have been submitted for possible publication in the following form:

> Magnus Jansson, A. Lee Swindlehurst and Björn Ottersten, "Weighted Subspace Fitting for General Array Error Models", *Submitted to IEEE Trans. on Signal Processing*, Jul. 1997.

Chapter 4

In many applications it is reasonable to assume that the signals that impinge on the array are independent of one another. In general, array processing methods do not presuppose any correlation among the signals. In case it is *a priori* known that the signals are uncorrelated it seems judicious to use this information to improve the performance of the estimator. A method which makes use of the *a priori* information in an optimal way is presented in Chapter 4. That is, it provides minimum variance direction estimates. Natural alternative approaches are the use of the maximum likelihood or the covariance matching method to impose the additional structure in the estimation problem. However, the proposed method appears to have computational advantages compared to the two aforementioned methods.

A version of Chapter 4 has been submitted as

> Magnus Jansson, Bo Göransson and Björn Ottersten, "A Subspace Method for Direction of Arrival Estimation of Uncorrelated Emitter Signals", *Submitted to IEEE Trans. on Signal Processing*, Aug. 1997.

Some of the results given in Chapter 4 have also appeared in

> Bo Göransson, Magnus Jansson and Björn Ottersten, "Spatial and Temporal Frequency Estimation of Uncorrelated Signals Using Subspace Fitting", In *Proceedings of 8th IEEE Signal Processing Workshop on Statistical Signal and Array Processing*, pp. 94-96, Corfu, Greece, June 1996.

Magnus Jansson, Bo Göransson and Björn Ottersten, "Analysis of a Subspace-Based Spatial Frequency Estimator", In *Proceedings of ICASSP'97*, pp. 4001-4004, Munich, Germany, Apr. 1997.

Chapter 5

The chapter contains the linear regression interpretation of the subspace system identification methods. The linear regression formulation is used to interpret existing estimates of the observability matrix as being the minimizing arguments of different cost functions. It is shown that the accuracy of the estimates strongly depends on the choice of a user specified parameter. An important observation is that the choice of this parameter is system dependent, which makes the task non-trivial. It is also shown that, asymptotically in the number of samples, the pole estimates are invariant to a specific weighting matrix employed in the identification schemes. Numerical examples are given to further illustrate the effect of different choices of weighting matrices.

With minor changes, this chapter contains the article,

Magnus Jansson and Bo Wahlberg. "A Linear Regression Approach to State-Space Subspace System Identification", *Signal Processing, Special Issue on Subspace Methods, Part II: System Identification*, Vol. 52, No. 2, pp. 103-129, July 1996.

Parts of this material have also appeared as

Bo Wahlberg and Magnus Jansson, "4SID Linear Regression", In *Proc. IEEE 33rd Conf. on Decision and Control*, pp. 2858-2863. Orlando, USA, Dec. 1994.

Magnus Jansson and Bo Wahlberg, "On Weighting in State-Space Subspace System Identification", In *Proc. European Control Conference, ECC'95*, pp. 435-440, Rome, Italy, Sep. 1995.

Magnus Jansson, "On Performance Analysis of Subspace Methods in System Identification and Sensor Array Processing", Licentiate Thesis (TRITA-REG-9503, ISSN 0347-1071), Automatic Control, Dept. of Signals, Sensors and Systems, KTH, Stockholm, June 1995.

Chapter 6

The consistency of the subspace estimate (or, equivalently, the extended observability matrix) is studied. Persistence of excitation conditions on the input signal are given, which proves consistency for systems where the output is perturbed by white measurement noise. If the system includes process noise, then it is shown that the subspace methods under consideration may fail to give a consistent estimate even though the input is persistently exciting to any order. An explicit example is given when such a failure occurs. It is also shown that this problem is eliminated if the input is a white noise process (or a low order ARMA process.)

A version of Chapter 6 has been submitted as

> Magnus Jansson and Bo Wahlberg, "On Consistency of Subspace Methods for System Identification", *Submitted to Automatica*, Jun. 1997.

Parts of the material in Chapter 6 have been presented at the following conferences:

> Magnus Jansson and Bo Wahlberg, "On Consistency of Subspace System Identification Methods", In *Preprints of the 13th IFAC World Congress*, pp. 181-186, vol. I, San Francisco, California, USA, Jul. 1996.

> Magnus Jansson and Bo Wahlberg, "Counterexample to General Consistency of Subspace System Identification Methods", In *Proc. 11th IFAC Symposium on System Identification*, pp. 1677-1682, Fukuoka, Japan, Jul. 1997.

1.4 Topics for Future Research

Forward-backward (FB) averaging is a topic that has received quite large attention in the array processing literature. Despite this, it seems not really known when FB averaging should or should not be used. For example, should FB averaging always be used when employing the MUSIC or ESPRIT estimators? It has been shown that, in the case of uncorrelated emitter signals, the asymptotic estimation error variance is not improved, but the resolution threshold is decreased [KP89]. There are also some results for the case of correlated emitter signals, but they seem to be less explicit [RH93, PK89]. If the true covariance matrix is

centro-Hermitian, then it is relatively straightforward to show that the FB sample covariance in (2.16) is the corresponding (structured) maximum likelihood (ML) estimate [Qua84]. Recall that the standard sample covariance is the unstructured ML estimate. It is then reasonable to expect that the FB sample estimate is a better estimate than the standard sample covariance with *lower* estimation error variance. This does not directly follow from the ML properties, but the author has proved this explicitly and a report is in progress. In view of this, the result of Chapter 2 becomes even more surprising. Although the FB covariance estimate is better, this does not necessarily lead to better direction estimates, as proved in Chapter 2 (see also [KP89]).

Similar to the development in [VS94b], one can extend the derivation of GWSF in Chapter 3 to also include particular errors in the noise model. In [VS94b], a statistical model that allows for the compensation of first order errors in the noise covariance is given. Using this model, an additional term in the weighting matrix for GWSF would result. It would also be interesting to evaluate GWSF on real array data.

The method (DEUCE) for direction estimation of uncorrelated emitter signals that is derived in Chapter 4 admittedly is quite cumbersome to implement. It would be interesting to investigate if there exists a simpler estimator preserving the performance of DEUCE. Some preliminary results indicate that this really is conceivable. Indeed, consider the case of uncorrelated emitter signals impinging on a uniform linear array. The covariance of the array output vector is then a Toeplitz matrix. This also implies that the matrix employed in DEUCE (see (4.3)) ideally is Toeplitz. The idea is to first perform a simple averaging along the diagonals of the sample estimate of the matrix in (4.3) to obtain a sufficient statistic of lower dimension. Compared to DEUCE, this will lead to an estimator which is computationally less complicated. The results of Chapter 4 may also find applications in "structured covariance estimation". Since DEUCE provides asymptotically maximum likelihood estimates of the parameters that parameterizes the Toeplitz covariance matrix, a structured covariance estimate can be constructed. More detailed results in this direction are expected in the near future. The ideas in Chapter 4 may also be useful to apply in other similar estimation problems such as, for example, blind channel identification.

The analysis of the state-space subspace system identification (4SID) methods in the thesis concerns the consistency of the methods and the asymptotic variance of the pole estimates. So far we have not been able to extend the analysis to obtain asymptotic variance expressions for the

estimated transfer function. We have only derived the asymptotic variance for the estimates of the $\mathbf{A}$ and $\mathbf{C}$ matrices obtained by the shift invariance method. Given estimates of $\mathbf{A}$ and $\mathbf{C}$, the $\mathbf{B}$ and $\mathbf{D}$ matrices are often estimated by linear regression in the input output relation. The estimates of $\mathbf{A}$ and $\mathbf{C}$ appear in the regression equations for estimating $\mathbf{B}$ and $\mathbf{D}$, which makes it very complicated to compute the asymptotic variance for the estimates. Deriving asymptotic variance expressions for the estimated transfer function is an important topic for future research. Such variance expressions can be used to show the relation between the subspace methods and the prediction error methods. They can also be used to estimate the quality of the identified model. There exist several alternatives for estimating the system matrices. A topic for research is to evaluate their relative performance. Another question that can be addressed is how the future inputs really should be treated in the subspace estimation step. In the elaborations in this chapter and in Chapter 5, the matrix $\mathbf{\Phi}_\alpha$ is estimated by linear regression without imposing any structure on the estimate. Recall that $\mathbf{\Phi}_\alpha$ is a lower triangular Toeplitz matrix. The simulation results in [PSD96] suggest that the performance can be improved by using a structured estimate of $\mathbf{\Phi}_\alpha$. As pointed out in the thesis, the subspace methods for system identification are quite sensitive to the input excitation. It would be interesting to find ways to decrease this sensitivity. Using more of the structure in the problem is likely the best approach to achieve this goal.

Part I

Sensor Array Signal Processing

Chapter 2

On Forward-Backward MODE for Array Signal Processing

In this chapter we apply the MODE (method of direction estimation) principle to the forward-backward (FB) covariance of the output vector of a sensor array to obtain what we call the FB-MODE procedure. The derivation of FB-MODE is an interesting exercise in matrix analysis, the outcome of which was somewhat unexpected: FB-MODE simply consists of applying the standard MODE approach to the eigenelements of the FB sample covariance matrix. By using an asymptotic expansion technique we also establish the surprising result that FB-MODE is outperformed, from a statistical standpoint, by the standard MODE applied to the forward-only sample covariance (F-MODE). We believe this to be an important result that shows that the FB approach, which proved quite useful for improving the performance of many suboptimal array processing methods, should *not* be used with a statistically optimal method such as F-MODE.

2.1 Introduction

MODE is a method of direction estimation by means of a sensor array, which is known to be statistically efficient in cases when either the num-

ber of data samples (N) or the signal-to-noise ratio (SNR) is sufficiently large [VO91, SS90a, SN90]. For uniform and linear arrays (ULAs) the implementation of MODE requires only standard matrix operations (such as an eigendecomposition) and is thus very straightforward. In fact in the ULA case MODE is a clear candidate for the best possible (i.e., computationally simple and statistically efficient) array processing method [KV96].

We stress that the aforementioned statistical efficiency of MODE holds asymptotically (in N or SNR). In short-sample or low-SNR cases other methods may provide better performance. The forward-backward (FB) approach is a well-known methodology that has been successfully used to enhance the performance of a number of array signal processing algorithms [RH93, KP89, Pil89]. Recently this approach has been used in conjunction with MODE probably in an attempt to obtain enhanced (finite sample or SNR) performance [Haa97b, Haa97a]. More exactly in the cited publications the standard MODE approach was applied to the eigenelements of the FB sample covariance matrix.

The first problem we deal with in this chapter concerns the formal application of the MODE principle to the FB sample covariance (see also [JO95]). After an exercise in matrix analysis we prove the somewhat unexpected result that FB-MODE should indeed consist of applying the standard MODE to the eigenelements of the FB sample covariance matrix.

Then we go on to establish the asymptotic statistical performance of FB-MODE. Because the standard F-MODE is asymptotically statistically efficient (in the sense that it achieves the Cramér-Rao bound (CRB)) [VO91, SS90a, SN90], we cannot expect FB-MODE to perform better in asymptotic regimes. What one might expect is that FB-MODE outperforms F-MODE in non-asymptotic regimes and that the two methods have the same asymptotic performance. We show that the conjecture on identical asymptotic performances, even though quite natural, is *false*: FB-MODE's asymptotic performance is usually inferior to that of F-MODE. Regarding the comparison of the two methods in non-asymptotic regimes, because the finite-sample/SNR analysis is intractable, we resort to Monte-Carlo simulations to show that F-MODE typically outperforms FB-MODE also in such cases.

In conclusion, the FB approach – which has been successfully employed to enhance the performance of several array signal processing algorithms – cannot be recommended for use with MODE. This result also shows that the related subspace fitting or asymptotic maximum likeli-

hood approaches of [VO91] and [SS90a], which produced the statistically efficient MODE in the forward-only case, may fail to yield statistically optimal estimators in other cases.

2.2 Data Model

Let $\mathbf{x}(t) \in \mathbb{C}^{m\times 1}$ denote the output vector of a ULA that comprises m elements. The variable t denotes the sampling point; hence, $t = 1, 2, \ldots, N$, where N is the number of available samples. Under the assumption that the signals impinging on the array are narrowband with the same center frequency, the array output can be described by the equation (see, e.g., [SM97])

$$\mathbf{x}(t) = \mathbf{A}\mathbf{s}(t) + \mathbf{n}(t). \tag{2.1}$$

Here, $\mathbf{s}(t) \in \mathbb{C}^{d\times 1}$ is the vector of the d signals (translated to baseband) that impinge on the array, $\mathbf{n}(t) \in \mathbb{C}^{m\times 1}$ is a noise term, and $\mathbf{A}$ is the Vandermonde matrix

$$\mathbf{A} = \begin{bmatrix} 1 & \cdots & 1 \\ e^{i\omega_1} & & e^{i\omega_d} \\ \vdots & & \vdots \\ e^{i(m-1)\omega_1} & \cdots & e^{i(m-1)\omega_d} \end{bmatrix},$$

where $\{\omega_k\}_{k=1}^{d}$ are the so-called *spatial frequencies* ($\omega_k = \phi_k$ defined in (1.15)). We assume that

$$\omega_k \neq \omega_j \quad \text{for} \quad k \neq j$$

and that $m > d$, which implies that

$$\operatorname{rank}(\mathbf{A}) = d.$$

The following assumption, frequently used in the array processing literature, is also made here: the signal vector and the noise are temporally white, zero-mean, circular Gaussian random variables that are independent of one another; additionally, the noise is spatially white and has the same power in all sensors. Mathematically, this assumption implies that

$$\mathrm{E}\{\mathbf{s}(t)\mathbf{s}^*(s)\} = \mathbf{P}_0\delta_{t,s}\,, \tag{2.2}$$

$$\mathrm{E}\{\mathbf{s}(t)\mathbf{s}^T(s)\} = \mathbf{0}, \tag{2.3}$$

$$\mathrm{E}\{\mathbf{n}(t)\mathbf{n}^*(s)\} = \sigma^2\mathbf{I}\delta_{t,s}\,, \tag{2.4}$$

$$\mathrm{E}\{\mathbf{n}(t)\mathbf{n}^T(s)\} = \mathbf{0}, \tag{2.5}$$

where E is the statistical expectation operator, $\mathbf{P}_0$ denotes the signal covariance matrix, σ^2 is the noise power in each element of the array, $\delta_{t,s}$ is the Kronecker delta, and the superscripts $*$ and T denote the conjugate transpose and the transpose, respectively. We also assume that

$$\text{rank}(\mathbf{P}_0) = d,$$

which is only done to simplify the notation (indeed, most of the results presented in what follows carry over to the case when $\text{rank}(\mathbf{P}_0) < d$).

A principal goal of array processing consists of estimating $\{\omega_k\}_{k=1}^d$ from $\{\mathbf{x}(t)\}_{t=1}^N$, without assuming knowledge of the incoming signals $\{\mathbf{s}(t)\}$ or (of course) the noise $\{\mathbf{n}(t)\}$. This is precisely the problem we will consider in this chapter. Once $\{\omega_k\}$ are estimated, the directions (also called angles-of-arrival) of the d signals can be easily obtained [VO91, SS90a, SN90, RH93, KP89, Pil89, SM97].

2.3 Preliminary Results

In this section, we present most of the mathematical results that are used in the next sections to derive and analyze FB-MODE. Some of these results are known, yet we provide simple proofs for all results, for completeness.

It follows from (2.1), (2.2)-(2.5) that the array output $\mathbf{x}(t)$ is a temporally white, zero-mean, circular Gaussian random variable with the covariance properties

$$\begin{aligned} &\mathrm{E}\{\mathbf{x}(t)\mathbf{x}^*(t)\} = \mathbf{A}\mathbf{P}_0\mathbf{A}^* + \sigma^2\mathbf{I} \triangleq \mathbf{R}_0, \\ &\mathrm{E}\{\mathbf{x}(t)\mathbf{x}^T(t)\} = \mathbf{0}. \end{aligned} \tag{2.6}$$

Let $\mathbf{J}$ denote the reversal matrix of dimension $m \times m$,

$$\mathbf{J} = \begin{bmatrix} 0 & \dots & 0 & 1 \\ 0 & & 1 & 0 \\ \vdots & \iddots & & \vdots \\ 1 & \dots & 0 & 0 \end{bmatrix}.$$

Similarly $\tilde{\mathbf{J}}$ will denote the $(m-d)\times(m-d)$ reversal matrix. It is readily checked that

$$\mathbf{J}\mathbf{A}^{\mathrm{c}} = \mathbf{A}\mathbf{\Phi}, \tag{2.7}$$

where the superscript c stands for the complex conjugate, and

$$\mathbf{\Phi} = \begin{bmatrix} e^{-i(m-1)\omega_1} & & \mathbf{0} \\ & \ddots & \\ \mathbf{0} & & e^{-i(m-1)\omega_d} \end{bmatrix}.$$

Hence, we have

$$\mathbf{J}\mathbf{x}^{\mathrm{c}}(t) = \mathbf{A}\mathbf{\Phi}\mathbf{s}^{\mathrm{c}}(t) + \mathbf{J}\mathbf{n}^{\mathrm{c}}(t) \tag{2.8}$$

and, accordingly,

$$\mathbf{J}\mathbf{R}_0^{\mathrm{c}}\mathbf{J} = \mathbf{A}\mathbf{\Phi}\mathbf{P}_0^{\mathrm{c}}\mathbf{\Phi}^*\mathbf{A}^* + \sigma^2\mathbf{I}.$$

Let

$$\mathbf{R} = \frac{1}{2}\big(\mathbf{R}_0 + \mathbf{J}\mathbf{R}_0^{\mathrm{c}}\mathbf{J}\big) = \mathbf{A}\mathbf{P}\mathbf{A}^* + \sigma^2\mathbf{I}, \tag{2.9}$$

where

$$\mathbf{P} = \frac{1}{2}\big(\mathbf{P}_0 + \mathbf{\Phi}\mathbf{P}_0^{\mathrm{c}}\mathbf{\Phi}^*\big).$$

In the equations above, $\mathbf{R}_0$ is the so-called "forward" covariance matrix, whereas $\mathbf{R}$ is called the "forward-backward" covariance. The reason for this terminology is that, while the indices of the elements of $\mathbf{x}(t)$ run forward (1, 2, ..., m), those of the elements of $\mathbf{J}\mathbf{x}^{\mathrm{c}}(t)$ run backward (m, ($m-1$), ..., 1). It will be useful for what follows to observe that $\mathbf{R}_0$ and $\mathbf{R}$ have the same structure: the only difference between the expressions in (2.6) and (2.9) for these two matrices is that $\mathbf{P}_0$ in $\mathbf{R}_0$ is replaced by $\mathbf{P}$ in $\mathbf{R}$.

Next, let us introduce the Toeplitz matrix

$$\mathbf{B}^* = \begin{bmatrix} b_0 & \dots & b_d & & \mathbf{0} \\ & \ddots & & \ddots & \\ \mathbf{0} & & b_0 & \dots & b_d \end{bmatrix} \qquad (m-d) \times m, \tag{2.10}$$

where the complex-valued coefficients $\{b_k\}$ are defined through

$$b_0 + b_1 z + \cdots + b_d z^d = b_d \prod_{k=1}^{d} \Big(z - e^{i\omega_k}\Big). \tag{2.11}$$

Because the polynomial in (2.11) has all the zeros on the unit circle, it can be written such that its coefficients satisfy the so-called "conjugate symmetry constraint" (see, e.g., [SS90b]):

$$b_k = b_{d-k}^c \qquad (\text{for } k = 0,\ 1,\ \ldots,\ d). \tag{2.12}$$

It follows easily from (2.10) and (2.11) that

$$\mathbf{B}^*\mathbf{A} = \mathbf{0}, \tag{2.13}$$

which, along with the fact that $\text{rank}(\mathbf{A}) = d$ and $\text{rank}(\mathbf{B}) = m - d$, implies that

$$\mathcal{R}(\mathbf{B}) = \mathcal{N}(\mathbf{A}^*). \tag{2.14}$$

Hereafter, $\mathcal{R}(\cdot)$ and $\mathcal{N}(\cdot)$ denote the range, respectively, the null space associated with the matrix in question.

To end up these notational preparations, let

$$\mathbf{R} = \begin{bmatrix} \underbrace{\mathbf{E}_s}_{d} & \underbrace{\mathbf{E}_n}_{m-d} \end{bmatrix} \begin{bmatrix} \mathbf{\Lambda}_s & \mathbf{0} \\ \mathbf{0} & \sigma^2\mathbf{I} \end{bmatrix} \begin{bmatrix} \mathbf{E}_s^* \\ \mathbf{E}_n^* \end{bmatrix} \tag{2.15}$$

denote the eigenvalue decomposition (EVD) of the matrix $\mathbf{R}$, where the matrix of eigenvectors $\begin{bmatrix} \mathbf{E}_s & \mathbf{E}_n \end{bmatrix}$ is unitary,

$$\mathbf{E}_s^*\mathbf{E}_s = \mathbf{I}; \quad \mathbf{E}_n^*\mathbf{E}_n = \mathbf{I}; \quad \mathbf{E}_s^*\mathbf{E}_n = \mathbf{0},$$

and where

$$\mathbf{\Lambda}_s = \begin{bmatrix} \lambda_1 & & \mathbf{0} \\ & \ddots & \\ \mathbf{0} & & \lambda_d \end{bmatrix}.$$

Here, $\{\lambda_k\}$ are the d largest eigenvalues of $\mathbf{R}$ arranged in a decreasing order: $\lambda_1 > \lambda_2 > \cdots > \lambda_d$. We assume that $\lambda_k \neq \lambda_p$ (for $k \neq p;\ k, p = 1, 2, \ldots, d$), which is generically true. Note from (2.15) that the smallest $(m-d)$ eigenvalues of $\mathbf{R}$ are identical and equal to σ^2, a fact that follows easily from (2.9). The EVD of $\mathbf{R}_0$ is similarly defined, but with $\mathbf{E}_s$, $\mathbf{E}_n$, and $\mathbf{\Lambda}_s$ replaced by $\mathbf{E}_{s_0}$, $\mathbf{E}_{n_0}$, and $\mathbf{\Lambda}_{s_0}$.

The sample covariance matrices corresponding to $\mathbf{R}_0$ and $\mathbf{R}$ are defined as

$$\hat{\mathbf{R}}_0 = \frac{1}{N}\sum_{t=1}^{N} \mathbf{x}(t)\mathbf{x}^*(t),$$

and

$$\hat{\mathbf{R}} = \frac{1}{2}\Big(\hat{\mathbf{R}}_0 + \mathbf{J}\hat{\mathbf{R}}_0^{\mathrm{c}}\mathbf{J}\Big). \tag{2.16}$$

It is well known that, under the assumptions made, $\hat{\mathbf{R}}_0$ and $\hat{\mathbf{R}}$ converge (with probability one and in mean square) to $\mathbf{R}_0$ and, respectively, $\mathbf{R}$, as N tends to infinity. Hence $\hat{\mathbf{R}}_0$ and $\hat{\mathbf{R}}$ are consistent estimates of the corresponding theoretical covariance matrices [SM97, And84, SS89]. In fact $\hat{\mathbf{R}}_0$ can be shown to be the (unstructured) maximum likelihood estimate (MLE) of $\mathbf{R}_0$ [And84, SS89]. By the invariance principle of ML estimation, it then follows that $\hat{\mathbf{R}}$ is the MLE of $\mathbf{R}$. We let

$$\hat{\mathbf{R}} = \big[\underbrace{\hat{\mathbf{E}}_s}_{d} \;\underbrace{\hat{\mathbf{E}}_n}_{m-d}\big] \begin{bmatrix} \hat{\mathbf{\Lambda}}_s & \mathbf{0} \\ \mathbf{0} & \hat{\mathbf{\Lambda}}_n \end{bmatrix} \begin{bmatrix} \hat{\mathbf{E}}_s^* \\ \hat{\mathbf{E}}_n^* \end{bmatrix}$$

denote the EVD of $\hat{\mathbf{R}}$, with the eigenvalues in

$$\begin{bmatrix} \hat{\mathbf{\Lambda}}_s & \mathbf{0} \\ \mathbf{0} & \hat{\mathbf{\Lambda}}_n \end{bmatrix}$$

arranged in a decreasing order. The EVD of $\hat{\mathbf{R}}_0$ is similarly defined, but with a subscript 0 attached to $\hat{\mathbf{E}}_s$, etc., to distinguish it from the EVD of $\hat{\mathbf{R}}$.

2.3.1 Results on A and B

R1. The matrix $\mathbf{B}$ satisfies

$$\mathbf{J}\mathbf{B}^{\mathrm{c}} = \mathbf{B}\tilde{\mathbf{J}} \tag{2.17}$$

and

$$\tilde{\mathbf{J}}\big(\mathbf{B}^*\mathbf{B}\big)\tilde{\mathbf{J}} = \big(\mathbf{B}^*\mathbf{B}\big)^{\mathrm{c}}. \tag{2.18}$$

Proof. Recall that the polynomial coefficients $\{b_k\}$ satisfy the conjugate symmetry constraint (2.14). Hence

$$\mathbf{J}\mathbf{B}^{\mathrm{c}} = \begin{bmatrix} \mathbf{0} & & b_d \\ & \iddots & \vdots \\ b_d & & b_0 \\ \vdots & \iddots & \\ b_0 & & \mathbf{0} \end{bmatrix} = \begin{bmatrix} \mathbf{0} & & b_0^{\mathrm{c}} \\ & \iddots & \vdots \\ b_0^{\mathrm{c}} & & b_d^{\mathrm{c}} \\ \vdots & \iddots & \\ b_d^{\mathrm{c}} & & \mathbf{0} \end{bmatrix} = \mathbf{B}\tilde{\mathbf{J}},$$

which proves (2.17). Equation (2.18) is a simple corollary of (2.17). □

R2. Let

$$\mathbf{a}(\omega) = \begin{bmatrix} 1 & e^{i\omega} & \dots & e^{i(m-1)\omega} \end{bmatrix}^T$$

denote a generic column of the matrix $\mathbf{A}$, and let

$$\mathbf{d}(\omega) \triangleq \frac{d\mathbf{a}(\omega)}{d\omega} = i \begin{bmatrix} 0 & e^{i\omega} & 2e^{i2\omega} & \dots & (m-1)e^{i(m-1)\omega} \end{bmatrix}^T.$$

Then

$$\mathbf{B}^*\mathbf{J}\mathbf{d}^{\mathrm{c}}(\omega) = e^{-i(m-1)\omega}\mathbf{B}^*\mathbf{d}(\omega) \quad \text{for } \omega = \omega_j \quad (j = 1, \dots, d). \tag{2.19}$$

Proof. From (2.7), we have

$$\mathbf{J}\mathbf{a}^{\mathrm{c}}(\omega) = e^{-i(m-1)\omega}\mathbf{a}(\omega).$$

Differentiating both sides with respect to ω gives

$$\mathbf{J}\mathbf{d}^{\mathrm{c}}(\omega) = e^{-i(m-1)\omega}\mathbf{d}(\omega) - i(m-1)e^{-i(m-1)\omega}\mathbf{a}(\omega). \tag{2.20}$$

In view of (2.13), $\mathbf{B}^*\mathbf{a}(\omega) = 0$ at $\omega = \omega_j$ $(j = 1, \dots, d)$, and hence (2.19) is obtained by pre-multiplying (2.20) by $\mathbf{B}^*$. □

2.3.2 Results on R

R3. Let $\mathbf{e}$ denote a generic eigenvector of $\mathbf{R}$, associated with a distinct eigenvalue λ. Then

$$\mathbf{J}\mathbf{e}^{\mathrm{c}} = e^{i\psi}\mathbf{e} \qquad \text{for some } \psi \in (-\pi, \pi]. \tag{2.21}$$

In particular, Equation (2.21) implies that

$$\mathbf{J}\mathbf{E}_s^{\mathrm{c}} = \mathbf{E}_s\mathbf{\Gamma},$$

where $\mathbf{E}_s$ is as defined in (2.15), and

$$\mathbf{\Gamma} = \begin{bmatrix} e^{i\psi_1} & & \mathbf{0} \\ & \ddots & \\ \mathbf{0} & & e^{i\psi_d} \end{bmatrix}; \qquad \psi_k \in (-\pi, \pi] \quad (k = 1, \dots, d).$$

Proof. Because λ is real-valued and $\mathbf{J}\mathbf{R}^{\mathrm{c}}\mathbf{J} = \mathbf{R}$, we have the following equivalences:

$$\mathbf{R}\mathbf{e} = \lambda\mathbf{e} \Longleftrightarrow \mathbf{J}\mathbf{R}^{\mathrm{c}}\mathbf{J}\mathbf{e} = \lambda\mathbf{e} \Longleftrightarrow \mathbf{R}\big(\mathbf{J}\mathbf{e}^{\mathrm{c}}\big) = \lambda\big(\mathbf{J}\mathbf{e}^{\mathrm{c}}\big).$$

Hence, $\mathbf{J}\mathbf{e}^{\mathrm{c}}$ is also an eigenvector associated with λ. Then it must be related to $\mathbf{e}$ as shown in (2.21), as λ is distinct by assumption. □

The above result is a consequence of the centro-Hermitian property of $\mathbf{R}$. Hence, a similar result holds for $\hat{\mathbf{R}}$ as well.

2.3.3 Results on P and R

R4. The condition number of $\mathbf{P}$

$$\mathrm{cond}(\mathbf{P}) \triangleq \frac{\lambda_{\max}(\mathbf{P})}{\lambda_{\min}(\mathbf{P})}$$

is never greater than that of $\mathbf{P}_0$. Here, $\lambda_{\max}(\mathbf{P})$ and $\lambda_{\min}(\mathbf{P})$ denote the largest and smallest eigenvalues of $\mathbf{P}$, respectively. A similar result holds for $\mathbf{R}$ and $\mathbf{R}_0$.

Proof. For a Hermitian matrix it holds that

$$\lambda_{\max}(\mathbf{P}) = \max_{\mathbf{x}} \frac{\mathbf{x}^*\mathbf{P}\mathbf{x}}{\mathbf{x}^*\mathbf{x}},$$
$$\lambda_{\min}(\mathbf{P}) = \min_{\mathbf{x}} \frac{\mathbf{x}^*\mathbf{P}\mathbf{x}}{\mathbf{x}^*\mathbf{x}}.$$

Hence, making use of the fact that $\mathbf{P}_0$ and $\mathbf{P}_0^{\mathrm{c}}$ have the same eigenvalues, we obtain

$$\begin{aligned}
\lambda_{\max}(\mathbf{P}_0 + \mathbf{\Phi}\mathbf{P}_0^{\mathrm{c}}\mathbf{\Phi}^*) &= \max_{\mathbf{x}} \frac{\mathbf{x}^*\mathbf{P}_0\mathbf{x} + \mathbf{x}^*\mathbf{\Phi}\mathbf{P}_0^{\mathrm{c}}\mathbf{\Phi}^*\mathbf{x}}{\mathbf{x}^*\mathbf{x}} \\
&\leq \max_{\mathbf{x}} \frac{\mathbf{x}^*\mathbf{P}_0\mathbf{x}}{\mathbf{x}^*\mathbf{x}} + \max_{\mathbf{y}} \frac{\mathbf{y}^*\mathbf{P}_0^{\mathrm{c}}\mathbf{y}}{\mathbf{y}^*\mathbf{y}} = 2\lambda_{\max}(\mathbf{P}_0), \\
\lambda_{\min}(\mathbf{P}_0 + \mathbf{\Phi}\mathbf{P}_0^{\mathrm{c}}\mathbf{\Phi}^*) &= \min_{\mathbf{x}} \frac{\mathbf{x}^*\mathbf{P}_0\mathbf{x} + \mathbf{x}^*\mathbf{\Phi}\mathbf{P}_0^{\mathrm{c}}\mathbf{\Phi}^*\mathbf{x}}{\mathbf{x}^*\mathbf{x}} \\
&\geq \min_{\mathbf{x}} \frac{\mathbf{x}^*\mathbf{P}_0\mathbf{x}}{\mathbf{x}^*\mathbf{x}} + \min_{\mathbf{y}} \frac{\mathbf{y}^*\mathbf{P}_0^{\mathrm{c}}\mathbf{y}}{\mathbf{y}^*\mathbf{y}} = 2\lambda_{\min}(\mathbf{P}_0),
\end{aligned}$$

from which the asserted result follows. □

Based on the above result we can say that the signals are less correlated in $\mathbf{R}$ than in $\mathbf{R}_0$. In particular, $\mathbf{P}$ may be nonsingular even though $\mathbf{P}_0$ is singular. This observation, along with the fact that the performance of many array processing algorithms deteriorates as the signal correlation increases, lies at the basis of the belief that the FB approach should outperform the F-only approach. This would really be true if one had two sets of independent data vectors with covariance matrices $\mathbf{R}_0$ and, respectively, $\mathbf{R}$. However, only $\mathbf{R}_0$ and $\hat{\mathbf{R}}_0$ correspond to such a data set, whereas $\mathbf{R}$ and $\hat{\mathbf{R}}$ do not. In fact, *the statistical properties of* $\hat{\mathbf{R}}$ *are quite different from those of* $\hat{\mathbf{R}}_0$*, and this may very well counterbalance the desirable property that* $\mathbf{P}$ *in* $\mathbf{R}$ *is better conditioned than* $\mathbf{P}_0$ *in* $\mathbf{R}_0$. Consequently, the FB approach may not lead to any performance enhancement. This discussion provides an intuitive motivation for the superiority of F-MODE over FB-MODE, which will be shown later in the chapter.

2.3.4 Results on $\mathbf{R}_0$ and $\mathbf{R}$

The following results are valid for *both* $\mathbf{R}_0$ *and* $\mathbf{R}$. However, for the sake of simplicity, we state them only for $\mathbf{R}$.

R5. The columns of $\mathbf{E}_s$, $\{\mathbf{e}_k\}_{k=1}^d$, belong to the range of $\mathbf{A}$:

$$\mathbf{e}_k \in \mathcal{R}(\mathbf{A}). \tag{2.22}$$

More exactly,

$$\mathbf{E}_s = \mathbf{A}\big(\mathbf{P}\mathbf{A}^*\mathbf{E}_s\tilde{\mathbf{\Lambda}}^{-1}\big),$$

where

$$\tilde{\mathbf{\Lambda}} = \mathbf{\Lambda}_s - \sigma^2\mathbf{I}. \tag{2.23}$$

Proof. A simple calculation shows that

$$\mathbf{R}\mathbf{E}_s = \mathbf{E}_s\mathbf{\Lambda}_s = \mathbf{A}\mathbf{P}\mathbf{A}^*\mathbf{E}_s + \sigma^2\mathbf{E}_s \quad \Rightarrow \quad \mathbf{E}_s\tilde{\mathbf{\Lambda}} = \mathbf{A}\big(\mathbf{P}\mathbf{A}^*\mathbf{E}_s\big),$$

from which (2.23) follows. □

R6. Under the assumption made that $\operatorname{rank}(\mathbf{P}) = d$,

$$\mathbf{E}_n^*\mathbf{A} = \mathbf{0} \qquad \Longleftrightarrow \quad \mathcal{R}(\mathbf{E}_n) = \mathcal{N}(\mathbf{A}^*).$$

Proof. This result follows at once from **R5** and the fact that $\mathbf{E}_n^*\mathbf{E}_s = \mathbf{0}$. □

R7. The following equality holds:

$$\mathbf{P}\mathbf{A}^*\mathbf{R}^{-1}\mathbf{A}\mathbf{P} = \big(\mathbf{A}^*\mathbf{A}\big)^{-1}\mathbf{A}^*\mathbf{E}_s\tilde{\mathbf{\Lambda}}^2\mathbf{\Lambda}_s^{-1}\mathbf{E}_s^*\mathbf{A}\big(\mathbf{A}^*\mathbf{A}\big)^{-1}. \tag{2.24}$$

Proof. From

$$\mathbf{R} = \mathbf{A}\mathbf{P}\mathbf{A}^* + \sigma^2\mathbf{I} = \mathbf{E}_s\mathbf{\Lambda}_s\mathbf{E}_s^* + \sigma^2\mathbf{E}_n\mathbf{E}_n^* = \mathbf{E}_s\tilde{\mathbf{\Lambda}}\mathbf{E}_s^* + \sigma^2\mathbf{I}$$

we obtain

$$\mathbf{P} = \big(\mathbf{A}^*\mathbf{A}\big)^{-1}\mathbf{A}^*\mathbf{E}_s\tilde{\mathbf{\Lambda}}\mathbf{E}_s^*\mathbf{A}\big(\mathbf{A}^*\mathbf{A}\big)^{-1}.$$

Inserting the above expression for $\mathbf{P}$ in the left-hand side of (2.24), and making use of **R5** and **R6**, yields

$$\begin{aligned}
&\big(\mathbf{A}^*\mathbf{A}\big)^{-1}\mathbf{A}^*\mathbf{E}_s\tilde{\mathbf{\Lambda}}\mathbf{E}_s^*\mathbf{A}\big(\mathbf{A}^*\mathbf{A}\big)^{-1}\mathbf{A}^* \\
&\quad\times\big[\mathbf{E}_s\mathbf{\Lambda}_s^{-1}\mathbf{E}_s^* + \frac{1}{\sigma^2}\mathbf{E}_n\mathbf{E}_n^*\big]\mathbf{A}\big(\mathbf{A}^*\mathbf{A}\big)^{-1}\mathbf{A}^*\mathbf{E}_s\tilde{\mathbf{\Lambda}}\mathbf{E}_s^*\mathbf{A}\big(\mathbf{A}^*\mathbf{A}\big)^{-1} \\
&\qquad\qquad = \big(\mathbf{A}^*\mathbf{A}\big)^{-1}\mathbf{A}^*\mathbf{E}_s\tilde{\mathbf{\Lambda}}^2\mathbf{\Lambda}_s^{-1}\mathbf{E}_s^*\mathbf{A}\big(\mathbf{A}^*\mathbf{A}\big)^{-1},
\end{aligned}$$

which we had to prove. □

R8. Let $\simeq$ denote an asymptotically valid equality, that is, an equality in which only the asymptotically dominant terms (in the mean square sense) have been retained. Then,

$$\mathbf{B}^*\hat{\mathbf{E}}_s \simeq \mathbf{B}^*\hat{\mathbf{R}}\mathbf{E}_s\tilde{\mathbf{\Lambda}}^{-1}. \tag{2.25}$$

Proof. From (2.3), we have

$$\begin{aligned}
\mathbf{B}^*\hat{\mathbf{R}}\hat{\mathbf{E}}_s &= \mathbf{B}^*\hat{\mathbf{E}}_s\hat{\mathbf{\Lambda}}_s, \\
\mathbf{B}^*\hat{\mathbf{R}}\mathbf{E}_s + \mathbf{B}^*\mathbf{R}\hat{\mathbf{E}}_s &= \mathbf{B}^*\hat{\mathbf{E}}_s\hat{\mathbf{\Lambda}}_s, \\
\mathbf{B}^*\hat{\mathbf{R}}\mathbf{E}_s &= \mathbf{B}^*\hat{\mathbf{E}}_s(\hat{\mathbf{\Lambda}}_s - \sigma^2\mathbf{I}), \\
\mathbf{B}^*\hat{\mathbf{E}}_s &\simeq \mathbf{B}^*\hat{\mathbf{R}}\mathbf{E}_s\tilde{\mathbf{\Lambda}}^{-1}.
\end{aligned}$$

The second and the third step follow from the facts that $\mathbf{B}^*\mathbf{R}\mathbf{E}_s = \mathbf{0}$ and $\mathbf{B}^*\mathbf{R} = \sigma^2\mathbf{B}^*$. Since $\hat{\mathbf{E}}_s \to \mathbf{E}_s$ and $\hat{\mathbf{\Lambda}}_s \to \mathbf{\Lambda}_s$ as $N \to \infty$, and since $\mathbf{B}^*\mathbf{E}_s = \mathbf{0}$, the first order approximation in the last step results. □

2.3.5 Results on ABC Estimation

Let $\mathbf{z}$ be a complex-valued random vector that depends on an unknown real-valued parameter vector $\boldsymbol{\omega}$, and whose mean and covariance matrix tend to zero (typically as $1/N$), as N increases. Then an asymptotically best (in the mean square sense) consistent (ABC) estimate of the parameter vector $\boldsymbol{\omega}$, based on $\mathbf{z}$, is given by the global minimizer of the function [SS89]

$$\boldsymbol{\mu}^T \mathbf{C}_{\boldsymbol{\mu}}^{-1} \boldsymbol{\mu}, \tag{2.26}$$

where

$$\boldsymbol{\mu} = \begin{bmatrix} \mathrm{Re}(\mathbf{z}) \\ \mathrm{Im}(\mathbf{z}) \end{bmatrix},$$

and where

$$\mathbf{C}_{\boldsymbol{\mu}} = \mathrm{E}\{\boldsymbol{\mu}\boldsymbol{\mu}^T\}$$

is assumed to be invertible. The ABC estimate above is the extension of the Markov linear estimator to a class of nonlinear regression equations. The minimization of (2.26) can also be given an approximate (asymptotically valid) ML interpretation (see, e.g., [SS90a]). The estimating criterion (2.26) also results in certain estimation problems, the solutions of which are derived by weighted subspace fitting techniques [VO91].

In most applications we derive $\mathrm{E}\{\mathbf{z}\mathbf{z}^*\}$ and $\mathrm{E}\{\mathbf{z}\mathbf{z}^T\}$, but not $\mathbf{C}_{\boldsymbol{\mu}}$ directly. It is hence more convenient to work with the vector

$$\boldsymbol{\rho} = \begin{bmatrix} \mathbf{z} \\ \mathbf{z}^{\mathrm{c}} \end{bmatrix} \tag{2.27}$$

rather than with $\boldsymbol{\mu}$. The next result obtains the function of $\boldsymbol{\rho}$ whose minimization is equivalent to that of (2.26).

R9. Let $\mathbf{C}_{\boldsymbol{\rho}} = \mathrm{E}\{\boldsymbol{\rho}\boldsymbol{\rho}^*\}$. Then,

$$\boldsymbol{\mu}^T \mathbf{C}_{\boldsymbol{\mu}}^{-1} \boldsymbol{\mu} = \boldsymbol{\rho}^* \mathbf{C}_{\boldsymbol{\rho}}^{-1} \boldsymbol{\rho}. \tag{2.28}$$

Proof. We have

$$\boldsymbol{\mu} = \mathbf{L}\boldsymbol{\rho},$$

where

$$\mathbf{L} = \frac{1}{2} \begin{bmatrix} \mathbf{I} & \mathbf{I} \\ -i\mathbf{I} & i\mathbf{I} \end{bmatrix}.$$

As $\mathbf{L}$ is nonsingular,

$$\boldsymbol{\mu}^T \mathbf{C}_{\boldsymbol{\mu}}^{-1} \boldsymbol{\mu} = \boldsymbol{\rho}^* \mathbf{L}^* \left(\mathbf{L} \mathbf{C}_{\boldsymbol{\rho}} \mathbf{L}^*\right)^{-1} \mathbf{L} \boldsymbol{\rho} = \boldsymbol{\rho}^* \mathbf{C}_{\boldsymbol{\rho}}^{-1} \boldsymbol{\rho},$$

which concludes the proof. □

2.4 Brief Review of F-MODE

Consider the ABC estimator (see Section 2.3) obtained from

$$\mathbf{z} = \mathrm{vec}(\mathbf{B}^* \hat{\mathbf{E}}_{s_0}), \tag{2.29}$$

where vec denotes column-wise vectorization. The ABC criterion corresponding to $\mathbf{z}$ above can be shown to be

$$\mathrm{Tr}\{\left(\mathbf{B}^* \mathbf{B}\right)^{-1} \mathbf{B}^* \hat{\mathbf{E}}_{s_0} \tilde{\boldsymbol{\Lambda}}_0^2 \boldsymbol{\Lambda}_{s0}^{-1} \hat{\mathbf{E}}_{s_0}^* \mathbf{B}\}, \tag{2.30}$$

where Tr denotes the trace operator. The F-MODE estimate of $\boldsymbol{\omega} \triangleq [\omega_1 \ \ldots \ \omega_d]^T$ is obtained as an asymptotically valid approximation to the minimizer of (2.30), in the following steps [SS90a]:

1. Obtain $\hat{\mathbf{E}}_{s_0}$, $\hat{\boldsymbol{\Lambda}}_{s_0}$, and $\hat{\tilde{\boldsymbol{\Lambda}}}_0$ from the EVD of $\hat{\mathbf{R}}_0$. Derive an initial estimate of $\{b_k\}$ by minimizing the quadratic function

$$\mathrm{Tr}\{\mathbf{B}^* \hat{\mathbf{E}}_{s_0} \hat{\tilde{\boldsymbol{\Lambda}}}_0^2 \hat{\boldsymbol{\Lambda}}_{s_0}^{-1} \hat{\mathbf{E}}_{s_0}^* \mathbf{B}\}.$$

2. Let $\left(\hat{\mathbf{B}}^* \hat{\mathbf{B}}\right)$ be the estimate of $\left(\mathbf{B}^* \mathbf{B}\right)$ made from the previously obtained estimates of $\{b_k\}$. Derive refined estimates of $\{b_k\}$ by minimizing the quadratic function

$$\mathrm{Tr}\{\left(\hat{\mathbf{B}}^* \hat{\mathbf{B}}\right)^{-1} \mathbf{B}^* \hat{\mathbf{E}}_{s_0} \hat{\tilde{\boldsymbol{\Lambda}}}_0^2 \hat{\boldsymbol{\Lambda}}_{s_0}^{-1} \hat{\mathbf{E}}_{s_0}^* \mathbf{B}\}.$$

   Possibly repeat this operation once more, using the latest estimate of $\{b_k\}$ to obtain $\left(\hat{\mathbf{B}}^* \hat{\mathbf{B}}\right)$. Finally, derive estimates of $\{\omega_k\}$ by rooting the polynomial $\sum_{k=0}^{d} \hat{b}_k z^k$ (see (2.11)).

The minimization in steps 1 and 2 above should be conducted under an appropriate constraint on $\{b_k\}$ (to prevent the trivial solution $\{b_k = 0\}$). Typically, one uses

$$\sum_{k=0}^{d} |b_k|^2 = 1.$$

Additionally the $\{b_k\}$ should satisfy (2.12).

Asymptotically (as N increases) the F-MODE estimate is Gaussian distributed with mean equal to the true parameter vector $\boldsymbol{\omega}$ and covariance matrix,

$$\mathbf{C}_{\mathrm{F}} = \frac{\sigma^2}{2N}\Big\{\mathrm{Re}\left[\mathbf{U} \odot \mathbf{Q}_0^T\right]\Big\}^{-1}, \tag{2.31}$$

where $\odot$ denotes the Hadamard product (i.e., element-wise multiplication),

$$\mathbf{U} = \mathbf{D}^* \boldsymbol{\Pi}_{\mathbf{A}}^{\perp} \mathbf{D}, \tag{2.32}$$

$$\mathbf{Q}_0 = \mathbf{P}_0 \mathbf{A}^* \mathbf{R}_0^{-1} \mathbf{A} \mathbf{P}_0, \tag{2.33}$$

and where

$$\mathbf{D} = \left[\mathbf{d}(\omega_1) \quad \dots \quad \mathbf{d}(\omega_d)\right]; \qquad \mathbf{d}(\omega) = \frac{d\mathbf{a}(\omega)}{d\omega}$$

and

$$\boldsymbol{\Pi}_{\mathbf{A}}^{\perp} = \mathbf{I} - \mathbf{A}\big(\mathbf{A}^*\mathbf{A}\big)^{-1}\mathbf{A}^*$$

is the orthogonal projector onto $\mathcal{N}(\mathbf{A}^*)$. Because (2.31) is also the CRB matrix for the estimation problem under consideration, it follows that F-MODE is asymptotically statistically efficient [VO91, SS90a, SN90].

2.5 Derivation of FB-MODE

Similarly to (2.29), the FB-MODE is associated with the ABC estimate derived from

$$\mathbf{z} = \mathrm{vec}(\mathbf{B}^* \hat{\mathbf{E}}_s) = \begin{bmatrix} \mathbf{B}^* \hat{\mathbf{e}}_1 \\ \vdots \\ \mathbf{B}^* \hat{\mathbf{e}}_d \end{bmatrix}.$$

As shown in Appendix A.1, asymptotically in N,

$$\mathrm{E}\{\mathbf{z}\mathbf{z}^*\} = \frac{\sigma^2}{2N}\big(\tilde{\boldsymbol{\Lambda}}^{-2}\boldsymbol{\Lambda}_s\big) \otimes \big(\mathbf{B}^*\mathbf{B}\big) \tag{2.34}$$

and

$$\mathrm{E}\{\mathbf{z}\mathbf{z}^T\} = \frac{\sigma^2}{2N}\big(\tilde{\boldsymbol{\Lambda}}^{-2}\boldsymbol{\Lambda}_s\boldsymbol{\Gamma}^*\big) \otimes \big(\mathbf{B}^*\mathbf{B}\tilde{\mathbf{J}}\big), \tag{2.35}$$

where $\otimes$ is the Kronecker matrix product operator. Consequently, see (2.27),

$$\begin{aligned}\mathbf{C}_{\boldsymbol{\rho}} &\triangleq \mathrm{E}\left\{\begin{bmatrix}\mathbf{z}\\ \mathbf{z}^{\mathrm{c}}\end{bmatrix}\begin{bmatrix}\mathbf{z}^{*} & \mathbf{z}^{T}\end{bmatrix}\right\}\\ &= \frac{\sigma^2}{2N}\begin{bmatrix}\left(\tilde{\boldsymbol{\Lambda}}^{-2}\boldsymbol{\Lambda}_s\right)\otimes\left(\mathbf{B}^{*}\mathbf{B}\right) & \left(\tilde{\boldsymbol{\Lambda}}^{-2}\boldsymbol{\Lambda}_s\boldsymbol{\Gamma}^{*}\right)\otimes\left(\mathbf{B}^{*}\mathbf{B}\tilde{\mathbf{J}}\right)\\ \left(\tilde{\boldsymbol{\Lambda}}^{-2}\boldsymbol{\Lambda}_s\boldsymbol{\Gamma}\right)\otimes\left(\tilde{\mathbf{J}}\mathbf{B}^{*}\mathbf{B}\right) & \left(\tilde{\boldsymbol{\Lambda}}^{-2}\boldsymbol{\Lambda}_s\right)\otimes\left(\mathbf{B}^{*}\mathbf{B}\right)^{\mathrm{c}}\end{bmatrix}.\end{aligned} \tag{2.36}$$

Using the fact that $\left(\mathbf{B}^{*}\mathbf{B}\right)^{\mathrm{c}} = \tilde{\mathbf{J}}\mathbf{B}^{*}\mathbf{B}\tilde{\mathbf{J}}$ (see **R1**), we can factor $\mathbf{C}_{\boldsymbol{\rho}}$ as (we omit the scalar factor $\sigma^2/2N$ in (2.36) since it has no influence on the estimate obtained by minimizing the ABC criterion)

$$\begin{aligned}\mathbf{C}_{\boldsymbol{\rho}} = &\begin{bmatrix}\left(\tilde{\boldsymbol{\Lambda}}^{-2}\boldsymbol{\Lambda}_s\right)\otimes\mathbf{I} & \mathbf{0}\\ \mathbf{0} & \left(\tilde{\boldsymbol{\Lambda}}^{-2}\boldsymbol{\Lambda}_s\right)\otimes\tilde{\mathbf{J}}\end{bmatrix}\\ &\times\begin{bmatrix}\mathbf{I}\otimes\mathbf{I} & \boldsymbol{\Gamma}^{*}\otimes\mathbf{I}\\ \boldsymbol{\Gamma}\otimes\mathbf{I} & \mathbf{I}\otimes\mathbf{I}\end{bmatrix}\begin{bmatrix}\mathbf{I}\otimes\left(\mathbf{B}^{*}\mathbf{B}\right) & \mathbf{0}\\ \mathbf{0} & \mathbf{I}\otimes\left(\mathbf{B}^{*}\mathbf{B}\tilde{\mathbf{J}}\right)\end{bmatrix}.\end{aligned} \tag{2.37}$$

The middle matrix in (2.37) can be rewritten as

$$\begin{bmatrix}\mathbf{I}\otimes\mathbf{I}\\ \boldsymbol{\Gamma}\otimes\mathbf{I}\end{bmatrix}\begin{bmatrix}\mathbf{I}\otimes\mathbf{I} & \boldsymbol{\Gamma}^{*}\otimes\mathbf{I}\end{bmatrix}$$

and it is evidently singular. Consequently $\mathbf{C}_{\boldsymbol{\rho}}$ is *singular* and hence the ABC estimating criterion in (2.28) cannot be used as it stands. There are several possibilities for overcoming this difficulty; see, e.g., [SS89, Gor97]. Here we adopt the approach of [Gor97], where it was shown that if $\mathbf{C}_{\boldsymbol{\rho}}(\varepsilon)$ denotes a nonsingular matrix obtained by a slight perturbation of $\mathbf{C}_{\boldsymbol{\rho}}$, then we can use (2.28) with $\mathbf{C}_{\boldsymbol{\rho}}(\varepsilon)$ in lieu of $\mathbf{C}_{\boldsymbol{\rho}}$. The minimizer of the so-obtained criterion,

$$\boldsymbol{\rho}^{*}\mathbf{C}_{\boldsymbol{\rho}}^{-1}(\varepsilon)\boldsymbol{\rho} \tag{2.38}$$

is then an ABC estimate, as the perturbation parameter ε goes to zero. If the limit of (2.38), as $\varepsilon \to 0$, cannot be evaluated analytically then we can obtain an (almost) ABC estimate by minimizing (2.38) with a "very small" ε value. Interestingly enough, in the case under discussion, we can obtain a closed-form expression for the limit criterion. To this end, let

$$\boldsymbol{\Gamma}_{\varepsilon} = (1-\varepsilon)\boldsymbol{\Gamma}$$

and let $\mathbf{C}_{\boldsymbol{\rho}}(\varepsilon)$ be given by (2.37) where $\boldsymbol{\Gamma}$ is replaced by $\boldsymbol{\Gamma}_\varepsilon$. It can be readily checked that (for $\varepsilon \neq 0$)

$$\begin{bmatrix} \mathbf{I}\otimes\mathbf{I} & \boldsymbol{\Gamma}_\varepsilon^* \times \mathbf{I} \\ \boldsymbol{\Gamma}_\varepsilon \otimes \mathbf{I} & \mathbf{I}\otimes\mathbf{I} \end{bmatrix}^{-1} = \frac{1}{\varepsilon(2-\varepsilon)} \begin{bmatrix} \mathbf{I}\otimes\mathbf{I} & -\boldsymbol{\Gamma}_\varepsilon^* \otimes \mathbf{I} \\ -\boldsymbol{\Gamma}_\varepsilon \otimes \mathbf{I} & \mathbf{I}\otimes\mathbf{I} \end{bmatrix},$$

which implies that

$$\begin{aligned} &\mathbf{C}_{\boldsymbol{\rho}}^{-1}(\varepsilon) \\ &= \frac{1}{\varepsilon(2-\varepsilon)} \begin{bmatrix} \mathbf{I}\otimes(\mathbf{B}^*\mathbf{B})^{-1} & \mathbf{0} \\ \mathbf{0} & \mathbf{I}\otimes\left[\tilde{\mathbf{J}}(\mathbf{B}^*\mathbf{B})^{-1}\right] \end{bmatrix} \\ &\quad \times \begin{bmatrix} \mathbf{I}\otimes\mathbf{I} & -\boldsymbol{\Gamma}_\varepsilon^* \otimes \mathbf{I} \\ -\boldsymbol{\Gamma}_\varepsilon \otimes \mathbf{I} & \mathbf{I}\otimes\mathbf{I} \end{bmatrix} \begin{bmatrix} (\tilde{\boldsymbol{\Lambda}}^2\boldsymbol{\Lambda}_s^{-1})\otimes\mathbf{I} & \mathbf{0} \\ \mathbf{0} & (\tilde{\boldsymbol{\Lambda}}^2\boldsymbol{\Lambda}_s^{-1})\otimes\tilde{\mathbf{J}} \end{bmatrix} \\ &= \frac{1}{\varepsilon(2-\varepsilon)} \\ &\quad \times \begin{bmatrix} (\tilde{\boldsymbol{\Lambda}}^2\boldsymbol{\Lambda}_s^{-1})\otimes(\mathbf{B}^*\mathbf{B})^{-1} & -(\boldsymbol{\Gamma}_\varepsilon\tilde{\boldsymbol{\Lambda}}^2\boldsymbol{\Lambda}_s^{-1})\otimes\left[(\mathbf{B}^*\mathbf{B})^{-1}\tilde{\mathbf{J}}\right] \\ -(\boldsymbol{\Gamma}_\varepsilon\tilde{\boldsymbol{\Lambda}}^2\boldsymbol{\Lambda}_s^{-1})\otimes\left[\tilde{\mathbf{J}}(\mathbf{B}^*\mathbf{B})^{-1}\right] & (\tilde{\boldsymbol{\Lambda}}^2\boldsymbol{\Lambda}_s^{-1})\otimes\left[\tilde{\mathbf{J}}(\mathbf{B}^*\mathbf{B})^{-1}\tilde{\mathbf{J}}\right] \end{bmatrix}. \end{aligned} \tag{2.39}$$

Inserting (2.39) into (2.38) yields

$$\begin{aligned} \varepsilon(2-\varepsilon)\boldsymbol{\rho}^*\mathbf{C}_{\boldsymbol{\rho}}^{-1}(\varepsilon)\boldsymbol{\rho} = \mathbf{z}^* &\underbrace{\left[(\tilde{\boldsymbol{\Lambda}}^2\boldsymbol{\Lambda}_s^{-1})\otimes(\mathbf{B}^*\mathbf{B})^{-1}\right]}_{\boldsymbol{\Omega}_1}\mathbf{z} \\ &- \mathbf{z}^T\underbrace{\left[(\boldsymbol{\Gamma}_\varepsilon\tilde{\boldsymbol{\Lambda}}^2\boldsymbol{\Lambda}_s^{-1})\otimes\left[\tilde{\mathbf{J}}(\mathbf{B}^*\mathbf{B})^{-1}\right]\right]}_{\boldsymbol{\Omega}_2}\mathbf{z} \\ &- \mathbf{z}^*\underbrace{\left[(\boldsymbol{\Gamma}_\varepsilon\tilde{\boldsymbol{\Lambda}}^2\boldsymbol{\Lambda}_s^{-1})\otimes\left[(\mathbf{B}^*\mathbf{B})^{-1}\tilde{\mathbf{J}}\right]\right]}_{\boldsymbol{\Omega}_3}\mathbf{z}^{\mathrm{c}} \\ &+ \mathbf{z}^T\underbrace{\left[(\tilde{\boldsymbol{\Lambda}}^2\boldsymbol{\Lambda}_s^{-1})\otimes\left[\tilde{\mathbf{J}}(\mathbf{B}^*\mathbf{B})^{-1}\tilde{\mathbf{J}}\right]\right]}_{\boldsymbol{\Omega}_4}\mathbf{z}^{\mathrm{c}}. \end{aligned} \tag{2.40}$$

Using **R1** we obtain (observe the definition of $\boldsymbol{\Omega}_1, \ldots, \boldsymbol{\Omega}_4$ above)

$$\boldsymbol{\Omega}_4 = \boldsymbol{\Omega}_1^{\mathrm{c}}$$

and

$$\boldsymbol{\Omega}_3 = \boldsymbol{\Omega}_2^{\mathrm{c}}.$$

Hence we can rewrite (2.40) in a more compact form:

$$\frac{\varepsilon(2-\varepsilon)}{2}\boldsymbol{\rho}^*\mathbf{C}_{\boldsymbol{\rho}}^{-1}(\varepsilon)\boldsymbol{\rho} = \mathbf{z}^*\boldsymbol{\Omega}_1\mathbf{z} - \mathrm{Re}\Big[\mathbf{z}^T\boldsymbol{\Omega}_2\mathbf{z}\Big]. \tag{2.41}$$

Next, we make use of the fact that, for conformable matrices $\mathbf{A}$, $\mathbf{X}$, $\mathbf{B}$, and $\mathbf{Y}$,

$$\mathrm{Tr}\{\mathbf{A}\mathbf{X}^*\mathbf{B}\mathbf{Y}\} = \big[\mathrm{vec}(\mathbf{X})\big]^*\big[\mathbf{A}^T \otimes \mathbf{B}\big]\,\mathrm{vec}(\mathbf{Y})$$

to obtain

$$\mathbf{z}^*\boldsymbol{\Omega}_1\mathbf{z} = \mathrm{Tr}\{\tilde{\boldsymbol{\Lambda}}^2\boldsymbol{\Lambda}_s^{-1}\hat{\mathbf{E}}_s^*\mathbf{B}(\mathbf{B}^*\mathbf{B})^{-1}\mathbf{B}^*\hat{\mathbf{E}}_s\} \tag{2.42}$$

and

$$\mathbf{z}^T\boldsymbol{\Omega}_2\mathbf{z} = \mathrm{Tr}\{\boldsymbol{\Gamma}_\varepsilon\tilde{\boldsymbol{\Lambda}}^2\boldsymbol{\Lambda}_s^{-1}\hat{\mathbf{E}}_s^T\mathbf{B}^{\mathrm{c}}\tilde{\mathbf{J}}(\mathbf{B}^*\mathbf{B})^{-1}\mathbf{B}^*\hat{\mathbf{E}}_s\}. \tag{2.43}$$

Finally, we use **R1** and **R3** to rewrite (2.43) as

$$\begin{aligned}\mathbf{z}^T\boldsymbol{\Omega}_2\mathbf{z} &= (1-\varepsilon)\,\mathrm{Tr}\{\tilde{\boldsymbol{\Lambda}}^2\boldsymbol{\Lambda}_s^{-1}\boldsymbol{\Gamma}\hat{\mathbf{E}}_s^T\mathbf{J}\mathbf{B}(\mathbf{B}^*\mathbf{B})^{-1}\mathbf{B}^*\hat{\mathbf{E}}_s\}\\ &= (1-\varepsilon)\,\mathrm{Tr}\{\tilde{\boldsymbol{\Lambda}}^2\boldsymbol{\Lambda}_s^{-1}\hat{\mathbf{E}}_s^*\mathbf{B}(\mathbf{B}^*\mathbf{B})^{-1}\mathbf{B}^*\hat{\mathbf{E}}_s\} = (1-\varepsilon)\mathbf{z}^*\boldsymbol{\Omega}_1\mathbf{z}.\end{aligned} \tag{2.44}$$

Combining (2.41), (2.42), and (2.44) leads to the function

$$\boldsymbol{\rho}^*\mathbf{C}_{\boldsymbol{\rho}}^{-1}(\varepsilon)\boldsymbol{\rho} = \frac{2}{2-\varepsilon}\big(\mathbf{z}^*\boldsymbol{\Omega}_1\mathbf{z}\big),$$

the limit of which, as $\varepsilon \to 0$, yields the *FB-MODE criterion*:

$$\mathrm{Tr}\{(\mathbf{B}^*\mathbf{B})^{-1}\mathbf{B}^*\hat{\mathbf{E}}_s\tilde{\boldsymbol{\Lambda}}^2\boldsymbol{\Lambda}_s^{-1}\hat{\mathbf{E}}_s^*\mathbf{B}\}. \tag{2.45}$$

Comparing (2.45) with (2.30) we see that *the FB-MODE criterion has exactly the same structure as the F-MODE criterion*, with the only difference that the former criterion depends on the eigenelements of the FB sample covariance matrix. Owing to this neat result, the FB-MODE estimate of $\boldsymbol{\omega}$ can be obtained by applying to $\hat{\mathbf{R}}$ the two- (or three-) step algorithm outlined in Section 2.4.

2.6 Analysis of FB-MODE

The FB-MODE criterion in (2.45) can be parameterized directly via the parameters of interest, $\{\omega_k\}$. Indeed, it follows from (2.14) that

$$\mathbf{B}(\mathbf{B}^*\mathbf{B})^{-1}\mathbf{B}^* = \mathbf{\Pi}_{\mathbf{A}}^{\perp}$$

and hence that (2.45) can be rewritten as

$$f(\boldsymbol{\omega}) \triangleq \mathrm{Tr}\{\hat{\mathbf{W}}\hat{\mathbf{E}}_s^*\mathbf{\Pi}_{\mathbf{A}}^{\perp}\hat{\mathbf{E}}_s\}, \tag{2.46}$$

where

$$\hat{\mathbf{W}} = \hat{\tilde{\mathbf{\Lambda}}}^2\hat{\mathbf{\Lambda}}_s^{-1}.$$

Later we will also use the notation $\mathbf{W} = \tilde{\mathbf{\Lambda}}^2\mathbf{\Lambda}_s^{-1}$. The reason that $\hat{\mathbf{W}}$ appears in (2.46), rather than $\mathbf{W}$ as in (2.45), is that the estimator should be based on the sample data. It will, however, be shown that it is only the limit matrix $\mathbf{W}$ that affects the asymptotic performance. Let

$$\mathbf{g} = \frac{\partial f(\boldsymbol{\omega})}{\partial \boldsymbol{\omega}}$$

denote the gradient vector of (2.46), let

$$\mathbf{H} = \frac{\partial^2 f(\boldsymbol{\omega})}{\partial \boldsymbol{\omega}\partial \boldsymbol{\omega}^T}$$

denote the corresponding Hessian matrix, and let

$$\mathbf{H}_\infty = \lim_{N\to\infty} \mathbf{H}$$

denote the asymptotic Hessian. Using this notation and a standard Taylor series expansion technique (the details of which are omitted in the interest of brevity, see [VO91, SS90a] and [SN90] for similar analyses), we can show that the covariance matrix of the FB-MODE estimate of $\boldsymbol{\omega}$ is asymptotically (for $N \gg 1$) given by

$$\mathbf{C}_{FB} = \mathbf{H}_\infty^{-1}\Big[\mathrm{E}(\mathbf{g}\mathbf{g}^T)\Big]\mathbf{H}_\infty^{-1}. \tag{2.47}$$

It remains to evaluate $\mathbf{H}_\infty$ and the middle matrix in (2.47).

Let $\mathbf{A}_i$ denote the derivative of $\mathbf{A}$ with respect to ω_i:

$$\mathbf{A}_i = \frac{\partial \mathbf{A}}{\partial \omega_i} = \mathbf{d}_i \mathbf{u}_i^*. \tag{2.48}$$

Here, $\mathbf{d}_i$ is a short notation for $\mathbf{d}(\omega_i)$, and $\mathbf{u}_i = [0,\ \ldots,\ 0,\ 1,\ 0,\ \ldots,\ 0]^T$ (with 1 in the ith position). A simple calculation shows that

$$\begin{aligned}\frac{\partial \mathbf{\Pi}_{\mathbf{A}}^{\perp}}{\partial \omega_i} &= -\mathbf{A}_i(\mathbf{A}^*\mathbf{A})^{-1}\mathbf{A}^* \\ &\quad + \mathbf{A}(\mathbf{A}^*\mathbf{A})^{-1}\big[\mathbf{A}_i^*\mathbf{A} + \mathbf{A}^*\mathbf{A}_i\big](\mathbf{A}^*\mathbf{A})^{-1}\mathbf{A}^* - \mathbf{A}(\mathbf{A}^*\mathbf{A})^{-1}\mathbf{A}_i^* \\ &= -\mathbf{\Pi}_{\mathbf{A}}^{\perp}\mathbf{A}_i(\mathbf{A}^*\mathbf{A})^{-1}\mathbf{A}^* - \mathbf{A}(\mathbf{A}^*\mathbf{A})^{-1}\mathbf{A}_i^*\mathbf{\Pi}_{\mathbf{A}}^{\perp}.\end{aligned} \tag{2.49}$$

Next note that – for conformable matrices $\mathbf{X}$ and $\mathbf{Y}$, with $\mathbf{Y}$ Hermitian – we have

$$\mathrm{Tr}\{(\mathbf{X} + \mathbf{X}^*)\mathbf{Y}\} = 2\,\mathrm{Re}\big[\mathrm{Tr}\{\mathbf{X}\mathbf{Y}\}\big]. \tag{2.50}$$

Using (2.49) and (2.50) we obtain

$$g_i = -2\,\mathrm{Re}\left\{\mathrm{Tr}[\hat{\mathbf{W}}\hat{\mathbf{E}}_s^*\mathbf{A}(\mathbf{A}^*\mathbf{A})^{-1}\mathbf{A}_i^*\mathbf{\Pi}_{\mathbf{A}}^{\perp}\hat{\mathbf{E}}_s]\right\}. \tag{2.51}$$

Inserting (2.48) in (2.51) gives

$$g_i \simeq -2\,\mathrm{Re}\left[\mathbf{d}_i^*\mathbf{\Pi}_{\mathbf{A}}^{\perp}\hat{\mathbf{E}}_s\mathbf{W}\mathbf{E}_s^*\mathbf{A}(\mathbf{A}^*\mathbf{A})^{-1}\mathbf{u}_i\right].$$

Taking the derivative of the right hand side of (2.51) with respect to ω_j, we obtain

$$\begin{aligned}\mathbf{H}_{ij} &\simeq 2\,\mathrm{Re}\left[\mathbf{d}_i^*\mathbf{\Pi}_{\mathbf{A}}^{\perp}\mathbf{A}_j(\mathbf{A}^*\mathbf{A})^{-1}\mathbf{A}^*\mathbf{E}_s\mathbf{W}\mathbf{E}_s^*\mathbf{A}(\mathbf{A}^*\mathbf{A})^{-1}\mathbf{u}_i\right] \\ &= 2\,\mathrm{Re}\left\{\left[\mathbf{d}_i^*\mathbf{\Pi}_{\mathbf{A}}^{\perp}\mathbf{d}_j\right]\left[\left((\mathbf{A}^*\mathbf{A})^{-1}\mathbf{A}^*\mathbf{E}_s\mathbf{W}\mathbf{E}_s^*\mathbf{A}(\mathbf{A}^*\mathbf{A})^{-1}\right)^T\right]_{ij}\right\} \\ &= \big(\mathbf{H}_{\infty}\big)_{ij}.\end{aligned}$$

Making use of **R7** yields the following expression for the asymptotic Hessian matrix,

$$\mathbf{H}_{\infty} = 2\,\mathrm{Re}\left[\mathbf{U} \odot \mathbf{Q}^T\right],$$

where $\mathbf{U}$ is as defined in (2.32), and $\mathbf{Q}$ is defined similarly to $\mathbf{Q}_0$ in (2.33),

$$\mathbf{Q} = \mathbf{P}\mathbf{A}^*\mathbf{R}^{-1}\mathbf{A}\mathbf{P}.$$

To derive an expression for the middle matrix in (2.47) we need the additional notation

$$\begin{aligned}\boldsymbol{\alpha}_i^* &= \mathbf{d}_i^*\mathbf{B}(\mathbf{B}^*\mathbf{B})^{-1},\\ \boldsymbol{\beta}_i &= \mathbf{W}\mathbf{E}_s^*\mathbf{A}(\mathbf{A}^*\mathbf{A})^{-1}\mathbf{u}_i,\end{aligned}$$

with the use of which we can write

$$-g_i \simeq 2\,\mathrm{Re}\left[\boldsymbol{\alpha}_i^*(\mathbf{B}^*\hat{\mathbf{E}}_s)\boldsymbol{\beta}_i\right] = 2\,\mathrm{Re}\left[(\boldsymbol{\beta}_i^T \otimes \boldsymbol{\alpha}_i^*)\mathbf{z}\right].$$

It follows that

$$\begin{aligned}&\mathrm{E}[g_i g_j]\\ &\quad\simeq 2\,\mathrm{Re}\left\{(\boldsymbol{\beta}_i^T \otimes \boldsymbol{\alpha}_i^*)\,\mathrm{E}[\mathbf{z}\mathbf{z}^*](\boldsymbol{\beta}_j^{\mathrm{c}} \otimes \boldsymbol{\alpha}_j) + (\boldsymbol{\beta}_i^T \otimes \boldsymbol{\alpha}_i^*)\,\mathrm{E}[\mathbf{z}\mathbf{z}^T](\boldsymbol{\beta}_j \otimes \boldsymbol{\alpha}_j^{\mathrm{c}})\right\}\\ &\quad\triangleq 2\,\mathrm{Re}(T_1 + T_2).\end{aligned} \tag{2.52}$$

Next, we note that (cf. (2.34))

$$\begin{aligned}\frac{2N}{\sigma^2}T_1 &= (\boldsymbol{\beta}_i^T\tilde{\boldsymbol{\Lambda}}^{-2}\boldsymbol{\Lambda}_s\boldsymbol{\beta}_j^{\mathrm{c}})(\boldsymbol{\alpha}_i^*\mathbf{B}^*\mathbf{B}\boldsymbol{\alpha}_j)\\ &= (\boldsymbol{\beta}_j^*\tilde{\boldsymbol{\Lambda}}^{-2}\boldsymbol{\Lambda}_s\boldsymbol{\beta}_i)(\boldsymbol{\alpha}_i^*\mathbf{B}^*\mathbf{B}\boldsymbol{\alpha}_j) = \mathbf{Q}_{ij}^T\mathbf{U}_{ij}.\end{aligned} \tag{2.53}$$

A convenient expression for T_2 is slightly more difficult to obtain. First, we note that (cf. (2.35))

$$\frac{2N}{\sigma^2}T_2 = (\boldsymbol{\beta}_i^T\tilde{\boldsymbol{\Lambda}}^{-2}\boldsymbol{\Lambda}_s\boldsymbol{\Gamma}^*\boldsymbol{\beta}_j)(\boldsymbol{\alpha}_i^*\mathbf{B}^*\mathbf{B}\tilde{\mathbf{J}}\boldsymbol{\alpha}_j^{\mathrm{c}}). \tag{2.54}$$

Next, we make use of **R3** and (2.7) to write

$$\begin{aligned}\boldsymbol{\Gamma}^*\boldsymbol{\beta}_j &= \mathbf{W}(\boldsymbol{\Gamma}^*\mathbf{E}_s^*)\mathbf{A}(\mathbf{A}^*\mathbf{A})^{-1}\mathbf{u}_j = \mathbf{W}\mathbf{E}_s^T(\mathbf{J}\mathbf{A})(\mathbf{A}^*\mathbf{A})^{-1}\mathbf{u}_j\\ &= \mathbf{W}\mathbf{E}_s^T\mathbf{A}^{\mathrm{c}}\boldsymbol{\Phi}^*(\mathbf{A}^*\mathbf{A})^{-1}\mathbf{u}_j = \mathbf{W}\mathbf{E}_s^T\mathbf{A}^{\mathrm{c}}(\mathbf{A}^*\mathbf{J}\mathbf{A}^{\mathrm{c}})^{-1}\mathbf{u}_j\\ &= \mathbf{W}\mathbf{E}_s^T\mathbf{A}^{\mathrm{c}}(\boldsymbol{\Phi}\mathbf{A}^T\mathbf{A}^{\mathrm{c}})^{-1}\mathbf{u}_j = \mathbf{W}\mathbf{E}_s^T\mathbf{A}^{\mathrm{c}}(\mathbf{A}^T\mathbf{A}^{\mathrm{c}})^{-1}e^{i(m-1)\omega_j}\mathbf{u}_j\\ &= \boldsymbol{\beta}_j^{\mathrm{c}}e^{i(m-1)\omega_j},\end{aligned}$$

which gives

$$\boldsymbol{\beta}_i^T \tilde{\boldsymbol{\Lambda}}^{-2} \boldsymbol{\Lambda}_s \boldsymbol{\Gamma}^* \boldsymbol{\beta}_j = \boldsymbol{\beta}_i^T \tilde{\boldsymbol{\Lambda}}^{-2} \boldsymbol{\Lambda}_s \boldsymbol{\beta}_j^{\mathrm{c}} e^{i(m-1)\omega_j} = (\boldsymbol{\beta}_j^* \tilde{\boldsymbol{\Lambda}}^{-2} \boldsymbol{\Lambda}_s \boldsymbol{\beta}_i) e^{i(m-1)\omega_j} = \mathbf{Q}_{ij}^T e^{i(m-1)\omega_j}. \quad (2.55)$$

Finally, we use **R1** and **R2** to obtain

$$\begin{aligned} \tilde{\mathbf{J}} \boldsymbol{\alpha}_j^{\mathrm{c}} &= (\mathbf{B}^T \mathbf{B}^{\mathrm{c}} \tilde{\mathbf{J}})^{-1} \mathbf{B}^T \mathbf{d}_j^{\mathrm{c}} = (\tilde{\mathbf{J}} \mathbf{B}^* \mathbf{B})^{-1} \mathbf{B}^T \mathbf{d}_j^{\mathrm{c}} \\ &= (\mathbf{B}^* \mathbf{B})^{-1} \mathbf{B}^* \mathbf{J} \mathbf{d}_j^{\mathrm{c}} = (\mathbf{B}^* \mathbf{B})^{-1} \mathbf{B}^* \mathbf{d}_j e^{-i(m-1)\omega_j}, \end{aligned}$$

which yields

$$\boldsymbol{\alpha}_i^* (\mathbf{B}^* \mathbf{B}) \tilde{\mathbf{J}} \boldsymbol{\alpha}_j^{\mathrm{c}} = \mathbf{d}_i^* \mathbf{B} (\mathbf{B}^* \mathbf{B})^{-1} \mathbf{B}^* \mathbf{d}_j e^{-i(m-1)\omega_j} = \mathbf{U}_{ij} e^{-i(m-1)\omega_j}. \quad (2.56)$$

Inserting (2.55) and (2.56) into (2.54) gives the desired expression for T_2:

$$\frac{2N}{\sigma^2} T_2 = \mathbf{Q}_{ij}^T \mathbf{U}_{ij}. \quad (2.57)$$

Combining (2.52), (2.53), and (2.57) leads to the following expression for *the asymptotic covariance matrix of FB-MODE*:

$$\mathbf{C}_{\mathrm{FB}} = \frac{\sigma^2}{2N} \Big\{ \mathrm{Re}\left[\mathbf{U} \odot \mathbf{Q}^T \right] \Big\}^{-1}. \quad (2.58)$$

Comparing (2.58) and (2.31) we see that the only difference between $\mathbf{C}_{\mathrm{FB}}$ and $\mathbf{C}_{\mathrm{F}}$ is that $\mathbf{Q}_0$ in $\mathbf{C}_{\mathrm{F}}$ is replaced by $\mathbf{Q}$ in $\mathbf{C}_{\mathrm{FB}}$. If $\mathbf{P}_0$ *is diagonal* then $\mathbf{Q} = \mathbf{Q}_0$ and hence $\mathbf{C}_{\mathrm{FB}} = \mathbf{C}_{\mathrm{F}}$. However, if $\mathbf{P}_0$ *is non-diagonal* (i.e., the signals are correlated) then, in general, $\mathbf{Q} \neq \mathbf{Q}_0$. To see this, consider for example a case where $\mathbf{P}_0$ is singular, which implies that $\mathbf{Q}_0$ is singular as well; however, $\mathbf{P}$, and hence $\mathbf{Q}$, may well be nonsingular. This example also shows that the difference matrix $\mathbf{Q}_0 - \mathbf{Q}$ is not necessarily positive semi-definite, in spite of the fact that, by the CRB inequality, we must have ($\mathbf{A} \geq \mathbf{B}$ below means that the matrix $\mathbf{A} - \mathbf{B}$ is positive semi-definite)

$$\mathbf{C}_{\mathrm{FB}} \geq \mathbf{C}_{\mathrm{F}} \quad (2.59)$$

$$\Longleftrightarrow$$

$$\mathrm{Re}\left[\mathbf{U} \odot (\mathbf{Q}_0 - \mathbf{Q}) \right] \geq \mathbf{0}. \quad (2.60)$$

(Of course, this is no contradiction because $\mathbf{Q}_0 \geq \mathbf{Q}$ is sufficient for (2.60) to hold, but it is not necessary.)

As already indicated above, the inequality in (2.59) is usually "strict" in the sense that $\mathbf{C}_{\mathrm{FB}} \neq \mathbf{C}_{\mathrm{F}}$. Every time this happens, *the FB-MODE is asymptotically statistically less efficient than the F-MODE*. To study the difference $(\mathbf{C}_{\mathrm{FB}} - \mathbf{C}_{\mathrm{F}})$ quantitatively, as well as the extent to which the asymptotic results derived above hold in samples of practical lengths, we resort to numerical simulations (see the next section).

2.7 Numerical Examples

In this section we will study the difference in performance between F-MODE and FB-MODE by means of a two signal scenario. It is a simple exercise to verify that the covariance matrices $\mathbf{P}$ and $\mathbf{P}_0$ are identical for a certain correlation phase between the two signals. Indeed, let the signal covariance matrix be given by

$$\mathbf{P}_0 = \begin{bmatrix} p_{11} & p_{12} \\ p_{12}^* & p_{22} \end{bmatrix}$$

with $p_{12} = \xi e^{i\phi}$. If the correlation phase is

$$\phi = \frac{1}{2}(m-1)(\omega_2 - \omega_1) + k\pi,$$

where k is any integer, then $\mathbf{P} = \mathbf{P}_0$. This implies that $\mathbf{R} = \mathbf{R}_0$ and hence that $\mathbf{C}_{\mathrm{F}} = \mathbf{C}_{\mathrm{FB}}$. Thus, in this special case, the large sample performance is the same for F-MODE and FB-MODE. However, as previously mentioned, in general $\mathbf{C}_{\mathrm{FB}} > \mathbf{C}_{\mathrm{F}}$. In the following, we choose ϕ so as to emphasize the difference between F-MODE and FB-MODE.

Consider a ULA consisting of four omni-directional and identical sensors separated by half of the carrier's wavelength. The two signals impinge on the array from $\theta_1 = -7.5^\circ$ and $\theta_2 = 7.5^\circ$ relative to broadside. These directions correspond to the spatial (angular) frequencies: $\omega_i = \pi \sin(\theta_i)$ $(i = 1,\ 2)$. The signal covariance is

$$\mathbf{P}_0 = 10^{\mathrm{SNR}/10} \begin{bmatrix} 1 & 0.99e^{i\pi/4} \\ 0.99e^{-i\pi/4} & 1 \end{bmatrix},$$

where SNR is expressed in decibels (dB). The correlation phase of $\pi/4 = 45^\circ$ is (close to) the "worst case," that is, the case where the difference between $\mathbf{C}_{\mathrm{FB}}$ and $\mathbf{C}_{\mathrm{F}}$ is most significant (given the other parameters). The noise variance is fixed to $\sigma^2 = 1$.

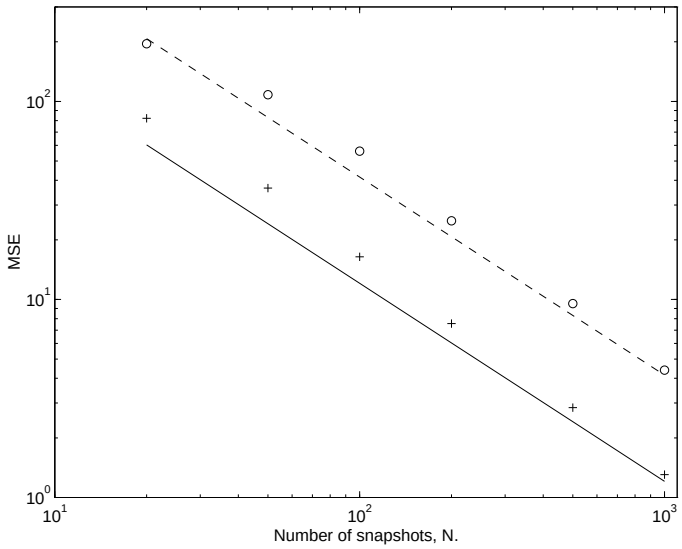

Figure 2.1: Mean square errors for θ_1 (in degrees^2) for F-MODE (+) and FB-MODE (o) versus the number of snapshots N. The solid line is the theoretical (asymptotic) MSE for F-MODE as given in (2.31), and the dashed line is the theoretical MSE for FB-MODE given in (2.58).

In the first example, SNR=0 dB. The mean-square errors (MSEs) for F-MODE and FB-MODE are compared for different sample lengths in Figure 2.1. (Only the MSE values for θ_1 are shown; the MSE plot corresponding to θ_2 is similar.) The sample MSEs are based on 1000 independent trials. In the simulations, two steps of the algorithm given in Section 2.4 were used both for F-MODE and FB-MODE. The MSE predicted by the large sample analysis is also depicted in Figure 2.1. It can be seen that the theoretical and simulation results are similar even for quite small sample lengths. It is clearly not useful to use FB-MODE in this case, not even for small samples.

In the second example, the number of samples is fixed to $N = 100$ and the SNR is varied. All other parameters are as before. The MSEs (computed from 1000 trials) are shown in Figure 2.2. We see that F-MODE outperforms FB-MODE for all SNR values.

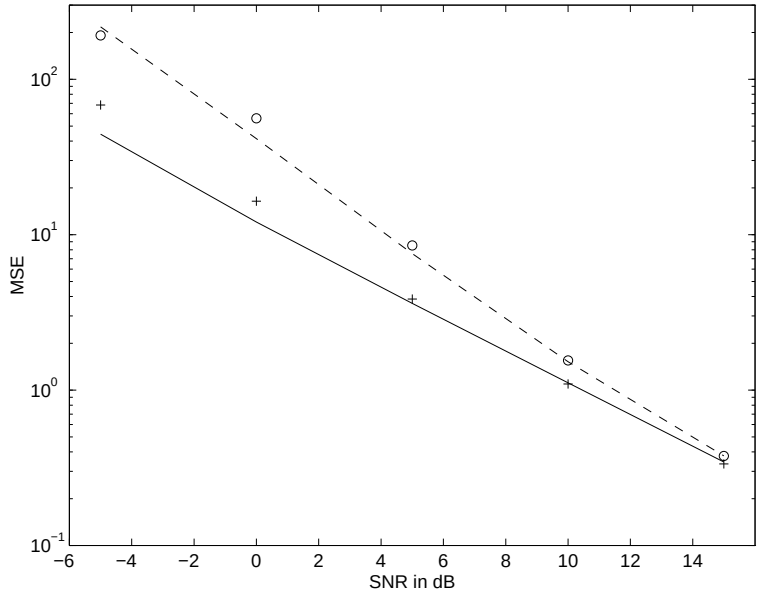

Figure 2.2: Mean square errors for θ_1 (in degrees^2) for F-MODE (+) and FB-MODE (o) versus the SNR. The solid line is the theoretical (asymptotic) MSE for F-MODE as given in (2.31), and the dashed line is the theoretical MSE for FB-MODE given in (2.58).

2.8 Conclusions

MODE is an angle-of-arrival estimator which is asymptotically statistically efficient. The standard MODE algorithm is used with the forward-only sample covariance matrix of the output of a sensor array. Here, we have applied the MODE principle to the *forward-backward* sample covariance matrix to obtain the *FB-MODE* estimator. We have shown that FB-MODE simply consists of applying the standard MODE algorithm to the eigenelements of the forward-backward covariance matrix. We have also shown that the standard MODE algorithm outperforms FB-MODE, from a statistical standpoint, in large samples. Numerical examples were presented to show that these results most often holds for small samples or

low signal-to-noise ratios as well. Thus, the forward-backward averaging should in general not be used in conjunction with MODE.

Chapter 3

Weighted Subspace Fitting for General Array Error Models

Model error sensitivity is an issue common to all high resolution direction of arrival estimators. Much attention has been directed to the design of algorithms for minimum variance estimation taking only finite sample errors into account. Approaches to reduce the sensitivity due to array calibration errors have also appeared in the literature. Herein, one such approach is adopted which assumes that the errors due to finite samples and model errors are of comparable size. Minimum variance estimators have previously been proposed for this case, but these estimators typically lead to non-linear optimization problems and are not in general consistent if the source signals are fully correlated. In this chapter, a weighted subspace fitting method for general array perturbation models is derived. This method provides minimum variance estimates under the assumption that the prior distribution of the perturbation model is known. Interestingly, the method reduces to the WSF (MODE) estimator if no model errors are present. Vice versa, assuming that model errors dominate, the method specializes to the corresponding "model-errors-only subspace fitting method". Unlike previous techniques for model errors, the estimator can be implemented using a two-step procedure if the nominal array is uniform and linear, and it is also consistent even if the signals are fully correlated. The chapter also contains a large sample analysis of one of the

alternative methods, namely, MAPprox. It is shown that MAPprox also provides minimum variance estimates under reasonable assumptions.

3.1 Introduction

All signal parameter estimation methods in array signal processing rely on information about the array response, and assume that the signal wavefronts impinging on the array have perfect spatial coherence (e.g., perfect plane waves). The array response may be determined by either empirical measurements, a process referred to as array *calibration*, or by making certain assumptions about the sensors in the array and their geometry (e.g., identical sensors in known locations).

Unfortunately, an array cannot be perfectly calibrated, and analytically derived array responses relying on the array geometry and wave propagation are at best good approximations. Due to changes in antenna location, temperature, and the surrounding environment, the response of the array may be significantly different than when it was last calibrated. Furthermore, the calibration measurements themselves are subject to gain and phase errors, and they can only be obtained for discrete angles, thus necessitating interpolation techniques for uncalibrated directions. For the case of analytically calibrated arrays of nominally identical, identically oriented elements, errors result since the elements are not really identical and their locations are not precisely known.

Because of the many sources of error listed above, the limiting factor in the performance of array signal processing algorithms is most often not measurement noise, but rather perturbations in the array response model. Depending on the size of such errors, estimates of the directions of arrival (DOAs) and the source signals may be significantly degraded. A number of studies have been conducted to quantify the performance degradation due to model errors for both DOA [ZW88, WWN88, SK90, Fri90a, Fri90b, SK92, SK93, LV92, VS94b, SH92, KSS94, KSS96] and signal estimation [RH80, Com82, Qua82, FW94, YS95]. These analyses have assumed either a deterministic model for the errors, using bias as the performance metric, or a stochastic model, where variance is typically calculated.

A number of techniques have also been considered for improving the robustness of array processing algorithms. In one such approach, the array response is parameterized not only by the DOAs of the signals, but also by perturbation or "nuisance" parameters that describe deviations

of the response from its nominal value. These parameters can include, for example, displacements of the antenna elements from their nominal positions, uncalibrated receiver gain and phase offsets, *etc.*. With such a model, a natural approach is to attempt to estimate the unknown nuisance parameters simultaneously with the signal parameters. Such methods are referred to as *auto-calibration* techniques, and have been proposed by a number of authors, including [PK85, RS87a, RS87b, WF89, WOV91, WRM94, VS94a, FFLC95, Swi96].

When auto-calibration techniques are employed, it is critical to determine whether both the signal and nuisance parameters are identifiable. In certain cases they are not; for example, one cannot uniquely estimate both DOAs and sensor positions unless of course additional information is available, such as sources in known locations [LM87, WF89, NN93, KF93], cyclostationary signals with two or more known cycle frequencies [YZ95], or partial information about the phase response of the array [MR94]. The identifiability problem can be alleviated if the perturbation parameters are assumed to be drawn from some known *a priori* distribution. While this itself represents a form of additional information, it has the advantage of allowing an optimal maximum *a posteriori* (MAP) solution to the problem to be formulated [VS94a]. In [VS94a] it is shown that, by using an asymptotically equivalent approximation to the resulting MAP criterion, the estimation of the signal and nuisance parameters can be decoupled, leading to a significant simplification of the problem.

Another technique for reducing the sensitivity of array processing algorithms to model errors is through the use of statistically optimal weightings based on probabilistic models for the errors. Optimal weightings that ignore the finite sample effects of noise have been developed for MUSIC [SK92] and the general subspace fitting technique [SK93]. A more general analysis in [VS94b] included the effects of noise, and presented a weighted subspace fitting (WSF) method whose DOA estimates asymptotically achieve the Cramér-Rao bound (CRB), but only for a very special type of array error model. On the other hand, the MAP approach in [VS94a] is asymptotically statistically efficient for very general error models. However, since it is implemented by means of *noise* subspace fitting [OVSN93], if the sources are highly correlated or closely spaced in angle, its finite sample performance may be poor. In fact, the method of [VS94a] is not a consistent estimator of the DOAs if the signals are perfectly coherent.

In this chapter, we develop a statistically efficient weighted *signal* subspace fitting (SSF) algorithm that holds for very general array per-

turbation models, that has much better finite sample performance than [VS94a] when the signals are highly correlated or closely spaced, and that yields consistent estimates when coherent sources are present. An additional advantage of our SSF formulation is that if the array is nominally uniform and linear, a two-step procedure similar to that for MODE [SS90a] can be used to eliminate the search for the DOAs. Furthermore, as part of our analysis we show that the so-called MAPprox technique described in [WOV91] also asymptotically achieves the CRB, and we draw some connections between it and the new SSF algorithm presented herein.

The weighted SSF method presented here differs from other WSF techniques like [VO91, SK93, VS94b] in that all of the elements of the vectors spanning the signal subspace have their own individual weighting [OAKP97]. In these earlier algorithms, the form of the weighting forced certain subsets of the elements to share a particular weight. It is the generalization to individual weights that is the key to the algorithm's optimality for very general array response perturbation models. For this reason, we will refer to the algorithm as generalized weighted subspace fitting (GWSF).

The chapter is organized as follows: In the next section, the data model is briefly introduced. In Section 3.3, more insight into the studied problem is given by presenting previous approaches. In Section 3.4, the proposed GWSF estimator is introduced, and its statistical properties are analyzed in Section 3.5. Details about the implementation of the algorithm are given in Section 3.6. In Section 3.7, we show that the MAPprox estimator has very close connections with GWSF and inherits the same asymptotic properties as GWSF. Finally, the theoretical observations are illustrated by numerical examples in Section 3.8.

3.2 Problem Formulation

Assume that the output of an array of m sensors is given by the model

$$\mathbf{x}(t) = \mathbf{A}(\boldsymbol{\theta}, \boldsymbol{\rho})\mathbf{s}(t) + \mathbf{n}(t),$$

where $\mathbf{s}(t)$ is a complex d-vector containing the emitted signal waveforms and $\mathbf{n}(t)$ is an additive noise vector. The array steering matrix is defined as

$$\mathbf{A}(\boldsymbol{\theta}, \boldsymbol{\rho}) = \left[\bar{\mathbf{a}}(\boldsymbol{\theta}_1, \boldsymbol{\rho}) \quad \ldots \quad \bar{\mathbf{a}}(\boldsymbol{\theta}_d, \boldsymbol{\rho})\right],$$

where $\bar{\mathbf{a}}(\boldsymbol{\theta}_i, \boldsymbol{\rho})$ denotes the array response to a unit waveform associated with the signal parameter $\boldsymbol{\theta}_i$ (possibly vector valued, although we will specialize to the scalar case). The parameters in the real n-vector $\boldsymbol{\rho}$ are used to model the uncertainty in the array steering matrix. It is assumed that $\mathbf{A}(\boldsymbol{\theta}, \boldsymbol{\rho})$ is known for a nominal value $\boldsymbol{\rho} = \boldsymbol{\rho}_0$ and that the columns in $\mathbf{A}(\boldsymbol{\theta}, \boldsymbol{\rho}_0)$ are linearly independent as long as $\boldsymbol{\theta}_i \neq \boldsymbol{\theta}_j,\ i \neq j$. The model for $\mathbf{A}(\boldsymbol{\theta}, \boldsymbol{\rho}_0)$ can be obtained for example by physical insight, or it could be the result of a calibration experiment. One may then have knowledge about the sensitivity of the nominal response to certain variations in $\boldsymbol{\rho}$, which can be modeled by considering $\boldsymbol{\rho}$ as a random vector. The *a priori* information is then in the form of a probability distribution which can be used in the design of an estimation algorithm to make it robust with regard to the model errors.

We will use a stochastic model for the signals; more precisely, $\mathbf{s}(t)$ is considered to be a zero-mean Gaussian random vector with second order moments

$$\begin{aligned} \mathrm{E}\{\mathbf{s}(t)\mathbf{s}^*(s)\} &= \mathbf{P}\delta_{t,s}, \\ \mathrm{E}\{\mathbf{s}(t)\mathbf{s}^T(s)\} &= \mathbf{0}, \end{aligned}$$

where $(\cdot)^*$ denotes complex conjugate transpose, $(\cdot)^T$ denotes transpose and $\delta_{t,s}$ is the Kronecker delta. Let d' denote the rank of the signal covariance matrix $\mathbf{P}$. Special attention will be given to cases where $d' < d$, i.e., cases in which the signals may be fully correlated (coherent). In particular, we show that the proposed method is consistent even under such severe conditions. The noise is modeled as a zero-mean spatially and temporally white complex Gaussian vector with second order moments

$$\begin{aligned} \mathrm{E}\{\mathbf{n}(t)\mathbf{n}^*(s)\} &= \sigma^2\mathbf{I}\delta_{t,s}, \\ \mathrm{E}\{\mathbf{n}(t)\mathbf{n}^T(s)\} &= \mathbf{0}. \end{aligned}$$

The perturbation parameter vector $\boldsymbol{\rho}$ is modeled as a Gaussian random variable with mean $\mathrm{E}\{\boldsymbol{\rho}\} = \boldsymbol{\rho}_0$ and covariance

$$\mathrm{E}\{(\boldsymbol{\rho} - \boldsymbol{\rho}_0)(\boldsymbol{\rho} - \boldsymbol{\rho}_0)^T\} = \boldsymbol{\Omega}.$$

It is assumed that both $\boldsymbol{\rho}_0$ and $\boldsymbol{\Omega}$ are known. Similar to [VS94b, VS94a], we consider small perturbations in $\boldsymbol{\rho}$ and more specifically assume that the effect of the array errors on the estimates of $\boldsymbol{\theta}$ is of comparable size to those due to the finite sample effects of the noise. To model this, we

assume that

$$\mathbf{\Omega} = \bar{\mathbf{\Omega}}/N,$$

where N is the number of samples and $\bar{\mathbf{\Omega}}$ is independent of N. This somewhat artificial assumption concerning the model errors is made only for convenience in showing the statistical optimality of the algorithm presented later. An identical result can be obtained for small $\boldsymbol{\rho} - \boldsymbol{\rho}_0$ if a first order perturbation analysis is used, but this approach is somewhat less elegant. The assumption that $\boldsymbol{\rho} - \boldsymbol{\rho}_0 = O_p(1/\sqrt{N})$ implies that the calibration errors and finite sample effects are of comparable size. (The notation $\boldsymbol{\xi} = O_p(1/\sqrt{N})$ means that $\sqrt{N}\boldsymbol{\xi}$ tends to a constant in probability as $N \to \infty$.) Despite this fact, we will see that the resulting algorithm is optimal also for the following limiting cases:

- $N \to \infty$ for fixed $(\boldsymbol{\rho} - \boldsymbol{\rho}_0)$ – (model errors only),
- $(\boldsymbol{\rho} - \boldsymbol{\rho}_0) \to 0$ for fixed N – (finite sample errors only).

In other words, for each of the above cases, the proposed technique converges to an algorithm that has previously been shown to be statistically efficient for that case. We can thus conclude that the algorithm is globally optimal, not just under the assumption $\boldsymbol{\rho} - \boldsymbol{\rho}_0 = O_p(1/\sqrt{N})$.

3.3 Robust Estimation

This section introduces some of the previous approaches taken to solve the problem considered in this chapter. The Cramér Rao lower bound is also restated from [VS94a].

3.3.1 MAP

As the problem has been formulated, it is natural to use a maximum a posteriori (MAP) estimator. Following [WOV91], the cost function to be minimized for simultaneous estimation of signal and perturbation parameters is

$$V_{\mathrm{MAP}}(\boldsymbol{\theta}, \boldsymbol{\rho}) = V_{\mathrm{ML}}(\boldsymbol{\theta}, \boldsymbol{\rho}) + \frac{1}{2}(\boldsymbol{\rho} - \boldsymbol{\rho}_0)^T \mathbf{\Omega}^{-1}(\boldsymbol{\rho} - \boldsymbol{\rho}_0).$$

$V_{\mathrm{ML}}(\boldsymbol{\theta}, \boldsymbol{\rho})$ is the concentrated negative log-likelihood function and is given by (see, e.g., [Böh86, Jaf88])

$$V_{\mathrm{ML}}(\boldsymbol{\theta}, \boldsymbol{\rho}) = N \log \det\{\mathbf{A}\hat{\mathbf{P}}\mathbf{A}^* + \hat{\sigma}^2\mathbf{I}\},$$

where for brevity we have suppressed the arguments and where constant terms have been neglected. Here, $\hat{\mathbf{P}} = \hat{\mathbf{P}}(\boldsymbol{\theta}, \boldsymbol{\rho})$ and $\hat{\sigma}^2 = \hat{\sigma}^2(\boldsymbol{\theta}, \boldsymbol{\rho})$ denote the maximum likelihood estimates of $\mathbf{P}$ and σ^2, respectively. They are explicitly given by:

$$\begin{aligned}\hat{\sigma}^2(\boldsymbol{\theta}, \boldsymbol{\rho}) &= \frac{1}{m-d} \operatorname{Tr}\{\boldsymbol{\Pi}_{\mathbf{A}}^{\perp}(\boldsymbol{\theta}, \boldsymbol{\rho})\hat{\mathbf{R}}\}, \\ \hat{\mathbf{P}}(\boldsymbol{\theta}, \boldsymbol{\rho}) &= \mathbf{A}^{\dagger}(\boldsymbol{\theta}, \boldsymbol{\rho}) \left(\hat{\mathbf{R}} - \hat{\sigma}^2(\boldsymbol{\theta}, \boldsymbol{\rho})\mathbf{I}\right) \mathbf{A}^{\dagger *}(\boldsymbol{\theta}, \boldsymbol{\rho}),\end{aligned} \tag{3.1}$$

where

$$\begin{aligned}\hat{\mathbf{R}} &= \frac{1}{N}\sum_{t=1}^{N} \mathbf{x}(t)\mathbf{x}^*(t), \\ \mathbf{A}^{\dagger} &= (\mathbf{A}^*\mathbf{A})^{-1}\mathbf{A}^*, \\ \boldsymbol{\Pi}_{\mathbf{A}}^{\perp} &= \mathbf{I} - \mathbf{A}\mathbf{A}^{\dagger}.\end{aligned}$$

For large N, it is further argued in [WOV91] that $V_{\mathrm{ML}}(\boldsymbol{\theta}, \boldsymbol{\rho})$ can be replaced with any other cost function that has the same large sample behavior as ML. In particular, it was proposed that the weighted subspace fitting (WSF) cost function [VO91] be used. This results in

$$V_{\text{MAP-WSF}}(\boldsymbol{\theta}, \boldsymbol{\rho}) = \frac{N}{\hat{\sigma}^2} V_{\mathrm{WSF}}(\boldsymbol{\theta}, \boldsymbol{\rho}) + \frac{1}{2}(\boldsymbol{\rho} - \boldsymbol{\rho}_0)^T \boldsymbol{\Omega}^{-1}(\boldsymbol{\rho} - \boldsymbol{\rho}_0), \tag{3.2}$$

where

$$V_{\mathrm{WSF}}(\boldsymbol{\theta}, \boldsymbol{\rho}) = \operatorname{Tr}\{\boldsymbol{\Pi}_{\mathbf{A}}^{\perp}(\boldsymbol{\theta}, \boldsymbol{\rho})\hat{\mathbf{E}}_s \hat{\mathbf{W}}_{\mathrm{WSF}} \hat{\mathbf{E}}_s^*\}. \tag{3.3}$$

Here, $\hat{\mathbf{E}}_s$ and $\hat{\mathbf{W}}_{\mathrm{WSF}}$ are defined via the eigendecomposition of $\hat{\mathbf{R}}$

$$\hat{\mathbf{R}} = \hat{\mathbf{E}}_s \hat{\boldsymbol{\Lambda}}_s \hat{\mathbf{E}}_s^* + \hat{\mathbf{E}}_n \hat{\boldsymbol{\Lambda}}_n \hat{\mathbf{E}}_n^*, \tag{3.4}$$

where $\hat{\boldsymbol{\Lambda}}_s$ is a diagonal matrix containing the d' largest eigenvalues and $\hat{\mathbf{E}}_s$ is composed of the corresponding eigenvectors. The WSF weighting matrix is defined as

$$\hat{\mathbf{W}}_{\mathrm{WSF}} = \hat{\tilde{\boldsymbol{\Lambda}}}^2 \hat{\boldsymbol{\Lambda}}_s^{-1},$$

where $\hat{\tilde{\boldsymbol{\Lambda}}} = \hat{\boldsymbol{\Lambda}}_s - \hat{\sigma}^2\mathbf{I}$ and $\hat{\sigma}^2$ is a consistent estimate of σ^2 (for example, the average of the $m - d'$ smallest eigenvalues of $\hat{\mathbf{R}}$). The normalizing factor $N/\hat{\sigma}^2$ in (3.2) is important to make the partial derivatives of

$N\,V_{\mathrm{WSF}}/\hat{\sigma}^2$ and V_{ML} with respect to $\boldsymbol{\theta}$ and $\boldsymbol{\rho}$ of comparable size locally around $\{\boldsymbol{\theta}_0, \boldsymbol{\rho}\}$. More precisely,

$$\left.\frac{\partial V_{\mathrm{ML}}}{\partial \eta}\right|_{\boldsymbol{\theta}_0,\boldsymbol{\rho}} = \frac{N}{\hat{\sigma}^2}\left.\frac{\partial V_{\mathrm{WSF}}}{\partial \eta}\right|_{\boldsymbol{\theta}_0,\boldsymbol{\rho}} + o_p(\sqrt{N}),$$

where η denotes a generic component of the vector $[\boldsymbol{\theta}^T\ \boldsymbol{\rho}^T]^T$, and where $o_p(\cdot)$ represents a term that tends to zero faster than its argument in probability. The minimization of either V_{MAP} or $V_{\text{MAP-WSF}}$ is over both $\boldsymbol{\theta}$ and $\boldsymbol{\rho}$. The idea of the methods presented in the following two sections is to eliminate the need for an explicit minimization over $\boldsymbol{\rho}$.

3.3.2 MAPprox

In [WOV91] it is suggested that the minimization of $V_{\text{MAP-WSF}}$ over $\boldsymbol{\rho}$ can be done implicitly. Assuming that $\boldsymbol{\rho} - \boldsymbol{\rho}_0$ is small, a second order Taylor expansion of $V_{\text{MAP-WSF}}$ around $\boldsymbol{\rho}_0$ is performed, and then the result is analytically minimized with regard to $\boldsymbol{\rho}$. This leads to a concentrated form of the cost function

$$\begin{aligned} &V_{\mathrm{MAPprox}}(\boldsymbol{\theta}) \\ &= \frac{N}{\hat{\sigma}^2}\left\{V_{\mathrm{WSF}} - \frac{1}{2}\partial_{\boldsymbol{\rho}} V_{\mathrm{WSF}}^T \left(\partial_{\boldsymbol{\rho}\boldsymbol{\rho}} V_{\mathrm{WSF}} + \frac{\hat{\sigma}^2}{N}\boldsymbol{\Omega}^{-1}\right)^{-1} \partial_{\boldsymbol{\rho}} V_{\mathrm{WSF}}\right\}, \end{aligned} \tag{3.5}$$

where $\partial_{\boldsymbol{\rho}} V_{\mathrm{WSF}}$ denotes the gradient of V_{WSF} with respect to $\boldsymbol{\rho}$ and $\partial_{\boldsymbol{\rho}\boldsymbol{\rho}} V_{\mathrm{WSF}}$ denotes the Hessian. The right hand side of (3.5) is evaluated at $\boldsymbol{\rho}_0$ and $\boldsymbol{\theta}$. The method is referred to as *MAPprox*. In Section 3.7 we analyze the asymptotic properties of the MAPprox estimates and point out its relationship to the GWSF estimator derived in Section 3.4.

3.3.3 MAP-NSF

Another method for approximating the MAP estimator is the MAP-NSF approach of [VS94a]. In MAP-NSF, one uses the fact that the noise subspace fitting (NSF) method is also asymptotically equivalent to ML [OVSN93]. Thus, in lieu of using the WSF criterion in (3.2), the NSF cost function

$$V_{\mathrm{NSF}} = \mathrm{Tr}\{\mathbf{A}^*\hat{\mathbf{E}}_n\hat{\mathbf{E}}_n^*\mathbf{A}\hat{\mathbf{U}}\} \tag{3.6}$$

is employed. Here, $\hat{\mathbf{U}}$ is a consistent estimate of the matrix

$$\mathbf{U} = \mathbf{A}^{\dagger}\mathbf{E}_s\widetilde{\mathbf{\Lambda}}^2\mathbf{\Lambda}_s^{-1}\mathbf{E}_s^*\mathbf{A}^{\dagger^*}.$$

As shown below, this also leads to an explicit solution for $\boldsymbol{\rho}$ when $\boldsymbol{\rho} - \boldsymbol{\rho}_0$ is small.

The NSF cost function can be rewritten using the following general identities:

$$\mathrm{Tr}\{\mathbf{AB}\} = \mathrm{vec}^T(\mathbf{A}^T)\,\mathrm{vec}(\mathbf{B}) \tag{3.7}$$

$$\mathrm{vec}(\mathbf{ABC}) = \left(\mathbf{C}^T \otimes \mathbf{A}\right)\mathrm{vec}(\mathbf{B}), \tag{3.8}$$

where $\mathrm{vec}(\cdot)$ is the vectorization operation and $\otimes$ denotes the Kronecker matrix product [Bre78, Gra81]. An equivalent form of (3.6) is then given by

$$V_{\mathrm{NSF}} = \mathbf{a}^*\hat{\mathbf{M}}\mathbf{a},$$

where

$$\begin{aligned}\mathbf{a} &= \mathrm{vec}(\mathbf{A}),\\ \hat{\mathbf{M}} &= \hat{\mathbf{U}}^T \otimes (\hat{\mathbf{E}}_n\hat{\mathbf{E}}_n^*).\end{aligned} \tag{3.9}$$

The next idea is to approximate the steering matrix around $\boldsymbol{\rho}_0$. A first-order Taylor expansion gives

$$\mathbf{a}(\boldsymbol{\theta}, \boldsymbol{\rho}) \approx \mathbf{a}_0 + \mathbf{D}_{\boldsymbol{\rho}}(\boldsymbol{\rho} - \boldsymbol{\rho}_0), \tag{3.10}$$

where

$$\begin{aligned}\mathbf{a}_0 &= \mathbf{a}(\boldsymbol{\theta}, \boldsymbol{\rho}_0),\\ \mathbf{D}_{\boldsymbol{\rho}} &= \left[\frac{\partial \mathbf{a}(\boldsymbol{\theta},\boldsymbol{\rho})}{\partial \boldsymbol{\rho}_1} \quad \dots \quad \frac{\partial \mathbf{a}(\boldsymbol{\theta},\boldsymbol{\rho})}{\partial \boldsymbol{\rho}_n}\right]\Big|_{\boldsymbol{\theta},\boldsymbol{\rho}_0}.\end{aligned} \tag{3.11}$$

Since the derivatives of both $\mathbf{a}$ and the approximation in (3.10) with respect to any parameter in $\boldsymbol{\theta}$ or $\boldsymbol{\rho}$ are identical when evaluated at $\boldsymbol{\rho}_0$, it can be shown that this approximation will not affect the asymptotic properties of the estimates. Inserting (3.10) in (3.6) and using the resulting cost function to replace V_{WSF} in (3.2) leads to

$$\frac{N}{\hat{\sigma}^2}(\mathbf{a}_0 + \mathbf{D}_{\boldsymbol{\rho}}\tilde{\boldsymbol{\rho}})^*\hat{\mathbf{M}}(\mathbf{a}_0 + \mathbf{D}_{\boldsymbol{\rho}}\tilde{\boldsymbol{\rho}}) + \frac{1}{2}\tilde{\boldsymbol{\rho}}^T\mathbf{\Omega}^{-1}\tilde{\boldsymbol{\rho}}, \tag{3.12}$$

where $\tilde{\boldsymbol{\rho}} = \boldsymbol{\rho} - \boldsymbol{\rho}_0$. This cost function is quadratic in $\boldsymbol{\rho}$ and can thus, for fixed $\boldsymbol{\theta}$, be explicitly minimized with respect to $\boldsymbol{\rho}$. Substituting the solution for $\boldsymbol{\rho}$ back into (3.12) gives

$$V_{\text{MAP-NSF}}(\boldsymbol{\theta}) = \mathbf{a}_0^* \hat{\mathbf{M}} \mathbf{a}_0 - \hat{\mathbf{f}}^T \hat{\boldsymbol{\Gamma}}^{-1} \hat{\mathbf{f}}, \tag{3.13}$$

where

$$\begin{aligned} \hat{\mathbf{f}} &= \text{Re}\{\mathbf{D}_{\boldsymbol{\rho}}^* \hat{\mathbf{M}} \mathbf{a}_0\}, \\ \hat{\boldsymbol{\Gamma}} &= \text{Re}\{\mathbf{D}_{\boldsymbol{\rho}}^* \hat{\mathbf{M}} \mathbf{D}_{\boldsymbol{\rho}} + \frac{\hat{\sigma}^2}{2} \bar{\boldsymbol{\Omega}}^{-1}\}. \end{aligned} \tag{3.14}$$

The function in (3.13) depends on $\boldsymbol{\theta}$ via $\mathbf{a}_0$ and $\mathbf{D}_{\boldsymbol{\rho}}$. It is noted in [VS94a] that $\mathbf{D}_{\boldsymbol{\rho}}$ (and $\hat{\mathbf{M}}$) can be replaced with a consistent estimate without affecting the large sample second order properties.

The following procedure is suggested by the derivations above:

1. Compute the eigendecomposition of $\hat{\mathbf{R}}$. Obtain a consistent estimate of $\boldsymbol{\theta}$ using, for example, MUSIC.

2. Based on the estimate from the first step, compute consistent estimates of $\mathbf{D}_{\boldsymbol{\rho}}$ and $\hat{\mathbf{M}}$. Insert these estimates in the cost function (3.13), which thus depends on $\boldsymbol{\theta}$ only via $\mathbf{a}_0$. Take the minimizing argument of the resulting cost function as the MAP-NSF estimate of $\boldsymbol{\theta}$.

In [VS94a], the statistical properties of the MAP-NSF estimate of $\boldsymbol{\theta}$ are analyzed. It is shown that MAP-NSF is a consistent and asymptotically efficient estimator if $d' = d$. This means that the asymptotic covariance matrix of the estimation error in $\boldsymbol{\theta}$ is equal to the Cramér-Rao lower bound given in the next section.

3.3.4 Cramér Rao Lower Bound

In [WOV91, VS94a] an asymptotically valid Cramér Rao lower bound is derived for the problem of interest herein. Below we give the lower bound on the signal parameters only.

Theorem 3.1. *Assuming that $\hat{\boldsymbol{\theta}}$ is an asymptotically unbiased estimate of $\boldsymbol{\theta}_0$, then for large N,*

$$\text{E}\{(\hat{\boldsymbol{\theta}} - \boldsymbol{\theta}_0)(\hat{\boldsymbol{\theta}} - \boldsymbol{\theta}_0)^T\} \geq \mathbf{CRB}_{\boldsymbol{\theta}} \triangleq \frac{\sigma^2}{2N} \left[\mathbf{C} - \mathbf{F}_{\boldsymbol{\theta}}^T \boldsymbol{\Gamma}^{-1} \mathbf{F}_{\boldsymbol{\theta}}\right]^{-1}, \tag{3.15}$$

where[1]

$$\begin{aligned}
\mathbf{C} &= \mathrm{Re}\{\mathbf{D}_{\boldsymbol{\theta}}^{*}\mathbf{M}\mathbf{D}_{\boldsymbol{\theta}}\}, \\
\mathbf{M} &= \mathbf{U}^{T} \otimes \boldsymbol{\Pi}_{\mathbf{A}}^{\perp}, \qquad (3.16) \\
\mathbf{D}_{\boldsymbol{\theta}} &= \left[\frac{\partial \mathbf{a}(\boldsymbol{\theta},\boldsymbol{\rho})}{\partial \boldsymbol{\theta}_1} \quad \cdots \quad \frac{\partial \mathbf{a}(\boldsymbol{\theta},\boldsymbol{\rho})}{\partial \boldsymbol{\theta}_d} \right], \\
\mathbf{F}_{\boldsymbol{\theta}} &= \mathrm{Re}\{\mathbf{D}_{\boldsymbol{\rho}}^{*}\mathbf{M}\mathbf{D}_{\boldsymbol{\theta}}\}, \qquad (3.17) \\
\boldsymbol{\Gamma} &= \mathrm{Re}\{\mathbf{D}_{\boldsymbol{\rho}}^{*}\mathbf{M}\mathbf{D}_{\boldsymbol{\rho}} + \frac{\sigma^2}{2}\bar{\boldsymbol{\Omega}}^{-1}\}. \qquad (3.18)
\end{aligned}$$

The above expressions are evaluated at $\boldsymbol{\theta}_0$ *and* $\boldsymbol{\rho}_0$.

Proof. See [WOV91, VS94a]. □

It is important to notice that the CRB for the case with no calibration errors is $\sigma^2\mathbf{C}^{-1}/2N$ and clearly is a lower bound for the MAP-CRB.

3.4 Generalized Weighted Subspace Fitting (GWSF)

It was shown in [VS94a] that the MAP-NSF method is asymptotically statistically efficient. One drawback with MAP-NSF is that it is not consistent if the sources are fully correlated, that is, if $d' < d$. This problem can be overcome in the *signal* subspace formulation. In this section, we derive a new method in the signal subspace fitting (SSF) class of algorithms. The method will be shown to possess the same large sample performance as MAP-NSF and is thus also asymptotically efficient. A further advantage of the proposed SSF approach is that the cost function depends on the parameters in a relatively simple manner and, if the nominal array is uniform and linear, the non-linear minimization can be replaced by a rooting technique (see Section 3.6).

According to the problem formulation, $\hat{\mathbf{R}} - \mathbf{R} = O_p(1/\sqrt{N})$, where

$$\mathbf{R} = \mathrm{E}\{\mathbf{x}(t)\mathbf{x}^{*}(t)\} = \mathbf{A}_0\mathbf{P}\mathbf{A}_0^{*} + \sigma^2\mathbf{I}$$

and $\mathbf{A}_0 = \mathbf{A}(\boldsymbol{\theta}_0, \boldsymbol{\rho}_0)$. This implies that $\hat{\mathbf{E}}_s \to \mathbf{E}_s = \mathbf{A}_0\mathbf{T}$ at the same rate, where $\mathbf{T}$ is a $d \times d'$ full rank matrix. The idea of the proposed method is to minimize a suitable norm of the residuals

$$\boldsymbol{\varepsilon} = \mathrm{vec}(\mathbf{B}^{*}(\boldsymbol{\theta})\hat{\mathbf{E}}_s),$$

[1] Notice that $\mathbf{M}$ is the limit of $\hat{\mathbf{M}}$ defined in (3.9) if $d' = d$.

where $\mathbf{B}(\boldsymbol{\theta})$ is an $m \times (m-d)$ full rank matrix whose columns span the null-space of $\mathbf{A}^*(\boldsymbol{\theta})$. This implies that $\mathbf{B}^*(\boldsymbol{\theta})\mathbf{A}(\boldsymbol{\theta}) = \mathbf{0}$ and $\mathbf{B}^*(\boldsymbol{\theta}_0)\mathbf{E}_s = \mathbf{0}$.

Remark 3.1. For general arrays, there is no known closed form parameterization of $\mathbf{B}$ in terms of $\boldsymbol{\theta}$. However, this will not introduce any problems since, as we show in Section 3.6, the final criterion can be written as an explicit function of $\boldsymbol{\theta}$.

For general array error models, we have to consider the real and imaginary parts of $\boldsymbol{\varepsilon}$ separately to get optimal (minimum variance) performance. Equivalently, we may study $\boldsymbol{\varepsilon}$ and its complex conjugate, which we denote by $\boldsymbol{\varepsilon}^c$ (cf. Section 2.3.5). We believe that the analysis of the method is clearer if $\boldsymbol{\varepsilon}$ and $\boldsymbol{\varepsilon}^c$ are used instead of the real and imaginary parts. However, from an implementational point of view, it may be more suitable to use real arithmetic. Before presenting the estimation criterion, we define:

$$\hat{\mathbf{e}}_s = \begin{bmatrix} \mathrm{vec}(\hat{\mathbf{E}}_s) \\ \mathrm{vec}(\hat{\mathbf{E}}_s^c) \end{bmatrix},$$

$$\bar{\mathbf{A}} = \begin{bmatrix} (\mathbf{I}_{d'} \otimes \mathbf{A}) & \mathbf{0} \\ \mathbf{0} & (\mathbf{I}_{d'} \otimes \mathbf{A}^c) \end{bmatrix},$$

$$\bar{\mathbf{B}} = \begin{bmatrix} (\mathbf{I}_{d'} \otimes \mathbf{B}) & \mathbf{0} \\ \mathbf{0} & (\mathbf{I}_{d'} \otimes \mathbf{B}^c) \end{bmatrix},$$

and

$$\bar{\boldsymbol{\varepsilon}} = \begin{bmatrix} \boldsymbol{\varepsilon} \\ \boldsymbol{\varepsilon}^c \end{bmatrix} = \bar{\mathbf{B}}^* \hat{\mathbf{e}}_s.$$

Notice that the columns of $\bar{\mathbf{B}}$ span the null-space of $\bar{\mathbf{A}}^*$.

We propose to estimate the signal parameters $\boldsymbol{\theta}$ as follows:

$$\hat{\boldsymbol{\theta}} = \arg\min_{\boldsymbol{\theta}} V_{\mathrm{GWSF}}(\boldsymbol{\theta}), \tag{3.19}$$

$$V_{\mathrm{GWSF}}(\boldsymbol{\theta}) = \bar{\boldsymbol{\varepsilon}}^*(\boldsymbol{\theta})\mathbf{W}\bar{\boldsymbol{\varepsilon}}(\boldsymbol{\theta}), \tag{3.20}$$

where $\mathbf{W}$ is a positive definite weighting matrix. The method will in the sequel be referred to as the *generalized weighted subspace fitting (GWSF)* method. To derive the weighting that leads to minimum variance estimates of $\boldsymbol{\theta}$, we need to compute the residual covariance matrix. As shown in Appendix A.2, the (asymptotic) second order moment of the residual

vector $\bar{\varepsilon}$ at $\boldsymbol{\theta}_0$

$$\mathbf{C}_{\bar{\varepsilon}} = \lim_{N\to\infty} N\ \mathrm{E}\{\bar{\varepsilon}\bar{\varepsilon}^*\} \tag{3.21}$$

can be written as

$$\mathbf{C}_{\bar{\varepsilon}} = \bar{\mathbf{L}} + \bar{\mathbf{G}}\bar{\mathbf{G}}^*, \tag{3.22}$$

where we have defined

$$\bar{\mathbf{L}} = \begin{bmatrix} \mathbf{L} & \mathbf{0} \\ \mathbf{0} & \mathbf{L}^c \end{bmatrix}, \tag{3.23}$$

$$\mathbf{L} = \left(\sigma^2 \widetilde{\boldsymbol{\Lambda}}^{-2} \boldsymbol{\Lambda}_s \otimes \mathbf{B}^*\mathbf{B}\right),$$

$$\bar{\mathbf{G}} = \begin{bmatrix} \mathbf{G} \\ \mathbf{G}^c \end{bmatrix}, \tag{3.24}$$

$$\mathbf{G} = \left(\mathbf{T}^T \otimes \mathbf{B}^*\right) \mathbf{D}_{\boldsymbol{\rho}} \bar{\boldsymbol{\Omega}}^{1/2}.$$

Here, $\bar{\boldsymbol{\Omega}}^{1/2}$ is a (symmetric) square root of $\bar{\boldsymbol{\Omega}}$ and $\mathbf{T} = \mathbf{A}_0^{\dagger}\mathbf{E}_s$. It is easy to see that $\mathbf{C}_{\bar{\varepsilon}}$ is positive definite since $\mathbf{L}$ is. It is then well known that (in the class of estimators based on $\bar{\varepsilon}$) the optimal choice of the weighting in terms of minimizing the parameter estimation error variance is

$$\mathbf{W}_{\mathrm{GWSF}} = \mathbf{C}_{\bar{\varepsilon}}^{-1} \tag{3.25}$$

(see, e.g., Section 2.3.5 and [SS89]). In the next section it is proven that this weighting in fact also gives asymptotically (in N) minimum variance estimates (in the class of unbiased estimators) for the estimation problem under consideration. The implementation of GWSF is discussed in Section 3.6. We conclude this section with two remarks regarding the GWSF formulation.

Remark 3.2. If there are no model errors, then GWSF reduces to the WSF estimator (3.3). This can easily be verified by setting $\bar{\boldsymbol{\Omega}} = \mathbf{0}$ and rewriting the GWSF criterion (3.20).

Remark 3.3. For the case of model errors only ($N \to \infty$ or $\sigma^2 \to 0$), GWSF becomes the "model errors only" algorithm [SK93]. The results obtained for GWSF are also consistent with weightings given in [VS94b] for special array error models.

Thus, the GWSF method can be considered to be optimal in general, and not just when the model errors and the finite sample effects are of the same order.

3.5 Performance Analysis

The asymptotic properties of the GWSF estimates are analyzed in this section. It is shown that the estimates are consistent and have a limiting Gaussian distribution. It is also shown that the asymptotic covariance matrix of the estimation error is equal to the CRB.

3.5.1 Consistency

The cost function (3.20) converges uniformly in $\boldsymbol{\theta}$ with probability one (w.p.1) to the limit

$$\bar{V}_{\mathrm{GWSF}}(\boldsymbol{\theta}) = \left[\mathrm{vec}^*(\mathbf{B}^*(\boldsymbol{\theta})\mathbf{E}_s) \quad \mathrm{vec}^T(\mathbf{B}^*(\boldsymbol{\theta})\mathbf{E}_s)\right] \mathbf{W} \begin{bmatrix} \mathrm{vec}(\mathbf{B}^*(\boldsymbol{\theta})\mathbf{E}_s) \\ \mathrm{vec}^c(\mathbf{B}^*(\boldsymbol{\theta})\mathbf{E}_s) \end{bmatrix}. \tag{3.26}$$

This implies that $\hat{\boldsymbol{\theta}}$ converges to the minimizing argument of (3.26). Since $\mathbf{W}$ is positive definite, $\bar{V}_{\mathrm{GWSF}}(\boldsymbol{\theta}) \geq 0$ with equality if and only if $\mathbf{B}^*(\boldsymbol{\theta})\mathbf{E}_s = \mathbf{0}$. However, it is proven by [WZ89] that this uniquely determines $\boldsymbol{\theta}_0$ if $d < (m + d')/2$. We have thus proven that $\hat{\boldsymbol{\theta}}$ in (3.19) tends to $\boldsymbol{\theta}_0$ w.p.1 as $N \to \infty$.

3.5.2 Asymptotic Distribution

In this section we derive the asymptotic distribution of the GWSF estimates (3.19). As already mentioned, there exists a certain weighting matrix (3.25) that minimizes the estimation error variance. This matrix depends on the true parameters and, in practice, has to be replaced with a consistent estimate. However, this will not change the second order asymptotic properties considered herein. In fact it is easy to see below that the derivative of the cost function with respect to $\mathbf{W}$ only leads to higher order terms. Thus, whether $\mathbf{W}$ is considered as a fixed matrix or a consistent estimate thereof does not matter for the analysis in this section.

The estimate that minimizes (3.20) satisfies by definition $V'(\hat{\boldsymbol{\theta}}) = \mathbf{0}$, and since $\hat{\boldsymbol{\theta}}$ is consistent, a Taylor series expansion of $V'(\hat{\boldsymbol{\theta}})$ around $\boldsymbol{\theta}_0$ leads to

$$\tilde{\boldsymbol{\theta}} = -\mathbf{H}^{-1}V' + o_p(1/\sqrt{N}), \tag{3.27}$$

where $\tilde{\boldsymbol{\theta}} = \hat{\boldsymbol{\theta}} - \boldsymbol{\theta}_0$, $\mathbf{H}$ is the limiting Hessian, and V' is the gradient of $V(\boldsymbol{\theta})$. Both V' and $\mathbf{H}$ are evaluated at $\boldsymbol{\theta}_0$. In the following, let the index

i denote the partial derivative with respect to $\boldsymbol{\theta}_i$. The derivative of $V(\boldsymbol{\theta})$ is given by

$$\begin{aligned} V_i' &= \bar{\boldsymbol{\varepsilon}}_i^* \mathbf{W} \bar{\boldsymbol{\varepsilon}} + \bar{\boldsymbol{\varepsilon}}^* \mathbf{W} \bar{\boldsymbol{\varepsilon}}_i \\ &= 2 \operatorname{Re} \{ \bar{\boldsymbol{\varepsilon}}_i^* \mathbf{W} \bar{\boldsymbol{\varepsilon}} \} . \end{aligned} \tag{3.28}$$

It is straightforward to verify that $\bar{\boldsymbol{\varepsilon}}_i^* \mathbf{W} \bar{\boldsymbol{\varepsilon}}$ is real for any weighting matrix having the form

$$\mathbf{W} = \begin{bmatrix} \mathbf{W}_{11} & \mathbf{W}_{12} \\ \mathbf{W}_{12}^c & \mathbf{W}_{11}^c \end{bmatrix} . \tag{3.29}$$

In particular, the matrix $\mathbf{W}_{\mathrm{GWSF}}$ in (3.25) has this structure. Next notice that $\bar{\boldsymbol{\varepsilon}} = \bar{\mathbf{B}}^* \hat{\mathbf{e}}_s$ and thus

$$\bar{\boldsymbol{\varepsilon}}_i = \bar{\mathbf{B}}_i^* \hat{\mathbf{e}}_s = \bar{\mathbf{B}}_i^* \mathbf{e}_s + o_p(1), \tag{3.30}$$

where $\mathbf{e}_s$ denotes the limit of $\hat{\mathbf{e}}_s$. Define the vector

$$\mathbf{k}_i = \bar{\mathbf{B}}_i^* \mathbf{e}_s = \begin{bmatrix} \operatorname{vec}(\mathbf{B}_i^* \mathbf{E}_s) \\ \operatorname{vec}(\mathbf{B}_i^* \mathbf{E}_s)^c \end{bmatrix} ,$$

and insert (3.30) in (3.28) to show that

$$V_i' \simeq 2 \mathbf{k}_i^* \mathbf{W} \bar{\boldsymbol{\varepsilon}}, \tag{3.31}$$

for any $\mathbf{W}$ satisfying (3.29), where $\simeq$ represents an equality up to first order; that is, terms of order $o_p(1/\sqrt{N})$ are omitted. Recall the relation (A.5) and that $\sqrt{N}(\hat{\mathbf{R}} - \mathbf{R})$ is asymptotically Gaussian by the central limit theorem. By (3.27) and (3.31) we thus conclude that the normalized estimation error has a limiting Gaussian distribution

$$\sqrt{N} \tilde{\boldsymbol{\theta}} \in \mathrm{AsN}(\mathbf{0}, \mathbf{H}^{-1} \mathbf{Q} \mathbf{H}^{-1}),$$

where

$$\mathbf{Q} = \lim_{N \to \infty} N \ \mathrm{E}\{ V' V'^T \}, \tag{3.32}$$

and where the notation AsN means asymptotically Gaussian distributed. In summary we have the following result.

Theorem 3.2. *If $d < (m + d')/2$, then the GWSF estimate* (3.19) *tends to $\boldsymbol{\theta}_0$ w.p.1 as $N \to \infty$, and*

$$\sqrt{N}(\hat{\boldsymbol{\theta}} - \boldsymbol{\theta}_0) \in \mathrm{AsN}(\mathbf{0}, \mathbf{H}^{-1} \mathbf{Q} \mathbf{H}^{-1}).$$

If $\mathbf{W} = \mathbf{W}_{GWSF}$ *given in* (3.25)*, then*

$$\mathbf{H}^{-1}\mathbf{Q}\mathbf{H}^{-1} = N\,\mathbf{CRB}_{\boldsymbol{\theta}}.$$

Expressions for $\mathbf{H}$ *and* $\mathbf{Q}$ *can be found in Appendix A.3 and* $\mathbf{CRB}_{\boldsymbol{\theta}}$ *is given in* (3.15)*. All quantities are evaluated at* $\boldsymbol{\theta}_0$*.*

Proof. The result follows from the analysis above and the calculations in Appendix A.3. □

This result is similar to what was derived for the MAP-NSF method in [VS94a]. It implies that GWSF and MAP-NSF are asymptotically equivalent and efficient for large N and small $\boldsymbol{\Omega}$ ($= \bar{\boldsymbol{\Omega}}/N$). An advantage of GWSF as compared to MAP-NSF is that GWSF is consistent even if $\mathbf{P}$ is rank deficient ($d' < d$). Another advantage is that the minimization of $V_{\mathrm{GWSF}}(\boldsymbol{\theta})$ can be performed without a search if the nominal array is uniform and linear, as we show in Section 3.6. In short, GWSF is a generalization of WSF [VO91] and MODE [SS90a] that allows one to include *a priori* knowledge of the array perturbations into the estimation criterion.

3.6 Implementation

We will in this section discuss in some detail the implementation of the GWSF estimator. Recall that the GWSF criterion is written in terms of the matrix $\bar{\mathbf{B}}(\boldsymbol{\theta})$ and that the parameterization of $\bar{\mathbf{B}}$ in general is not known. In this section we first rewrite the GWSF criterion so that it becomes explicitly parameterized by $\boldsymbol{\theta}$. This function can then be minimized numerically to give the GWSF estimate of $\boldsymbol{\theta}$. Next, in Section 3.6.2, we present the implementation for the common special case when the nominal array is uniform and linear. For this case, it is possible to implement GWSF without the need for gradient search methods. Thus, GWSF is an interesting direction of arrival estimator which combines statistical efficiency with computational simplicity (relative to other efficient estimators).

3.6.1 Implementation for General Arrays

The GWSF cost function in (3.20) reads

$$V_{\mathrm{GWSF}}(\boldsymbol{\theta}) = \bar{\boldsymbol{\varepsilon}}^*(\boldsymbol{\theta})\mathbf{W}\bar{\boldsymbol{\varepsilon}}(\boldsymbol{\theta}) = \hat{\mathbf{e}}_s^*\bar{\mathbf{B}}(\boldsymbol{\theta})\mathbf{W}\bar{\mathbf{B}}^*(\boldsymbol{\theta})\hat{\mathbf{e}}_s. \tag{3.33}$$

What complicates matters is that the functional form of $\bar{\mathbf{B}}(\boldsymbol{\theta})$ is not known for general array geometries. However, if the optimal weighting in (3.25) is used in (3.33), then it is possible to rewrite (3.33) so that it depends explicitly on $\boldsymbol{\theta}$. To see how this can be done, we will use the following two lemmas.

Lemma 3.1. *Let* $\mathbf{X}$ *and* $\mathbf{Y}$ *be two full column rank matrices of dimension* $m \times n$ *and* $m \times (m-n)$*, respectively. If* $\mathbf{X}^*\mathbf{Y} = \mathbf{0}$ *then*

$$\begin{bmatrix}\mathbf{X} & \mathbf{Y}\end{bmatrix}^{-1} = \begin{bmatrix}\mathbf{X}^\dagger \\ \mathbf{Y}^\dagger\end{bmatrix},$$

where $(\cdot)^\dagger$ *denotes the Moore-Penrose pseudo-inverse of the matrix in question* ($\mathbf{X}^\dagger = (\mathbf{X}^*\mathbf{X})^{-1}\mathbf{X}^*$).

Proof. By direct verification we have

$$\begin{bmatrix}\mathbf{X} & \mathbf{Y}\end{bmatrix}\begin{bmatrix}\mathbf{X}^\dagger \\ \mathbf{Y}^\dagger\end{bmatrix} = \begin{bmatrix}\mathbf{X}^\dagger \\ \mathbf{Y}^\dagger\end{bmatrix}\begin{bmatrix}\mathbf{X} & \mathbf{Y}\end{bmatrix} = \mathbf{I}_m.$$

□

Lemma 3.2. *Let* $\mathbf{X}$ $(m \times n)$ *and* $\mathbf{Y}$ $(m \times (m-n))$ *be two full column rank matrices. Furthermore, assume that* $\mathbf{X}^*\mathbf{Y} = \mathbf{0}$*, and let* $\mathbf{C}$ *and* $\mathbf{D}$ *be two non-singular matrices. Then*

$$\mathbf{X}\mathbf{C}^{-1}\mathbf{X}^* = \boldsymbol{\Pi}_{\mathbf{X}}\left(\mathbf{X}^{\dagger^*}\mathbf{C}\mathbf{X}^\dagger + \mathbf{Y}^{\dagger^*}\mathbf{D}\mathbf{Y}^\dagger\right)^{-1}\boldsymbol{\Pi}_{\mathbf{X}},$$

where $\boldsymbol{\Pi}_{\mathbf{X}} = \mathbf{X}(\mathbf{X}^*\mathbf{X})^{-1}\mathbf{X}^*$ *is the projection matrix projecting orthogonally onto the range-space of* $\mathbf{X}$*.*

Proof. Note that $\boldsymbol{\Pi}_{\mathbf{X}}\mathbf{Y} = \mathbf{0}$. The lemma is proven by the following set of equalities:

$$\begin{aligned}
\mathbf{X}\mathbf{C}^{-1}\mathbf{X}^* &= \boldsymbol{\Pi}_{\mathbf{X}}\mathbf{X}\mathbf{C}^{-1}\mathbf{X}^*\boldsymbol{\Pi}_{\mathbf{X}} \\
&= \boldsymbol{\Pi}_{\mathbf{X}}\begin{bmatrix}\mathbf{X} & \mathbf{Y}\end{bmatrix}\begin{bmatrix}\mathbf{C}^{-1} & \mathbf{0} \\ \mathbf{0} & \mathbf{D}^{-1}\end{bmatrix}\begin{bmatrix}\mathbf{X}^* \\ \mathbf{Y}^*\end{bmatrix}\boldsymbol{\Pi}_{\mathbf{X}} \\
&= \boldsymbol{\Pi}_{\mathbf{X}}\left(\begin{bmatrix}\mathbf{X}^* \\ \mathbf{Y}^*\end{bmatrix}^{-1}\begin{bmatrix}\mathbf{C} & \mathbf{0} \\ \mathbf{0} & \mathbf{D}\end{bmatrix}\begin{bmatrix}\mathbf{X} & \mathbf{Y}\end{bmatrix}^{-1}\right)^{-1}\boldsymbol{\Pi}_{\mathbf{X}} \\
&= \boldsymbol{\Pi}_{\mathbf{X}}\left(\begin{bmatrix}\mathbf{X}^{\dagger^*} & \mathbf{Y}^{\dagger^*}\end{bmatrix}\begin{bmatrix}\mathbf{C} & \mathbf{0} \\ \mathbf{0} & \mathbf{D}\end{bmatrix}\begin{bmatrix}\mathbf{X}^\dagger \\ \mathbf{Y}^\dagger\end{bmatrix}\right)^{-1}\boldsymbol{\Pi}_{\mathbf{X}} \\
&= \boldsymbol{\Pi}_{\mathbf{X}}\left(\mathbf{X}^{\dagger^*}\mathbf{C}\mathbf{X}^\dagger + \mathbf{Y}^{\dagger^*}\mathbf{D}\mathbf{Y}^\dagger\right)^{-1}\boldsymbol{\Pi}_{\mathbf{X}},
\end{aligned}$$

where use was made of Lemma 3.1 in the fourth step. □

Now apply Lemma 3.2 to the GWSF criterion (3.33). With reference to Lemma 3.2, take $\mathbf{X} = \bar{\mathbf{B}}$, $\mathbf{Y} = \bar{\mathbf{A}}$, $\mathbf{C} = \mathbf{W}^{-1}$ and, for example, $\mathbf{D} = (\bar{\mathbf{A}}^*\bar{\mathbf{A}})^2$ to show that

$$V_{\mathrm{GWSF}}(\boldsymbol{\theta}) = \hat{\mathbf{e}}_s^* \boldsymbol{\Pi}_{\bar{\mathbf{A}}}^{\perp} \tilde{\mathbf{W}} \boldsymbol{\Pi}_{\bar{\mathbf{A}}}^{\perp} \hat{\mathbf{e}}_s, \tag{3.34}$$

where

$$\tilde{\mathbf{W}} = \left(\bar{\mathbf{B}}^{\dagger^*} \mathbf{W}^{-1} \bar{\mathbf{B}}^{\dagger} + \bar{\mathbf{A}} \bar{\mathbf{A}}^* \right)^{-1}. \tag{3.35}$$

In (3.34), we used the fact that $\boldsymbol{\Pi}_{\bar{\mathbf{B}}} = \boldsymbol{\Pi}_{\bar{\mathbf{A}}}^{\perp}$. Let $\mathbf{W}$ be chosen according to (3.25). It is then readily verified that

$$\bar{\mathbf{B}}^{\dagger^*} \mathbf{W}^{-1} \bar{\mathbf{B}}^{\dagger} = \bar{\mathbf{B}}^{\dagger^*} \mathbf{C}_{\bar{\boldsymbol{\varepsilon}}} \bar{\mathbf{B}}^{\dagger} = \begin{bmatrix} \tilde{\mathbf{L}} & \mathbf{0} \\ \mathbf{0} & \tilde{\mathbf{L}}^c \end{bmatrix} + \begin{bmatrix} \tilde{\mathbf{G}} \\ \tilde{\mathbf{G}}^c \end{bmatrix} \begin{bmatrix} \tilde{\mathbf{G}}^* & \tilde{\mathbf{G}}^T \end{bmatrix}, \tag{3.36}$$

where

$$\tilde{\mathbf{L}} = \left(\sigma^2 \widetilde{\boldsymbol{\Lambda}}^{-2} \boldsymbol{\Lambda}_s \otimes \boldsymbol{\Pi}_{\mathbf{A}}^{\perp} \right),$$
$$\tilde{\mathbf{G}} = \left(\mathbf{T}^T \otimes \boldsymbol{\Pi}_{\mathbf{A}}^{\perp} \right) \mathbf{D}_{\boldsymbol{\rho}} \bar{\boldsymbol{\Omega}}^{1/2}.$$

Combining (3.36), (3.35) and (3.34), we see that the criterion is now explicitly parameterized by $\boldsymbol{\theta}$. The GWSF algorithm for general array geometries can be summarized as follows:

1. Based on $\hat{\mathbf{R}}$, compute $\hat{\mathbf{E}}_s$, $\hat{\boldsymbol{\Lambda}}_s$, and

$$\hat{\sigma}^2 = \frac{1}{m - d'} \left\{ \mathrm{Tr}(\hat{\mathbf{R}}) - \mathrm{Tr}(\hat{\boldsymbol{\Lambda}}_s) \right\},$$
$$\hat{\widetilde{\boldsymbol{\Lambda}}} = \hat{\boldsymbol{\Lambda}}_s - \hat{\sigma}^2 \mathbf{I}.$$

2. The GWSF estimate of $\boldsymbol{\theta}$ is then given by

$$\hat{\boldsymbol{\theta}} = \arg\min_{\boldsymbol{\theta}} \hat{\mathbf{e}}_s^* \boldsymbol{\Pi}_{\bar{\mathbf{A}}}^{\perp} \hat{\tilde{\mathbf{W}}} \boldsymbol{\Pi}_{\bar{\mathbf{A}}}^{\perp} \hat{\mathbf{e}}_s,$$

where $\hat{\tilde{\mathbf{W}}}$ is given by (3.35) and (3.36) with the sample estimates from the first step inserted in place of the true quantities.

This results in a non-linear optimization problem where $\boldsymbol{\theta}$ enters in a complicated way. From the analysis in Section 3.5 it follows that the asymptotic second order properties of $\hat{\boldsymbol{\theta}}$ are not affected if the weighting matrix $\tilde{\mathbf{W}}$ is replaced by a consistent estimate. Hence, if a consistent estimate of $\boldsymbol{\theta}_0$ is used to compute $\tilde{\mathbf{W}}$, then the criterion in the second step only depends on $\boldsymbol{\theta}$ via $\boldsymbol{\Pi}_{\tilde{\mathbf{A}}}^{\perp}$. This may lead to some computational savings, but it still results in a non-linear optimization problem. In the next section, we turn to the common special case of a uniform linear array, for which it is possible to avoid gradient search methods.

3.6.2 Implementation for Uniform Linear Arrays

In this section, we present a way to significantly simplify the implementation of GWSF if the nominal array is linear and uniform. The form of the estimator is in the spirit of IQML [BM86] and MODE [SS90b, SS90a]. Many of the details concerning the implementation are borrowed from [SS90b]. Define the following polynomial with d roots on the unit circle corresponding to the DOAs:

$$b_0 z^d + b_1 z^{d-1} + \cdots + b_d = b_0 \prod_{k=1}^{d} (z - e^{j\omega_k}), \qquad b_0 \neq 0, \tag{3.37}$$

where $\omega_k = 2\pi\delta \sin(\boldsymbol{\theta}_k)$ and where δ is the separation between the sensors measured in wavelengths. The idea is to re-parameterize the minimization problem in terms of the polynomial coefficients instead of $\boldsymbol{\theta}$. As will be seen below, this leads to a considerable computational simplification. Observe that the roots of (3.37) lie on the unit circle. A common way to impose this constraint on the coefficients in the estimation procedure is to enforce the conjugate symmetry property

$$b_k = b_{d-k}^c; \quad k = 0, \ldots, d. \tag{3.38}$$

This only approximately ensures that the roots are on the unit circle. However, notice that if z_i is a root of (3.37) with conjugate symmetric coefficients, then so is z_i^{-c}. Assume now that we have a set of perturbed polynomial coefficients satisfying (3.38). As long as the perturbation is small enough, the d roots of (3.37) will be on the unit circle since the true DOAs are distinct. That is, for large enough N, the conjugate symmetry property in fact guarantees that the roots are on the unit circle and the asymptotic properties of the estimates will not be affected.

Next, define the $m \times (m-d)$ Toeplitz matrix $\mathbf{B}$ as

$$\mathbf{B}^* = \begin{bmatrix} b_d & \cdots & b_1 & b_0 & 0 & \cdots & 0 \\ 0 & b_d & \cdots & b_1 & b_0 & \ddots & 0 \\ \vdots & \ddots & \ddots & & \ddots & \ddots & \vdots \\ 0 & \dots & 0 & b_d & \dots & b_1 & b_0 \end{bmatrix}. \tag{3.39}$$

It is readily verified that $\mathbf{B}^*\mathbf{A}(\boldsymbol{\theta}) = \mathbf{0}$, and since the rank of $\mathbf{B}$ is $m-d$ (by construction, since $b_0 \neq 0$), it follows that the columns of $\mathbf{B}$ span the null-space of $\mathbf{A}^*$. This implies that we can use $\mathbf{B}$ in (3.39) in the GWSF criterion, minimize with respect to the polynomial coefficients, and then compute $\boldsymbol{\theta}$ from the roots of the polynomial (3.37). In the following we give the details on how this can be performed.

It is useful to rewrite the GWSF criterion as follows (cf. (3.20) and (3.25)):

$$V_{\mathrm{GWSF}} = \bar{\boldsymbol{\varepsilon}}^* \mathbf{W}_{\mathrm{GWSF}} \bar{\boldsymbol{\varepsilon}} = \begin{bmatrix} \mathrm{vec}(\mathbf{B}^*\hat{\mathbf{E}}_W) \\ \mathrm{vec}(\mathbf{B}^T\hat{\mathbf{E}}_W^c) \end{bmatrix}^* \bar{\mathbf{W}} \begin{bmatrix} \mathrm{vec}(\mathbf{B}^*\hat{\mathbf{E}}_W) \\ \mathrm{vec}(\mathbf{B}^T\hat{\mathbf{E}}_W^c) \end{bmatrix}, \tag{3.40}$$

where

$$\hat{\mathbf{E}}_W = \frac{1}{\sqrt{\hat{\sigma}^2}} \hat{\mathbf{E}}_s \hat{\bar{\mathbf{\Lambda}}} \hat{\mathbf{\Lambda}}_s^{-1/2}, \tag{3.41}$$

$$\bar{\mathbf{W}}^{-1} = \begin{bmatrix} (\bar{\mathbf{W}}^{-1})_{11} & (\bar{\mathbf{W}}^{-1})_{12} \\ (\bar{\mathbf{W}}^{-1})_{12}^c & (\bar{\mathbf{W}}^{-1})_{11}^c \end{bmatrix}. \tag{3.42}$$

The blocks in $\bar{\mathbf{W}}^{-1}$ are given by

$$\begin{aligned} (\bar{\mathbf{W}}^{-1})_{11} &= (\mathbf{I}_{d'} \otimes \mathbf{B}^*\mathbf{B}) + \left(\bar{\mathbf{T}}^T \otimes \mathbf{B}^*\right) \mathbf{D}_{\boldsymbol{\rho}} \bar{\mathbf{\Omega}} \mathbf{D}_{\boldsymbol{\rho}}^* \left(\bar{\mathbf{T}}^c \otimes \mathbf{B}\right), \\ (\bar{\mathbf{W}}^{-1})_{12} &= \left(\bar{\mathbf{T}}^T \otimes \mathbf{B}^*\right) \mathbf{D}_{\boldsymbol{\rho}} \bar{\mathbf{\Omega}} \mathbf{D}_{\boldsymbol{\rho}}^T \left(\bar{\mathbf{T}} \otimes \mathbf{B}^c\right), \end{aligned}$$

where $\bar{\mathbf{T}} = \mathbf{T}\hat{\bar{\mathbf{\Lambda}}}\hat{\mathbf{\Lambda}}_s^{-1/2}/\sqrt{\hat{\sigma}^2} = \mathbf{A}^\dagger \hat{\mathbf{E}}_W$. Let $\hat{\mathbf{E}}_{W_{\bullet k}}$ denote column k and $\hat{\mathbf{E}}_{W_{i,j}}$ the (i,j)th element of $\hat{\mathbf{E}}_W$, and define the vector

$$\mathbf{b} = \begin{bmatrix} b_0 & b_1 & \dots & b_d \end{bmatrix}^T.$$

Observe that

$$\mathbf{B}^*\hat{\mathbf{E}}_{W_{\bullet k}} = \begin{bmatrix} \hat{\mathbf{E}}_{W_{d+1,k}} & \hat{\mathbf{E}}_{W_{d,k}} & \dots & \hat{\mathbf{E}}_{W_{1,k}} \\ \hat{\mathbf{E}}_{W_{d+2,k}} & \hat{\mathbf{E}}_{W_{d+1,k}} & \dots & \hat{\mathbf{E}}_{W_{2,k}} \\ \vdots & & & \vdots \\ \hat{\mathbf{E}}_{W_{m,k}} & \hat{\mathbf{E}}_{W_{m-1,k}} & \dots & \hat{\mathbf{E}}_{W_{m-d,k}} \end{bmatrix} \mathbf{b} \triangleq \tilde{\mathbf{S}}_k \mathbf{b}$$

for $k = 1, \ldots, d'$, and define

$$\mathbf{S} = \begin{bmatrix} \tilde{\mathbf{S}}_1 \\ \vdots \\ \tilde{\mathbf{S}}_{d'} \end{bmatrix}.$$

Then we have

$$\mathrm{vec}(\mathbf{B}^* \hat{\mathbf{E}}_W) = \mathbf{S}\mathbf{b}.$$

Let $\boldsymbol{\beta} = \begin{bmatrix} b_0 & \ldots & b_{\lfloor (d-1)/2 \rfloor} \end{bmatrix}^T$, where $\lfloor (\cdot) \rfloor$ denotes the largest integer less than or equal to $(\cdot)$. In view of the conjugate symmetry constraint (3.38),

$$\mathbf{b} = \begin{bmatrix} \boldsymbol{\beta} \\ (b_{d/2}) \\ \tilde{\mathbf{I}}\boldsymbol{\beta}^c \end{bmatrix},$$

where the real valued parameter $b_{d/2}$ only appears if d is even. Here, $\tilde{\mathbf{I}}$ is the exchange matrix with ones along the anti-diagonal and zeros elsewhere. Clearly, we have

$$\begin{aligned} \mathbf{S}\mathbf{b} &= \begin{bmatrix} \mathbf{S}_1 & (\mathbf{s}) & \mathbf{S}_2 \end{bmatrix} \begin{bmatrix} \boldsymbol{\beta}_r + j\boldsymbol{\beta}_i \\ (b_{d/2}) \\ \tilde{\mathbf{I}}(\boldsymbol{\beta}_r - j\boldsymbol{\beta}_i) \end{bmatrix} \\ &= \begin{bmatrix} \mathbf{S}_1 + \mathbf{S}_2\tilde{\mathbf{I}} & (\mathbf{s}) & j(\mathbf{S}_1 - \mathbf{S}_2\tilde{\mathbf{I}}) \end{bmatrix} \begin{bmatrix} \boldsymbol{\beta}_r \\ (b_{d/2}) \\ \boldsymbol{\beta}_i \end{bmatrix} \\ &\triangleq \mathbf{F}\boldsymbol{\mu}, \end{aligned}$$

where the subscripts r and i denote real and imaginary parts, respectively. With the notation introduced above, the criterion (3.40) can be written as

$$V_{\mathrm{GWSF}} = \boldsymbol{\mu}^T \begin{bmatrix} \mathbf{F} \\ \mathbf{F}^c \end{bmatrix}^* \bar{\mathbf{W}} \begin{bmatrix} \mathbf{F} \\ \mathbf{F}^c \end{bmatrix} \boldsymbol{\mu}.$$

To obtain a proper parameterization we should also include a non-triviality constraint to avoid the solution $\mathbf{b} = \mathbf{0}$ ($\boldsymbol{\mu} = \mathbf{0}$). In [SS90b] it is proposed that either b_{0r} or b_{0i} can be set to one. In what follows we assume, for simplicity, that it is possible to put $b_{0r} = \boldsymbol{\mu}_1 = 1$. For particular cases

this may not be possible. In such cases one should instead use the constraint $b_{0i} = 1$. As an alternative to these linear constraints, one can use a norm constraint on $\boldsymbol{\mu}$ (see, e.g., [NK94]). The key advantage of the reformulation of the problem in terms of $\boldsymbol{\mu}$ is that V_{GWSF} is quadratic in $\boldsymbol{\mu}$, and thus it can be solved explicitly.

A consistent estimate of $\boldsymbol{\theta}_0$ can be obtained by minimizing $\|\mathrm{vec}(\mathbf{B}^*\hat{\mathbf{E}}_W)\|_2^2$ since $\mathbf{B}^*\mathbf{E}_s = \mathbf{0}$ uniquely determines $\boldsymbol{\theta}_0$. Furthermore, this also implies that replacing the weighting matrix $\bar{\mathbf{W}}$ in (3.40) by a consistent estimate does not change the asymptotic distribution of the estimates. In summary, we have the following GWSF algorithm for uniform linear arrays:

1. Based on $\hat{\mathbf{R}}$, compute $\hat{\mathbf{E}}_s$, $\hat{\boldsymbol{\Lambda}}_s$, and
$$\hat{\sigma}^2 = \frac{1}{m-d'}\left\{\mathrm{Tr}(\hat{\mathbf{R}}) - \mathrm{Tr}(\hat{\boldsymbol{\Lambda}}_s)\right\},$$
$$\hat{\bar{\boldsymbol{\Lambda}}} = \hat{\boldsymbol{\Lambda}}_s - \hat{\sigma}^2\mathbf{I}.$$

2. Using the notation introduced above, an initial estimate can be obtained by minimizing
$$\|\mathrm{vec}(\mathbf{B}^*\hat{\mathbf{E}}_W)\|_2^2 = \|\mathbf{S}\mathbf{b}\|_2^2 = \|\mathbf{F}\boldsymbol{\mu}\|_2^2 = \|\mathbf{J}\boldsymbol{\eta} + \mathbf{c}\|_2^2 \tag{3.43}$$
over $\boldsymbol{\eta} \in \mathbb{R}^d$, where $\boldsymbol{\eta}$, $\mathbf{J}$ and $\mathbf{c}$ are defined via
$$\mathbf{F}\boldsymbol{\mu} = \begin{bmatrix}\mathbf{c} & \mathbf{J}\end{bmatrix}\begin{bmatrix}1\\ \boldsymbol{\eta}\end{bmatrix} = \mathbf{J}\boldsymbol{\eta} + \mathbf{c}.$$
The norm should be interpreted as $\|\mathbf{x}\|_2^2 = \mathbf{x}^*\mathbf{x}$. Using the minimizer $\hat{\boldsymbol{\eta}}$ of (3.43), an estimate of $\mathbf{b}$ can be constructed. The initial estimate of $\boldsymbol{\theta}_0$ is then found via the roots of (3.37). Notice that $\hat{\boldsymbol{\eta}}$ is the least-squares solution to the over-determined set of equations given in (3.43).

3. Given $\bar{\boldsymbol{\Omega}}$ and an initial estimate $\hat{\boldsymbol{\theta}}$ (and $\hat{\mathbf{b}}$), compute $\hat{\bar{\mathbf{T}}} = \mathbf{A}^\dagger(\hat{\boldsymbol{\theta}})\hat{\mathbf{E}}_W$, $\mathbf{B}(\hat{\mathbf{b}})$ and $\mathbf{D}_{\boldsymbol{\rho}}(\hat{\boldsymbol{\theta}})$. Use these quantities to obtain a consistent estimate of $\bar{\mathbf{W}}^{-1}$ in (3.42). Let $\bar{\mathbf{W}}^{-1/2}$ denote the Cholesky factor of $\bar{\mathbf{W}}^{-1}$ such that $\bar{\mathbf{W}}^{-1} = \bar{\mathbf{W}}^{-1/2}\bar{\mathbf{W}}^{-*/2}$. Solve the following linear system of equations for $\mathbf{F}_w$
$$\bar{\mathbf{W}}^{-1/2}\mathbf{F}_w = \begin{bmatrix}\mathbf{F}\\ \mathbf{F}^c\end{bmatrix},$$

and define $\mathbf{J}_w$ and $\mathbf{c}_w$ via

$$\mathbf{F}_w\boldsymbol{\mu} = \begin{bmatrix}\mathbf{c}_w & \mathbf{J}_w\end{bmatrix}\begin{bmatrix}1\\ \boldsymbol{\eta}\end{bmatrix} = \mathbf{J}_w\boldsymbol{\eta} + \mathbf{c}_w.$$

The solution of this step is given by

$$\hat{\boldsymbol{\eta}} = \arg\min_{\boldsymbol{\eta}\in\mathbb{R}^d} \|\mathbf{J}_w\boldsymbol{\eta} + \mathbf{c}_w\|_2^2.$$

The GWSF estimate $\hat{\boldsymbol{\theta}}$ is then constructed from $\hat{\boldsymbol{\eta}}$ as described before.

In finite samples and difficult scenarios it may be useful to reiterate the third step several times; however, this does not improve the asymptotic statistical properties of the estimate.

In this section, we have shown that GWSF can be implemented in a very attractive manner if the nominal array is uniform and linear. In particular, the solution can be obtained in a "closed form" by solving a set of linear systems of equations and rooting the polynomial in (3.37). Thus, there is no need for an iterative optimization procedure like that necessary in, for example, MAP-NSF.

3.7 Performance Analysis of MAPprox

The MAPprox cost function (3.5) was derived by a second order approximation of the MAP-WSF cost function (3.2) around $\boldsymbol{\rho}_0$. The MAPprox estimates are thus expected to have a performance similar to ML. This has also been observed in simulations [WOV91, VS94a]. However, a formal analysis of the asymptotic properties of MAPprox has not been conducted. In this section we show that, using asymptotic approximations, the MAPprox cost function in fact can be rewritten to coincide with the GWSF cost function. This establishes the observed asymptotic efficiency of the MAPprox method.

Consider the normalized MAPprox cost function (cf. (3.5))

$$\frac{1}{N}V_{\mathrm{MAPprox}}(\boldsymbol{\theta}) = V(\boldsymbol{\theta}) - \frac{1}{2}\partial_{\boldsymbol{\rho}}V^T(\boldsymbol{\theta})\left[\partial_{\boldsymbol{\rho}\boldsymbol{\rho}}V(\boldsymbol{\theta}) + \bar{\boldsymbol{\Omega}}^{-1}\right]^{-1}\partial_{\boldsymbol{\rho}}V(\boldsymbol{\theta}), \tag{3.44}$$

where

$$V(\boldsymbol{\theta}) = V(\boldsymbol{\theta}, \boldsymbol{\rho}_0) \tag{3.45}$$

and

$$V(\boldsymbol{\theta},\boldsymbol{\rho}) = \frac{1}{\hat{\sigma}^2}\,\mathrm{Tr}\{\boldsymbol{\Pi}_{\mathbf{A}}^{\perp}(\boldsymbol{\theta},\boldsymbol{\rho})\hat{\mathbf{E}}_s\hat{\mathbf{W}}_{\mathrm{WSF}}\hat{\mathbf{E}}_s^*\}. \tag{3.46}$$

The gradient and the Hessian in (3.44) are evaluated at $\boldsymbol{\rho}_0$. One problem with $V_{\mathrm{MAPprox}}(\boldsymbol{\theta})$ is that the inverse $(\partial_{\boldsymbol{\rho}\boldsymbol{\rho}}V(\boldsymbol{\theta}) + \bar{\boldsymbol{\Omega}}^{-1})^{-1}$ may not exist for all $\boldsymbol{\theta}$. This implies that the consistency of the MAPprox estimate cannot be guaranteed. However, locally around $\boldsymbol{\theta}_0$ the function is well behaved. In the following we will approximate (3.44) around $\boldsymbol{\theta}_0$. The approximation retains the second order behavior of $V_{\mathrm{MAPprox}}(\boldsymbol{\theta})$ around $\boldsymbol{\theta}_0$ and is well defined for all $\boldsymbol{\theta}$, implying that the consistency problem is eliminated. More precisely, we will study (3.44) for $\boldsymbol{\theta}$ such that $\boldsymbol{\theta} - \boldsymbol{\theta}_0 = O_p(1/\sqrt{N})$.

Let us start by deriving the gradient $\partial_{\boldsymbol{\rho}}V$. In what follows we write $\boldsymbol{\Pi}^{\perp}$ in place of $\boldsymbol{\Pi}_{\mathbf{A}}^{\perp}$, for simplicity of notation. The derivative of (3.46) with respect to $\boldsymbol{\rho}_i$ is

$$\partial_{\boldsymbol{\rho}_i}V = \frac{1}{\hat{\sigma}^2}\,\mathrm{Tr}\{\boldsymbol{\Pi}_i^{\perp}\hat{\mathbf{E}}_s\hat{\mathbf{W}}_{\mathrm{WSF}}\hat{\mathbf{E}}_s^*\} = -\frac{2}{\hat{\sigma}^2}\,\mathrm{Re}\left[\mathrm{Tr}\{\boldsymbol{\Pi}^{\perp}\mathbf{A}_i\mathbf{A}^{\dagger}\hat{\mathbf{E}}_s\hat{\mathbf{W}}_{\mathrm{WSF}}\hat{\mathbf{E}}_s^*\}\right],$$

where we have used the following result:

$$\boldsymbol{\Pi}_i^{\perp} = -\boldsymbol{\Pi}^{\perp}\mathbf{A}_i\mathbf{A}^{\dagger} - \mathbf{A}^{\dagger^*}\mathbf{A}_i^*\boldsymbol{\Pi}^{\perp}.$$

Using the definition (3.11) and the formula (3.7), we can write

$$\begin{aligned}\partial_{\boldsymbol{\rho}}V(\boldsymbol{\theta}) &= \partial_{\boldsymbol{\rho}}V|_{\boldsymbol{\theta},\boldsymbol{\rho}_0}\\ &= -\frac{2}{\hat{\sigma}^2}\,\mathrm{Re}\left[\mathbf{D}_{\boldsymbol{\rho}}^*\,\mathrm{vec}(\boldsymbol{\Pi}^{\perp}\hat{\mathbf{E}}_s\hat{\mathbf{W}}_{\mathrm{WSF}}\hat{\mathbf{E}}_s^*\mathbf{A}^{\dagger^*})\right] = O_p(1/\sqrt{N}).\end{aligned} \tag{3.47}$$

Consider next the (i,j)th element of the Hessian matrix

$$\begin{aligned}\partial_{\boldsymbol{\rho}_i\boldsymbol{\rho}_j}V = -\frac{2}{\hat{\sigma}^2}\,\mathrm{Re}\Big[\mathrm{Tr}\{&\underbrace{\boldsymbol{\Pi}_j^{\perp}\mathbf{A}_i\mathbf{A}^{\dagger}\hat{\mathbf{E}}_s\hat{\mathbf{W}}_{\mathrm{WSF}}\hat{\mathbf{E}}_s^*}_{O_p(1)}\\ &+\underbrace{\boldsymbol{\Pi}^{\perp}\mathbf{A}_{ij}\mathbf{A}^{\dagger}\hat{\mathbf{E}}_s\hat{\mathbf{W}}_{\mathrm{WSF}}\hat{\mathbf{E}}_s^*}_{O_p(1/\sqrt{N})} + \underbrace{\boldsymbol{\Pi}^{\perp}\mathbf{A}_i\mathbf{A}_j^{\dagger}\hat{\mathbf{E}}_s\hat{\mathbf{W}}_{\mathrm{WSF}}\hat{\mathbf{E}}_s^*}_{O_p(1/\sqrt{N})}\}\Big].\end{aligned} \tag{3.48}$$

Notice that

$$\frac{1}{N}V_{\text{MAPprox}} = \underbrace{V}_{O_p(1/N)} - \frac{1}{2}\underbrace{\partial_{\boldsymbol{\rho}} V^T}_{O_p(1/\sqrt{N})}(\underbrace{\partial_{\boldsymbol{\rho}\boldsymbol{\rho}} V}_{O_p(1)} + \underbrace{\bar{\boldsymbol{\Omega}}^{-1}}_{O(1)})^{-1}\underbrace{\partial_{\boldsymbol{\rho}} V}_{O_p(1/\sqrt{N})} = O_p(1/N).$$

All of the order relations above are valid locally around $\boldsymbol{\theta}_0$. Next, study the derivative of $\frac{1}{N}V_{MAPprox}$ with respect to $\boldsymbol{\theta}_i$ (here, an index i denotes a partial derivative with respect to $\boldsymbol{\theta}_i$)

$$\begin{aligned}\frac{\partial}{\partial\boldsymbol{\theta}_i}\frac{1}{N}V_{\text{MAPprox}} &= \underbrace{V_i}_{O_p(1/\sqrt{N})} - \frac{1}{2}\underbrace{\partial_{\boldsymbol{\rho}} V_i^T}_{O_p(1)}(\underbrace{\partial_{\boldsymbol{\rho}\boldsymbol{\rho}} V}_{O_p(1)} + \underbrace{\bar{\boldsymbol{\Omega}}^{-1}}_{O(1)})^{-1}\underbrace{\partial_{\boldsymbol{\rho}} V}_{O_p(1/\sqrt{N})} \\ &+ \frac{1}{2}\underbrace{\partial_{\boldsymbol{\rho}} V^T}_{O_p(1/\sqrt{N})}(\underbrace{\partial_{\boldsymbol{\rho}\boldsymbol{\rho}} V}_{O_p(1)} + \underbrace{\bar{\boldsymbol{\Omega}}^{-1}}_{O(1)})^{-1}\underbrace{\partial_{\boldsymbol{\rho}\boldsymbol{\rho}} V_i}_{O_p(1)}(\underbrace{\partial_{\boldsymbol{\rho}\boldsymbol{\rho}} V}_{O_p(1)} + \underbrace{\bar{\boldsymbol{\Omega}}^{-1}}_{O(1)})^{-1}\underbrace{\partial_{\boldsymbol{\rho}} V}_{O_p(1/\sqrt{N})} \\ &- \frac{1}{2}\underbrace{\partial_{\boldsymbol{\rho}} V^T}_{O_p(1/\sqrt{N})}(\underbrace{\partial_{\boldsymbol{\rho}\boldsymbol{\rho}} V}_{O_p(1)} + \underbrace{\bar{\boldsymbol{\Omega}}^{-1}}_{O(1)})^{-1}\underbrace{\partial_{\boldsymbol{\rho}} V_i}_{O_p(1)}.\end{aligned} \tag{3.49}$$

Since the term containing $\partial_{\boldsymbol{\rho}\boldsymbol{\rho}} V_i$ is of order $O_p(1/N)$, we conclude that $\partial_{\boldsymbol{\rho}\boldsymbol{\rho}} V$ can be replaced by a consistent estimate without affecting the asymptotic second order properties. This implies in particular that we can neglect the last two terms in (3.48) and only retain the first. (Notice that all three terms in $\partial_{\boldsymbol{\rho}\boldsymbol{\rho}} V_i$ are of order $O_p(1)$. If the second term in (3.49) were $O_p(1/\sqrt{N})$, then all three terms in (3.48) would have contributed.) Similarly, it can be shown that asymptotically the two last terms in (3.48) do not affect the second order derivatives of $V_{MAPprox}/N$

with respect to $\boldsymbol{\theta}$. Recall (3.48) and rewrite it as

$$\begin{aligned}
\partial_{\boldsymbol{\rho}_i\boldsymbol{\rho}_j} V &= -\frac{2}{\hat{\sigma}^2}\,\mathrm{Re}\left[\mathrm{Tr}\{\boldsymbol{\Pi}_j^{\perp}\mathbf{A}_i\mathbf{A}^{\dagger}\hat{\mathbf{E}}_s\hat{\mathbf{W}}_{\mathrm{WSF}}\hat{\mathbf{E}}_s^{*}\}\right] + o_p(1) \\
&= -\frac{2}{\hat{\sigma}^2}\,\mathrm{Re}\left[\mathrm{Tr}\{(-\boldsymbol{\Pi}^{\perp}\mathbf{A}_j\mathbf{A}^{\dagger} - \mathbf{A}^{\dagger^*}\mathbf{A}_j^{*}\boldsymbol{\Pi}^{\perp})\mathbf{A}_i\mathbf{A}^{\dagger}\hat{\mathbf{E}}_s\hat{\mathbf{W}}_{\mathrm{WSF}}\hat{\mathbf{E}}_s^{*}\}\right] + o_p(1) \\
&= \frac{2}{\hat{\sigma}^2}\,\mathrm{Re}\left[\mathrm{Tr}\{\mathbf{A}^{\dagger^*}\mathbf{A}_j^{*}\boldsymbol{\Pi}^{\perp}\mathbf{A}_i\mathbf{A}^{\dagger}\hat{\mathbf{E}}_s\hat{\mathbf{W}}_{\mathrm{WSF}}\hat{\mathbf{E}}_s^{*}\}\right] + o_p(1) \\
&= \frac{2}{\hat{\sigma}^2}\,\mathrm{Re}\left[\mathrm{vec}^{*}(\mathbf{A}_i)\left(\left(\mathbf{A}^{\dagger}\hat{\mathbf{E}}_s\hat{\mathbf{W}}_{\mathrm{WSF}}\hat{\mathbf{E}}_s^{*}\mathbf{A}^{\dagger^*}\right)^{T}\otimes\boldsymbol{\Pi}^{\perp}\right)\mathrm{vec}(\mathbf{A}_j)\right] + o_p(1).
\end{aligned} \tag{3.50}$$

The dominating term of (3.50) can be written in matrix form as

$$\begin{aligned}
\tilde{V}_{\boldsymbol{\rho}\boldsymbol{\rho}}(\boldsymbol{\theta}) &\triangleq \frac{2}{\hat{\sigma}^2}\,\mathrm{Re}\left[\mathbf{D}_{\boldsymbol{\rho}}^{*}\left(\left(\mathbf{A}^{\dagger}\hat{\mathbf{E}}_s\hat{\mathbf{W}}_{\mathrm{WSF}}\hat{\mathbf{E}}_s^{*}\mathbf{A}^{\dagger^*}\right)^{T}\otimes\boldsymbol{\Pi}^{\perp}\right)\mathbf{D}_{\boldsymbol{\rho}}\right] \\
&= \frac{2}{\hat{\sigma}^2}\,\mathrm{Re}\left[\mathbf{D}_{\boldsymbol{\rho}}^{*}\hat{\mathbf{M}}\mathbf{D}_{\boldsymbol{\rho}}\right].
\end{aligned} \tag{3.51}$$

If $\tilde{V}_{\boldsymbol{\rho}\boldsymbol{\rho}}(\boldsymbol{\theta})$ is used in lieu of $\partial_{\boldsymbol{\rho}\boldsymbol{\rho}}V(\boldsymbol{\theta})$ in (3.44), we get the following alternate cost function:

$$V_{\mathrm{MAPprox2}}(\boldsymbol{\theta}) = V(\boldsymbol{\theta}) - \frac{1}{2}\partial_{\boldsymbol{\rho}}V^{T}(\boldsymbol{\theta})\left[\tilde{V}_{\boldsymbol{\rho}\boldsymbol{\rho}}(\boldsymbol{\theta}) + \bar{\boldsymbol{\Omega}}^{-1}\right]^{-1}\partial_{\boldsymbol{\rho}}V(\boldsymbol{\theta}).$$

It can be seen that (3.51) is non-negative definite, which ensures that the inverse $(\tilde{V}_{\boldsymbol{\rho}\boldsymbol{\rho}}(\boldsymbol{\theta}) + \bar{\boldsymbol{\Omega}}^{-1})^{-1}$ always exists. Furthermore, we have (cf. (3.14))

$$\tilde{V}_{\boldsymbol{\rho}\boldsymbol{\rho}}(\boldsymbol{\theta}) + \bar{\boldsymbol{\Omega}}^{-1} = \frac{2}{\hat{\sigma}^2}\hat{\boldsymbol{\Gamma}}.$$

It can also be verified that $V(\boldsymbol{\theta})$ and $\partial_{\boldsymbol{\rho}}V(\boldsymbol{\theta})$, as defined in (3.45) and (3.47), can be written as

$$\begin{aligned}
V(\boldsymbol{\theta}) &= \frac{1}{2}\bar{\boldsymbol{\varepsilon}}^{*}\hat{\bar{\mathbf{L}}}^{-1}\bar{\boldsymbol{\varepsilon}}, \\
\partial_{\boldsymbol{\rho}}V(\boldsymbol{\theta}) &= -\bar{\boldsymbol{\Omega}}^{-1/2}\hat{\bar{\mathbf{G}}}^{*}\hat{\bar{\mathbf{L}}}^{-1}\bar{\boldsymbol{\varepsilon}},
\end{aligned}$$

where $\hat{\bar{\mathbf{L}}}$ and $\hat{\bar{\mathbf{G}}}$ are defined similarly to (3.23) and (3.24) but computed with sample data quantities and in $\boldsymbol{\theta}$ (not in $\boldsymbol{\theta}_0$). This implies that

$$V_{\mathrm{MAPprox2}}(\boldsymbol{\theta}) = \frac{1}{2}\bar{\boldsymbol{\varepsilon}}^{*}\hat{\mathbf{W}}_{\mathrm{M2}}\bar{\boldsymbol{\varepsilon}},$$

where

$$\hat{\mathbf{W}}_{\mathrm{M2}} = \left(\hat{\bar{\mathbf{L}}}^{-1} - \hat{\bar{\mathbf{L}}}^{-1} \hat{\mathbf{G}} \bar{\mathbf{\Omega}}^{-1/2} \frac{\hat{\sigma}^2}{2} \hat{\mathbf{\Gamma}}^{-1} \bar{\mathbf{\Omega}}^{-1/2} \hat{\mathbf{G}}^* \hat{\bar{\mathbf{L}}}^{-1} \right). \tag{3.52}$$

The MAPprox2 cost function can thus be written in the same form as the GWSF criterion (see (3.20)). The weighting matrix in (3.52) depends on $\boldsymbol{\theta}$ and on sample data quantities. However, in Section 3.5 it was shown that any two weighting matrices related as $\mathbf{W}_1 = \mathbf{W}_2 + o_p(1)$ give the same asymptotic performance. This implies that in the following we can consider the "limit" of (3.52) in lieu of $\hat{\mathbf{W}}_{\mathrm{M2}}$. In what follows, let $\mathbf{W}_{\mathrm{M2}}$ denote $\hat{\mathbf{W}}_{\mathrm{M2}}$ evaluated in $\boldsymbol{\theta}_0$ and for infinite data. Thus, if we can show that

$$\mathbf{W}_{\mathrm{M2}} \propto \mathbf{W}_{\mathrm{GWSF}}$$

then we have proven that MAPprox2 has the same asymptotic performance as GWSF, and hence that MAPprox2 is asymptotically efficient. (The symbol $\propto$ denotes equality up to a multiplicative scalar constant.) Combining (3.25), (A.19), and (A.21) it is immediately clear that $\mathbf{W}_{\mathrm{M2}} = \mathbf{W}_{\mathrm{GWSF}}$.

In this section, the MAPprox cost function was approximated so as to retain the local properties that affect the estimation error variance. The approximation (MAPprox2) was then shown to coincide with the GWSF cost function (with a "consistent" estimate of the weighting matrix), and hence it can be concluded that MAPprox(2) provides minimum variance estimates of the DOAs. However, the MAPprox cost function depends on $\boldsymbol{\theta}$ in quite a complicated manner. In Section 3.8 we compare MAPprox2 and GWSF by means of several simulations, and the strong similarities between these two approaches are clearly visible. Since the implementation of GWSF is much easier, its use is preferred.

3.8 Simulation Examples

In this section, we illustrate the findings of this chapter by means of simulation examples. The MAP-NSF, MAPprox2 and GWSF methods are compared with one another, as well as with methods like WSF (MODE) that do not take the array perturbations into account. In [VS94a], the asymptotic performance of WSF was analyzed for the case under study. Unfortunately, the result given in that paper contains a printing error and, therefore, we provide the following result.

Theorem 3.3. *Let $\hat{\boldsymbol{\theta}}_{WSF}$ be the minimizing argument of $V_{WSF}(\boldsymbol{\theta}) = V_{WSF}(\boldsymbol{\theta}, \boldsymbol{\rho}_0)$, where $V_{WSF}(\boldsymbol{\theta}, \boldsymbol{\rho})$ is given in* (3.3)*. Then*

$$\sqrt{N}(\hat{\boldsymbol{\theta}}_{WSF} - \boldsymbol{\theta}_0) \in \mathrm{AsN}(\mathbf{0}, \mathbf{C}_{WSF}),$$

where

$$\mathbf{C}_{WSF} = \frac{\sigma^2}{2}\mathbf{C}^{-1} + \mathbf{C}^{-1}\mathbf{F}_{\boldsymbol{\theta}}^T\bar{\boldsymbol{\Omega}}\mathbf{F}_{\boldsymbol{\theta}}\mathbf{C}^{-1}. \tag{3.53}$$

Proof. Since WSF is a special case of GWSF, the result follows from the analysis in Section 3.5. Indeed, if in GWSF we use the weighting $\mathbf{W} = \bar{\mathbf{L}}^{-1}$ (which makes $V_{\mathrm{GWSF}} \propto V_{\mathrm{WSF}}$) then $\mathbf{C}_{\mathrm{WSF}} = \mathbf{H}^{-1}\mathbf{Q}\mathbf{H}^{-1}$, where $\mathbf{H}$ and $\mathbf{Q}$ are given in (A.16) and (A.17), respectively. □

It can be seen from the expression (3.53) that the first term corresponds to the CRB for the case with no model errors. The second term in (3.53) reflects the performance degradation of WSF due to model errors.

3.8.1 Example 1

Consider a uniform linear array consisting of $m = 10$ sensors separated by a half wavelength. Two signals impinge from the directions $\boldsymbol{\theta}_0 = [0^\circ\ 5^\circ]^T$ relative to broadside. The signals are uncorrelated and the SNR is 5 dB:

$$\mathbf{P}/\sigma^2 = 10^{5/10}\mathbf{I}_2.$$

The nominal unit gain sensors are perturbed by additive Gaussian random variables with variance 0.01. This corresponds to an uncertainty in the gain with a standard deviation of 10%. Figure 3.1 depicts the root-mean-square (RMS) error versus the sample size for different methods. (Only the RMS values for $\boldsymbol{\theta}_1$ are displayed; the results corresponding to $\boldsymbol{\theta}_2$ are similar.) In Figure 3.1 and in the graphs that follow, we show simulation results using different symbols, while the theoretical results are displayed by lines. The empirical RMS values are computed from 1000 independent trials in all simulations. The MAP-NSF and MAPprox2 cost functions are minimized with Newton-type methods initialized by the WSF estimate. WSF (or, equivalently, MODE [SS90a]) is implemented in the "rooting form" described in [SS90b] (see Section 2.4). The GWSF method is implemented as described in Section 3.6.2. In the examples presented here, we reiterated the third step of the algorithm three times. The poor performance of MAP-NSF in Figure 3.1 is due to two

Figure 3.1: RMS errors for $\boldsymbol{\theta}_1$ versus N.

main reasons. First, MAP-NSF fails to resolve the two signals in many cases. Second, the numerical search is sometimes trapped in a local minima. The performance of GWSF and MAPprox2 is excellent and close to the accuracy predicted by the asymptotic analysis. However, the numerical minimization of the MAPprox2 cost function is complicated. In this example, MAPprox2 produced "outliers" in about five percent of the 1000 trials. These outliers were removed before the RMS value for MAPprox2 was calculated. For small N, GWSF and WSF have a similar performance since the finite sample effects dominate. However, for larger N (when calibration errors affect the performance), it can be seen that GWSF and MAPprox2 are significantly better than the standard WSF method.

Figure 3.2: RMS errors for $\boldsymbol{\theta}_1$ versus the variance of the uncertainty in the gain of the sensors.

3.8.2 Example 2

Here, we have the same set-up as in the previous example, but the sample size is fixed to $N = 200$ and the variance of the gain uncertainty is varied. In Figure 3.2, the RMS errors for $\boldsymbol{\theta}_1$ are plotted versus the variance of the sensor gains. The curve denoted by CRB in Figure 3.2 is the Cramér-Rao lower bound for the case with no model errors; that is, CRB = $\sigma^2 \mathbf{C}^{-1}/2N$. Notice that GWSF and MAPprox2 begin to differ for large model errors. Indeed, the equivalence of GWSF and MAPprox shown in Section 3.7 holds for large N and small model errors. The three methods (GWSF, MAPprox2 and MAP-NSF) are known to be asymptotically efficient estimators for this case only; the performance for large model errors is not predicted by the theory in this chapter.

3.8.3 Example 3

This example involves uncertainty in the phase response of the sensors and is taken from [WOV91]. Two plane waves are incident on a uniform linear array of $m = 6$ sensors with half wavelength inter-element spacing. The signals are uncorrelated and 10 dB above the noise, and have DOAs $\boldsymbol{\theta}_0 = [0^\circ \ 10^\circ]^T$ relative to broadside. The uncertainty in the phase of the sensors is modeled by adding uncorrelated zero-mean Gaussian random variables with covariance

$$\boldsymbol{\Omega} = 10^{-3} \begin{bmatrix} 10 & 0 & 0 & 0 & 0 & 0 \\ 0 & 1 & 0 & 0 & 0 & 0 \\ 0 & 0 & 1 & 0 & 0 & 0 \\ 0 & 0 & 0 & 1 & 0 & 0 \\ 0 & 0 & 0 & 0 & 1 & 0 \\ 0 & 0 & 0 & 0 & 0 & 10 \end{bmatrix}$$

to the nominal phase, which is zero for all sensors. RMS errors for $\boldsymbol{\theta}_1$ are shown in Figure 3.3. It appears that MAP-NSF has a higher small sample threshold than GWSF and MAPprox2. For large samples, the performance of the methods is similar. Again, it is clearly useful to take the array uncertainty into account when designing the estimator.

3.8.4 Example 4

Here, we consider the same set-up as in the previous example, but the signals are correlated. More precisely, the signal covariance matrix is

$$\mathbf{P} = 10 \begin{bmatrix} 1 & -0.99 \\ -0.99 & 1 \end{bmatrix}$$

and the noise variance is $\sigma^2 = 1$. The RMS errors for $\boldsymbol{\theta}_1$ are shown in Figure 3.4. It can be seen that the two *signal* subspace fitting methods GWSF and WSF can resolve the two signals, while the *noise* subspace fitting method MAP-NSF has a much higher threshold.

3.9 Conclusions

This chapter has studied the problem of developing robust weighted signal subspace fitting algorithms for arrays with calibration errors. It was shown that if the second-order statistics of the calibration errors

Figure 3.3: RMS errors for $\boldsymbol{\theta}_1$ versus the number of snapshots, N.

are known, then asymptotically statistically efficient weightings can be derived for very general perturbation models. Earlier research had resulted in optimal weightings that were applicable only for very special cases. The GWSF technique derived herein unifies earlier work and also enjoys several advantages over the MAP-NSF approach, another statistically efficient technique developed for calibration errors. In particular, since GWSF is based on the signal rather than noise subspace, it is a consistent estimator even when the signals are perfectly coherent, and has better finite sample performance than MAP-NSF when the signals are highly correlated or closely spaced. In addition, unlike MAP-NSF, when the array is nominally uniform and linear, the GWSF criterion can be re-parameterized in such a way that the directions of arrival may be solved for by rooting a polynomial rather than via a gradient search. As a byproduct of our analysis, we also demonstrated the asymptotic statistical efficiency of the MAPprox algorithm, another robust DOA estimator for perturbed arrays. While the MAPprox and GWSF estimators have a

Figure 3.4: RMS errors for $\boldsymbol{\theta}_1$ versus the number of snapshots, N.

very similar performance, GWSF depends on the parameters in a simpler way than MAPprox and this facilitates the implementation. Our simulations indicate that, in the presence of calibration errors with known statistics, both algorithms can yield a significant performance improvement over techniques that ignore such errors.

Chapter 4

A Direction Estimator for Uncorrelated Emitters

In this chapter, a novel eigenstructure-based method for direction estimation is presented. The method assumes that the emitter signals are uncorrelated. Ideas from subspace and covariance matching methods are combined to yield a non-iterative estimation algorithm when a uniform linear array is employed. The large sample performance of the estimator is analyzed. It is shown that the asymptotic variance of the direction estimates coincides with the relevant Cramér-Rao lower bound (CRB). A compact expression for the CRB is derived for the case when it is known that the signals are uncorrelated, and it is lower than the CRB usually used in the array processing literature (assuming no particular structure for the signal covariance matrix). The difference between the two CRBs can be large in difficult scenarios. This implies that, in such scenarios, the proposed method has significantly better performance than existing subspace methods such as, for example, WSF, MUSIC and ESPRIT. Numerical examples are provided to illustrate the obtained results.

4.1 Introduction

The problem of estimating the directions of arrival (DOAs) of signals from array data is well documented in the literature. A number of high resolution algorithms or eigenstructure methods have been presented and analyzed (see, e.g., [VO91, Sch81, RK89, SS90a, SS91, BM86, RH89,

SN89b]). In some applications, such as, radio astronomy, communications etc., it is reasonable to assume that the signals are spatially uncorrelated. One disadvantage with eigenstructure or, so-called, subspace based methods is that it is difficult to incorporate prior knowledge of the signal correlation into the eigendecomposition. Hence, it is difficult to use this prior information to increase the estimation accuracy.

Herein, we propose an estimator which combines ideas from subspace and covariance matching methods [TO96, WSW95] which makes it possible to incorporate prior knowledge of the signal correlation into the estimator. It should be noted that the Cramér-Rao lower bound (CRB) usually used when comparing estimators in array signal processing is not the proper one in this scenario. As will be shown here, the CRB that should be used to compare estimators that use priors on the source correlation is in general lower than that presented in, e.g., [SN89a, VO91]. We derive the relevant CRB for the case under study and give a compact matrix expression for the CRB on the DOA parameters. It is also shown that the proposed method yields estimates that asymptotically attain this CRB on the estimation error covariance.

The proposed estimator is based on a weighted least squares fit of certain elements in the eigendecomposition of the output covariance of the array. In general, this leads to a multi-modal cost function which has to be minimized with some multi-dimensional search technique. This will, of course, lead to a computationally rather unattractive problem. However, for the common special case of a uniform linear array (ULA), the cost function can be reparameterized in a similar manner as in MODE and IQML [SS90b, SS90a, BM86] (see also [JGO97b]). In this case, the estimates of the directions can be found from the roots of a certain polynomial. This leads to a significant computational simplification. Note that a similar reparameterization and "non-iterative" scheme has not yet been found for maximum-likelihood (ML) or covariance matching techniques. Thus, the presented method has the important property to yield a non-iterative solution with the same asymptotic accuracy as ML.

This chapter is organized as follows. In Section 4.2, the model and assumptions are given. In Section 4.3, we present the DOA estimator. In Section 4.4, the Cramér-Rao bound for uncorrelated sources is derived. The proposed estimator is analyzed in Section 4.5, where the large sample properties of the estimates are derived. In Section 4.5, we also derive the optimal weighting matrix leading to minimum variance estimates of the DOA. The numerical implementation of the method when a ULA is employed, is discussed in Section 4.6. Numerical examples are provided in

Section 4.7, to demonstrate the performance of the proposed algorithm. Finally, some conclusions are given in Section 4.8.

4.2 Data Model and Assumptions

Consider d uncorrelated, narrow-band, plane waves impinging on an unambiguous array consisting of m sensors. The spatial response of the array is assumed to be parameterized by the directions of arrival, $\boldsymbol{\theta} = [\theta_1, \ldots, \theta_d]^T$. The functional form of the array response vector, $\mathbf{a}(\theta)$, is assumed to be known. This scenario is described by the model

$$\mathbf{x}(t) = \mathbf{A}(\boldsymbol{\theta})\mathbf{s}(t) + \mathbf{n}(t),$$

where the array response matrix, $\mathbf{A}(\boldsymbol{\theta}) = [\mathbf{a}(\theta_1), \ldots, \mathbf{a}(\theta_d)]$, is the collection of the array response vectors. The source signals, $\mathbf{s}(t)$, and the additive noise, $\mathbf{n}(t)$, are assumed to be zero-mean Gaussian random sequences with second-order moments given by

$$\begin{aligned} \mathrm{E}\{\mathbf{s}(t)\mathbf{s}^{\mathrm{T}}(\tau)\} &= \mathbf{0}, \qquad \mathrm{E}\{\mathbf{n}(t)\mathbf{n}^{\mathrm{T}}(\tau)\} = \mathbf{0}, \\ \mathrm{E}\{\mathbf{s}(t)\mathbf{s}^{*}(\tau)\} &= \mathbf{P}\delta_{t,\tau}, \ \mathrm{E}\{\mathbf{n}(t)\mathbf{n}^{*}(\tau)\} = \sigma^2\mathbf{I}\delta_{t,\tau}, \end{aligned}$$

where δ is the Kronecker delta function, and where the superscripts T and $*$ stand for transposition and complex conjugate transposition, respectively. For later use, we also introduce the superscript c for complex conjugation. Notice that, since the sources are assumed to be spatially uncorrelated, the signal covariance matrix, $\mathbf{P}$, is diagonal. With the definitions above and under the assumption that $\mathbf{s}(t)$ and $\mathbf{n}(t)$ are uncorrelated, the output covariance matrix of the array is given by

$$\mathbf{R} = \mathrm{E}\{\mathbf{x}(t)\mathbf{x}^{*}(t)\} = \mathbf{A}(\boldsymbol{\theta})\mathbf{P}\mathbf{A}^{*}(\boldsymbol{\theta}) + \sigma^2\mathbf{I} \ . \tag{4.1}$$

It is further assumed that the number of signals is known, or has been consistently estimated [VOK91a, Wax92].

4.3 Estimating the Parameters

The problem under consideration is that of estimating the unknown parameters in (4.1) from sensor array data. Of main interest are the DOAs, $\boldsymbol{\theta}$. The estimation procedure should use the prior knowledge that the signals are uncorrelated to increase the estimation accuracy.

The subspace estimation techniques rely on the properties of the eigendecomposition of the output covariance matrix $\mathbf{R}$. Let

$$\mathbf{R} = \mathbf{E}_s \mathbf{\Lambda}_s \mathbf{E}_s^* + \mathbf{E}_n \mathbf{\Lambda}_n \mathbf{E}_n^* = \mathbf{E}_s \mathbf{\Lambda}_s \mathbf{E}_s^* + \sigma^2 \mathbf{E}_n \mathbf{E}_n^* \tag{4.2}$$

be a partitioned eigendecomposition of $\mathbf{R}$. Here, $\mathbf{\Lambda}_s$ is a diagonal matrix containing the $d < m$ largest eigenvalues and the columns of $\mathbf{E}_s$ are the corresponding eigenvectors. We will assume that the eigenvalues in $\mathbf{\Lambda}_s$ are distinct, which is generically true. Similarly, $\mathbf{\Lambda}_n$ contains the $m - d$ smallest eigenvalues and $\mathbf{E}_n$ is composed of the remaining eigenvectors. The fact that $\mathbf{\Lambda}_n = \sigma^2 \mathbf{I}$ follows from the assumption that $\mathbf{A}$ is full rank and since $\mathbf{P}$ is positive definite. Comparing (4.1) and (4.2) gives

$$\mathbf{A}\mathbf{P}\mathbf{A}^* = \mathbf{E}_s \mathbf{\Lambda}_s \mathbf{E}_s^* + \sigma^2 \mathbf{E}_n \mathbf{E}_n^* - \sigma^2 \mathbf{I} = \mathbf{E}_s \mathbf{\Lambda} \mathbf{E}_s^*, \tag{4.3}$$

where the definition

$$\mathbf{\Lambda} = \mathbf{\Lambda}_s - \sigma^2 \mathbf{I}$$

has been used. The last step in (4.3) follows from the fact that $\mathbf{E}_n \mathbf{E}_n^* = \mathbf{I} - \mathbf{E}_s \mathbf{E}_s^*$. Applying the vectorization operator (vec) [Gra81] on (4.3), we obtain[1]

$$(\mathbf{A}^{\mathrm{c}} \otimes \mathbf{A}) \operatorname{vec}(\mathbf{P}) = (\mathbf{E}_s^{\mathrm{c}} \otimes \mathbf{E}_s) \operatorname{vec}(\mathbf{\Lambda}), \tag{4.4}$$

where $\otimes$ denotes the Kronecker matrix product. Since the matrices $\mathbf{P}$ and $\mathbf{\Lambda}$ are diagonal, there exists a $(d^2 \times d)$ selection matrix $\mathbf{L}$ such that

$$\operatorname{vec}(\mathbf{P}) = \mathbf{L}\mathbf{p} \quad \text{and} \quad \operatorname{vec}(\mathbf{\Lambda}) = \mathbf{L}\boldsymbol{\lambda} \ ,$$

where $\mathbf{p}$ and $\boldsymbol{\lambda}$ are $(d \times 1)$ vectors consisting of the diagonal entries of $\mathbf{P}$ and $\mathbf{\Lambda}$, respectively. Notice that

$$(\mathbf{A}^{\mathrm{c}} \otimes \mathbf{A})\, \mathbf{L} = (\mathbf{A}^{\mathrm{c}} \circ \mathbf{A}) \ ,$$

where $\circ$ is the Khatri-Rao matrix product, which is a column-wise Kronecker product [Bre78]. The relation in (4.4) will now be used to formulate an estimator of the DOA.

Let $\hat{\mathbf{R}}$ denote the sample estimate of the covariance matrix in (4.1); i.e.,

$$\hat{\mathbf{R}} = \frac{1}{N} \sum_{t=1}^{N} \mathbf{x}(t) \mathbf{x}^*(t),$$

[1] $\operatorname{vec}(\mathbf{ABC}) = (\mathbf{C}^{\mathrm{T}} \otimes \mathbf{A}) \operatorname{vec}(\mathbf{B})$

where N is the number of snapshots. Let

$$\hat{\mathbf{R}} = \hat{\mathbf{E}}_s \hat{\mathbf{\Lambda}}_s \hat{\mathbf{E}}_s^* + \hat{\mathbf{E}}_n \hat{\mathbf{\Lambda}}_n \hat{\mathbf{E}}_n^*$$

be an eigendecomposition of $\hat{\mathbf{R}}$, similar to (4.2). A consistent estimate of the noise variance is given by

$$\hat{\sigma}^2 = \frac{1}{m-d} \operatorname{Tr}\{\hat{\mathbf{\Lambda}}_n\} = \frac{1}{m-d} \left[\operatorname{Tr}\{\hat{\mathbf{R}}\} - \operatorname{Tr}\{\hat{\mathbf{\Lambda}}_s\} \right].$$

Replacing $\mathbf{E}_s$ and $\mathbf{\Lambda}$ in (4.4) by $\hat{\mathbf{E}}_s$ and $\hat{\mathbf{\Lambda}} = \hat{\mathbf{\Lambda}}_s - \hat{\sigma}^2 \mathbf{I}$ yields

$$(\mathbf{A}^{\mathrm{c}} \circ \mathbf{A})\, \mathbf{p} \approx \left(\hat{\mathbf{E}}_s^{\mathrm{c}} \circ \hat{\mathbf{E}}_s \right) \hat{\boldsymbol{\lambda}} \ . \tag{4.5}$$

Using the definitions

$$\begin{aligned} \mathbf{B}(\boldsymbol{\theta}) &= (\mathbf{A}^{\mathrm{c}}(\boldsymbol{\theta}) \circ \mathbf{A}(\boldsymbol{\theta})) = \left[(\mathbf{a}^{\mathrm{c}}(\theta_1) \otimes \mathbf{a}(\theta_1)) \quad \dots \quad (\mathbf{a}^{\mathrm{c}}(\theta_d) \otimes \mathbf{a}(\theta_d)) \right] \\ &= \left[\operatorname{vec}(\mathbf{a}(\theta_1)\mathbf{a}^*(\theta_1)) \quad \dots \quad \operatorname{vec}(\mathbf{a}(\theta_d)\mathbf{a}^*(\theta_d)) \right], \qquad (4.6) \\ \hat{\mathbf{f}} &= \left(\hat{\mathbf{E}}_s^{\mathrm{c}} \circ \hat{\mathbf{E}}_s \right) \hat{\boldsymbol{\lambda}}, \qquad (4.7) \end{aligned}$$

we can, from (4.5), formulate the least squares problem

$$\min_{\boldsymbol{\theta},\, \mathbf{p}} \|\hat{\mathbf{f}} - \mathbf{B}(\boldsymbol{\theta})\mathbf{p}\|_2^2. \tag{4.8}$$

For fixed $\boldsymbol{\theta}$, the solution of (4.8) with respect to $\mathbf{p}$ is

$$\hat{\mathbf{p}} = \mathbf{B}^{\dagger}(\boldsymbol{\theta})\hat{\mathbf{f}}, \tag{4.9}$$

where $\mathbf{B}^{\dagger} = (\mathbf{B}^*\mathbf{B})^{-1}\mathbf{B}^*$ denotes the Moore-Penrose pseudo-inverse of $\mathbf{B}$. By substituting $\hat{\mathbf{p}}$ back into (4.8), we get

$$\min_{\boldsymbol{\theta}} \|\hat{\mathbf{f}} - \mathbf{B}(\boldsymbol{\theta})\mathbf{B}^{\dagger}(\boldsymbol{\theta})\hat{\mathbf{f}}\|_2^2 = \min_{\boldsymbol{\theta}} \|\mathbf{\Pi}^{\perp}_{\mathbf{B}(\boldsymbol{\theta})}\hat{\mathbf{f}}\|_2^2, \tag{4.10}$$

where $\mathbf{\Pi}^{\perp}_{\mathbf{B}(\boldsymbol{\theta})} = \mathbf{I} - \mathbf{B}(\boldsymbol{\theta})\mathbf{B}^{\dagger}(\boldsymbol{\theta})$. In general, we will use the notation $\mathbf{\Pi}^{\perp}_{\mathbf{X}}$ for the orthogonal projection onto the null-space of $\mathbf{X}^*$. Similarly, $\mathbf{\Pi}_{\mathbf{X}} = \mathbf{I} - \mathbf{\Pi}^{\perp}_{\mathbf{X}}$ will denote the orthogonal projection onto the range-space of $\mathbf{X}$. An estimate of $\boldsymbol{\theta}$ can be obtained by minimizing the criterion in (4.10) (see [GJO96]). However, it is useful to introduce a weighting in

the criterion to improve the accuracy of the estimates. More precisely, we suggest to estimate $\boldsymbol{\theta}$ as

$$\hat{\boldsymbol{\theta}} = \arg\min_{\boldsymbol{\theta}} V(\boldsymbol{\theta}) \tag{4.11}$$

$$V(\boldsymbol{\theta}) = \|\boldsymbol{\Pi}^{\perp}_{\mathbf{B}(\boldsymbol{\theta})}\hat{\mathbf{f}}\|^2_{\mathbf{W}} = \hat{\mathbf{f}}^*\boldsymbol{\Pi}^{\perp}_{\mathbf{B}(\boldsymbol{\theta})}\mathbf{W}\boldsymbol{\Pi}^{\perp}_{\mathbf{B}(\boldsymbol{\theta})}\hat{\mathbf{f}} \ , \tag{4.12}$$

where $\mathbf{W}$ is a Hermitian positive definite weighting matrix yet to be determined (see Section 4.5).

Remark 4.1. It is readily shown that $\hat{\mathbf{p}}$ in (4.9) is real valued by making use of the results in Appendix A.8. However, $\hat{\mathbf{p}}$ is not guaranteed to be positive for small N. For large N, this is not a problem since $\hat{\mathbf{p}}$ is a consistent estimate of $\mathbf{p}$. This implies that $\hat{\mathbf{p}}$ is positive for sufficiently large N and the large sample performance of the estimates is not affected.

Minimizing (4.12) to obtain the estimates $\hat{\boldsymbol{\theta}}$ can be accomplished with a Newton-type algorithm. The gradient and Hessian of the cost function, needed in such an implementation, are given as by-products in the statistical analysis of the estimator in Section 4.5. The criterion is in general multi-modal, rendering the multi-dimensional search for a global extremum computationally expensive. However, when a ULA is employed it is possible to reparameterize the criterion and convert it to a linear problem, where the estimate is obtained by rooting a polynomial. This is further discussed in Section 4.6, where the reparameterization is shown in detail.

4.4 The CRB for Uncorrelated Sources

The Cramér-Rao bound (CRB) is a commonly used lower bound on the estimation error covariance of any unbiased estimator [Cra46]. Let $\boldsymbol{\eta} = [\boldsymbol{\theta}^{\mathrm{T}}, \mathbf{p}^{\mathrm{T}}, \sigma^2]^{\mathrm{T}}$ denote the vector that parameterizes the covariance matrix $\mathbf{R}$. Notice that we here will derive the CRB when it is known that the emitter signals are uncorrelated. When the asymptotic estimation error covariance of an estimator is equal to the CRB it is referred to as being asymptotically statistically efficient. We are mainly interested in the bound on the direction parameters $\boldsymbol{\theta}$. Let us denote this bound by $\mathrm{CRB}_{\boldsymbol{\theta}}$. We can now formulate the following result:

Theorem 4.1. *Under the assumptions given in Section 4.2, the Cramér-Rao lower bound on the estimation error covariance for any unbiased*

estimate of $\boldsymbol{\theta}$ *is*

$$\mathrm{CRB}_{\boldsymbol{\theta}} = \left(\mathbf{P}\mathbf{D}^*\mathbf{G}(\mathbf{G}^*\tilde{\mathbf{C}}\mathbf{G})^{-1}\mathbf{G}^*\mathbf{D}\mathbf{P}\right)^{-1}. \tag{4.13}$$

Here,

$$\tilde{\mathbf{C}} = \left(\mathbf{R}^{\mathrm{T}} \otimes \mathbf{R}\right) + \frac{\sigma^4}{m-d}\,\mathrm{vec}(\mathbf{\Pi}_{\mathbf{A}})\,\mathrm{vec}^*(\mathbf{\Pi}_{\mathbf{A}}), \tag{4.14}$$

$$\mathbf{D} = \left(\bar{\mathbf{D}}^{\mathrm{c}} \circ \mathbf{A}\right) + \left(\mathbf{A}^{\mathrm{c}} \circ \bar{\mathbf{D}}\right), \tag{4.15}$$

$$\bar{\mathbf{D}} = \begin{bmatrix} \frac{\partial \mathbf{a}(\theta_1)}{\partial \theta_1} & \cdots & \frac{\partial \mathbf{a}(\theta_d)}{\partial \theta_d} \end{bmatrix}, \tag{4.16}$$

and $\mathbf{G}$ *is any matrix whose columns span the null-space of* $\mathbf{B}^*$ *(see also Section 4.6).*

Proof. The proof is given in Appendix A.5. □

The CRB for the "standard" case, when $\mathbf{P}$ is any Hermitian positive definite matrix is, e.g., given in [SN89a, VO91]. A comparison of (4.13) with the corresponding CRB-expressions in [SN89a, VO91] can be used to quantify the gain in performance of using the prior information about the signal correlation. An example of such a comparison is given in Section 4.7.

4.5 Asymptotic Analysis

The asymptotic (in N) behavior of the estimates given by (4.11) is analyzed in this section. The derivation of the estimator in Section 4.3 is rather ad hoc. However, below we show that the estimator in fact is asymptotically statistically efficient. We will start the asymptotic analysis by establishing the consistency of the estimates.

4.5.1 Consistency

In what follows, we use $\boldsymbol{\theta}_0$ to distinguish the true DOA vector from a generic vector $\boldsymbol{\theta}$. Notice that $\hat{\mathbf{f}}$ converges to

$$\mathbf{f} = (\mathbf{E}_s^{\mathrm{c}} \circ \mathbf{E}_s)\,\boldsymbol{\lambda} = (\mathbf{A}^{\mathrm{c}}(\boldsymbol{\theta}_0) \circ \mathbf{A}(\boldsymbol{\theta}_0))\,\mathbf{p} = \mathbf{B}(\boldsymbol{\theta}_0)\mathbf{p}$$

with probability one as $N \to \infty$. Since the norm of $\mathbf{\Pi}^{\perp}_{\mathbf{B}(\boldsymbol{\theta})}$ is bounded, the criterion (4.12) tends to

$$\bar{V} = \mathbf{f}^*\mathbf{\Pi}^{\perp}_{\mathbf{B}(\boldsymbol{\theta})}\mathbf{W}\mathbf{\Pi}^{\perp}_{\mathbf{B}(\boldsymbol{\theta})}\mathbf{f}$$

uniformly in $\boldsymbol{\theta}$ with probability one. The consistency of $\hat{\boldsymbol{\theta}}$ in (4.11) then follows if $\boldsymbol{\theta} = \boldsymbol{\theta}_0$ is the unique solution to $\bar{V} = 0$. Notice that $\bar{V} = 0$ if and only if $\boldsymbol{\Pi}^{\perp}_{\mathbf{B}(\boldsymbol{\theta})}\mathbf{f} = \boldsymbol{\Pi}^{\perp}_{\mathbf{B}(\boldsymbol{\theta})}\mathbf{B}(\boldsymbol{\theta}_0)\mathbf{p} = \mathbf{0}$ since $\mathbf{W} > \mathbf{0}$ by assumption. Assume that (without loss of generality), the first n DOAs are equal but not all; that is, $\theta_i = \theta_{0_i}$ for $i = 1, \ldots, n$, where $0 \leq n < d$. Then

$$\begin{aligned}\boldsymbol{\Pi}^{\perp}_{\mathbf{B}(\boldsymbol{\theta})}\mathbf{f} &= \boldsymbol{\Pi}^{\perp}_{\mathbf{B}(\boldsymbol{\theta})}\begin{bmatrix}\mathbf{B}_1 & \mathbf{B}_2\end{bmatrix}\begin{bmatrix}\mathbf{p}_1 \\ \mathbf{p}_2\end{bmatrix} = \boldsymbol{\Pi}^{\perp}_{\mathbf{B}(\boldsymbol{\theta})}\mathbf{B}_2\mathbf{p}_2 \\ &= \underbrace{\begin{bmatrix}\mathbf{B}_2 & \mathbf{B}(\boldsymbol{\theta})\end{bmatrix}}_{2d-n}\begin{bmatrix}\mathbf{I}_{d-n} \\ -\mathbf{B}^{\dagger}(\boldsymbol{\theta})\mathbf{B}_2\end{bmatrix}\mathbf{p}_2,\end{aligned}$$

where $\mathbf{B}_1$ and $\mathbf{B}_2$ contain the first n and the last $d-n$ columns of $\mathbf{B}(\boldsymbol{\theta}_0)$, respectively, and where $\mathbf{p}$ has been partitioned accordingly. In Appendix A.6 it is proved that $\begin{bmatrix}\mathbf{B}_2 & \mathbf{B}(\boldsymbol{\theta})\end{bmatrix}$ is full rank if $m > (2d-n)/2$. This condition is satisfied for all admissible n if $m > d$. Clearly, the only solution to $\boldsymbol{\Pi}^{\perp}_{\mathbf{B}(\boldsymbol{\theta})}\mathbf{f} = \mathbf{0}$ is $\mathbf{p}_2 = \mathbf{0}$, which contradicts the fact that $\mathbf{p}$ consists of the signal powers. Thus, the only valid solution is $\boldsymbol{\theta} = \boldsymbol{\theta}_0$ and strong consistency of the estimates follows.

Remark 4.2. The identifiability condition $d < m$ is natural if no additional assumptions are made. Consider, for example, the case of a ULA for which $\mathbf{A}(\boldsymbol{\theta})$ is a Vandermonde matrix. The array covariance matrix (4.1) is then a Toeplitz matrix since $\mathbf{P}$ is diagonal. It is well known from the Carathéodory parameterization that any Hermitian, positive definite, Toeplitz matrix can be written in the form

$$\mathbf{R} = \mathbf{APA}^* + \sigma^2\mathbf{I},$$

with $d < m$ (see, e.g., [SM97]). This implies that if $d \geq m$ signals are received by the array, then it cannot be distinguished from another scenario with $d < m$ (based on the information in $\mathbf{R}$). On the other hand, for particular array geometries, it is possible to estimate more signals than the number of sensors ($d \geq m$) under the assumption of uncorrelated emitter signals (see, e.g., [PPL90]).

4.5.2 Asymptotic Distribution

After establishing consistency, the asymptotic distribution of the estimates from (4.11) can be derived through a Taylor series expansion approach (see, e.g., [VO91, SS89]). Let $V'(\boldsymbol{\theta})$ and $V''(\boldsymbol{\theta})$ denote the gradient and the Hessian of $V(\boldsymbol{\theta})$, respectively. By definition $V'(\hat{\boldsymbol{\theta}}) = \mathbf{0}$, and since

$\hat{\boldsymbol{\theta}}$ is consistent, a first order Taylor series expansion of $V'(\hat{\boldsymbol{\theta}})$ around $\boldsymbol{\theta}_0$ leads to

$$\tilde{\boldsymbol{\theta}} = \hat{\boldsymbol{\theta}} - \boldsymbol{\theta}_0 \simeq -\mathbf{H}^{-1} V'(\boldsymbol{\theta}_0), \tag{4.17}$$

where $\simeq$ denotes equality in probability up to first order. The notation $\mathbf{H}$ refers to the limiting Hessian matrix,

$$\mathbf{H} = \lim_{N\to\infty} V''(\boldsymbol{\theta}_0) \ . \tag{4.18}$$

The derivative of (4.12) with respect to θ_k (i.e., the kth element in the parameter vector $\boldsymbol{\theta}$) is given by

$$\begin{aligned} V'_k &= \hat{\mathbf{f}}^* \{\boldsymbol{\Pi}_{\mathbf{B}}^{\perp}\}_k \mathbf{W} \boldsymbol{\Pi}_{\mathbf{B}}^{\perp} \hat{\mathbf{f}} + \hat{\mathbf{f}}^* \boldsymbol{\Pi}_{\mathbf{B}}^{\perp} \mathbf{W} \{\boldsymbol{\Pi}_{\mathbf{B}}^{\perp}\}_k \hat{\mathbf{f}} \\ &\simeq -2\,\mathrm{Re}\{\mathbf{f}^* \mathbf{B}^{\dagger *} \mathbf{B}_k^* \boldsymbol{\Pi}_{\mathbf{B}}^{\perp} \mathbf{W} \boldsymbol{\Pi}_{\mathbf{B}}^{\perp} \hat{\mathbf{f}}\}, \end{aligned} \tag{4.19}$$

where, for notational simplicity, the argument $(\boldsymbol{\theta}_0)$ is omitted. In (4.19), we made use of the following expression for the derivative of the projection matrix:

$$\{\boldsymbol{\Pi}_{\mathbf{B}}^{\perp}\}_k = -\boldsymbol{\Pi}_{\mathbf{B}}^{\perp} \mathbf{B}_k \mathbf{B}^{\dagger} - \mathbf{B}^{\dagger *} \mathbf{B}_k^* \boldsymbol{\Pi}_{\mathbf{B}}^{\perp} \ . \tag{4.20}$$

We have also used the fact that $\hat{\mathbf{f}} \to \mathbf{f}$ as $N \to \infty$ and $\boldsymbol{\Pi}_{\mathbf{B}}^{\perp} \mathbf{f} = \mathbf{0}$. Next, we will relate $\hat{\mathbf{f}}$ to the sample covariance. From the definition of $\hat{\mathbf{f}}$ in (4.7), we have

$$\begin{aligned} \hat{\mathbf{f}} &= \mathrm{vec}\left(\hat{\mathbf{E}}_s (\hat{\boldsymbol{\Lambda}}_s - \hat{\sigma}^2 \mathbf{I}) \hat{\mathbf{E}}_s^*\right) \\ &= \mathrm{vec}\left(\hat{\mathbf{R}} - \hat{\sigma}^2 \mathbf{I} - \hat{\mathbf{E}}_n (\hat{\boldsymbol{\Lambda}}_n - \hat{\sigma}^2 \mathbf{I}) \hat{\mathbf{E}}_n^*\right) \\ &= \mathrm{vec}\left(\hat{\mathbf{R}} - \hat{\sigma}^2 \mathbf{I} - \hat{\mathbf{E}}_n \hat{\mathbf{E}}_n^* (\hat{\mathbf{R}} - \hat{\sigma}^2 \mathbf{I}) \hat{\mathbf{E}}_n \hat{\mathbf{E}}_n^*\right) \\ &\simeq \mathrm{vec}\left(\hat{\mathbf{R}} - \hat{\sigma}^2 \mathbf{I} - \boldsymbol{\Pi}_{\mathbf{A}}^{\perp} (\hat{\mathbf{R}} - \hat{\sigma}^2 \mathbf{I}) \boldsymbol{\Pi}_{\mathbf{A}}^{\perp}\right) \\ &= \mathrm{vec}\left(\hat{\mathbf{R}} - \boldsymbol{\Pi}_{\mathbf{A}}^{\perp} \hat{\mathbf{R}} \boldsymbol{\Pi}_{\mathbf{A}}^{\perp} - \hat{\sigma}^2 \boldsymbol{\Pi}_{\mathbf{A}}\right) \ , \end{aligned} \tag{4.21}$$

where $\boldsymbol{\Pi}_{\mathbf{A}}^{\perp} = \mathbf{I} - \boldsymbol{\Pi}_{\mathbf{A}} = \boldsymbol{\Pi}_{\mathbf{A}(\boldsymbol{\theta}_0)}^{\perp}$. In (4.21), use is made of the facts that $\hat{\mathbf{E}}_n \hat{\mathbf{E}}_n^* \to \mathbf{E}_n \mathbf{E}_n^* = \boldsymbol{\Pi}_{\mathbf{A}}^{\perp}$ and $\boldsymbol{\Pi}_{\mathbf{A}}^{\perp}(\hat{\mathbf{R}} - \hat{\sigma}^2 \mathbf{I}) \to \mathbf{0}$ as $N \to \infty$. Recall that the noise variance is estimated as the average of the noise eigenvalues in

$\hat{\mathbf{\Lambda}}_n$ and notice that

$$\begin{aligned}(m-d)(\hat{\sigma}^2-\sigma^2) &= \mathrm{Tr}\{\hat{\mathbf{\Lambda}}_n - \sigma^2\mathbf{I}_{m-d}\} = \mathrm{Tr}\{\hat{\mathbf{E}}_n^*\left(\hat{\mathbf{R}}-\sigma^2\mathbf{I}_m\right)\hat{\mathbf{E}}_n\}\\ &= \mathrm{Tr}\{\hat{\mathbf{E}}_n\hat{\mathbf{E}}_n^*\left(\hat{\mathbf{R}}-\sigma^2\mathbf{I}_m\right)\hat{\mathbf{E}}_n\hat{\mathbf{E}}_n^*\}\\ &\simeq \mathrm{Tr}\{\mathbf{E}_n\mathbf{E}_n^*\left(\hat{\mathbf{R}}-\sigma^2\mathbf{I}_m\right)\mathbf{E}_n\mathbf{E}_n^*\}\\ &= \mathrm{Tr}\{\mathbf{\Pi}_{\mathbf{A}}^{\perp}\hat{\mathbf{R}}\}-(m-d)\sigma^2 \ ,\end{aligned}$$

where $\mathbf{I}_k$ denotes a $k\times k$ identity matrix. This implies that[2]

$$\hat{\sigma}^2 \simeq \frac{1}{m-d}\,\mathrm{Tr}\{\mathbf{\Pi}_{\mathbf{A}}^{\perp}\hat{\mathbf{R}}\} = \frac{1}{m-d}\,\mathrm{vec}^*(\mathbf{\Pi}_{\mathbf{A}}^{\perp})\,\mathrm{vec}(\hat{\mathbf{R}}) \ . \tag{4.22}$$

Using (4.22) in (4.21), we get

$$\begin{aligned}\hat{\mathbf{f}} &= \left[\mathbf{I}-\left(\mathbf{\Pi}_{\mathbf{A}}^{\perp\mathrm{T}}\otimes\mathbf{\Pi}_{\mathbf{A}}^{\perp}\right)-\frac{1}{m-d}\,\mathrm{vec}(\mathbf{\Pi}_{\mathbf{A}})\,\mathrm{vec}^*(\mathbf{\Pi}_{\mathbf{A}}^{\perp})\right]\mathrm{vec}(\hat{\mathbf{R}})\\ &\triangleq \mathbf{M}\,\mathrm{vec}(\hat{\mathbf{R}}).\end{aligned} \tag{4.23}$$

From the central limit theorem it follows that the elements in $\sqrt{N}(\hat{\mathbf{R}}-\mathbf{R})$ are asymptotically zero-mean Gaussian distributed. The relations (4.19), (4.17) and (4.23) then show that this holds for $\sqrt{N}V'(\boldsymbol{\theta}_0)$ and $\sqrt{N}\hat{\boldsymbol{\theta}}$ as well. We have

$$\sqrt{N}V'(\boldsymbol{\theta}_0) \in \mathrm{AsN}(\mathbf{0},\mathbf{Q}),$$

where

$$\mathbf{Q} = \lim_{N\to\infty} N\,\mathrm{E}\{V'V'^{\mathrm{T}}\}, \tag{4.24}$$

and where the notation AsN means asymptotically Gaussian distributed. The asymptotic second-order properties of $\tilde{\boldsymbol{\theta}}$ are given by the following result:

Theorem 4.2. *If $m>d$, then the estimate $\hat{\boldsymbol{\theta}}$ obtained from (4.11) is a consistent estimate of $\boldsymbol{\theta}_0$ and the normalized estimation error is asymptotically Gaussian distributed according to*

$$\sqrt{N}(\hat{\boldsymbol{\theta}}-\boldsymbol{\theta}_0) \in \mathrm{AsN}(\mathbf{0},\mathbf{\Gamma}),$$

[2] $\mathrm{Tr}\{\mathbf{AB}\} = \mathrm{vec}^*(\mathbf{A}^*)\,\mathrm{vec}(\mathbf{B})$

where

$$\mathbf{\Gamma} = \mathbf{H}^{-1}\mathbf{Q}\mathbf{H}^{-1} \ .$$

The matrices $\mathbf{H}$ *and* $\mathbf{Q}$ *are given by*

$$\mathbf{H} = 2\,\mathrm{Re}\{\mathbf{P}\mathbf{D}^*\mathbf{\Pi}_{\mathbf{B}}^{\perp}\mathbf{W}\mathbf{\Pi}_{\mathbf{B}}^{\perp}\mathbf{D}\mathbf{P}\}, \tag{4.25}$$

$$\mathbf{Q} = 2\,\mathrm{Re}\{\mathbf{U}^*\bar{\mathbf{C}}\mathbf{U}^{\mathrm{c}} + \mathbf{U}^*\mathbf{C}\mathbf{U}\}, \tag{4.26}$$

where

$$\mathbf{U} = \mathbf{\Pi}_{\mathbf{B}}^{\perp}\mathbf{W}\mathbf{\Pi}_{\mathbf{B}}^{\perp}\mathbf{D}\mathbf{P}, \tag{4.27}$$

and where $\mathbf{D}$ *is defined in* (4.15)*. The two covariance matrices* $\mathbf{C}$ *and* $\bar{\mathbf{C}}$ *are defined as*

$$\mathbf{C} = \lim_{N\to\infty} N\,\mathrm{E}\{\tilde{\mathbf{f}}\tilde{\mathbf{f}}^*\}, \tag{4.28}$$

$$\bar{\mathbf{C}} = \lim_{N\to\infty} N\,\mathrm{E}\{\tilde{\mathbf{f}}\tilde{\mathbf{f}}^{\mathrm{T}}\}, \tag{4.29}$$

where $\tilde{\mathbf{f}} = \hat{\mathbf{f}} - \mathbf{f}$*. Explicit expressions for* $\mathbf{C}$ *and* $\bar{\mathbf{C}}$ *are given in Appendix A.7. All quantities are evaluated at the true DOA* $\boldsymbol{\theta}_0$*.*

Proof. The derivation of $\mathbf{H}$ and $\mathbf{Q}$ can be found in Appendix A.7. □

4.5.3 Optimal Weighting

The result in Theorem 4.2 is valid for any positive definite weighting $\mathbf{W}$. However, it is of course of interest to find a weighting such that the asymptotic covariance matrix $\mathbf{\Gamma}$ is minimized (in the sense of positive definiteness). A lower bound on $\mathbf{\Gamma}$ is given by the CRB in Theorem 4.1. Next, we show that there indeed exists a weighting matrix $\mathbf{W}$ such that $\mathbf{\Gamma}$ attains the CRB. This implies that the estimate in (4.11) is asymptotically statistically efficient.

Theorem 4.3. *If*

$$\mathbf{W} = \mathbf{W}_{\mathrm{opt}} = \left[\mathbf{\Pi}_{\mathbf{B}}^{\perp}\tilde{\mathbf{C}}\mathbf{\Pi}_{\mathbf{B}}^{\perp} + \mathbf{B}\mathbf{B}^*\right]^{-1}, \tag{4.30}$$

where $\tilde{\mathbf{C}}$ *is defined in* (4.14)*, then*

$$\mathbf{\Gamma} = \mathrm{CRB}_{\boldsymbol{\theta}}.$$

Here, $\mathrm{CRB}_{\boldsymbol{\theta}}$ *is the Cramér-Rao lower bound on the estimation error covariance of* $\boldsymbol{\theta}$ *corresponding to the prior knowledge that the signals are uncorrelated (see Theorem 4.1).*

Proof. The proof can be found in Appendix A.8. □

Note that the optimal weighting matrix in (4.30) depends on the true parameters. However, since $\mathbf{\Pi}^{\perp}_{\mathbf{B}(\boldsymbol{\theta}_0)}\mathbf{f} = \mathbf{0}$, it can be shown that $\mathbf{W}_{\text{opt}}$ can be replaced by a consistent estimate without changing the asymptotic analysis given above. In particular, this implies that the estimator can be implemented as a two-step procedure as further explained in Section 4.6.

Remark 4.3. By making use of the results in Appendix A.5 and Appendix A.8, it is possible to show that $\hat{\mathbf{f}}$ can be replaced by $\text{vec}\{\hat{\mathbf{R}} - \hat{\sigma}^2\mathbf{I}\}$ in the criterion (4.12), without changing the asymptotic second order properties of $\hat{\boldsymbol{\theta}}$ [GO97]. We will not elaborate more on this here.

4.6 Implementation

This section deals with the implementation of the estimator (4.11) when a uniform linear array is employed. For general arrays, the criterion in (4.12) can be minimized by a Newton-type method. In the following we will discuss a way to avoid gradient search algorithms. For ULAs, a technique similar to the one used in MODE [SS90b, SS90a] can be utilized. Note that, when the array consists of uniformly spaced omnidirectional sensors, the steering matrix, $\mathbf{A}$, takes the form

$$\mathbf{A} = \begin{pmatrix} 1 & \cdots & 1 \\ \mathrm{e}^{i\omega_1} & \cdots & \mathrm{e}^{i\omega_d} \\ \vdots & & \vdots \\ \mathrm{e}^{i(m-1)\omega_1} & \cdots & \mathrm{e}^{i(m-1)\omega_d} \end{pmatrix},$$

where ω_k ($k = 1, \ldots, d$) are the so-called spatial frequencies. The relationship between ω_k and θ_k is given by

$$\omega_k = 2\pi\Delta \sin(\theta_k),$$

where Δ is the element spacing measured in wavelengths, and where θ_k is measured relative to array broadside.

The idea is to find a basis for the null-space of $\mathbf{B}^*$ that depends linearly on a minimal set of parameters. For that purpose, introduce the following polynomial

$$g_0 z^d + g_1 z^{d-1} + \cdots + g_d = g_0 \prod_{k=1}^{d} (z - \mathrm{e}^{i\omega_k}) \qquad (4.31)$$
$$g_0 \neq 0 \ .$$

From the definition of $\mathbf{B}$ in (4.6), it follows that the kth column of $\mathbf{B}$ is given by

$$\begin{aligned}\mathbf{B}_{\bullet k} = [1 \; z_k \; \cdots \; z_k^{m-1} \big| z_k^{-1} \; 1 \; \cdots \; z_k^{m-2} \big| z_k^{-2} \; z_k^{-1} \; \cdots \; z_k^{m-3} \big| \cdots \\ \cdots \big| \, z_k^{-(m-1)} \;\; z_k^{-(m-2)} \;\; \cdots \;\; 1]^{\mathrm{T}} \;\; , \end{aligned} \tag{4.32}$$

where $z_k = \mathrm{e}^{i\omega_k}$. The goal is to find a full rank matrix $\mathbf{G}$ of dimension $m^2 \times (m^2 - d)$ such that

$$\mathbf{G}^* \mathbf{B} = \mathbf{0} \;\; .$$

In this regard, it is useful to permute the rows of $\mathbf{B}$, and correspondingly the columns of $\mathbf{G}^*$, such that the permuted version of (4.32) reads

$$\begin{aligned}\tilde{\mathbf{B}}_{\bullet k} = [z_k^{-m+1} \big| z_k^{-m+2} \; z_k^{-m+2} \big| z_k^{-m+3} \; z_k^{-m+3} \; z_k^{-m+3} \big| \cdots \\ \cdots \big| \, z_k^{m-2} \; z_k^{m-2} \big| z_k^{m-1}]^{\mathrm{T}} \;\; . \end{aligned}$$

Notice that the permutation is made such that elements containing z_k of the same power are collected next to each other. This permutation will simplify the construction of $\tilde{\mathbf{G}}^*$, the permuted version of $\mathbf{G}^*$. The parameterization is best described by examples. The generalization of the parameterization will be straightforward from the examples given next.

Example 4.1. Let $m = 3$ and $d = 1$ which implies that we need $m^2 - d = 8$ independent rows to form $\tilde{\mathbf{G}}^*$. One such $\tilde{\mathbf{G}}^*$ is given by

$$\tilde{\mathbf{G}}^* = \left[\begin{array}{c|cc|ccc|ccc} g_1 & g_0 & 0 & 0 & 0 & 0 & 0 & 0 & 0 \\ g_1 & 0 & g_0 & 0 & 0 & 0 & 0 & 0 & 0 \\ 0 & g_1 & 0 & g_0 & 0 & 0 & 0 & 0 & 0 \\ 0 & g_1 & 0 & 0 & g_0 & 0 & 0 & 0 & 0 \\ 0 & g_1 & 0 & 0 & 0 & g_0 & 0 & 0 & 0 \\ 0 & 0 & 0 & g_1 & 0 & 0 & g_0 & 0 & 0 \\ 0 & 0 & 0 & g_1 & 0 & 0 & 0 & g_0 & 0 \\ 0 & 0 & 0 & 0 & 0 & 0 & g_1 & 0 & g_0 \end{array}\right] , \tag{4.33}$$

which is easily seen to be full rank and to satisfy the key relation $\tilde{\mathbf{G}}^* \tilde{\mathbf{B}} = \mathbf{0}$. The column partitioning in (4.33) corresponds to the different powers of z_k in $\tilde{\mathbf{B}}_{\bullet k}$. Notice that there exists several alternative positions for g_1 in the last six rows. ■

Example 4.2. In this example, let $m = 3$ and $d = 2$; i.e., $m^2 - d = 7$ independent rows are needed. In this case we may take

$$\tilde{\mathbf{G}}^* = \left[\begin{array}{c|cc|ccc|ccc} 0 & -1 & 1 & 0 & 0 & 0 & 0 & 0 & 0 \\ g_2 & g_1 & 0 & g_0 & 0 & 0 & 0 & 0 & 0 \\ g_2 & g_1 & 0 & 0 & g_0 & 0 & 0 & 0 & 0 \\ g_2 & g_1 & 0 & 0 & 0 & g_0 & 0 & 0 & 0 \\ 0 & g_2 & 0 & g_1 & 0 & 0 & g_0 & 0 & 0 \\ 0 & g_2 & 0 & g_1 & 0 & 0 & 0 & g_0 & 0 \\ 0 & 0 & 0 & g_2 & 0 & 0 & g_1 & 0 & g_0 \end{array}\right] . \tag{4.34}$$

Clearly, the matrix $\tilde{\mathbf{G}}^*$ in (4.34) is full rank and $\tilde{\mathbf{G}}^*\tilde{\mathbf{B}} = \mathbf{0}$. Again, notice that there are several alternative positions for g_1 and g_2 in many rows. The first row containing ± 1 appears because the pattern of the last six rows in (4.34) cannot be continued since the degree of the polynomial is "too large". ■

By extending the pattern given in the examples above, it can be seen that there are $d(d-1)/2$ rows with ± 1 and $m^2 - d^2/2 - d/2$ rows with g-coefficients in the general case. Altogether this becomes $m^2 - d$ rows, and by construction these rows are linearly independent. The matrix $\mathbf{G}^*$ is obtained by a column permutation of $\tilde{\mathbf{G}}^*$.

Observe that the polynomial (4.31) should have its roots on the unit circle. By imposing the conjugate symmetry constraint $g_k = g_{d-k}^c$, $(k = 0, ..., d)$, it is more likely that the roots will lie on the unit circle (see [SS90b] for details). Notice that the parameterization remains linear with this constraint. To get a minimal (invertible) reparameterization we need one additional constraint. It is common to use either a linear or a norm constraint on the polynomial coefficients (see [SS90b, NK94]).

Next, notice that $\mathbf{\Pi}_{\mathbf{B}}^{\perp} = \mathbf{\Pi}_{\mathbf{G}} = \mathbf{G}\mathbf{G}^{\dagger}$ and rewrite the criterion (4.12) as (see (A.46))

$$\hat{\mathbf{f}}^*\mathbf{\Pi}_{\mathbf{B}}^{\perp}\mathbf{W}_{\text{opt}}\mathbf{\Pi}_{\mathbf{B}}^{\perp}\hat{\mathbf{f}} = \hat{\mathbf{f}}^*\mathbf{G}(\mathbf{G}^*\check{\mathbf{C}}\mathbf{G})^{-1}\mathbf{G}^*\hat{\mathbf{f}} \ . \tag{4.35}$$

Since $\mathbf{G}^*\mathbf{f} = \mathbf{0}$, it is possible to show that the inverse in (4.35) can be replaced with a consistent estimate without altering the asymptotic properties of the estimates. The proposed procedure for estimating $\boldsymbol{\theta}$ can be summarized as follows:

1. Compute a consistent estimate of $\boldsymbol{\theta}_0$ by minimizing the *quadratic* function $\|\mathbf{G}^*\hat{\mathbf{f}}\|_2^2$. Observe that there are only d free real parameters in $\mathbf{G}$ under the constraints mentioned above. Alternatively, one

can use any other consistent estimator, for example, root-MUSIC or ESPRIT.

2. Based on sample data and the initial estimate of $\boldsymbol{\theta}_0$ from the first step, calculate consistent estimates $\hat{\tilde{\mathbf{C}}}$ and $\hat{\mathbf{G}}$ of $\tilde{\mathbf{C}}$ and $\mathbf{G}$, respectively. Minimize the following *quadratic* criterion

$$\hat{\mathbf{f}}^* \mathbf{G} (\hat{\mathbf{G}}^* \hat{\tilde{\mathbf{C}}} \hat{\mathbf{G}})^{-1} \mathbf{G}^* \hat{\mathbf{f}}$$

over the d free real parameters in $\mathbf{G}$. Once the polynomial coefficients are given, $\hat{\boldsymbol{\theta}}$ can be retrieved from the phase angle of the roots of the polynomial (4.31).

Exactly how the minimization of the two quadratic functions above is performed depends on the constraint on the polynomial coefficients. For the constraints previously mentioned, the minimization can be accomplished either by solving an eigenvalue problem or by solving an over-determined system of linear equations (see [SS90b, NK94] for details).

4.7 Numerical Examples

In this section, some numerical examples and simulations are provided to illustrate the performance of the proposed estimator. Henceforth, the proposed method will be called DEUCE (direction estimator for uncorrelated emitters).

Example 4.3. First, we will study the relative improvement in estimation accuracy which can be obtained by making use of the prior knowledge that the signals are uncorrelated. We will consider a ULA with $m = 3$ sensor elements separated by a half wavelength. There are two uncorrelated plane-waves impinging on the array from different directions. The first source is located at 0° while the direction to the other is varied. The SNRs of the sources are varied, but the second source is always 10 decibel (dB) stronger than the first source. That is, if the SNR of the first source is denoted by SNR_1, then

$$\mathbf{P}/\sigma^2 = \begin{bmatrix} \mathrm{SNR}_1 & 0 \\ 0 & 10\,\mathrm{SNR}_1 \end{bmatrix}.$$

The CRB on the estimation error variance on $\boldsymbol{\theta}_2$ is calculated with and without the prior on the signal correlation. The CRB for the case with

uncorrelated signals is given in (4.13). The expression for the CRB on $\boldsymbol{\theta}$ without any prior on $\mathbf{P}$ is given by the following expression (see [SN89a, VO91]):

$$\frac{\sigma^2}{2N}\left\{\mathrm{Re}\left[(\bar{\mathbf{D}}^*\boldsymbol{\Pi}_{\mathbf{A}}^{\perp}\bar{\mathbf{D}})\odot(\mathbf{P}\mathbf{A}^*\mathbf{R}^{-1}\mathbf{A}\mathbf{P})^T\right]\right\}^{-1}, \tag{4.36}$$

where $\odot$ denotes elementwise multiplication. In Figure 4.1, the ratio between the two CRBs on θ_2 given by (4.36) and (4.13) is shown for different θ_2 and SNR_1. Clearly, the ratio between the two CRBs can

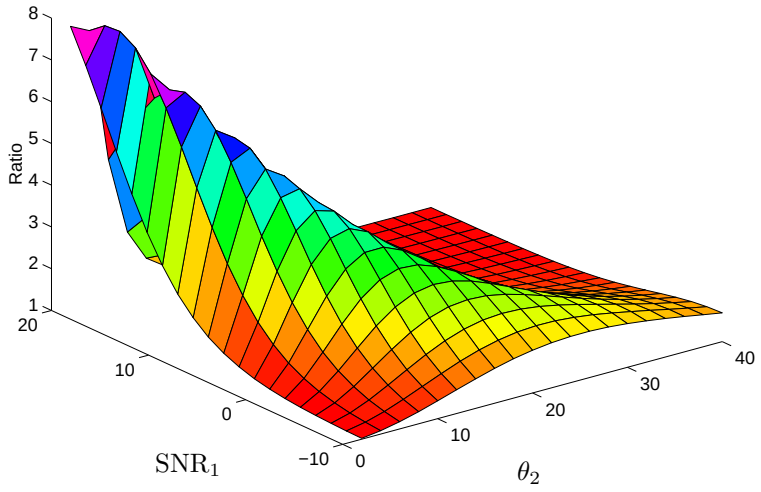

Figure 4.1: The ratio between the two CRBs for θ_2, versus θ_2 in degrees and SNR_1 in dB.

be significantly larger than one in certain scenarios. Hence, there is motivation for a method that can utilize the prior information about the signal correlation. In the next example, we show that the performance of DEUCE predicted by the large sample analysis also holds for samples of practical lengths. ■

Example 4.4. In the second example, we study the small sample behavior of DEUCE. Again, we consider a ULA with $m = 3$ sensor elements

separated by a half wavelength. Two uncorrelated sources are located at $\boldsymbol{\theta} = [0^\circ, 20^\circ]^{\mathrm{T}}$ relative to array broadside. The signal covariance matrix is

$$\mathbf{P} = \begin{bmatrix} 10^{(3/10)} & 0 \\ 0 & 10^{(20/10)} \end{bmatrix}$$

and the noise variance is $\sigma^2 = 1$. The root-mean-square (RMS) error of the second source is depicted in Figure 4.2, along with the corresponding RMS error for the root-MUSIC estimates [Bar83, RH89]. The RMS errors

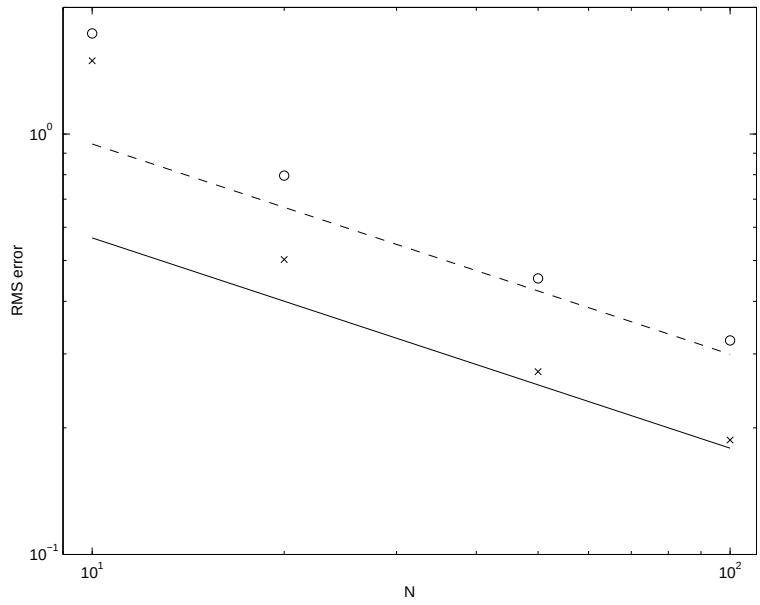

Figure 4.2: RMS error in degrees for θ_2 versus the number of snapshots, N: 'x' – DEUCE, 'o' – root-MUSIC. The solid line represents the CRB when it is known that the sources are uncorrelated and the dashed line is the CRB without this knowledge.

are based on 200 independent trials. For comparison, the corresponding CRBs are plotted as well. The solid line represents the CRB when the prior is incorporated (see (4.13)), and the dashed line denotes the CRB

without the prior (see (4.36)). It can be seen that the RMS error for DEUCE reaches the appropriate CRB at rather small sample values. In this example, we made use of the root-MUSIC estimate in the first step of the algorithm given in Section 4.6. A linear constraint ($\mathrm{Re}(g_0) = 1$) on the polynomial coefficients was employed in the second step of the algorithm. The finite sample performance can be improved slightly by iterating the second step several times. However, the RMS errors in Figure 4.2 are calculated for the estimates obtained from the two-step procedure outlined in Section 4.6. ■

Example 4.5. Another important issue is the robustness. That is, what happens if the sources are correlated? The following example is provided to partially answer this question. The setup is the same as in Example 4.4 except for the signal correlation. The signal covariance matrix is in this example given by

$$\mathbf{P} = \begin{bmatrix} p_1 & p_{12} \\ p_{12}^c & p_2 \end{bmatrix},$$

where $p_1 = 10^{(3/10)}$, $p_2 = 10^{(20/10)}$, and where the cross-correlation is defined as $p_{12} = \sqrt{(p_1 p_2)}\rho \mathrm{e}^{i\phi}$. In the simulations, the correlation coefficient, ρ, as well as the correlation phase, ϕ, are varied. The DOAs are estimated from a batch of 100 snapshots. The RMS error for θ_2, computed from 200 independent trials, is plotted as a function of the correlation coefficient in Figure 4.3. For comparison, the corresponding RMS error for the root-MUSIC estimates is shown as well. The CRB given by (4.36) is also displayed in Figure 4.3. It is seen that DEUCE has a better performance than root-MUSIC for small ρ as expected. It is interesting to observe that the two methods have a similar performance when the correlation increases. ■

4.8 Conclusions

In this chapter, a method (DEUCE) for estimating the locations of uncorrelated emitter signals from array data was proposed and analyzed. The asymptotic distribution for the direction estimates was derived. The asymptotic variance was shown to coincide with the Cramér-Rao lower bound including knowledge of uncorrelated signals. This means that DEUCE is asymptotically statistically efficient. It was also shown that DEUCE can be implemented as a two-step procedure for uniform linear arrays. This makes the method quite attractive since it provides

minimum variance estimates without having to resort to non-linear iterative minimization. Some computer simulated examples indicate that DEUCE is rather robust against the assumption that the emitters are uncorrelated. For *correlated* emitters, DEUCE behaves similar to root-MUSIC. However, since DEUCE is statistically efficient, it outperforms root-MUSIC for the case of *uncorrelated* emitters.

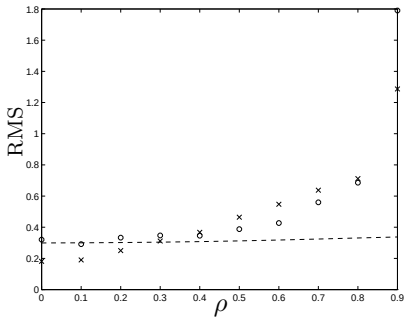

Figure 4.3a: Correlation phase, $\phi = 0°$.

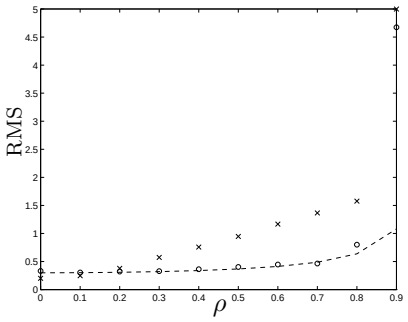

Figure 4.3b: Correlation phase, $\phi = 60°$.

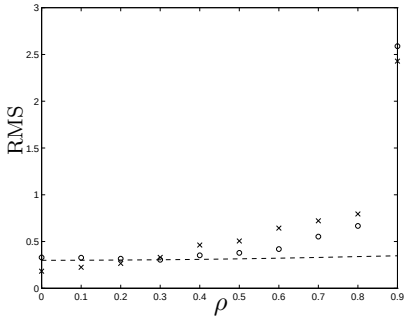

Figure 4.3c: Correlation phase, $\phi = 120°$.

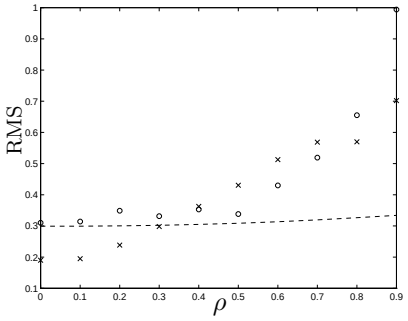

Figure 4.3d: Correlation phase, $\phi = 180°$.

Figure 4.3: The RMS error (in degrees) for θ_2 versus the correlation coefficient, ρ : 'x' – DEUCE, 'o' – root-MUSIC. The dashed line represents the CRB without prior knowledge given in (4.36).

Part II

Subspace System Identification

Chapter 5

A Linear Regression Approach to Subspace System Identification

Recently, state-space subspace system identification (4SID) has been suggested as an alternative to the more traditional prediction error system identification. The aim of this chapter is to analyze the connections between these two different approaches to system identification. The conclusion is that 4SID can be viewed as a linear regression multistep-ahead prediction error method with certain rank constraints. This allows us to describe 4SID methods within the standard framework of system identification and linear regression estimation. For example, this observation is used to compare different cost-functions which occur rather implicitly in the ordinary framework of 4SID. From the cost-functions, estimates of the extended observability matrix are derived and related to previous work. Based on the estimates of the observability matrix, the asymptotic properties of two pole estimators, namely the shift invariance method and a weighted subspace fitting method, are analyzed. Expressions for the asymptotic variances of the pole estimation error are given. From these expressions, difficulties in choosing user-specified parameters are pointed out. Furthermore, it is found that a row-weighting in the subspace estimation step does not affect the pole estimation error asymptotically.

5.1 Introduction

Algorithms for state-space subspace system identification (4SID) have attracted a large interest recently [VD94b, Lar90, Ver94, VOWL93]. An overview of 4SID methods can be found in [VD94a, Vib94]. The schemes for subspace system identification considered are very attractive since they estimate a state-space representation directly from input-output data. This is done without requiring a canonical parameterization as is often necessary in traditional prediction error methods [Lju87, SS89]. This requirement has been relaxed in [McK94b, McK94a] where it is shown that an over-parameterization of the state-space model does not necessarily lead to performance degradation. However the estimation method analyzed therein requires a large parameter search. The 4SID methods use reliable numerical tools such as QR-decomposition and singular value decomposition (SVD) which lead to numerically effective implementations. The nonlinear iterative optimization schemes that are usually necessary in the traditional framework are avoided. However, at the same time, this introduces new problems in terms of understanding the properties of the algorithms. Perhaps the most tractable property of 4SID is that the computations for multi-variable systems are just as easy as for single input single output systems. Another interesting property is the connection to model reduction [VD95a].

In the last few years, several new 4SID algorithms have been tested both in practice and by computer simulations. The results have been compared with results obtained with classical tools. In general, 4SID methods seem to perform very well, even close to optimal. The motivation for our work is to further increase the understanding of 4SID methods. The objective is to study the quality of the estimated models, to try to understand the performance limitations and capabilities of 4SID methods and, if possible, to suggest improvements and give user guidelines.

In this chapter, 4SID methods are phrased in a linear regression framework. This allows us to analyze the problem in a more traditional way. One advantage is that this explains more clearly the partition of data in the past and future which is done in 4SID. Also the linear regression formulation is useful to relate different approaches to 4SID. Specifically, the estimation of the extended observability matrix (the subspace estimation) is discussed in some detail based on different cost-functions. The estimates are shown to be identical to estimates used in existing algorithms. To compare different methods, we consider the asymptotic performance of two pole estimation techniques which are based on an estimate of

the extended observability matrix. The methods are the shift invariance method [Kun78, HK66] and the weighted subspace fitting method proposed in [OV94]. We give explicit expressions for the asymptotic covariance of the estimates. These expressions are rather involved, and it is difficult to interpret the results. However, one interesting general observation is that a row-weighting in the subspace estimation step does not affect the pole estimation error asymptotically. This result holds both for the shift invariance method and for the optimally weighted subspace fitting method. In order to gain further insight, we specialize to certain numerical examples which show that the choice of method and user-provided parameters is not obvious.

The rest of this chapter is organized as follows. In Section 5.2 the problem description is given along with the general assumptions made. In Section 5.3, we present the linear regression interpretation of 4SID. Based on the linear regression model, subspace estimation is discussed in some detail in Section 5.4. Section 5.5 introduces the two pole estimation algorithms considered. In Section 5.6, we analyze the asymptotic performance of these two methods and give numerical illustrations of the results in Section 5.7. Section 5.8 concludes the chapter.

5.2 Model and Assumptions

Consider a linear time-invariant system and assume that the dynamics of the system can be described by an nth order state-space realization

$$\mathbf{x}(t+1) = \mathbf{A}\mathbf{x}(t) + \mathbf{B}\mathbf{u}(t) + \mathbf{w}(t) \tag{5.1a}$$

$$\mathbf{y}(t) = \mathbf{C}\mathbf{x}(t) + \mathbf{D}\mathbf{u}(t) + \mathbf{v}(t)\,. \tag{5.1b}$$

Here, $\mathbf{x}(t)$ is an n-dimensional state-vector, $\mathbf{u}(t)$ is a vector of m input signals, $\mathbf{w}(t)$ represents the process noise, the vector $\mathbf{y}(t)$ contains l output signals, and $\mathbf{v}(t)$ is additive measurement noise. The system matrices have appropriate dimensions. The system is assumed to be asymptotically stable, i.e., the eigenvalues of $\mathbf{A}$ lie strictly inside the unit circle. Furthermore, for certain theoretical derivations, $\mathbf{A}$ is assumed to be diagonalizable.

It is well known that the realization in (5.1) is not unique. In fact, any realization characterized by the set

$$\{\mathbf{A},\, \mathbf{B},\, \mathbf{C},\, \mathbf{D}\}$$

has the same input-output description as the realization given by the set

$$\{\mathbf{T}^{-1}\mathbf{A}\mathbf{T},\, \mathbf{T}^{-1}\mathbf{B},\, \mathbf{C}\mathbf{T},\, \mathbf{D}\}$$

(if the process noise is properly scaled), where $\mathbf{T}$ is any full rank matrix. This is known as a similarity transformation, and the two realizations are said to be similar. The objective of an identification of the system description in (5.1) can be stated as: estimate the system order n, a matrix set $\{\mathbf{A}, \mathbf{B}, \mathbf{C}, \mathbf{D}\}$ which is similar to the true description and possibly the noise covariances from the measured data $\{\mathbf{u}(t), \mathbf{y}(t)\}_{t=1}^{N}$.

5.2.1 4SID Basic Equation

Subspace estimation techniques rely on a model that has an informative part which inherits a low-rank property plus a possible noise part. In 4SID, the model is obtained through a stacking of input-output data. Introduce a $l\alpha \times 1$ vector of stacked consecutive outputs as

$$\mathbf{y}_\alpha(t) = \frac{1}{\sqrt{N-\alpha-\beta+1}}\Big[\mathbf{y}(t)^T, \mathbf{y}(t+1)^T, \ldots, \mathbf{y}(t+\alpha-1)^T\Big]^T\,, \tag{5.2}$$

where α is a user-specified integer. To assure a low-rank property, α is required to be larger than the system order n. The scaling factor in (5.2) $(1/\sqrt{N-\alpha-\beta+1})$ is introduced in order to simplify the definition of sample covariance matrices in what follows. The parameter β is introduced below. Similarly, define vectors of stacked inputs, process, and measurement noises as $\mathbf{u}_\alpha(t)$, $\mathbf{w}_\alpha(t)$, and $\mathbf{v}_\alpha(t)$, respectively. Now it is straightforward to iterate the system equations in (5.1) to obtain the equation for the stacked quantities

$$\mathbf{y}_\alpha(t) = \mathbf{\Gamma}_\alpha\mathbf{x}(t) + \mathbf{\Phi}_\alpha\mathbf{u}_\alpha(t) + \mathbf{n}_\alpha(t)\,, \tag{5.3}$$

where $\mathbf{n}_\alpha(t) = \mathbf{\Psi}_\alpha \mathbf{w}_\alpha(t) + \mathbf{v}_\alpha(t)$ contains the noise and where the following block matrices have been introduced,

$$\mathbf{\Gamma}_\alpha = \begin{bmatrix} \mathbf{C} \\ \mathbf{CA} \\ \vdots \\ \mathbf{CA}^{\alpha-1} \end{bmatrix}, \tag{5.4}$$

$$\mathbf{\Phi}_\alpha = \begin{bmatrix} \mathbf{D} & \mathbf{0} & \cdots & \mathbf{0} \\ \mathbf{CB} & \mathbf{D} & \ddots & \mathbf{0} \\ \vdots & \ddots & \ddots & \vdots \\ \mathbf{CA}^{\alpha-2}\mathbf{B} & \mathbf{CA}^{\alpha-3}\mathbf{B} & \cdots & \mathbf{D} \end{bmatrix},$$

$$\mathbf{\Psi}_\alpha = \begin{bmatrix} \mathbf{0} & \cdots & \mathbf{0} & \mathbf{0} \\ \mathbf{C} & \ddots & \mathbf{0} & \mathbf{0} \\ \vdots & \ddots & \vdots & \vdots \\ \mathbf{CA}^{\alpha-2} & \cdots & \mathbf{C} & \mathbf{0} \end{bmatrix}.$$

Equation (5.3) is the basic model in 4SID. Notice that $\mathbf{\Gamma}_\alpha$ is the extended observability matrix and is of rank n if the system is observable.

5.2.2 General Assumptions

Some general assumptions are stated here. More specific assumptions will be made when needed.

- The process and measurement noise are assumed to be stationary zero-mean ergodic white Gaussian random processes with covariance given by

$$\mathrm{E} \begin{bmatrix} \mathbf{w}(t) \\ \mathbf{v}(t) \end{bmatrix} \begin{bmatrix} \mathbf{w}(t) \\ \mathbf{v}(t) \end{bmatrix}^T = \begin{bmatrix} \mathbf{r_w} & \mathbf{r_{wv}} \\ \mathbf{r}_{\mathbf{wv}}^T & \mathbf{r_v} \end{bmatrix}$$

  where E is the expectation operator.

- The measurable input, $\mathbf{u}(t)$, is assumed to be a quasi-stationary deterministic sequence [Lju87] uncorrelated with $\mathbf{w}(t)$ and $\mathbf{v}(t)$. The correlation sequence of $\mathbf{u}(t)$ is defined as

$$\mathbf{r_u}(s) = \bar{\mathrm{E}}\{\mathbf{u}(t+s)\mathbf{u}^T(t)\}$$

where $\bar{\mathrm{E}}$ is defined as

$$\bar{\mathrm{E}}\{\cdot\} = \lim_{N\to\infty} \frac{1}{N} \sum_{t=1}^{N} \mathrm{E}\{\cdot\} \, .$$

Furthermore, assume that the input is persistently exciting (PE) of order $\alpha + \beta$, [Lju87], where the parameter β is described below.

- The system is assumed to be observable which implies that the (extended) observability matrix, (5.4), has full rank, equal to the system order n.

5.3 Linear Regression

As a first step, the key idea of subspace identification is to estimate the n dimensional range space of $\mathbf{\Gamma}_\alpha$ from Equation (5.3). This can be done with more or less clever projections on the data. The traditional framework of 4SID can be a bit difficult in terms of advanced numerical linear algebra, concealing the statistical properties. Here, 4SID will be formulated in a linear regression framework. First we will provide motivation before introducing a linear regression model.

5.3.1 Motivation

Consider the basic equation (5.3). The idea is to replace the unknown state $\mathbf{x}(t)$ with an estimate from an optimal stochastic state observer. Let

$$\hat{\mathbf{x}}(t) = \mathbf{K}_1 \mathbf{y}_\beta(t-\beta) + \mathbf{K}_2 \mathbf{u}_\beta(t-\beta) + \mathbf{K}_3 \mathbf{u}_\alpha(t) \tag{5.5}$$

be the linear mean square error optimal estimate of $\mathbf{x}(t)$, given $\mathbf{y}_\beta(t-\beta)$, $\mathbf{u}_\beta(t-\beta)$ and $\mathbf{u}_\alpha(t)$. Here, β is a user-specified parameter which clearly can be interpreted as the size of the "memory" of past data used for estimating the state. The estimation error $\mathbf{x}(t) - \hat{\mathbf{x}}(t)$ is then orthogonal to $\mathbf{y}_\beta(t-\beta)$, $\mathbf{u}_\beta(t-\beta)$ and $\mathbf{u}_\alpha(t)$. Rewrite (5.3) to give the input-output relation

$$\begin{aligned}
\mathbf{y}_\alpha(t) &= \mathbf{\Gamma}_\alpha \hat{\mathbf{x}}_t + \mathbf{\Phi}_\alpha \mathbf{u}_\alpha(t) + \mathbf{\Gamma}_\alpha(\mathbf{x}(t) - \hat{\mathbf{x}}(t)) + \mathbf{n}_\alpha(t) \\
&= \mathbf{\Gamma}_\alpha \left(\mathbf{K}_1 \mathbf{y}_\beta(t-\beta) + \mathbf{K}_2 \mathbf{u}_\beta(t-\beta) + \mathbf{K}_3 \mathbf{u}_\alpha(t)\right) + \mathbf{\Phi}_\alpha \mathbf{u}_\alpha(t) + \mathbf{e}_\alpha(t) \\
&= \mathbf{L}_1 \mathbf{y}_\beta(t-\beta) + \mathbf{L}_2 \mathbf{u}_\beta(t-\beta) + \mathbf{L}_3 \mathbf{u}_\alpha(t) + \mathbf{e}_\alpha(t) \, ,
\end{aligned} \tag{5.6}$$

where we have introduced the notation

$$\begin{aligned}\begin{bmatrix}\mathbf{L}_1 & \mathbf{L}_2\end{bmatrix} &= \mathbf{\Gamma}_\alpha \begin{bmatrix}\mathbf{K}_1 & \mathbf{K}_2\end{bmatrix}, \\ \mathbf{L}_3 &= \mathbf{\Gamma}_\alpha \mathbf{K}_3 + \mathbf{\Phi}_\alpha ,\end{aligned} \tag{5.7}$$

and where $\mathbf{e}_\alpha(t)$ is defined as

$$\mathbf{e}_\alpha(t) = \mathbf{\Gamma}_\alpha(\mathbf{x}(t) - \hat{\mathbf{x}}(t)) + \mathbf{n}_\alpha(t) .$$

Thus, the "future" outputs, $\mathbf{y}_\alpha(t)$, are given by certain linear combinations of the data. For example, the combination of past inputs and outputs is constrained to lie in the range space of the extended observability matrix. Also notice that by construction, the noise term $\mathbf{e}_\alpha(t)$ is uncorrelated with the other terms on the right hand side of (5.6). From the construction above it is also clear that $\mathbf{y}_\alpha(t) - \mathbf{e}_\alpha(t)$ contains the mean-square optimal multistep ahead predictions of $\mathbf{y}_\alpha(t)$ given $\mathbf{y}_\beta(t-\beta)$, $\mathbf{u}_\beta(t-\beta)$ and $\mathbf{u}_\alpha(t)$. This is in general an approximation of the true predictions since we only have finite memory. As will be apparent later, another approximation made is that we consider time independent $\mathbf{K}$-matrices. In [VD94b], the relation between subspace projections and Kalman filtering is discussed in detail.

Remark 5.1. It should be remarked that even though we introduce an estimate of the states in (5.5), this is merely a help quantity in the elaborations to follow. In this chapter, we consider methods based on an estimate of $\mathbf{\Gamma}_\alpha$ and the matrices $\mathbf{K}_1$, $\mathbf{K}_2$, $\mathbf{K}_3$ will be eliminated along the way (see Section 5.4).

Special Cases

Deterministic systems: For the deterministic case with no noise, a dead-beat observer can be constructed which estimates the state exactly in at most n steps. Hence, the state vector can be obtained as

$$\mathbf{x}(t) = \mathbf{K}_1 \mathbf{y}_\beta(t-\beta) + \mathbf{K}_2 \mathbf{u}_\beta(t-\beta) , \tag{5.8}$$

for a specific choice of $\mathbf{K}_1$ and $\mathbf{K}_2$ ($\mathbf{K}_3 = 0$).

ARX systems: In [WJ94], the properties of ARX models in 4SID are studied in some detail. Since the predictor for ARX models has finite memory, this implies that even in this case the state can be exactly recovered in n steps, i.e.,

$$\mathbf{x}(t) = \mathbf{K}_1 \mathbf{y}_\beta(t-\beta) + \mathbf{K}_2 \mathbf{u}_\beta(t-\beta), \quad \beta \geq n,$$

even if we have noise! Observe that we have the same expression as in the deterministic case, so $\mathbf{L}_3 = \mathbf{\Phi}_\alpha$. This also implies that $\mathbf{e}_\alpha(t) = \mathbf{n}_\alpha(t)$ which is precisely the prediction error in the ARX case (see [WJ94]). Thus, for ARX systems the 4SID output-vector, $\mathbf{y}_\alpha(t)$, consists of the true multistep-ahead predictions plus the prediction errors, i.e.,

$$\mathbf{y}_\alpha(t) = [\hat{\mathbf{y}}_{t|t-1}^T, \dots, \hat{\mathbf{y}}_{t+\alpha-1|t-1}^T]^T + \mathbf{e}_\alpha(t) \,,$$

where $\hat{\mathbf{y}}_{t+k|t-1}$ denotes the prediction of $\mathbf{y}(t+k)$ given data up to time $t-1$.

5.3.2 4SID Linear Regression Model

Inspired by the elaborations made above, a linear regression form of the 4SID output equation (5.3) will be introduced. The explicit relation to linear regression will hopefully clarify certain things in 4SID.

Definition. The 4SID linear regression model is defined by

$$\mathbf{y}_\alpha(t) = \mathbf{L}_1\mathbf{y}_\beta(t-\beta) + \mathbf{L}_2\mathbf{u}_\beta(t-\beta) + \mathbf{L}_3\mathbf{u}_\alpha(t) + \mathbf{e}_\alpha(t) \,. \tag{5.9}$$

As seen above, the linear regression model will inherit certain properties. The noise vector $\mathbf{e}_\alpha(t)$ is orthogonal to $\mathbf{y}_\beta(t-\beta)$, $\mathbf{u}_\beta(t-\beta)$, $\mathbf{u}_\alpha(t)$, and

$$\operatorname{rank}[\mathbf{L}_1 \ \mathbf{L}_2] = n \,, \tag{5.10a}$$

$$\mathcal{R}[\mathbf{L}_1 \ \mathbf{L}_2] = \mathcal{R}[\mathbf{\Gamma}_\alpha] \,, \tag{5.10b}$$

where $\mathcal{R}[\cdot]$ denotes the range space of $[\cdot]$.

Remark 5.2. While it is obvious that $\operatorname{rank}[\mathbf{L}_1 \ \mathbf{L}_2] \leq n$, it is not easy to establish explicit conditions when equality holds. Loosely speaking, this requires the states to be sufficiently excited. We will not elaborate further on this here, but assume (5.10a) to hold true throughout this chapter. A thorough discussion about the rank condition is made in the next chapter.

In [VD94b], a similar idea to replace the state with an estimate is elaborated. They consider the estimated state-sequence as obtained from a bank of non-steady state Kalman filters and derive explicit expressions for the matrices $\mathbf{L}_i, \ i = 1, 2, 3$ in the case of infinite data.

In 4SID algorithms, it is common to use $\alpha = \beta$, and no general rule exists for how to choose them. It is also a quite common idea that the performance improves if α and β are increased. However in this chapter,

a simple example is provided to show that this is not always the case. The numerical complexity of 4SID methods increases with the size of α and β, thus these parameters should be as small as possible. The linear regression interpretation (think of the state observers in (5.5) and (5.8), and think also of the ARX case) suggests that β most often could be chosen close to the system order, n, as is also indicated in the numerical examples in Section 5.7. While α is required to be greater than the system order, it is not that obvious what the corresponding condition on β is. The interpretation in terms of state observers suggests that $\beta \geq n$ is a necessary condition. However, an instrumental variable interpretation of 4SID (see [VOWL93, Vib94]) indicates that it may suffice to take $\beta \geq n/(l+m)$. This can also be seen by inspection of the necessary conditions for the dimension of quantities used in the subspace estimation in Section 5.4. The question of the required size of β is closely tied to the rank condition (5.10a); see Remark 5.2 and Chapter 6.

5.4 Subspace Estimation

Most 4SID methods start the estimation procedure by estimating the extended observability matrix. This section discusses the so-called subspace estimation. To be able to compare the effects of different weightings (different algorithms), the estimation of the system poles is considered in Section 5.5.

The idea in this section is to estimate $\mathbf{\Gamma}_\alpha$ by minimizing two cost-functions which arise naturally from the linear regression formulation. The so-obtained estimates are then related to previously published estimates. We believe that this comparison/unification aids in understanding the nature of the subspace estimation procedure.

Using (5.9), the observations can be modeled by the matrix equation

$$\mathbf{Y}_\alpha = \mathbf{L}_1\mathbf{Y}_\beta + \mathbf{L}_2\mathbf{U}_\beta + \mathbf{L}_3\mathbf{U}_\alpha + \mathbf{E}_\alpha \ , \tag{5.11}$$

where the block Hankel matrices of outputs are defined as

$$\mathbf{Y}_\beta = [\mathbf{y}_\beta(1), \ldots, \mathbf{y}_\beta(N-\alpha-\beta+1)] \, , \tag{5.12a}$$
$$\mathbf{Y}_\alpha = [\mathbf{y}_\alpha(1+\beta), \ldots, \mathbf{y}_\alpha(N-\alpha+1)] \, , \tag{5.12b}$$

and similarly for $\mathbf{U}_\alpha$, $\mathbf{U}_\beta$, and $\mathbf{E}_\alpha$. The 4SID linear regression model (5.9) corresponds to an approximate multistep-ahead prediction error model. It is quite natural to base an estimation procedure on the minimization of

the prediction error[1] in some suitable norm. Thus, consider the prediction error covariance matrix

$$\mathbf{\Theta}(\mathbf{L}_1, \mathbf{L}_2, \mathbf{L}_3) = \mathbf{E}_\alpha \mathbf{E}_\alpha^T = \sum_{t=1+\beta}^{N-\alpha+1} \mathbf{e}_\alpha(t)\mathbf{e}_\alpha^T(t) \, .$$

where only the explicit dependence on the regression coefficients has been stressed. In general, the matrices $\mathbf{L}_1$, $\mathbf{L}_2$ and $\mathbf{L}_3$ depend on the system matrices, noise covariances, and the initial state. The structure of these matrices can be incorporated in the minimization of $\mathbf{\Theta}$. However the resulting nonlinear minimization problem is quite complicated.

We will obtain estimates by minimizing two different norms of $\mathbf{\Theta}$. In the minimization, the structure of the problem will be relaxed in the sense that $\mathbf{L}_3$ is considered to be a completely unknown matrix, and the only restriction of $[\mathbf{L}_1 \ \mathbf{L}_2]$ will be the rank n constraint of (5.10a). Thus the minimization is a rank-constrained problem; however, it can be transformed to an unconstrained one by the reparameterization (cf. (5.7))

$$\begin{bmatrix} \mathbf{L}_1 & \mathbf{L}_2 \end{bmatrix} = \mathbf{\Gamma}_\alpha \bar{\mathbf{K}} \, . \tag{5.13}$$

The factorization in (5.13) is clearly not unique since $\mathbf{\Gamma}_\alpha \bar{\mathbf{K}} = \mathbf{\Gamma}_\alpha \mathbf{T}\mathbf{T}^{-1}\bar{\mathbf{K}}$ for any invertible $\mathbf{T}$. However, it turns out that this non-uniqueness is not a problem. The minimization problem to be solved in this section can now be formulated as

$$\min_{\mathbf{\Gamma}_\alpha, \, \bar{\mathbf{K}}, \, \mathbf{L}_3} V(\mathbf{\Gamma}_\alpha, \bar{\mathbf{K}}, \mathbf{L}_3)$$

for one of the following two functions

$$V(\mathbf{\Gamma}_\alpha, \bar{\mathbf{K}}, \mathbf{L}_3) = \mathrm{Tr}\{\mathbf{W}\mathbf{\Theta}(\mathbf{\Gamma}_\alpha, \bar{\mathbf{K}}, \mathbf{L}_3)\} \tag{5.14}$$

or

$$V(\mathbf{\Gamma}_\alpha, \bar{\mathbf{K}}, \mathbf{L}_3) = \det\{\mathbf{\Theta}(\mathbf{\Gamma}_\alpha, \bar{\mathbf{K}}, \mathbf{L}_3)\}. \tag{5.15}$$

Here $\mathrm{Tr}\{\cdot\}$ denotes the trace operator, $\mathbf{W}$ is any symmetric positive definite weighting matrix, and $\det\{\cdot\}$ is the determinant function. In an obvious notation, the argument of $\mathbf{\Theta}$ has been altered according to the

[1] For simplicity, we will call the residuals in the linear regression model for *the prediction error* in the sequel.

reparameterization. As already mentioned, we are only interested in an estimate of the extended observability matrix $\mathbf{\Gamma}_\alpha$; hence $\bar{\mathbf{K}}$ and $\mathbf{L}_3$ can be seen as auxiliary variables.

The next idea is to minimize $\mathbf{\Theta}$ with respect to $\mathbf{L}_3$ and $\mathbf{\Gamma}_\alpha$ in terms of matrix inequalities. (For two matrices $\mathbf{A}$ and $\mathbf{B}$, the inequality $\mathbf{A}-\mathbf{B} \geq 0$ means that $\mathbf{A}-\mathbf{B}$ is positive semi-definite.) The reason is that these results are valid for *any* nondecreasing function of $\mathbf{\Theta}$ and thus specifically for the two choices (5.14) and (5.15) (see [SS89]). To minimize with respect to $\bar{\mathbf{K}}$, however, we have to consider the functions separately. This is done in two subsequent sections.

In order to proceed, it is convenient to introduce the notation

$$\mathbf{p}_\beta(t) = \begin{bmatrix} \mathbf{y}_\beta(t) \\ \mathbf{u}_\beta(t) \end{bmatrix}, \qquad \mathbf{P}_\beta = \begin{bmatrix} \mathbf{Y}_\beta \\ \mathbf{U}_\beta \end{bmatrix},$$
$$\bar{\mathbf{L}} = \begin{bmatrix} \mathbf{L}_1 & \mathbf{L}_2 \end{bmatrix} = \mathbf{\Gamma}_\alpha \bar{\mathbf{K}}, \qquad \mathbf{U}_\alpha^\dagger = \mathbf{U}_\alpha^T (\mathbf{U}_\alpha \mathbf{U}_\alpha^T)^{-1}.$$

Rewrite $\mathbf{\Theta}$ as

$$\begin{aligned} \mathbf{\Theta}(\mathbf{\Gamma}_\alpha, \bar{\mathbf{K}}, \mathbf{L}_3) &= \big[\mathbf{Y}_\alpha - \bar{\mathbf{L}}\mathbf{P}_\beta - \mathbf{L}_3\mathbf{U}_\alpha\big]\big[\mathbf{Y}_\alpha - \bar{\mathbf{L}}\mathbf{P}_\beta - \mathbf{L}_3\mathbf{U}_\alpha\big]^T \\ &= \big[\mathbf{L}_3 - (\mathbf{Y}_\alpha - \bar{\mathbf{L}}\mathbf{P}_\beta)\mathbf{U}_\alpha^\dagger\big]\mathbf{U}_\alpha\mathbf{U}_\alpha^T\big[\mathbf{L}_3 - (\mathbf{Y}_\alpha - \bar{\mathbf{L}}\mathbf{P}_\beta)\mathbf{U}_\alpha^\dagger\big]^T \\ &\quad + \big[\mathbf{Y}_\alpha - \bar{\mathbf{L}}\mathbf{P}_\beta\big]\big[\mathbf{Y}_\alpha - \bar{\mathbf{L}}\mathbf{P}_\beta\big]^T - \big[\mathbf{Y}_\alpha - \bar{\mathbf{L}}\mathbf{P}_\beta\big]\mathbf{U}_\alpha^\dagger\mathbf{U}_\alpha\big[\mathbf{Y}_\alpha - \bar{\mathbf{L}}\mathbf{P}_\beta\big]^T. \end{aligned} \tag{5.16}$$

Since $\mathbf{U}_\alpha\mathbf{U}_\alpha^T$ is positive definite by assumption, the unconstrained $\mathbf{L}_3$ minimizing *any* nondecreasing function of $\mathbf{\Theta}$ is given by

$$\hat{\mathbf{L}}_3 = \big[\mathbf{Y}_\alpha - \bar{\mathbf{L}}\mathbf{P}_\beta\big]\mathbf{U}_\alpha^\dagger. \tag{5.17}$$

Let

$$\mathbf{\Pi}_\alpha^\perp = \mathbf{I} - \mathbf{U}_\alpha^\dagger\mathbf{U}_\alpha$$

denote the projection matrix on the null-space of $\mathbf{U}_\alpha$. Insert (5.17) in (5.16) and again rewrite in a similar way using the factorization $\bar{\mathbf{L}} = \mathbf{\Gamma}_\alpha\bar{\mathbf{K}}$

$$\begin{aligned} \mathbf{\Theta}(\mathbf{\Gamma}_\alpha, \bar{\mathbf{K}}) &= \big[\mathbf{Y}_\alpha - \mathbf{\Gamma}_\alpha\bar{\mathbf{K}}\mathbf{P}_\beta\big]\mathbf{\Pi}_\alpha^\perp\big[\mathbf{Y}_\alpha - \mathbf{\Gamma}_\alpha\bar{\mathbf{K}}\mathbf{P}_\beta\big]^T \\ &= \big[\mathbf{\Gamma}_\alpha - \mathbf{Y}_\alpha\mathbf{\Pi}_\alpha^\perp\mathbf{P}_\beta^T\bar{\mathbf{K}}^T(\bar{\mathbf{K}}\mathbf{P}_\beta\mathbf{\Pi}_\alpha^\perp\mathbf{P}_\beta^T\bar{\mathbf{K}}^T)^{-1}\big]\bar{\mathbf{K}}\mathbf{P}_\beta\mathbf{\Pi}_\alpha^\perp\mathbf{P}_\beta^T\bar{\mathbf{K}}^T \\ &\quad \times \big[\mathbf{\Gamma}_\alpha - \mathbf{Y}_\alpha\mathbf{\Pi}_\alpha^\perp\mathbf{P}_\beta^T\bar{\mathbf{K}}^T(\bar{\mathbf{K}}\mathbf{P}_\beta\mathbf{\Pi}_\alpha^\perp\mathbf{P}_\beta^T\bar{\mathbf{K}}^T)^{-1}\big]^T \\ &\quad + \mathbf{Y}_\alpha\mathbf{\Pi}_\alpha^\perp\mathbf{Y}_\alpha^T - \mathbf{Y}_\alpha\mathbf{\Pi}_\alpha^\perp\mathbf{P}_\beta^T\bar{\mathbf{K}}^T(\bar{\mathbf{K}}\mathbf{P}_\beta\mathbf{\Pi}_\alpha^\perp\mathbf{P}_\beta^T\bar{\mathbf{K}}^T)^{-1}\bar{\mathbf{K}}\mathbf{P}_\beta\mathbf{\Pi}_\alpha^\perp\mathbf{Y}_\alpha^T. \end{aligned} \tag{5.18}$$

The factor $\bar{\mathbf{K}}\mathbf{P}_\beta\mathbf{\Pi}_\alpha^\perp\mathbf{P}_\beta^T\bar{\mathbf{K}}^T$ is positive definite by assumption. (This is because $\bar{\mathbf{K}}$ has full row rank and, $\mathbf{P}_\beta\mathbf{\Pi}_\alpha^\perp\mathbf{P}_\beta^T$ is positive definite under weak conditions on the noise and if $\mathbf{u}(t)$ is persistently exciting of order $\alpha+\beta$; see [SS89] Complement C5.1.) Hence, if $\bar{\mathbf{K}}$ is given, the estimate of the extended observability matrix is

$$\hat{\mathbf{\Gamma}}_\alpha = \mathbf{Y}_\alpha\mathbf{\Pi}_\alpha^\perp\mathbf{P}_\beta^T\bar{\mathbf{K}}^T(\bar{\mathbf{K}}\mathbf{P}_\beta\mathbf{\Pi}_\alpha^\perp\mathbf{P}_\beta^T\bar{\mathbf{K}}^T)^{-1} \tag{5.19}$$

and the concentrated form of the covariance matrix equals

$$\mathbf{\Theta}(\bar{\mathbf{K}}) = \mathbf{Y}_\alpha\mathbf{\Pi}_\alpha^\perp\mathbf{Y}_\alpha^T - \mathbf{Y}_\alpha\mathbf{\Pi}_\alpha^\perp\mathbf{P}_\beta^T\bar{\mathbf{K}}^T(\bar{\mathbf{K}}\mathbf{P}_\beta\mathbf{\Pi}_\alpha^\perp\mathbf{P}_\beta^T\bar{\mathbf{K}}^T)^{-1}\bar{\mathbf{K}}\mathbf{P}_\beta\mathbf{\Pi}_\alpha^\perp\mathbf{Y}_\alpha^T\,. \tag{5.20}$$

Until now, the estimates were independent of the precise norm of $\mathbf{\Theta}$ chosen. However to proceed and minimize with respect to $\bar{\mathbf{K}}$, we have to consider the two cost-functions (5.14) and (5.15) separately.

5.4.1 Weighted Least Squares (WLS)

In this section, we derive the estimate of $\mathbf{\Gamma}_\alpha$ by minimizing the cost-function (5.14), i.e., the weighted sum of the residuals in the linear regression model. This estimate will be called the weighted least squares (WLS) estimate. Using the concentrated form of $\mathbf{\Theta}$, (5.20), the minimizing $\bar{\mathbf{K}}$ is given by

$$\hat{\bar{\mathbf{K}}} = \arg\min_{\bar{\mathbf{K}}} \operatorname{Tr}\{\mathbf{W}\mathbf{\Theta}(\bar{\mathbf{K}})\}\,. \tag{5.21}$$

The details of the optimization is deferred to Appendix A.9. The solution to (5.21) is

$$\hat{\bar{\mathbf{K}}} = \bar{\mathbf{T}}^T\hat{\mathbf{V}}_s^T(\mathbf{P}_\beta\mathbf{\Pi}_\alpha^\perp\mathbf{P}_\beta^T)^{-1/2} \tag{5.22}$$

where $\bar{\mathbf{T}}$ is any $n\times n$ full rank matrix and where $\hat{\mathbf{V}}_s$ is given by the SVD

$$\hat{\mathbf{Q}}\hat{\mathbf{S}}\hat{\mathbf{V}}^T = \begin{bmatrix}\hat{\mathbf{Q}}_s & \hat{\mathbf{Q}}_n\end{bmatrix}\begin{bmatrix}\hat{\mathbf{S}}_s & \mathbf{0}\\ \mathbf{0} & \hat{\mathbf{S}}_n\end{bmatrix}\begin{bmatrix}\hat{\mathbf{V}}_s^T\\ \hat{\mathbf{V}}_n^T\end{bmatrix} = \mathbf{W}^{1/2}\mathbf{Y}_\alpha\mathbf{\Pi}_\alpha^\perp\mathbf{P}_\beta^T(\mathbf{P}_\beta\mathbf{\Pi}_\alpha^\perp\mathbf{P}_\beta^T)^{-1/2}\,. \tag{5.23}$$

$\hat{\mathbf{S}}_s$ is a diagonal matrix containing the n largest singular values, and the columns of $\hat{\mathbf{V}}_s$ are the corresponding right singular vectors. $\mathbf{W}^{1/2}$ is a

symmetric square-root of $\mathbf{W}$. Inserting (5.22) in (5.19) yields the WLS subspace estimate

$$\begin{aligned}\hat{\mathbf{\Gamma}}_\alpha &= \mathbf{W}^{-1/2}\mathbf{W}^{1/2}\mathbf{Y}_\alpha\mathbf{\Pi}_\alpha^\perp\mathbf{P}_\beta^T(\mathbf{P}_\beta\mathbf{\Pi}_\alpha^\perp\mathbf{P}_\beta^T)^{-1/2}\hat{\mathbf{V}}_s\bar{\mathbf{T}}(\bar{\mathbf{T}}^T\hat{\mathbf{V}}_s^T\hat{\mathbf{V}}_s\bar{\mathbf{T}})^{-1} \\ &= \mathbf{W}^{-1/2}\hat{\mathbf{Q}}\hat{\mathbf{S}}\hat{\mathbf{V}}^T\hat{\mathbf{V}}_s\bar{\mathbf{T}}^{-T} = \mathbf{W}^{-1/2}\hat{\mathbf{Q}}_s\hat{\mathbf{S}}_s\bar{\mathbf{T}}^{-T}\,.\end{aligned} \tag{5.24}$$

As mentioned previously, the estimate of the extended observability matrix concludes the first step in many 4SID techniques. The appearance of the factor $\hat{\mathbf{S}}_s\bar{\mathbf{T}}^{-T}$ in (5.24) and $\bar{\mathbf{T}}^T$ in (5.22) reflects the fact that different state-space realizations are related by a similarity transformation (cf., the non-uniqueness in the factorization (5.13)). $\bar{\mathbf{T}}$ does not affect the minimization but determines which realization is obtained. Some common choices are: $\bar{\mathbf{T}} = \hat{\mathbf{S}}_s^{1/2}$ and $\bar{\mathbf{T}} = \hat{\mathbf{S}}_s$.

5.4.2 Approximate Maximum Likelihood (AML)

It is well known that under certain assumptions, prediction error methods have the same performance as maximum likelihood (ML) estimators. More precisely, it is required that the prediction error is Gaussian noise, white in time, and that the cost-function is properly chosen, e.g., the determinant of the prediction error covariance matrix [Lju87, SS89]. However in the present problem, the prediction errors are not white, and taking the determinant cost-function will not be the ML estimate. Instead it will be called the Approximate ML (AML) estimate. Actually there are more profound considerations in an ML approach. This is due to the rank constraint on the regression coefficients (5.10a). For the derivation of the maximum likelihood estimator for a reduced-rank linear regression model, we refer to [SV95, SV96] which also served as inspiration to the presentation in this section.

The criterion in this section will be chosen as the determinant of the prediction error covariance matrix, i.e., (5.15). Due to the general "minimization" of $\mathbf{\Theta}$ in Section 5.4, the minimizing $\hat{\mathbf{L}}_3$ and $\hat{\mathbf{\Gamma}}_\alpha$ are given by (5.17) and (5.19), respectively, with the minimizing $\bar{\mathbf{K}}$ inserted. Using (5.20), the estimate of $\bar{\mathbf{K}}$ is given by

$$\hat{\bar{\mathbf{K}}} = \arg\min_{\bar{\mathbf{K}}} \det\bigl\{\mathbf{\Theta}(\bar{\mathbf{K}})\bigr\}\,. \tag{5.25}$$

The details of the minimization are deferred to Appendix A.10. Intro-

ducing the SVD similar to (5.23),

$$\begin{aligned}\hat{\mathbf{Q}}\hat{\mathbf{S}}\hat{\mathbf{V}}^T &= \begin{bmatrix}\hat{\mathbf{Q}}_s & \hat{\mathbf{Q}}_n\end{bmatrix}\begin{bmatrix}\hat{\mathbf{S}}_s & \mathbf{0}\\ \mathbf{0} & \hat{\mathbf{S}}_n\end{bmatrix}\begin{bmatrix}\hat{\mathbf{V}}_s^T\\ \hat{\mathbf{V}}_n^T\end{bmatrix}\\ &= (\mathbf{Y}_\alpha\mathbf{\Pi}_\alpha^\perp\mathbf{Y}_\alpha^T)^{-1/2}\mathbf{Y}_\alpha\mathbf{\Pi}_\alpha^\perp\mathbf{P}_\beta^T(\mathbf{P}_\beta\mathbf{\Pi}_\alpha^\perp\mathbf{P}_\beta^T)^{-1/2}\,, \end{aligned} \tag{5.26}$$

the solution to (5.25) is given by

$$\hat{\bar{\mathbf{K}}} = \bar{\mathbf{T}}^T\hat{\mathbf{V}}_s^T(\mathbf{P}_\beta\mathbf{\Pi}_\alpha^\perp\mathbf{P}_\beta^T)^{-1/2} \tag{5.27}$$

where $\bar{\mathbf{T}}$ is any $n \times n$ full rank matrix. The AML estimate of $\mathbf{\Gamma}_\alpha$ is obtained by using (5.27) in (5.19)

$$\begin{aligned}\hat{\mathbf{\Gamma}}_\alpha &= (\mathbf{Y}_\alpha\mathbf{\Pi}_\alpha^\perp\mathbf{Y}_\alpha^T)^{1/2}(\mathbf{Y}_\alpha\mathbf{\Pi}_\alpha^\perp\mathbf{Y}_\alpha^T)^{-1/2}\mathbf{Y}_\alpha\mathbf{\Pi}_\alpha^\perp\mathbf{P}_\beta^T\\ &\quad\times(\mathbf{P}_\beta\mathbf{\Pi}_\alpha^\perp\mathbf{P}_\beta^T)^{-1/2}\hat{\mathbf{V}}_s\bar{\mathbf{T}}(\bar{\mathbf{T}}^T\hat{\mathbf{V}}_s^T\hat{\mathbf{V}}_s\bar{\mathbf{T}})^{-1}\\ &= (\mathbf{Y}_\alpha\mathbf{\Pi}_\alpha^\perp\mathbf{Y}_\alpha^T)^{1/2}\hat{\mathbf{Q}}\hat{\mathbf{S}}\hat{\mathbf{V}}^T\hat{\mathbf{V}}_s\bar{\mathbf{T}}^{-T} = (\mathbf{Y}_\alpha\mathbf{\Pi}_\alpha^\perp\mathbf{Y}_\alpha^T)^{1/2}\hat{\mathbf{Q}}_s\hat{\mathbf{S}}_s\bar{\mathbf{T}}^{-T}\,. \end{aligned} \tag{5.28}$$

5.4.3 Discussion

The weighting matrix introduced in the weighted least squares method is by user choice. A couple of different choices correspond to estimates previously suggested in the literature.

PO-MOESP: The PO-MOESP method was introduced in [Ver94]. It is straightforward to verify that choosing $\mathbf{W} = \mathbf{I}$ gives the same estimate of $\mathbf{\Gamma}_\alpha$ (and the same singular values) as in PO-MOESP (cf. [VD94a, Vib94]).

CVA: The choice $\mathbf{W} = (\mathbf{Y}_\alpha\mathbf{\Pi}_\alpha^\perp\mathbf{Y}_\alpha^T)^{-1}$ results in the canonical variate analysis (CVA) solution [Lar83, Lar90]. A natural interpretation of the algorithmic details of Larimore's is given in [VD94a]. Here it is called the CVA solution even if Larimore does not explicitly use the extended observability matrix. Larimore does actually propose a generalization of the canonical variate analysis method and introduces a general weighting matrix corresponding to $\mathbf{W}$ in our notation.

Comparing (5.23) and (5.24) with (5.26) and (5.28), it is clear that if $\mathbf{W} = (\mathbf{Y}_\alpha\mathbf{\Pi}_\alpha^\perp\mathbf{Y}_\alpha^T)^{-1}$, the two estimates are identical and equal to the

CVA estimate. This means that AML is a special case of WLS, and it suffices to consider WLS in the sequel.

In [VD94a], an interpretation of $\mathbf{W}$ as a shaping filter in the frequency domain is given. More precisely, $\mathbf{W}$ contains impulse response coefficients of a shaping filter specifying important frequency bands. These ideas are further extended in [VD95a].

A further observation on the selection of the weighting matrix, $\mathbf{W}$, concerns the model order selection. The estimate of the model order is often obtained by studying the singular values of (5.23). $\mathbf{W}$ clearly affects the singular value distribution. Thus, it would be nice if $\mathbf{W}$ could increase the gap between the n dominating singular values and the rest. In [Lar94], it is claimed by a numerical example that CVA is optimal (ML) for model order selection.

A popular subspace identification algorithm is the N4SID method [VD94b]. Hence, a short note on the relation of the linear regression framework to the estimate in N4SID is warranted. The N4SID estimate of $\mathbf{\Gamma}_\alpha$ can not be obtained directly from our WLS solution because of the rank constraint on $\bar{\mathbf{L}}$. In N4SID, this constraint is invoked in a later stage. This may be seen as follows. Consider the unconstrained least squares estimate of $\bar{\mathbf{L}}$ and $\mathbf{L}_3$ from the cost-function $\mathrm{Tr}\{\mathbf{\Theta}\}$

$$\hat{\bar{\mathbf{L}}} = \mathbf{Y}_\alpha \mathbf{\Pi}_\alpha^\perp \mathbf{P}_\beta^T \left(\mathbf{P}_\beta \mathbf{\Pi}_\alpha^\perp \mathbf{P}_\beta^T \right)^{-1} , \tag{5.29a}$$

$$\hat{\mathbf{L}}_3 = \mathbf{Y}_\alpha \mathbf{\Pi}_{\mathbf{P}_\beta}^\perp \mathbf{U}_\alpha^T \left(\mathbf{U}_\alpha \mathbf{\Pi}_{\mathbf{P}_\beta}^\perp \mathbf{U}_\alpha^T \right)^{-1} , \tag{5.29b}$$

where $\mathbf{\Pi}_{\mathbf{P}_\beta}^\perp = \mathbf{I} - \mathbf{P}_\beta^T (\mathbf{P}_\beta \mathbf{P}_\beta^T)^{-1} \mathbf{P}_\beta$ is the projection onto the nullspace of $\mathbf{P}_\beta$. Define the least squares residuals by

$$\hat{\mathbf{E}}_\alpha = \mathbf{Y}_\alpha - \hat{\bar{\mathbf{L}}} \mathbf{P}_\beta - \hat{\mathbf{L}}_3 \mathbf{U}_\alpha,$$

where $\hat{\mathbf{E}}_\alpha$ is orthogonal to $\mathbf{P}_\beta$ and $\mathbf{U}_\alpha$. Rewrite the true residuals as

$$\mathbf{E}_\alpha = \mathbf{Y}_\alpha - \bar{\mathbf{L}} \mathbf{P}_\beta - \mathbf{L}_3 \mathbf{U}_\alpha = \hat{\mathbf{E}}_\alpha - (\bar{\mathbf{L}} - \hat{\bar{\mathbf{L}}}) \mathbf{P}_\beta - (\mathbf{L}_3 - \hat{\mathbf{L}}_3) \mathbf{U}_\alpha \, .$$

Due to the orthogonality, the cost-function reads

$$\begin{aligned} \mathrm{Tr}\{\mathbf{\Theta}\} &= \mathrm{Tr}\{\mathbf{E}_\alpha \mathbf{E}_\alpha^T\} = \left\| \mathbf{E}_\alpha \right\|_F^2 \\ &= \left\| \hat{\mathbf{E}}_\alpha \right\|_F^2 + \left\| (\bar{\mathbf{L}} - \hat{\bar{\mathbf{L}}}) \mathbf{P}_\beta + (\mathbf{L}_3 - \hat{\mathbf{L}}_3) \mathbf{U}_\alpha \right\|_F^2 , \end{aligned}$$

where $\|\cdot\|_F$ denotes Frobenius norm. Hence if $\mathbf{L}_3$ is taken as the (unconstrained) least-squares estimate in (5.29b) and we minimize under the constraint that the rank of $\bar{\mathbf{L}}\mathbf{P}_\beta$ should be n, the approximation is obtained from the SVD of $\hat{\bar{\mathbf{L}}}\mathbf{P}_\beta$ which is exactly what is used in N4SID. Clearly the difference between N4SID and our derivation is at which stage the rank constraint is used. It is expected that the estimate should be more accurate if the constraint is invoked as early as possible.

5.5 Pole Estimation

Given an estimate of the extended observability matrix $\mathbf{\Gamma}_\alpha$, different approaches for deriving the system matrices exist, see [Kun78, Ver94, McK94b, VD94b, Van95]. This chapter focuses on the estimation of the poles. The reasons for this are two-fold:

- For comparing the quality of the estimates from different methods, we need to consider a canonical parameter set. The perhaps simplest and most useful set is the system poles.
- Initial work on the performance of 4SID methods has been reported in [VOWL91, VOWL93, OV94], and the results presented therein rely on the pole estimation error. We will heavily draw from their results.

In this section, we introduce two pole estimation methods appearing in the literature. The asymptotic (in number of data samples N) properties of these two methods are then analyzed in Section 5.6.

5.5.1 The Shift Invariance Method

For deriving the system matrix, $\mathbf{A}$, a straightforward method is to use the shift invariance structure of $\mathbf{\Gamma}_\alpha$, [Kun78, HK66]. Define the selection matrices

$$\mathbf{J}_1 = \begin{bmatrix} \mathbf{I}_{(\alpha-1)l} & \mathbf{0}_{(\alpha-1)l\times l} \end{bmatrix},$$
$$\mathbf{J}_2 = \begin{bmatrix} \mathbf{0}_{(\alpha-1)l\times l} & \mathbf{I}_{(\alpha-1)l} \end{bmatrix},$$

where $\mathbf{I}_n$ denotes the $n \times n$ identity matrix and $\mathbf{0}_{n\times m}$ denotes an $n \times m$ matrix of zeros. Then the estimate of the system matrix is

$$\hat{\mathbf{A}} = \left(\mathbf{J}_1\hat{\mathbf{\Gamma}}_\alpha\right)^\dagger \left(\mathbf{J}_2\hat{\mathbf{\Gamma}}_\alpha\right), \tag{5.30}$$

where $(\cdot)^\dagger$ denotes the Moore-Penrose pseudo inverse of $(\cdot)$. Let $\boldsymbol{\mu}$ be a vector with components μ_k, $k = 1, \ldots, n$, where μ_k denotes the kth pole of the true system. The estimated poles are then, of course, given by the eigenvalues of $\hat{\mathbf{A}}$, i.e.,

$$\hat{\boldsymbol{\mu}} = \text{the eigenvalues of } \hat{\mathbf{A}} \,. \tag{5.31}$$

5.5.2 Subspace Fitting

The second pole estimation technique considered was proposed in [OV94] (see also [SROK95]). Let $\boldsymbol{\Gamma}_\alpha(\boldsymbol{\theta})$ denote the parameterized observability matrix of some realization. The estimated observability matrix, $\hat{\boldsymbol{\Gamma}}_\alpha$, may then be written

$$\hat{\boldsymbol{\Gamma}}_\alpha = \boldsymbol{\Gamma}_\alpha(\boldsymbol{\theta})\mathbf{T} + \tilde{\boldsymbol{\Gamma}}_\alpha, \tag{5.32}$$

where $\mathbf{T}$ denotes an unknown similarity transformation matrix and $\tilde{\boldsymbol{\Gamma}}_\alpha$ is the error. The idea in the subspace fitting approach is to obtain parameter estimates so as to achieve the best fit between the two subspaces spanned by the columns of $\boldsymbol{\Gamma}_\alpha(\boldsymbol{\theta})$ and $\hat{\boldsymbol{\Gamma}}_\alpha$. To be more specific, the unknown parameters ($\boldsymbol{\theta}$ and the elements in $\mathbf{T}$) can be estimated by minimizing some suitable norm of $\tilde{\boldsymbol{\Gamma}}_\alpha$, for example,

$$\|\text{vec}(\hat{\boldsymbol{\Gamma}}_\alpha - \boldsymbol{\Gamma}_\alpha(\boldsymbol{\theta})\mathbf{T})\|^2_{\boldsymbol{\Phi}} \,. \tag{5.33}$$

Here, $\text{vec}(\mathbf{A})$ denotes a vector obtained by stacking the columns of $\mathbf{A}$, $\boldsymbol{\Phi}$ is a positive definite weighting matrix, and $\|\mathbf{x}\|^2_{\boldsymbol{\Phi}} = \mathbf{x}^T\boldsymbol{\Phi}\mathbf{x}$. In [OV94] it was shown that, for minimum variance parameter estimates (of $\boldsymbol{\theta}$), we may equivalently study the following minimization problem

$$\hat{\boldsymbol{\theta}} = \arg\min_{\boldsymbol{\theta}} V(\boldsymbol{\theta}), \tag{5.34}$$

where $V(\boldsymbol{\theta})$ is defined by[2]

$$V(\boldsymbol{\theta}) = \text{vec}^T(\boldsymbol{\Pi}^\perp_{\mathbf{W}^{1/2}\boldsymbol{\Gamma}_\alpha}\hat{\mathbf{Q}}_s)\boldsymbol{\Lambda}\,\text{vec}(\boldsymbol{\Pi}^\perp_{\mathbf{W}^{1/2}\boldsymbol{\Gamma}_\alpha}\hat{\mathbf{Q}}_s) \tag{5.35}$$

for some symmetric positive semi-definite weighting matrix $\boldsymbol{\Lambda}$. Here

$$\boldsymbol{\Pi}^\perp_{\mathbf{W}^{1/2}\boldsymbol{\Gamma}_\alpha} = \mathbf{I} - \mathbf{W}^{1/2}\boldsymbol{\Gamma}_\alpha(\boldsymbol{\Gamma}^*_\alpha\mathbf{W}\boldsymbol{\Gamma}_\alpha)^{-1}\boldsymbol{\Gamma}^*_\alpha\mathbf{W}^{1/2} \tag{5.36}$$

[2] We use the notation $V(\cdot)$ to denote different cost-functions; we believe that this will not cause any confusion.

is a projection matrix on the null space of $(\mathbf{W}^{1/2}\boldsymbol{\Gamma}_\alpha)^*$, and $(\cdot)^*$ denotes the complex conjugate transpose. The argument $(\boldsymbol{\theta})$ has been suppressed for notational convenience.

Remark 5.3. A few comments about the formulation in (5.34) follow. The cost-function (5.35) can be formulated in different ways leading to similar (or identical) results. The choice made herein differs slightly from [OV94]. Instead of $\boldsymbol{\Pi}^{\perp}_{\mathbf{W}^{1/2}\boldsymbol{\Gamma}_\alpha}\hat{\mathbf{Q}}_s$, we could equally well consider $\boldsymbol{\Pi}^{\perp}_{\boldsymbol{\Gamma}_\alpha}\mathbf{W}^{-1/2}\hat{\mathbf{Q}}_s$ or $\mathbf{P}^T\mathbf{W}^{-1/2}\hat{\mathbf{Q}}_s$ where the columns of $\mathbf{P}$ are a parameterized basis for the null space of $\boldsymbol{\Gamma}^*_\alpha(\boldsymbol{\theta})$; see [OV94, VWO97]. See Section 5.6.3 for further comments.

Regarding the parameterization, $\boldsymbol{\Gamma}_\alpha(\boldsymbol{\theta})$ is considered to be parameterized in any way such that the true d-dimensional parameter vector, $\boldsymbol{\theta}_0$, is uniquely given by the identity, $\boldsymbol{\Pi}^{\perp}_{\mathbf{W}^{1/2}\boldsymbol{\Gamma}_\alpha}(\boldsymbol{\theta}_0)\mathbf{Q}_s = \mathbf{0}$. In particular, $\boldsymbol{\Gamma}_\alpha$ in the diagonal realization can be parameterized by the system poles, and for multi-output systems, possibly some of the coefficients in $\mathbf{C}$, see [OV94]. Notice that the parameterization should be such that the projection matrix in (5.36) is real valued. We also refer to [VWO97] for an interesting discussion about the parameterization issue. Therein, it is shown that the null space of $\boldsymbol{\Gamma}^*_\alpha$ can be linearly parameterized which implies that the estimator (5.34) can be implemented in a non-iterative (two-step) fashion (see [OV94, VWO97]).

5.6 Performance Analysis

In this section, the asymptotic performance of the two pole estimation methods described in Section 5.5 is analyzed. A short discussion on consistency is made whereafter the asymptotic distribution of the pole estimates is derived.

5.6.1 Consistency

Consider the subspace estimate obtained through the WLS minimization in Section 5.4.1 (as mentioned previously, this covers the AML case, as well). Thus, we assume the estimate of the extended observability matrix to be given by

$$\hat{\boldsymbol{\Gamma}}_\alpha = \mathbf{W}^{-1/2}\hat{\mathbf{Q}}_s \tag{5.37}$$

where $\hat{\mathbf{Q}}_s$ is obtained from the SVD (cf. (5.23))

$$\hat{\mathbf{Q}}_s\hat{\mathbf{S}}_s\hat{\mathbf{V}}_s^T + \hat{\mathbf{Q}}_n\hat{\mathbf{S}}_n\hat{\mathbf{V}}_n^T = \mathbf{W}^{1/2}\mathbf{Y}_\alpha\mathbf{\Pi}_\alpha^\perp\mathbf{P}_\beta^T\left(\mathbf{P}_\beta\mathbf{\Pi}_\alpha^\perp\mathbf{P}_\beta^T\right)^{-1/2} . \tag{5.38}$$

In the asymptotic analysis, we consider $\mathbf{W}$ to be a fix full rank matrix or, in the data dependent case, a consistent estimate of a full rank matrix. Let $\mathbf{\Gamma}_\alpha^\bullet$ denote the extended observability matrix of a fix realization of (5.1) and let

$$\mathbf{X} = [\mathbf{x}(1+\beta)\,\mathbf{x}(2+\beta)\,\ldots\,\mathbf{x}(N-\alpha+1)] .$$

be the corresponding state trajectory. In the analysis of the shift invariance method we let $\mathbf{\Gamma}_\alpha^\bullet$ be the extended observability matrix of the diagonal realization ($\mathbf{\Gamma}_\alpha^\bullet = \mathbf{\Gamma}_\alpha^d$), whereas $\mathbf{\Gamma}_\alpha^\bullet = \mathbf{\Gamma}_\alpha(\boldsymbol{\theta}_0)$ is the natural choice in the analysis of the subspace fitting method. Next notice that the block Hankel matrix of outputs from a fixed realization of (5.1) is given by (cf. (5.3))

$$\mathbf{Y}_\alpha = \mathbf{\Gamma}_\alpha^\bullet\mathbf{X} + \mathbf{\Phi}_\alpha\mathbf{U}_\alpha + \mathbf{N}_\alpha \tag{5.39}$$

where $\mathbf{N}_\alpha$ is defined similar to (5.12b). By assumption, the noise is uncorrelated with the past inputs and outputs and with the future inputs. By ergodicity, this implies that

$$\lim_{N\to\infty}\mathbf{N}_\alpha\mathbf{U}_\alpha^T = \mathbf{0} , \tag{5.40}$$

$$\lim_{N\to\infty}\mathbf{N}_\alpha\mathbf{P}_\beta^T = \mathbf{0} , \tag{5.41}$$

where the limits are interpreted in terms of convergence w.p.1. Observe that all signals are assumed to be properly scaled such that multiplications as in (5.41) converge to the corresponding covariance. Using these observations, the following limit

$$\lim_{N\to\infty}\mathbf{W}^{1/2}\mathbf{Y}_\alpha\mathbf{\Pi}_\alpha^\perp\mathbf{P}_\beta^T(\mathbf{P}_\beta\mathbf{\Pi}_\alpha^\perp\mathbf{P}_\beta^T)^{-1/2} = \mathbf{W}^{1/2}\mathbf{\Gamma}_\alpha^\bullet\mathbf{R}^\bullet \tag{5.42}$$

is obtained (w.p.1) where, for notational convenience, we have defined

$$\mathbf{R}^\bullet = [\mathbf{R}_{\mathbf{xp}}(\beta) - \mathbf{R}_{\mathbf{xu}}(\beta)\mathbf{R}_{\mathbf{u}}^{-1}\mathbf{R}_{\mathbf{up}}][\mathbf{R}_{\mathbf{p}} - \mathbf{R}_{\mathbf{up}}^T\mathbf{R}_{\mathbf{u}}^{-1}\mathbf{R}_{\mathbf{up}}]^{-1/2} \tag{5.43}$$

and where

$$\begin{aligned}
\mathbf{R}_{\mathbf{xp}}(\tau) &= \bar{\mathrm{E}}\left\{\mathbf{x}(t+\tau)\mathbf{p}_\beta^T(t)\right\} ,\\
\mathbf{R}_{\mathbf{xu}}(\tau) &= \bar{\mathrm{E}}\left\{\mathbf{x}(t+\tau)\mathbf{u}_\alpha^T(t+\beta)\right\} ,\\
\mathbf{R}_{\mathbf{u}} &= \bar{\mathrm{E}}\left\{\mathbf{u}_\alpha(t)\mathbf{u}_\alpha^T(t)\right\} ,\\
\mathbf{R}_{\mathbf{up}} &= \bar{\mathrm{E}}\left\{\mathbf{u}_\alpha(t+\beta)\mathbf{p}_\beta^T(t)\right\} .
\end{aligned}$$

Notice that the covariances involving system states are well defined since the realization is fixed in the analysis. The notation $\mathbf{R}^\bullet$ is in correspondence with the notation for $\mathbf{\Gamma}_\alpha^\bullet$ ($\mathbf{\Gamma}_\alpha^d \leftrightarrow \mathbf{R}^d$, $\mathbf{\Gamma}_\alpha(\boldsymbol{\theta}_0) \leftrightarrow \mathbf{R}^{\boldsymbol{\theta}_0}$). Let $\mathbf{Q}_s\mathbf{S}_s\mathbf{V}_s^T$ be the SVD of the right hand side of (5.42) or, equivalently, the limit of the SVD in (5.38). Assuming the matrix $\mathbf{R}^\bullet$ in (5.42) has full rank equal to n, it is clear that the range space of $\mathbf{Q}_s$ ($\hat{\mathbf{Q}}_s \to \mathbf{Q}_s$ as $N \to \infty$) is a consistent estimate of the range space of $\mathbf{W}^{1/2}\mathbf{\Gamma}_\alpha^\bullet$. Thus, (5.37) is a consistent estimate of the extended observability matrix of some realization. Any reasonable choice of estimator for $\mathbf{C}$ and $\mathbf{A}$ would then provide consistent estimates. In particular, the two pole estimation methods introduced in Section 5.5 will give consistent estimates. Observe that the consistency result in [PSD95] does not apply here since we consider a fix β. For a more complete analysis along the lines of this section, see Chapter 6.

5.6.2 Analysis of the Shift Invariance Method

In this section, the asymptotic properties of the pole estimates from the shift invariance method are analyzed. These results are a straightforward extension of the analysis by [VOWL91, VOWL93] (see also [SS91, RH89]). The modification is needed because the subspace estimate is different and because a weighting ($\mathbf{W}$) is included. A direct application of the shift invariance method can, in some cases, lead to a quite strange behavior of the accuracy of the estimates as function of the dimension parameter α (see [WJ94]). However in [WJ94], the weighting matrix, $\mathbf{W}$, was not included in the analysis. It would therefore be interesting to investigate the effect of the weighting on the pole estimation error. It could be conjectured that a proper choice of such a weighting (for instance, a weighting that makes the residuals white) would improve the accuracy of the pole estimates. However, a quite surprising result obtained below shows that this is not the case; the weighting does not affect the asymptotic pole estimation error.

In order to state the results of this section, we need the following

notation:

$$
\begin{aligned}
\tilde{\mu}_k &= \hat{\mu}_k - \mu_k \,, \\
\mathbf{R}_{\mathbf{n}_\alpha}(\tau) &= \bar{\mathrm{E}}\left\{\mathbf{n}_\alpha(t+\tau)\mathbf{n}_\alpha^T(t)\right\} \,, \\
\boldsymbol{\zeta}(t) &= [\mathbf{y}_\beta^T(t)\ \mathbf{u}_\beta^T(t)\ \mathbf{u}_\alpha^T(t+\beta)]^T = [\mathbf{p}_\beta^T(t)\ \mathbf{u}_\alpha^T(t+\beta)]^T \,, \\
\mathbf{R}_{\boldsymbol{\zeta}}(\tau) &= \bar{\mathrm{E}}\left\{\boldsymbol{\zeta}(t+\tau)\boldsymbol{\zeta}^T(t)\right\} \,, \\
\mathbf{f}_k^* &= \left(\mathbf{J}_1\boldsymbol{\Gamma}_\alpha^d\right)_{k\bullet}^\dagger \left(\mathbf{J}_2 - \mathbf{J}_1\mu_k\right) \,, \qquad (5.44) \\
\mathbf{R}_H &= \begin{bmatrix} \mathbf{I} \\ -\mathbf{R}_{\mathbf{u}}^{-1}\mathbf{R}_{\mathbf{up}} \end{bmatrix} \left(\mathbf{R}_{\mathbf{p}} - \mathbf{R}_{\mathbf{up}}^T\mathbf{R}_{\mathbf{u}}^{-1}\mathbf{R}_{\mathbf{up}}\right)^{-1/2} \,, \\
\boldsymbol{\Omega}_d &= \mathbf{R}_H\mathbf{R}^{d\dagger} \qquad (5.45)
\end{aligned}
$$

where $\mathbf{A}_{k\bullet}$ ($\mathbf{A}_{\bullet k}$) denotes row (column) k of the matrix $\mathbf{A}$. The notation $(\cdot)^c$ will be used to denote complex conjugate.

Theorem 5.1. *Let the subspace estimate be given by* (5.37)-(5.38) *and let the estimates of the system poles be as in* (5.31). *Then* $\sqrt{N}\tilde{\mu}_k$ *is asymptotically zero-mean Gaussian with second moments*

$$
\lim_{N\to\infty} N\,\mathrm{E}\left\{\tilde{\mu}_k\tilde{\mu}_l^c\right\} = \sum_{|\tau|<\alpha} [(\boldsymbol{\Omega}_d)_{\bullet k}]^T\mathbf{R}_{\boldsymbol{\zeta}}(\tau)[(\boldsymbol{\Omega}_d)_{\bullet l}]^c\mathbf{f}_k^*\mathbf{R}_{\mathbf{n}_\alpha}(\tau)\mathbf{f}_l \,, \quad (5.46a)
$$

$$
\lim_{N\to\infty} N\,\mathrm{E}\left\{\tilde{\mu}_k\tilde{\mu}_l\right\} = \sum_{|\tau|<\alpha} [(\boldsymbol{\Omega}_d)_{\bullet k}]^T\mathbf{R}_{\boldsymbol{\zeta}}(\tau)(\boldsymbol{\Omega}_d)_{\bullet l}\mathbf{f}_k^*\mathbf{R}_{\mathbf{n}_\alpha}(\tau)\mathbf{f}_l^c \,. \quad (5.46b)
$$

Proof. The proof is given in Appendix A.11. □

It is not easy to interpret the result of Theorem 5.1 in more general terms. The main merit is the possibility of numerically evaluating the asymptotic performance of the estimator without having to resort to simulations (see Section 5.7). However one specific observation based on the result in Theorem 5.1 is stated next.

Corollary 5.2. *The asymptotic second-order moments of the pole estimation error from the shift invariance method* (5.31) *do not depend on the weighting matrix* $\mathbf{W}$ *introduced in the WLS subspace estimation* (5.37)-(5.38).

Proof. Clearly, the formulae in (5.46) are not affected by the choice of $\mathbf{W}$. □

Remark 5.4. Corollary 5.2 is in fact true for a larger class of subspace estimates than considered in this chapter, e.g., the set of subspace estimates obtained from the unifying theorem in [VD94a].

Remark 5.5. One should keep in mind that Corollary 5.2 holds for large data records. For finite data, the weighting may indeed improve the estimates. Furthermore, the weighting can be useful for other reasons, e.g., model order selection, finite sample bias shaping, and for coping with un-modeled dynamics. We also remind the reader that the result only concerns the pole estimates.

5.6.3 Analysis of the Subspace Fitting Method

In this section, we analyze the asymptotic properties of the parameter estimates from the subspace fitting method (5.34). In [OV94], this estimation problem is solved by invoking the general theory of asymptotically best consistent estimation of nonlinear regression parameters (for instance, see [SS89]). Furthermore, the projection matrix is reparameterized in the coefficients of the characteristic polynomial of $\mathbf{A}$ and a non-iterative procedure for solving (5.34) is described. To some extent, the results of the analysis below will be parallel to the one in [OV94]. Specifically, the optimal weighted method derived below is the same as in [OV94] though phrased slightly different and tailored to our subspace estimate, (5.38)-(5.37), with the weight $\mathbf{W}$ included. Our derivation also provides an expression for the parameter estimation error covariance with a general weighting matrix, not just for the optimal weighting. This will make it possible to compare different weightings. Moreover, the results concern parameters in the extended observability matrix explicitly. This makes it possible to directly apply the result to the pole estimation error (see Section 5.7).

In Appendix A.12, the asymptotic distribution of the estimates from (5.34) is derived through a standard Taylor series expansion approach [Lju87, SS89]. Before presenting the main results of this analysis we

define

$$\mathbf{G} = \Big\{\Big[(\mathbf{W}^{1/2}\boldsymbol{\Gamma}_\alpha)^\dagger \mathbf{Q}_s\Big]^T \otimes \boldsymbol{\Pi}^\perp_{\mathbf{W}^{1/2}\boldsymbol{\Gamma}_\alpha}\mathbf{W}^{1/2}\Big\} \times \big[\mathrm{vec}(\boldsymbol{\Gamma}_{\alpha_1})\ \mathrm{vec}(\boldsymbol{\Gamma}_{\alpha_2})\ \ldots\ \mathrm{vec}(\boldsymbol{\Gamma}_{\alpha_d})\big]\,, \tag{5.47}$$

$$\boldsymbol{\Sigma} = \sum_{|\tau|<\alpha} \big(\mathbf{H}^T\mathbf{R}_{\boldsymbol{\zeta}}(\tau)\mathbf{H}\big) \otimes \big(\boldsymbol{\Pi}^\perp_{\mathbf{W}^{1/2}\boldsymbol{\Gamma}_\alpha}\mathbf{W}^{1/2}\mathbf{R}_{\mathbf{n}_\alpha}(\tau)\mathbf{W}^{1/2}\boldsymbol{\Pi}^\perp_{\mathbf{W}^{1/2}\boldsymbol{\Gamma}_\alpha}\big)\,, \tag{5.48}$$

$$\boldsymbol{\Omega}_{\boldsymbol{\theta}_0} = \mathbf{R}_H \mathbf{R}^{\boldsymbol{\theta}_0\,\dagger}\,, \tag{5.49}$$

where $\boldsymbol{\Gamma}_{\alpha_i}$ denotes the partial derivative of $\boldsymbol{\Gamma}_\alpha = \boldsymbol{\Gamma}_\alpha(\boldsymbol{\theta})$ with respect to $\boldsymbol{\theta}_i$ ($i = 1, \ldots, d$) and $\otimes$ denotes Kronecker product. $\mathbf{H}$ is defined as

$$\mathbf{H} = \mathbf{R}_H \mathbf{V}_s \mathbf{S}_s^{-1}\,. \tag{5.50}$$

Theorem 5.3. *The normalized parameter estimation error*

$$\sqrt{N}\tilde{\boldsymbol{\theta}} = \sqrt{N}(\hat{\boldsymbol{\theta}} - \boldsymbol{\theta}_0),$$

when using the estimator (5.34), is asymptotically zero-mean Gaussian and the asymptotic covariance is given by

$$\lim_{N\to\infty} N\ \mathrm{E}\big\{\tilde{\boldsymbol{\theta}}\tilde{\boldsymbol{\theta}}^T\big\} = (\mathbf{G}^T\boldsymbol{\Lambda}\mathbf{G})^{-1}(\mathbf{G}^T\boldsymbol{\Lambda}\boldsymbol{\Sigma}\boldsymbol{\Lambda}\mathbf{G})(\mathbf{G}^T\boldsymbol{\Lambda}\mathbf{G})^{-1}\,, \tag{5.51}$$

if the inverse exists.

Minimum variance parameter estimates are obtained if the weighting matrix[3] $\boldsymbol{\Lambda}$ *is chosen as*

$$\boldsymbol{\Lambda} = \boldsymbol{\Sigma}^\dagger\,. \tag{5.52}$$

With the choice (5.52)*, the covariance matrix in* (5.51) *can be rewritten*

[3] This weighting is not unique; it is easy to see that any matrix in the null space of $\mathbf{G}^T$ can be added.

as

$$\begin{aligned}\lim_{N\to\infty} N\ \mathrm{E}\{\tilde{\boldsymbol{\theta}}\tilde{\boldsymbol{\theta}}^T\} &= (\mathbf{G}^T\boldsymbol{\Sigma}^\dagger\mathbf{G})^{-1} \\ &= \Big\{[\mathrm{vec}(\boldsymbol{\Gamma}_{\alpha_1})\ \mathrm{vec}(\boldsymbol{\Gamma}_{\alpha_2})\ \cdots\ \mathrm{vec}(\boldsymbol{\Gamma}_{\alpha_d})]^T \\ &\quad \times \Big(\sum_{|\tau|<\alpha} \boldsymbol{\Omega}_{\boldsymbol{\theta}_0}^T \mathbf{R}_{\boldsymbol{\zeta}}(\tau)\boldsymbol{\Omega}_{\boldsymbol{\theta}_0} \otimes \boldsymbol{\Pi}_{\boldsymbol{\Gamma}_\alpha}^\perp \mathbf{R}_{\mathbf{n}_\alpha}(\tau)\boldsymbol{\Pi}_{\boldsymbol{\Gamma}_\alpha}^\perp\Big)^\dagger \\ &\quad \times [\mathrm{vec}(\boldsymbol{\Gamma}_{\alpha_1})\ \mathrm{vec}(\boldsymbol{\Gamma}_{\alpha_2})\ \cdots\ \mathrm{vec}(\boldsymbol{\Gamma}_{\alpha_d})]\Big\}^{-1}.\end{aligned} \tag{5.53}$$

Proof. The proof is given in Appendix A.12. □

As for the shift invariance method, the formulae in Theorem 5.3 are not easy to interpret. It is interesting to compare the asymptotic covariances in the two cases. Clearly the expressions in (5.46) and (5.53) are similar. For the optimally weighted subspace fitting method, we can also give a corollary corresponding to Corollary 5.2 in the shift invariance case.

Corollary 5.4. *Assume the subspace fitting method* (5.34) *is optimally weighted (with* (5.52)*), then the asymptotic parameter estimation error covariance is not affected by the weighting* $\mathbf{W}$ *in the WLS subspace estimation.*

Proof. This is apparent from the derivations leading to (5.53). □

Remark 5.6. Corollary 5.4 is true for a larger class of subspace estimates than considered in this chapter, e.g., the set of subspace estimates obtained from the unifying theorem in [VD94a] (cf. Remark 5.4).

Remark 5.7. In this case, the result of Corollary 5.4 is more intuitive than the corresponding result for the shift invariance method. The intuition could be explained: there is no need to introduce weighting in the subspace estimation step since in the parameter estimation step, we can compensate with a proper choice of $\boldsymbol{\Lambda}$. However, this is in general not true! For example, the same argument would lead to the idea that different choices of *column* weighting in the subspace estimation step (in the SVD (5.38)) also lead to the same asymptotic performance which is not true.

Remark 5.8. As the optimally weighted subspace fitting method has been formulated here, it is not particularly well suited for implementation. We refer to [OV94, VWO97] for further comments and details about the implementation.

In the analysis above, it was assumed that a subspace estimate was given in which the parameters were estimated in a second step. One could ask why not introduce the parameterization of $\mathbf{\Gamma}_\alpha$ directly in (5.14) before a specific subspace estimate is derived? The rest of this section will be concerned with the analysis of the accuracy of the so-obtained estimates. The derived results also lead to an interesting connection to a previously published 4SID parameter estimation algorithm [SROK95] (see Remark 5.10).

If the cost-function (5.14) is minimized with respect to $\mathbf{L}_3$ and then with respect to $\bar{\mathbf{K}}$, the following estimate is obtained

$$\hat{\bar{\mathbf{K}}} = (\mathbf{\Gamma}_\alpha^T \mathbf{W} \mathbf{\Gamma}_\alpha)^{-1} \mathbf{\Gamma}_\alpha^T \mathbf{W} \mathbf{Y}_\alpha \mathbf{\Pi}_\alpha^\perp \mathbf{P}_\beta^T (\mathbf{P}_\beta \mathbf{\Pi}_\alpha^\perp \mathbf{P}_\beta^T)^{-1} .$$

The concentrated cost-function, omitting terms independent of $\mathbf{\Gamma}_\alpha(\boldsymbol{\theta})$, reads

$$V(\boldsymbol{\theta}) = \mathrm{Tr}\left\{ \mathbf{\Pi}^\perp_{\mathbf{W}^{1/2}\mathbf{\Gamma}_\alpha} \mathbf{W}^{1/2} \mathbf{Y}_\alpha \mathbf{\Pi}_\alpha^\perp \mathbf{P}_\beta^T (\mathbf{P}_\beta \mathbf{\Pi}_\alpha^\perp \mathbf{P}_\beta^T)^{-1} \mathbf{P}_\beta \mathbf{\Pi}_\alpha^\perp \mathbf{Y}_\alpha^T \mathbf{W}^{1/2} \right\} . \tag{5.54}$$

Consider the parameter estimates obtained through

$$\hat{\boldsymbol{\theta}}_1 = \arg \min_{\boldsymbol{\theta}} V(\boldsymbol{\theta}) . \tag{5.55}$$

An interesting question is how this estimate is related to the one from (5.34). This can be answered (asymptotically) by using the following result.

Theorem 5.5. *The estimator* (5.55) *is asymptotically equivalent to*

$$\hat{\boldsymbol{\theta}}_2 = \arg \min_{\boldsymbol{\theta}} \mathrm{Tr}\{ \mathbf{\Pi}^\perp_{\mathbf{W}^{1/2}\mathbf{\Gamma}_\alpha} \hat{\mathbf{Q}}_s \mathbf{S}_s^2 \hat{\mathbf{Q}}_s^T \} , \tag{5.56}$$

i.e., $\sqrt{N}(\hat{\boldsymbol{\theta}}_1 - \hat{\boldsymbol{\theta}}_2) \to 0$ *in probability as* $N \to \infty$*, implying that* $\hat{\boldsymbol{\theta}}_1$ *and* $\hat{\boldsymbol{\theta}}_2$ *have the same asymptotic distribution.*

Proof. The proof is given in Appendix A.13. □

Now, it is possible to rewrite the cost-function in (5.56) to yield

$$\mathrm{vec}^T(\mathbf{\Pi}^{\perp}_{\mathbf{W}^{1/2}\mathbf{\Gamma}_\alpha}\hat{\mathbf{Q}}_s)(\mathbf{S}_s^2 \otimes \mathbf{I})\,\mathrm{vec}(\mathbf{\Pi}^{\perp}_{\mathbf{W}^{1/2}\mathbf{\Gamma}_\alpha}\hat{\mathbf{Q}}_s) \tag{5.57}$$

where the facts that $\mathrm{Tr}\{\mathbf{AB}\} = \mathrm{vec}^T(\mathbf{A}^T)\,\mathrm{vec}(\mathbf{B})$ and (A.76) have been used. Comparing (5.57) and (5.35), it is obvious that (5.57) is a special case with

$$\mathbf{\Lambda} = \mathbf{S}_s^2 \otimes \mathbf{I}\,. \tag{5.58}$$

The following theorem is then immediate.

Theorem 5.6. *The estimator in (5.55) yields less accurate estimates than using* (5.34) *with the optimal weighting (5.52).*

Remark 5.9. The performance comparison in Theorem 5.6 is not completely proper since the optimally weighted estimator is considerably more involved (the norms are different). Of course, if we decide to estimate the parameters directly from (5.11), we can do better than (5.55). However, it is interesting that by this we have an expression for the asymptotic covariance for the estimates from (5.55).

Remark 5.10. The last two results should also be compared with the subspace formulation in [SROK95]. They consider a weighted subspace fitting method applied to another subspace estimate than used here. However, if their approach is adopted on the estimate herein, the estimator would be (5.56), and the performance given by (5.51) with the weight (5.58).

Remark 5.11. It is shown in [Jan95] that the estimator (5.56) also has the same asymptotic performance as if the term $\tau = 0$ in (5.52) is only used as weight in (5.34) and $\mathbf{W} = (\mathbf{Y}_\alpha \mathbf{\Pi}_\alpha^{\perp} \mathbf{Y}_\alpha^T)^{-1}$.

Remark 5.12. Our experience is that the accuracy of the estimates from (5.56) in general is the same or worse than what is obtained by the shift invariance method. This is also the reason why this method is not included in the numerical examples in Section 5.7.

5.7 Examples

In this section, we provide two examples in order to compare the shift invariance and the optimally weighted subspace fitting method.

Example 5.1. As briefly mentioned in Section 5.5, a rather strange behavior of the pole estimation accuracy as a function of the prediction horizon parameter α has been noted in [WJ94]. Therein, the system poles were estimated by the shift invariance method, i.e., by (5.31). It was noted that the accuracy does not necessarily increase monotonically with a larger α but it can, in fact, even decrease. With the example below, the importance of proper weighting when recovering the poles from the subspace estimate is clearly visible. The theoretical expression for the estimation error covariance for the weighted subspace fitting estimator (5.53) will be compared with the corresponding result for the shift invariance method (5.46).

Consider the same example as in [WJ94, JW95]. The true system is described by a first-order state-space model

$$x(t+1) = 0.7x(t) + u(t) + w(t)\,, \tag{5.59a}$$

$$y(t) = x(t) + v(t)\,. \tag{5.59b}$$

The measurable input, $u(t)$, is a realization of a white Gaussian process with variance $r_u = 1$. The process noise, $w(t)$, and the measurement noise, $v(t)$, are individually independent white Gaussian processes and uncorrelated with $u(t)$. The variance of $v(t)$ is fixed to $r_v = 1$ while the variance of the process noise will take on two different values, namely $r_w = 0.2$ and $r_w = 2$. The first choice makes the system to be approximately of output error type while the second choice makes the system approximately ARX.

In order to use (5.34), a parameterization of $\mathbf{\Gamma}_\alpha$ has to be chosen. If C is fixed to 1, $\mathbf{\Gamma}_\alpha$ takes the form

$$\mathbf{\Gamma}_\alpha = \begin{bmatrix} 1 & \lambda & \lambda^2 & \cdots & \lambda^{\alpha-1} \end{bmatrix}^T\,,$$

where λ is the pole to be estimated. For details about the implementation of the subspace fitting method, we refer to [OV94].

The theoretical expressions (5.46) and (5.53) will be compared for different variance of the process noise and different combinations of α and β. Fig. 5.1 shows the normalized (by $\sqrt{N}$) asymptotic standard deviation of the pole estimate for the shift invariance method. The two subplots correspond to a different variance of the process noise. Next, the normalized asymptotic standard deviation of the pole estimate from (5.53) is plotted in Fig. 5.2. It is seen that the degradation in accuracy when increasing α for high process noise variance in Fig. 5.1, is overcome in the optimal weighting case, Fig. 5.2. The shift invariance method does

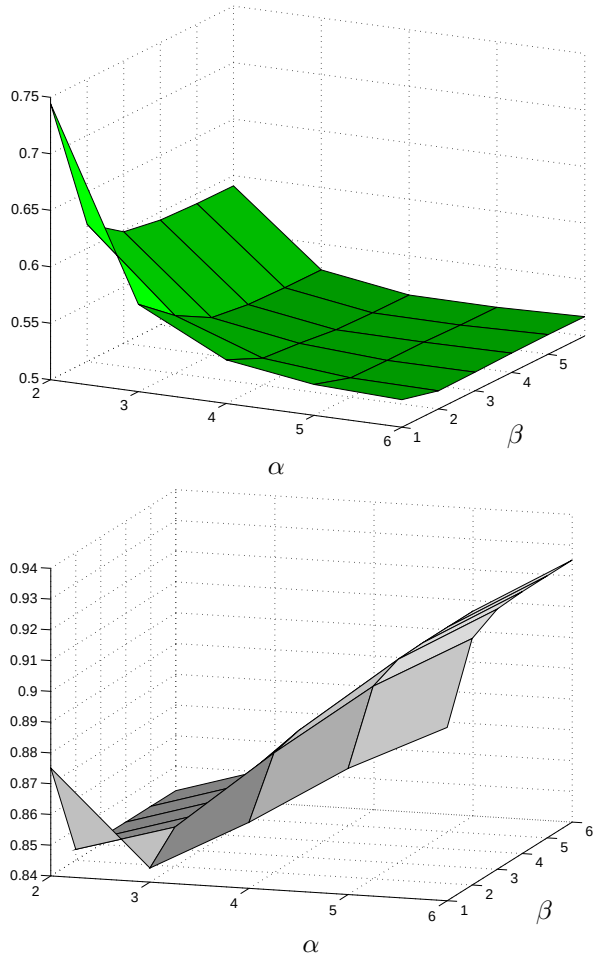

Figure 5.1: The basic shift invariance approach. Normalized asymptotic standard deviation of the estimated pole as a function of α and β. In the first plot, the variance of the process noise is $r_w = 0.2$. In the second, it is $r_w = 2$. For comparison, the Cramér-Rao lower bounds are 0.506 and 0.830, respectively.

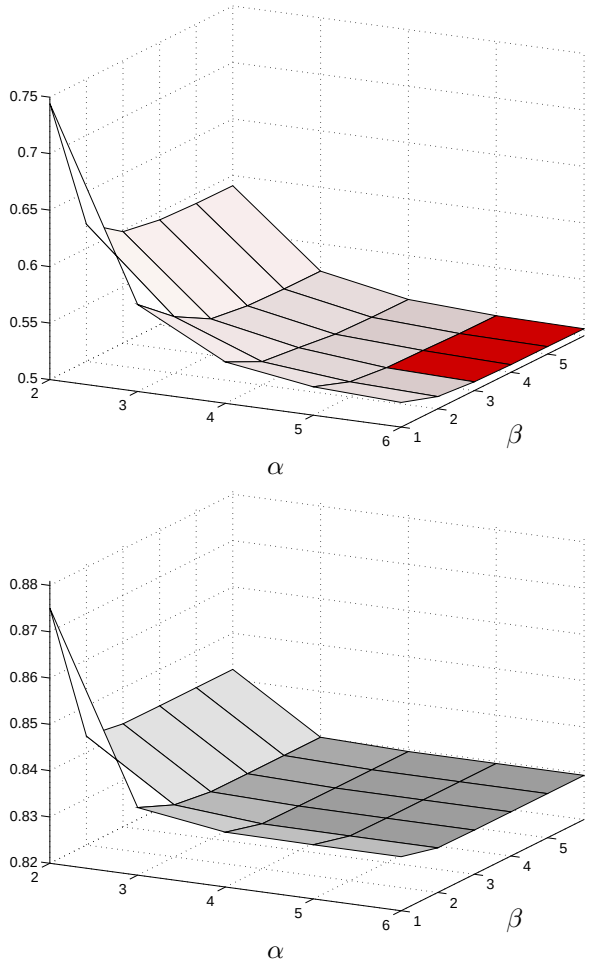

Figure 5.2: The optimally weighted subspace fitting approach. Normalized asymptotic standard deviation of the estimated pole as a function of α and β. In the first plot, the variance of the process noise is $r_w = 0.2$. In the second, it is $r_w = 2$. The Cramér-Rao lower bounds are 0.506 and 0.830, respectively.

not have any inherent weighting compensating for bad scaling, and thus it is impossible to give any rule for the choice of the prediction horizon α. In the weighted subspace fitting method, the weighting assures a more robust or consistent behavior. The performance clearly improves with α, but the computational burden increases, and a trade-off is necessary. For the choice of the observer dimension, β, it is observed that the performance is quite independent of β. Thus, a choice close to the system order would be recommended since the computational cost increases with β. The choice of variance for the input is of no major importance for the point to be made; this value determines (approximatively) the level of the curves, not the shape. The shapes of the curves are determined by the relation between process and measurement noise in combination with how well damped the system is.

For the example, it is possible to calculate a lower bound on the variance of the estimation error for any unbiased estimator of the pole, the Cramér-Rao lower Bound (CRB). This may be done by converting the system (5.59) to a first-order ARMAX system with identical second-order properties as that of the model (5.59). The CRB for the parameters in this ARMAX model is then readily calculated (see, e.g., [SS89]). For this example, the bounds on the pole estimation error standard deviation were calculated to 0.506 and 0.830 for the low and high process noise, respectively. An interesting observation is that the CRB seems to be attained by the method which uses the complete structure of $\mathbf{\Gamma}_\alpha$ for large α and β. ■

Example 5.2. For white input signals, the pole estimators based on $\hat{\mathbf{\Gamma}}_\alpha$ from either N4SID or PO-MOESP give the same asymptotic accuracy. This equivalence does not hold true for colored input signals. In this example, we study the difference between the subspace estimates ($\hat{\mathbf{\Gamma}}_\alpha$) from N4SID and PO-MOESP by comparing the asymptotic pole estimation error variance. The expressions for the variance in the N4SID case are given in [VOWL93] for the shift invariance method and in [OV94] for the weighted subspace fitting method. (Observe that the N4SID subspace estimate is equivalent to the instrumental variable subspace estimate in [VOWL93, OV94], see [VD94a].)

Let the system be as in Example 5.1. We consider the low process noise scenario, i.e., $r_v = 1$ and $r_w = 0.2$. The difference in this example is that the input is a colored signal. More precisely, the input signal $u(t)$

is generated as

$$u(t) = 0.3\frac{q^2 + 2q + 1}{q^2 - 0.17}\eta(t) + \nu(t)$$

where q is the forward shift operator. The zero-mean white noise processes $\eta(t)$ and $\nu(t)$ are independent and have the variances $r_\eta = 10$ and $r_\nu = 10^{-4}$, respectively. Consider the pole estimates from the shift invariance and the optimally weighted subspace fitting method based on the PO-MOESP estimate of $\mathbf{\Gamma}_\alpha$. In Fig. 5.3, the normalized asymptotic standard deviations of the pole estimates are shown as a function of α and β. We see that the variances still are approximatively constant with respect to β. Also notice that the variance of the weighted subspace fitting estimates does not decay monotonically with increasing α.

The corresponding results for the pole estimates based on the N4SID estimate of $\mathbf{\Gamma}_\alpha$ are given in Fig. 5.4. The performance is dramatically affected by the choice of α and β. To avoid misunderstanding it should be noted that the standard deviations in Fig. 5.4 are not what is obtained by the N4SID *algorithm*. In [VD94b], the system matrices and thus the poles are estimated in a completely different way. However, the results presented here indicates that the N4SID estimate of $\mathbf{\Gamma}_\alpha$ may not be the best choice, and this was also alluded to when the subspace estimation was discussed in Section 5.4.3. Monte Carlo type simulations indicate that the N4SID algorithm [VD94b] has a performance similar to the shift invariance method based on the PO-MOESP subspace estimate.

We may also compare the standard deviations in Fig. 5.3 and Fig. 5.4 with the CRB. The CRB for this example was calculated to 0.176. Clearly all the surfaces are above this limit.

In closing this example we remind the reader of Corollary 5.2 and Corollary 5.4 which imply that the asymptotic accuracy of the pole estimates based on either the PO-MOESP or the CVA subspace estimate is identical. ■

5.8 Conclusions

We have used a linear regression formulation to link state-space subspace system identification (4SID) to traditional identification methods. This has been used to compare some cost-functions which arise implicitly in the ordinary framework of 4SID. From the cost-functions, estimates of

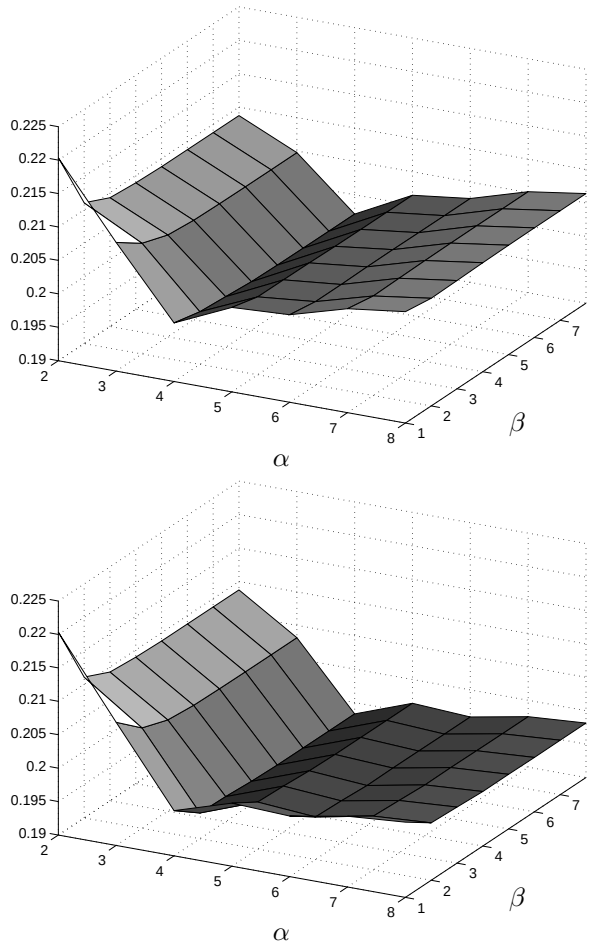

Figure 5.3: The normalized asymptotic standard deviation of the estimated pole as a function of α and β. The first plot is for the shift invariance method and the second for the optimally weighted subspace fitting method. The two pole estimation algorithms are based on the PO-MOESP estimate of $\mathbf{\Gamma}_\alpha$.

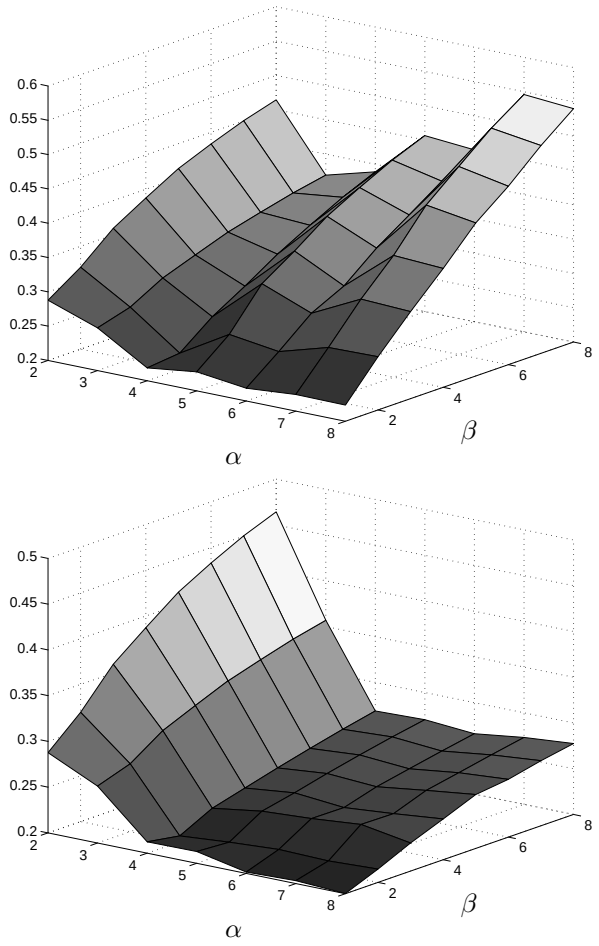

Figure 5.4: The normalized asymptotic standard deviation of the estimated pole as a function of α and β. The first plot is for the shift invariance method and the second for the optimally weighted subspace fitting method. The two pole estimation algorithms are based on the N4SID estimate of $\mathbf{\Gamma}_\alpha$.

the extended observability matrix have been derived and related to existing 4SID methods. Based on these estimates, the estimation of certain parameters were analyzed. In particular the problem of estimating the poles was considered. The asymptotic properties of the estimates of two different methods were analyzed. The first method is common in 4SID and makes use of the shift invariance structure of the observability matrix, while the second method is a recently proposed weighted subspace fitting method. From these results, the choice of user-specified parameters was discussed, and it was shown that this choice indeed may not be obvious for the shift invariance method. This problem can be mitigated by using more of the structure of the system. It was also shown that a proposed row-weighting matrix in the subspace estimation step does not affect the asymptotic properties of the estimates.

Chapter 6

On Consistency of Subspace Methods for System Identification

Subspace methods for the identification of linear time-invariant dynamical systems typically consist of two main steps. First, a so-called subspace estimate is constructed. This first step usually consists of estimating the range space of the extended observability matrix. Secondly, an estimate of system parameters is obtained, based on the subspace estimate. In this chapter, the consistency of a large class of methods for estimating the extended observability matrix is analyzed. Persistence of excitation conditions on the input signal are given which guarantee consistency for systems with only measurement noise. For systems including process noise, it is shown that a persistence of excitation condition on the input is not sufficient. More precisely, an example for which the subspace methods fail to give a consistent estimate of the transfer function is given. This failure occurs even though the input is persistently exciting, to any order. It is also shown that this problem is eliminated if stronger conditions are imposed on the input signal.

6.1 Introduction

The large interest in subspace methods for system identification is motivated by the need for useful engineering tools to model linear multivariable dynamical systems [VD94b, Lar90, Ver94, Vib95]. These methods, sometimes referred to as 4SID (subspace state-space system identification) methods, are easy to apply to identification of multivariable systems. Reliable numerical algorithms form the basis of these methods. The statistical properties, however, are not yet fully understood. Initial work in this direction is exemplified by [VOWL91, PSD96, JW96a, VWO97, BDS97].

Conditions for consistency of the methods in the literature have often involved assumptions on the rank of certain matrices used in the schemes. It would be more useful to have explicit conditions on the input signals and on the system. The consistency of combined deterministic and stochastic subspace identification methods has been analyzed in [PSD96]. In that paper, consistency is proven under two assumptions. One, is the assumption that the input is an ARMA process. Secondly, it is assumed that a dimension parameter tends to infinity at a certain rate as the number of samples approaches infinity. This assumption is needed to consistently estimate the stochastic sub-system and the system order. Subspace methods are typically applied with fixed dimension parameters. A consistency analysis under these conditions is given in [JW96b, JW97a]. The analysis is further extended in this chapter. The analysis focuses on the crucial first step of the subspace identification methods. That is, the focus is on estimating the extended observability matrix, or the "subspace estimation" step. The methods analyzed herein, are called *Basic-4SID* and *IV-4SID*.

The Basic-4SID method [DVVM88, Liu92] has been analyzed in [Gop69, VOWL91, Liu92, VD92]. Herein, we extend the analysis and give persistence of excitation conditions on the input signal. The more recent IV-4SID class of methods include N4SID [VD94b], MOESP [Ver94] and CVA [Lar90]. An open question regarding the IV-4SID methods has been whether or not only a persistence of excitation condition on the input is sufficient for consistency. The current contribution employs a counterexample to show that this is not the case. For systems with only measurement noise, however, it is possible to show that a persistently exciting input of a given order ensures consistency of the IV-4SID subspace estimate. For systems including process noise, IV-4SID methods may suffer from consistency problems. This is explicitly shown in the afore-

mentioned counterexample. A simple proof shows that a white noise (or a low order ARMA) input signal guarantees consistency in this case.

The rest of the chapter is organized as follows. In Section 6.2, the system model is defined and general assumptions are stated. Some preliminary results are also collected in this section. In Section 6.3, the ideas of the Basic 4SID and IV-4SID methods are presented. In Section 6.4, the consistency of the Basic-4SID method is analyzed. In Section 6.5, the critical relation for consistency of IV-4SID methods is presented. Conditions for this relation to hold are given. In Section 6.6, the counterexample is given, describing a system for which the critical relation does not hold. In Section 6.7, some simulations are presented to illustrate the theoretical results. Finally, conclusions are provided in Section 6.8.

6.2 Preliminaries

Assume that the true system is linear, time-invariant and described by the following state-space equations:

$$\mathbf{x}(t+1) = \mathbf{A}\mathbf{x}(t) + \mathbf{B}\mathbf{u}(t) + \mathbf{w}(t), \tag{6.1a}$$

$$\mathbf{y}(t) = \mathbf{C}\mathbf{x}(t) + \mathbf{D}\mathbf{u}(t) + \mathbf{e}(t). \tag{6.1b}$$

Here, $\mathbf{x}(t) \in \mathbb{R}^n$ is the state-vector, $\mathbf{u}(t) \in \mathbb{R}^m$ consists of the observed input signals, and $\mathbf{y}(t) \in \mathbb{R}^l$ contains the observed output signals. The system is perturbed by the process noise $\mathbf{w}(t) \in \mathbb{R}^n$ and the measurement noise $\mathbf{e}(t) \in \mathbb{R}^l$.

Let us introduce the following general assumptions:

A1: The noise process $[\mathbf{w}^T(t)\ \mathbf{e}^T(t)]^T$ is a stationary, ergodic, zero-mean, white noise process with covariance matrix,

$$\mathrm{E}\{\begin{bmatrix}\mathbf{w}(t)\\ \mathbf{e}(t)\end{bmatrix}\begin{bmatrix}\mathbf{w}(t)\\ \mathbf{e}(t)\end{bmatrix}^T\} = \begin{bmatrix}\mathbf{r}_w & \mathbf{r}_{we}\\ \mathbf{r}_{we}^T & \mathbf{r}_e\end{bmatrix}.$$

It will be convenient to introduce an $n \times p$ matrix $\mathbf{K}$ such that $\mathbf{r}_w = \mathbf{K}\mathbf{K}^T$, where p is the rank of $\mathbf{r}_w$. This implies that $\mathbf{w}(t) = \mathbf{K}\mathbf{v}(t)$. Here, $\mathrm{E}\{\mathbf{v}(t)\mathbf{v}^T(t)\} = \mathbf{I}_p$ and $\mathbf{I}_p$ denotes a $p \times p$ identity matrix.

A2: The input $\mathbf{u}(t)$ is a quasi-stationary signal [Lju87]. The correlation sequence is defined by

$$\mathbf{r}_u(\tau) = \bar{\mathrm{E}}\{\mathbf{u}(t+\tau)\mathbf{u}^T(t)\}$$

where $\bar{\mathrm{E}}$ is defined as

$$\bar{\mathrm{E}}\{\cdot\} = \lim_{N\to\infty} \frac{1}{N} \sum_{t=1}^{N} \mathrm{E}\{\cdot\}\,.$$

The input $\mathbf{u}(t)$ and the noise process are assumed to be uncorrelated.

A3: The system (6.1) is asymptotically stable. That is, the eigenvalues of $\mathbf{A}$ lie strictly inside the unit circle.

A4: The description (6.1) is minimal in the sense that the pair $(\mathbf{A}, \mathbf{C})$ is observable and the pair $(\mathbf{A}, [\mathbf{B}\ \mathbf{K}])$ is reachable.

The concept of persistently exciting signals is defined in the following way:

Definition 6.1. A (quasi-stationary) signal $\mathbf{u}(t)$ is said to be persistently exciting of order n, denoted by PE(n), if the following matrix is positive definite;

$$\begin{bmatrix} \mathbf{r}_u(0) & \mathbf{r}_u(1) & \dots & \mathbf{r}_u(n-1) \\ \mathbf{r}_u(-1) & \mathbf{r}_u(0) & & \mathbf{r}_u(n-2) \\ \vdots & & \ddots & \vdots \\ \mathbf{r}_u(1-n) & \mathbf{r}_u(2-n) & \dots & \mathbf{r}_u(0) \end{bmatrix}.$$

The following two lemmas will be useful in the consistency analysis.

Lemma 6.1. *Consider the (block) matrix*

$$\mathbf{S} = \begin{bmatrix} \mathbf{A} & \mathbf{B} \\ \mathbf{C} & \mathbf{D} \end{bmatrix}, \tag{6.2}$$

where $\mathbf{A}$ *is* $n \times n$ *and* $\mathbf{D}$ *is a non-singular* $m \times m$ *matrix. Then*

$$\mathrm{rank}\{\mathbf{S}\} = m + \mathrm{rank}\{\mathbf{A} - \mathbf{B}\mathbf{D}^{-1}\mathbf{C}\}.$$

Proof. The result follows directly from the identity,

$$\begin{bmatrix} \mathbf{I} & -\mathbf{B}\mathbf{D}^{-1} \\ \mathbf{0} & \mathbf{I} \end{bmatrix} \begin{bmatrix} \mathbf{A} & \mathbf{B} \\ \mathbf{C} & \mathbf{D} \end{bmatrix} \begin{bmatrix} \mathbf{I} & \mathbf{0} \\ -\mathbf{D}^{-1}\mathbf{C} & \mathbf{I} \end{bmatrix} = \begin{bmatrix} \boldsymbol{\Delta} & \mathbf{0} \\ \mathbf{0} & \mathbf{D} \end{bmatrix}, \tag{6.3}$$

where $\boldsymbol{\Delta} = \mathbf{A} - \mathbf{B}\mathbf{D}^{-1}\mathbf{C}$. □

Using (6.3), the next lemma is readily proven.

Lemma 6.2. *Let* $\mathbf{S}$ *be as in* (6.2) *but symmetric (*$\mathbf{C} = \mathbf{B}^T$*), and let* $\mathbf{D}$ *be positive definite. Conclude then, that* $\mathbf{S}$ *is positive (semi) definite if and only if* $(\mathbf{A} - \mathbf{B}\mathbf{D}^{-1}\mathbf{B}^T)$ *is positive (semi) definite.*

6.3 Background

In this section, the basic equations used in subspace state-space system identification (4SID) methods are reviewed. Define the $l\alpha \times 1$ vector of stacked outputs as

$$\mathbf{y}_\alpha(t) = \left[\mathbf{y}^T(t), \mathbf{y}^T(t+1), \ldots, \mathbf{y}^T(t+\alpha-1)\right]^T ,$$

where α is a user-specified parameter which is required to be greater than the observability index (or, for simplicity, the system order n). In a similar manner, define vectors made of stacked inputs, process and measurement noises as $\mathbf{u}_\alpha(t)$, $\mathbf{w}_\alpha(t)$ and $\mathbf{e}_\alpha(t)$, respectively. By iteration of the state equations in (6.1), it is straightforward to verify the following equation for the stacked quantities;

$$\mathbf{y}_\alpha(t) = \mathbf{\Gamma}_\alpha \mathbf{x}(t) + \mathbf{\Phi}_\alpha \mathbf{u}_\alpha(t) + \mathbf{n}_\alpha(t) , \tag{6.4}$$

where

$$\mathbf{n}_\alpha(t) = \mathbf{\Psi}_\alpha \mathbf{w}_\alpha(t) + \mathbf{e}_\alpha(t) ,$$

and where the following block matrices have been introduced:

$$\mathbf{\Gamma}_\alpha = \begin{bmatrix} \mathbf{C} \\ \mathbf{CA} \\ \vdots \\ \mathbf{CA}^{\alpha-1} \end{bmatrix},$$

$$\mathbf{\Phi}_\alpha = \begin{bmatrix} \mathbf{D} & \mathbf{0} & \cdots & \mathbf{0} \\ \mathbf{CB} & \mathbf{D} & \ddots & \mathbf{0} \\ \vdots & \ddots & \ddots & \vdots \\ \mathbf{CA}^{\alpha-2}\mathbf{B} & \mathbf{CA}^{\alpha-3}\mathbf{B} & \cdots & \mathbf{D} \end{bmatrix},$$

$$\mathbf{\Psi}_\alpha = \begin{bmatrix} \mathbf{0} & \mathbf{0} & \cdots & \mathbf{0} \\ \mathbf{C} & \mathbf{0} & \ddots & \mathbf{0} \\ \vdots & \ddots & \ddots & \vdots \\ \mathbf{CA}^{\alpha-2} & \mathbf{CA}^{\alpha-3} & \cdots & \mathbf{0} \end{bmatrix}.$$

The key idea of subspace identification methods is to first estimate the n-dimensional range space of the (extended) observability matrix $\mathbf{\Gamma}_\alpha$. Based

on the first step, the system parameters are subsequently estimated in various ways. For consistency of 4SID methods it is crucial that the estimate of $\mathbf{\Gamma}_\alpha$ is consistent.

There have been several suggestions in the literature for estimating $\mathbf{\Gamma}_\alpha$. Most of them, however, are closely related to one another [VD95c, Vib95]. To describe the methods considered, additional notation is needed. Assume there are $N + \alpha + \beta - 1$ data samples available and introduce the block Hankel matrices

$$\mathbf{Y}_\alpha = [\mathbf{y}_\alpha(1+\beta), \ldots, \mathbf{y}_\alpha(N+\beta)], \tag{6.5}$$

$$\mathbf{Y}_\beta = [\mathbf{y}_\beta(1), \ldots, \mathbf{y}_\beta(N)]. \tag{6.6}$$

The parameter β is to be chosen by the user. Intuitively, β can be interpreted as the dimension of the observer used to estimate the current state [WJ94] (see also Chapter 1 and Chapter 5). The partitioning of data into $\mathbf{Y}_\beta$ and $\mathbf{Y}_\alpha$ is sometimes referred to as "past" and "future". Define $\mathbf{U}_\alpha$ and $\mathbf{U}_\beta$ as block Hankel matrices of inputs similar to (6.5) and (6.6), respectively. Comparing (6.5) and (6.4), it is clear that $\mathbf{Y}_\alpha$ is given by the relation

$$\mathbf{Y}_\alpha = \mathbf{\Gamma}_\alpha \mathbf{X}_f + \mathbf{\Phi}_\alpha \mathbf{U}_\alpha + \mathbf{N}_\alpha \,, \tag{6.7}$$

where

$$\mathbf{X}_f = \begin{bmatrix} \mathbf{x}(1+\beta) & \mathbf{x}(2+\beta) & \ldots & \mathbf{x}(N+\beta) \end{bmatrix} \,,$$

and $\mathbf{N}_\alpha$ is defined from $\mathbf{n}_\alpha(t)$ similar to (6.5). Two methods of estimating the range space of $\mathbf{\Gamma}_\alpha$ from data are presented next. The methods are based on (6.7).

6.3.1 Basic 4SID

The method described in this section is sometimes referred to as the Basic 4SID method [DVVM88, Liu92]. When considering this method, it is not necessary to partition the data into past and future. Hence it can be assumed that $\beta = 0$. The idea is to study the residuals in the regression of $\mathbf{y}_\alpha(t)$ on $\mathbf{u}_\alpha(t)$ in (6.4). Introduce the orthogonal projection matrix on the null space of $\mathbf{U}_\alpha$ as

$$\mathbf{\Pi}^{\perp}_{\mathbf{U}_\alpha^T} = \mathbf{I} - \mathbf{U}_\alpha^T (\mathbf{U}_\alpha \mathbf{U}_\alpha^T)^{-1} \mathbf{U}_\alpha.$$

If the input $\mathbf{u}(t)$ is PE(α), then the inverse of $\mathbf{U}_\alpha \mathbf{U}_\alpha^T$ exists for sufficiently large N. The residual vectors in the regression of $\mathbf{y}_\alpha(t)$ on $\mathbf{u}_\alpha(t)$ are now given by the columns of the following expression:

$$\frac{1}{\sqrt{N}}\mathbf{Y}_\alpha \mathbf{\Pi}_{\mathbf{U}_\alpha^T}^\perp = \frac{1}{\sqrt{N}}\mathbf{\Gamma}_\alpha \mathbf{X}_f \mathbf{\Pi}_{\mathbf{U}_\alpha^T}^\perp + \frac{1}{\sqrt{N}}\mathbf{N}_\alpha \mathbf{\Pi}_{\mathbf{U}_\alpha^T}^\perp, \tag{6.8}$$

where the normalizing factor $1/\sqrt{N}$ has been introduced for later convenience. The approach taken in Basic 4SID to estimate the range space of $\mathbf{\Gamma}_\alpha$ is the following: retain the n left principal singular vectors in the singular value decomposition (SVD) of (6.8). The Basic 4SID estimate of $\mathbf{\Gamma}_\alpha$ is then given by

$$\hat{\mathbf{\Gamma}}_\alpha = \hat{\mathbf{Q}}_s \,, \tag{6.9}$$

where $\hat{\mathbf{Q}}_s$ is obtained from the SVD

$$\begin{bmatrix}\hat{\mathbf{Q}}_s & \hat{\mathbf{Q}}_n\end{bmatrix}\begin{bmatrix}\hat{\mathbf{S}}_s & \mathbf{0} \\ \mathbf{0} & \hat{\mathbf{S}}_n\end{bmatrix}\begin{bmatrix}\hat{\mathbf{V}}_s^T \\ \hat{\mathbf{V}}_n^T\end{bmatrix} = \frac{1}{\sqrt{N}}\mathbf{Y}_\alpha \mathbf{\Pi}_{\mathbf{U}_\alpha^T}^\perp.$$

Here, $\hat{\mathbf{S}}_s$ is a diagonal matrix containing the n largest singular values and $\hat{\mathbf{Q}}_s$ contains the corresponding left singular vectors.

6.3.2 IV-4SID

The second type of estimator that will be analyzed is called IV-4SID [VD94b, Lar90, Ver94]. The reason for this name is that this approach is most easily explained in terms of instrumental variables (IVs) (see e.g. [Vib95, Gus97]). The advantage of IV-4SID (compared to Basic 4SID) is that IV-4SID can handle more general noise correlations. The main idea here is to use an instrumental variable, which not only removes the effect of $\mathbf{u}_\alpha(t)$ in (6.4) (as in the Basic 4SID), but also reduces the effect of $\mathbf{n}_\alpha(t)$. The first step is to remove the future inputs. This is the same as in Basic 4SID. The second step is to remove the noise term in (6.8). This is accomplished by multiplying from the right by the "instrumental variable matrix"

$$\mathbf{P}_\beta = \begin{bmatrix}\mathbf{Y}_\beta \\ \mathbf{U}_\beta\end{bmatrix}. \tag{6.10}$$

Post-multiplying both sides of (6.8) with the matrix in (6.10), and normalizing by $1/\sqrt{N}$ yields,

$$\frac{1}{N}\mathbf{Y}_\alpha \mathbf{\Pi}_{\mathbf{U}_\alpha^T}^\perp \mathbf{P}_\beta^T = \frac{1}{N}\mathbf{\Gamma}_\alpha \mathbf{X}_f \mathbf{\Pi}_{\mathbf{U}_\alpha^T}^\perp \mathbf{P}_\beta^T + \frac{1}{N}\mathbf{N}_\alpha \mathbf{\Pi}_{\mathbf{U}_\alpha^T}^\perp \mathbf{P}_\beta^T,$$

$\hat{\mathbf{W}}_c$	$\hat{\mathbf{W}}_r$	Method
$\left(\frac{1}{N}\mathbf{P}_\beta\mathbf{\Pi}^\perp_{\mathbf{U}^T_\alpha}\mathbf{P}^T_\beta\right)^{-1/2}$	$\mathbf{I}$	PO-MOESP
$\left(\frac{1}{N}\mathbf{P}_\beta\mathbf{\Pi}^\perp_{\mathbf{U}^T_\alpha}\mathbf{P}^T_\beta\right)^{-1}\left(\frac{1}{N}\mathbf{P}_\beta\mathbf{P}^T_\beta\right)^{1/2}$	$\mathbf{I}$	N4SID
$\left(\frac{1}{N}\mathbf{P}_\beta\mathbf{P}^T_\beta\right)^{-1/2}$	$\left(\frac{1}{N}\mathbf{Y}_\alpha\mathbf{\Pi}^\perp_{\mathbf{U}^T_\alpha}\mathbf{Y}^T_\alpha\right)^{-1/2}$	IVM
$\left(\frac{1}{N}\mathbf{P}_\beta\mathbf{\Pi}^\perp_{\mathbf{U}^T_\alpha}\mathbf{P}^T_\beta\right)^{-1/2}$	$\left(\frac{1}{N}\mathbf{Y}_\alpha\mathbf{\Pi}^\perp_{\mathbf{U}^T_\alpha}\mathbf{Y}^T_\alpha\right)^{-1/2}$	CVA

Table 6.1: Weighting matrices corresponding to specific methods. Notice that some of the weightings may not be as they appear in the referred papers. These weightings, however, give estimates of $\mathbf{\Gamma}_\alpha$ identical to those obtained using the original choice of weighting.

where, due to the assumptions, the second term on the right tends to zero with probability one (w.p.1) as N tends to infinity (since the input and the noise process are uncorrelated, and since there is a "time shift" between $\mathbf{N}_\alpha$ and the noise in $\mathbf{Y}_\beta$). A quite general estimate of $\mathbf{\Gamma}_\alpha$ is then given by

$$\hat{\mathbf{\Gamma}}_\alpha = \hat{\mathbf{W}}_r^{-1}\hat{\mathbf{Q}}_s\,, \tag{6.11}$$

where $\hat{\mathbf{Q}}_s$ is the $\alpha l \times n$ matrix made of the n left singular vectors of

$$\frac{1}{N}\hat{\mathbf{W}}_r\mathbf{Y}_\alpha\mathbf{\Pi}^\perp_{\mathbf{U}^T_\alpha}\mathbf{P}^T_\beta\hat{\mathbf{W}}_c \tag{6.12}$$

corresponding to the n largest singular values. The (data dependent) weighting matrices $\hat{\mathbf{W}}_r$ and $\hat{\mathbf{W}}_c$ can be chosen in different ways to yield a class of estimators. This class includes most of the known methods appearing in the literature; see Table 6.1, cf. [VD95c, Vib95]. The methods PO-MOESP, N4SID, IVM and CVA appear in [Ver94, VD94b, Vib95, Lar90], respectively. For some results regarding the effect of the choice of the weighting matrices, see [JW95, JW96a, VD95b].

6.4 Analysis of Basic 4SID

In this section, conditions are established by which the Basic 4SID estimate $\hat{\mathbf{\Gamma}}_\alpha$ in (6.9) becomes consistent. Here, consistency means that the

column span of $\hat{\mathbf{\Gamma}}_\alpha$ tends to the column span of $\mathbf{\Gamma}_\alpha$ as N tends to infinity (w.p.1). This method has been analyzed previously (see [Gop69, VOWL91, Liu92, VD92]). This problem is reconsidered here, however, for two reasons. First, the proof to be presented appears to be more explicit than previous ones (known to the authors). Second, these results are useful in the analysis of the more interesting IV-based methods given in the next section.

Recall Equation (6.4). No correlation exists between the noise $\mathbf{n}_\alpha(t)$ and $\mathbf{u}_\alpha(t)$ or $\mathbf{x}(t)$. It is therefore relatively straightforward to show that the sample covariance matrix of the residuals in (6.8)

$$\hat{\mathbf{R}}_\varepsilon = \frac{1}{N}\mathbf{Y}_\alpha \mathbf{\Pi}^\perp_{\mathbf{U}_\alpha^T} \mathbf{Y}_\alpha^T$$

tends to

$$\mathbf{R}_\varepsilon = \mathbf{\Gamma}_\alpha(\mathbf{r}_x - \mathbf{r}_{xu}\mathbf{R}_u^{-1}\mathbf{r}_{xu}^T)\mathbf{\Gamma}_\alpha^T + \mathbf{R}_n \tag{6.13}$$

with probability one, as $N \to \infty$. Here, the various correlation matrices are defined as:

$$\begin{aligned}
\mathbf{r}_x &= \bar{\mathrm{E}}\{\mathbf{x}(t)\mathbf{x}^T(t)\},\\
\mathbf{r}_{xu} &= \bar{\mathrm{E}}\{\mathbf{x}(t)\mathbf{u}_\alpha^T(t)\},\\
\mathbf{R}_u &= \bar{\mathrm{E}}\{\mathbf{u}_\alpha(t)\mathbf{u}_\alpha^T(t)\},\\
\mathbf{R}_n &= \bar{\mathrm{E}}\{\mathbf{n}_\alpha(t)\mathbf{n}_\alpha^T(t)\}.
\end{aligned}$$

Recall that $\mathbf{u}(t)$ is assumed to be PE(α). This implies that $\mathbf{R}_u$ is positive definite. From (6.13) it can be concluded that the estimate of $\mathbf{\Gamma}_\alpha$ in (6.9) is consistent if and only if,[1]

$$\mathbf{R}_n = \sigma^2\mathbf{I}, \tag{6.14}$$

$$\mathbf{r}_x - \mathbf{r}_{xu}\mathbf{R}_u^{-1}\mathbf{r}_{xu}^T > \mathbf{0} \tag{6.15}$$

for some scalar σ^2. If (6.14) and (6.15) hold, then the limit of $\hat{\mathbf{\Gamma}}_\alpha$ (as defined in (6.9)), is given by $\mathbf{\Gamma}_\alpha\mathbf{T}$ for some non-singular $n \times n$ matrix $\mathbf{T}$. The condition (6.14) is essentially only true for output error systems perturbed by a measurement noise of equal power in each output channel.

[1] There may exist particular cases when Basic 4SID is consistent even when $\mathbf{R}_n \neq \sigma^2\mathbf{I}$. However, these cases depend on the system parameters and are not of interest here.

That is, if $\mathbf{K} = \mathbf{0}$ and $\mathbf{r}_e = \sigma^2\mathbf{I}$. In the following it is shown under what conditions (on the input signals) the condition (6.15) is fulfilled.

In view of Lemma 6.2, the condition (6.15) is equivalent to

$$\bar{\mathrm{E}}\left\{\begin{bmatrix}\mathbf{x}(t)\\ \mathbf{u}_\alpha(t)\end{bmatrix}\begin{bmatrix}\mathbf{x}(t)\\ \mathbf{u}_\alpha(t)\end{bmatrix}^T\right\} = \begin{bmatrix}\mathbf{r}_x & \mathbf{r}_{xu}\\ \mathbf{r}_{xu}^T & \mathbf{R}_u\end{bmatrix} > \mathbf{0}. \tag{6.16}$$

Next, the state is decomposed into two terms $\mathbf{x}(t) = \mathbf{x}^d(t) + \mathbf{x}^s(t)$, where the "deterministic" term $\mathbf{x}^d(t)$ is due to the observed inputs and the "stochastic" term $\mathbf{x}^s(t)$ is driven by the process noise $\mathbf{w}(t)$. Due to assumption **A2**, no correlation exists between $\mathbf{x}^s(t)$ and $\mathbf{x}^d(t)$ or $\mathbf{u}_\alpha(t)$. Furthermore, introduce a transfer function (operator) description of $\mathbf{x}^d(t)$ as

$$\mathbf{x}^d(t) = \frac{\mathbf{F}^u(q^{-1})}{a(q^{-1})}\mathbf{u}(t),$$

where q^{-1} is the backward shift operator. That is, $q^{-1}\mathbf{u}(t) = \mathbf{u}(t-1)$. The polynomials $\mathbf{F}^u(q^{-1})$ and $a(q^{-1})$ are defined by the relations

$$\begin{aligned}\mathbf{F}^u(q^{-1}) &= \frac{\mathrm{Adj}\{q\mathbf{I}-\mathbf{A}\}\mathbf{B}}{q^n}\\ &= \mathbf{F}_1^u q^{-1} + \mathbf{F}_2^u q^{-2} + \cdots + \mathbf{F}_n^u q^{-n}, \qquad (6.17)\\ a(q^{-1}) &= \frac{\det\{q\mathbf{I}-\mathbf{A}\}}{q^n}\\ &= a_0 + a_1 q^{-1} + \cdots + a_n q^{-n}, \quad (a_0 = 1), \qquad (6.18)\end{aligned}$$

where $\mathrm{Adj}\{\mathbf{A}\}$ denotes the adjugate matrix of $\mathbf{A}$ and $\det\{\cdot\}$ is the determinant function. The polynomial coefficients a_i $(i = 0, \ldots, n)$ are scalars while all $\mathbf{F}_i^u$ $(i = 1, \ldots, n)$ are $n \times m$ matrices. Analogously to $\mathbf{F}^u(q^{-1})$, define the matrix polynomial $\mathbf{F}^w(q^{-1})$, with $\mathbf{K}$ replacing $\mathbf{B}$:

$$\mathbf{F}^w(q^{-1}) = \mathbf{F}_1^w q^{-1} + \mathbf{F}_2^w q^{-2} + \cdots + \mathbf{F}_n^w q^{-n},$$

where $\mathbf{F}_i^w$ $(i = 1, \ldots, n)$ are $n \times p$ matrices and $\mathbf{K}$ is defined in assumption **A1**. Thus, $\mathbf{x}^s(t)$ is given by the relation

$$\mathbf{x}^s(t) = \frac{\mathbf{F}^w(q^{-1})}{a(q^{-1})}\mathbf{v}(t).$$

Also define the Sylvester-like matrix

$$\mathcal{S} = \underbrace{\begin{bmatrix} \mathbf{F}_n^u & \dots & \mathbf{F}_1^u & \mathbf{0} & \dots & \mathbf{0} & \mathbf{F}_n^w & \dots & \mathbf{F}_1^w \\ a_n\mathbf{I}_m & \dots & a_1\mathbf{I}_m & a_0\mathbf{I}_m & & \mathbf{0} & \mathbf{0} & \dots & \mathbf{0} \\ & \ddots & & & \ddots & & \vdots & & \vdots \\ \mathbf{0} & & a_n\mathbf{I}_m & \dots & \dots & a_0\mathbf{I}_m & \mathbf{0} & \dots & \mathbf{0} \end{bmatrix}}_{(n+\alpha m)\times((\alpha+n)m+np)}. \quad (6.19)$$

Using the notation introduced above, it can be verified that

$$\begin{bmatrix} \mathbf{x}(t) \\ \mathbf{u}_\alpha(t) \end{bmatrix} = \mathcal{S}\frac{1}{a(q^{-1})} \begin{bmatrix} \mathbf{u}(t-n) \\ \vdots \\ \mathbf{u}(t+\alpha-1) \\ \mathbf{v}(t-n) \\ \vdots \\ \mathbf{v}(t-1) \end{bmatrix}.$$

It is shown in Appendix A.14 that $\mathcal{S}$ has full row rank under assumption **A4**. This implies that the condition (6.16) is satisfied if the following matrix is positive definite:

$$\bar{\mathrm{E}}\left\{ \frac{1}{a(q^{-1})} \begin{bmatrix} \mathbf{u}(t-n) \\ \vdots \\ \mathbf{u}(t+\alpha-1) \\ \mathbf{v}(t-n) \\ \vdots \\ \mathbf{v}(t-1) \end{bmatrix} \frac{1}{a(q^{-1})} \begin{bmatrix} \mathbf{u}(t-n) \\ \vdots \\ \mathbf{u}(t+\alpha-1) \\ \mathbf{v}(t-n) \\ \vdots \\ \mathbf{v}(t-1) \end{bmatrix}^T \right\}. \quad (6.20)$$

Since $\mathbf{u}(t)$ and $\mathbf{v}(t)$ are uncorrelated, the covariance matrix in (6.20) will be block diagonal. The lower diagonal block is positive definite since $\mathrm{E}\{\mathbf{v}(t)\mathbf{v}^T(\tau)\} = \mathbf{I}\delta_{t,\tau}$. The upper diagonal block can be shown to be positive definite if $\mathbf{u}(t)$ is PE($\alpha+n$); see Lemma A.3.7 in [SS83], modified to quasi-stationary signals. In conclusion, the following theorem has been proven.

Theorem 6.1. *Under the general assumptions **A1-A4**, the Basic 4SID subspace estimate* (6.9) *is consistent if the following conditions are true:*

1. *The covariance matrix of the stacked noise is proportional to the identity matrix. That is,* $\mathbf{R}_n = \sigma^2\mathbf{I}$.

2. The input signal $\mathbf{u}(t)$ *is persistently exciting of order* $\alpha + n$.

Remark 6.1. As previously mentioned, condition (1) of the theorem is essentially only true if $\mathbf{K} = \mathbf{0}$ and if $\mathbf{r}_e = \sigma^2\mathbf{I}$. Furthermore, $\mathbf{K} = \mathbf{0}$ implies that the system must be reachable from $\mathbf{u}(t)$.

6.5 Analysis of IV-4SID

In this section, conditions for the IV-4SID estimate $\hat{\mathbf{\Gamma}}_\alpha$ in (6.11) to be consistent are established. As $N \to \infty$, the limit of the quantity in (6.12) is w.p.1 given by

$$\mathbf{W}_r\mathbf{\Gamma}_\alpha(\mathbf{r}_{xp} - \mathbf{r}_{xu}\mathbf{R}_u^{-1}\mathbf{R}_{up})\mathbf{W}_c, \tag{6.21}$$

where $\mathbf{W}_r$ and $\mathbf{W}_c$ are the limits of $\hat{\mathbf{W}}_r$ and $\hat{\mathbf{W}}_c$, respectively. The correlation matrices appearing in (6.21) are defined as follows:

$$\begin{aligned}
\mathbf{r}_{xp} &= \bar{\mathrm{E}}\{\mathbf{x}(t+\beta)\mathbf{p}_\beta^T(t)\},\\
\mathbf{r}_{xu} &= \bar{\mathrm{E}}\{\mathbf{x}(t)\mathbf{u}_\alpha^T(t)\},\\
\mathbf{R}_u &= \bar{\mathrm{E}}\{\mathbf{u}_\alpha(t)\mathbf{u}_\alpha^T(t)\},\\
\mathbf{R}_{up} &= \bar{\mathrm{E}}\{\mathbf{u}_\alpha(t+\beta)\mathbf{p}_\beta^T(t)\},
\end{aligned}$$

where $\mathbf{p}_\beta(t),\ t = 1, \ldots, N$, are defined as the columns of $\mathbf{P}_\beta$ in (6.10). If the weighting matrices $\mathbf{W}_r$ and $\mathbf{W}_c$ are positive definite, the estimate (6.11) is consistent if and only if the following matrix has full rank equal to n:

$$\mathbf{r}_{xp} - \mathbf{r}_{xu}\mathbf{R}_u^{-1}\mathbf{R}_{up}. \tag{6.22}$$

This is because the limiting principal left singular vectors of (6.12) will be equal to $\mathbf{W}_r\mathbf{\Gamma}_\alpha\mathbf{T}$ for some non-singular $n \times n$ matrix $\mathbf{T}$. Hence, the limit of $\hat{\mathbf{\Gamma}}_\alpha$ in (6.11) is $\mathbf{\Gamma}_\alpha\mathbf{T}$. In view of Lemma 6.1, the condition that (6.22) should have full rank can be reformulated as

$$\operatorname{rank} \bar{\mathrm{E}} \left\{ \begin{bmatrix} \mathbf{x}(t+\beta) \\ \mathbf{u}_\alpha(t+\beta) \end{bmatrix} \begin{bmatrix} \mathbf{y}_\beta(t) \\ \mathbf{u}_\beta(t) \\ \mathbf{u}_\alpha(t+\beta) \end{bmatrix}^T \right\} = n + \alpha m. \tag{6.23}$$

This is the *critical relation* for consistency of IV-4SID methods.

Method	Order of PE	Condition on noise
PO-MOESP	$\alpha+\beta$	$\bar{\mathrm{E}}\{\mathbf{n}_\beta(t)\mathbf{n}_\beta^T(t)\} > \mathbf{0}$
N4SID	$\alpha+\beta$	$\bar{\mathrm{E}}\{\mathbf{n}_\beta(t)\mathbf{n}_\beta^T(t)\} > \mathbf{0}$
IVM	$\xi \triangleq \max(\alpha,\beta)$	$\bar{\mathrm{E}}\{\mathbf{n}_\xi(t)\mathbf{n}_\xi^T(t)\} > \mathbf{0}$
CVA	$\alpha+\beta$	$\bar{\mathrm{E}}\{\mathbf{n}_\xi(t)\mathbf{n}_\xi^T(t)\} > \mathbf{0}$

Table 6.2: Sufficient conditions for the weighting matrices $\mathbf{W}_r$ and $\mathbf{W}_c$ to be positive definite.

Let us begin by deriving conditions which ensure that the weighting matrices in Table 6.1 exist (i.e., are positive definite). Consider for example the limit of the column weighting $\mathbf{W}_c$ for the PO-MOESP method. We need to establish that $\mathbf{P}_\beta \mathbf{\Pi}^\perp_{\mathbf{U}_\alpha^T} \mathbf{P}_\beta^T/N$ is non-singular for large N. Using Lemma 6.2, the condition $\mathbf{W}_c^{-2} > \mathbf{0}$ can be written as

$$\bar{\mathrm{E}}\left\{ \begin{bmatrix} \mathbf{y}_\beta(t) \\ \mathbf{u}_\beta(t) \\ \mathbf{u}_\alpha(t+\beta) \end{bmatrix} \begin{bmatrix} \mathbf{y}_\beta(t) \\ \mathbf{u}_\beta(t) \\ \mathbf{u}_\alpha(t+\beta) \end{bmatrix}^T \right\} > \mathbf{0}. \tag{6.24}$$

This is recognized as a similar requirement appearing in least-squares linear regression estimation [SS89, Complement C5.1]. The condition (6.24) holds if $\mathbf{u}(t)$ is PE$(\alpha+\beta)$ and if $\bar{\mathrm{E}}\{\mathbf{n}_\beta(t)\mathbf{n}_\beta^T(t)\} > \mathbf{0}$. Similarly, conditions for all cases in Table 6.1 can be obtained. The result is summarized in Table 6.2.

Having established that the weighting matrices are positive definite, condition (6.23) may now be examined. The correlation matrix in (6.23) can be written as the sum of two terms:

$$\bar{\mathrm{E}}\left\{ \begin{bmatrix} \mathbf{x}^d(t+\beta) \\ \mathbf{u}_\alpha(t+\beta) \end{bmatrix} \begin{bmatrix} \mathbf{y}_\beta^d(t) \\ \mathbf{u}_\beta(t) \\ \mathbf{u}_\alpha(t+\beta) \end{bmatrix}^T \right\} + \bar{\mathrm{E}}\left\{ \begin{bmatrix} \mathbf{x}^s(t+\beta) \\ \mathbf{0} \end{bmatrix} \begin{bmatrix} \mathbf{y}_\beta^s(t) \\ \mathbf{0} \\ \mathbf{0} \end{bmatrix}^T \right\}, \tag{6.25}$$

where the superscripts $(\cdot)^d$ and $(\cdot)^s$ denote the deterministic part and the stochastic part, respectively. Below we show that the first term in (6.25) has full row rank under a PE condition on $\mathbf{u}(t)$. This implies that (6.23) is fulfilled for systems *with no process noise* (since $\mathbf{x}^s(t) \equiv \mathbf{0}$ in that case). For systems with process noise, one may in exceptional cases lose rank when adding the two terms in (6.25). One example of such a

situation is given in the next section. Generally, loss of rank is unlikely to occur (at least if $\beta l \gg n$). If $\beta l \gg n$ then the matrix in (6.25) has many more columns than rows. Hence it is more likely that the matrix has full rank. This last point can be made more strict (see Theorem 6.5 and [PSD96]).

In the following it is shown that the first term in (6.25) has full row rank under certain conditions. It can be verified that the correlation matrix is equivalent to;

$$\begin{bmatrix} \mathbf{A}^\beta & \mathcal{C}_\beta(\mathbf{A},\mathbf{B}) & \mathbf{0} \\ \mathbf{0} & \mathbf{0} & \mathbf{I}_{\alpha m} \end{bmatrix} \times \bar{\mathrm{E}} \left\{ \begin{bmatrix} \mathbf{x}^d(t) \\ \mathbf{u}_\beta(t) \\ \mathbf{u}_\alpha(t+\beta) \end{bmatrix} \begin{bmatrix} \mathbf{x}^d(t) \\ \mathbf{u}_\beta(t) \\ \mathbf{u}_\alpha(t+\beta) \end{bmatrix}^T \right\} \begin{bmatrix} \mathbf{\Gamma}_\beta^T & \mathbf{0} & \mathbf{0} \\ \mathbf{\Phi}_\beta^T & \mathbf{I}_{\beta m} & \mathbf{0} \\ \mathbf{0} & \mathbf{0} & \mathbf{I}_{\alpha m} \end{bmatrix}, \tag{6.26}$$

where $\mathcal{C}_\beta(\mathbf{A},\mathbf{B})$ denotes the reversed reachability matrix. That is,

$$\mathcal{C}_\beta(\mathbf{A},\mathbf{B}) = \begin{bmatrix} \mathbf{A}^{\beta-1}\mathbf{B} & \mathbf{A}^{\beta-2}\mathbf{B} & \dots & \mathbf{B} \end{bmatrix}. \tag{6.27}$$

Clearly, the first factor has full row rank $(n + \alpha m)$ if the system (6.1) is reachable from $\mathbf{u}(t)$ and if β is greater than or equal to the controllability index. Notice that the last factor has full row rank, provided β is greater than or equal to the observability index. A sufficient condition is then obtained if the covariance matrix in the middle of (6.26) is positive definite. We have

$$\begin{aligned} &\bar{\mathrm{E}} \left\{ \begin{bmatrix} \mathbf{x}^d(t) \\ \mathbf{u}_\beta(t) \\ \mathbf{u}_\alpha(t+\beta) \end{bmatrix} \begin{bmatrix} \mathbf{x}^d(t) \\ \mathbf{u}_\beta(t) \\ \mathbf{u}_\alpha(t+\beta) \end{bmatrix}^T \right\} \\ &\quad = \underline{\mathcal{S}}\, \bar{\mathrm{E}} \left\{ \left(\frac{1}{a(q^{-1})} \mathbf{u}_{\alpha+\beta+n}(t-n) \right) \left(\frac{1}{a(q^{-1})} \mathbf{u}_{\alpha+\beta+n}^T(t-n) \right) \right\} \underline{\mathcal{S}}^T, \end{aligned} \tag{6.28}$$

where

$$\underline{\mathcal{S}} = \underbrace{\begin{bmatrix} \mathbf{F}_n^u & \dots & \mathbf{F}_1^u & \mathbf{0} & \dots & \mathbf{0} \\ a_n\mathbf{I}_m & \dots & a_1\mathbf{I}_m & a_0\mathbf{I}_m & & \mathbf{0} \\ & \ddots & & & \ddots & \\ \mathbf{0} & & a_n\mathbf{I}_m & \dots & \dots & a_0\mathbf{I}_m \end{bmatrix}}_{(n+\alpha m+\beta m)\times((\alpha+\beta+n)m)}. \tag{6.29}$$

If the system is reachable from $\mathbf{u}(t)$ then $\underline{\mathcal{S}}$ is full row rank according to Appendix A.14. The matrix in (6.28) then, is positive definite if $\mathbf{u}(t)$ is PE($\alpha + \beta + n$). The result is summarized in the following theorem.

Theorem 6.2. *The IV-4SID subspace estimate* $\hat{\mathbf{\Gamma}}_\alpha$ *given by* (6.11) *is consistent if the general assumptions* ***A1-A4*** *apply in addition to the following conditions:*

1. $(\mathbf{A},\ \mathbf{B})$ *is reachable.*
2. $\beta \geq \max($*observability index, controllability index*$)$.
3. $\mathbf{r}_w = \mathbf{0}$.
4. $\mathbf{r}_e > \mathbf{0}$.
5. *The input is persistently exciting of order* $\alpha + \beta + n$.

Remark 6.2. The condition $\mathbf{r}_w = \mathbf{0}$ ensures that the second term in (6.25) is zero. Furthermore, the conditions for the weighting matrices in Table 6.2 are fulfilled if the last two conditions hold.

We conclude this section by giving three alternate consistency theorems for IV-4SID. The first relaxes the order of PE on $\mathbf{u}(t)$ for *single* input systems, while the second strengthens the conditions on $\mathbf{u}(t)$ in order to prove consistency for systems with process noise. Finally, the third theorem considers single input ARMA (autoregressive moving average) signals.

Theorem 6.3. *For single input systems, the IV-4SID subspace estimate* $\hat{\mathbf{\Gamma}}_\alpha$ *given by* (6.11) *is consistent if the general assumptions* ***A1-A4*** *apply in addition to the following conditions:*

1. $(\mathbf{A},\ \mathbf{B})$ *is reachable.*
2. $\beta \geq$ *the observability index.*
3. $\mathbf{r}_w = \mathbf{0}$.
4. $\mathbf{r}_e > \mathbf{0}$.
5. *The input is persistently exciting of order* $\alpha + n$.

Proof. Consider a single input system and define the vector polynomial in q^{-1}:

$$\begin{aligned}\mathbf{F}^y(q^{-1}) &= \frac{\mathbf{C}\mathrm{Adj}\{q\mathbf{I}-\mathbf{A}\}\mathbf{B}}{q^n}+\mathbf{D}\\ &= \mathbf{F}_0^y+\mathbf{F}_1^y q^{-1}+\mathbf{F}_2^y q^{-2}+\cdots+\mathbf{F}_n^y q^{-n},\end{aligned}$$

where $\mathbf{F}_i^y$ $(i=0,\ ...,\ n)$ are $l\times 1$ vectors. This implies that

$$\mathbf{y}^d(t)=\frac{\sum_{k=0}^n \mathbf{F}_k^y q^{-k}}{\sum_{k=0}^n a_k q^{-k}}\mathbf{u}(t), \tag{6.30}$$

where $\{a_i\}$ is defined in (6.18). Next, define the Sylvester matrix

$$\mathcal{S}_y=\underbrace{\begin{bmatrix}\mathbf{F}_n^y & \dots & \mathbf{F}_0^y & & \mathbf{0} & \mathbf{0} & \dots & \mathbf{0}\\ & \ddots & & \ddots & & \vdots & & \vdots\\ \mathbf{0} & & \mathbf{F}_n^y & \dots & \mathbf{F}_0^y & \mathbf{0} & \dots & \mathbf{0}\\ a_n & \dots & a_0 & & \mathbf{0} & \mathbf{0} & \dots & \mathbf{0}\\ & \ddots & & \ddots & & \vdots & & \vdots\\ \mathbf{0} & & a_n & \dots & a_0 & \mathbf{0} & \dots & \mathbf{0}\\ \mathbf{0} & \dots & \mathbf{0} & a_n & \dots & a_0 & & \mathbf{0}\\ \vdots & & \vdots & & \ddots & & \ddots & \\ \mathbf{0} & \dots & \mathbf{0} & \mathbf{0} & & a_n & \dots & a_0\end{bmatrix}}_{(\alpha+\beta+\beta l)\times(n+\alpha+\beta)}\begin{matrix}\left.\begin{matrix}\\ \\ \\ \\ \\ \\ \\ \\ \\ \end{matrix}\right\}\beta l \text{ rows}\\ \left.\begin{matrix}\\ \\ \\ \\ \\ \end{matrix}\right\}\beta \text{ rows}\\ \left.\begin{matrix}\\ \\ \\ \end{matrix}\right\}\alpha \text{ rows}\end{matrix}. \tag{6.31}$$

It can be shown that the rank of $\mathcal{S}_y$ is $n+\alpha+\beta$ if the system is observable and reachable from $\mathbf{u}(t)$, and if β is greater than or equal to the observability index [AJ76, BKAK78]. A straightforward (simple) proof of this fact is given in Appendix A.15, using the notation introduced in this chapter. The first term in (6.25) can now be written as

$$\bar{\mathrm{E}}\left\{\begin{bmatrix}\mathbf{x}^d(t+\beta)\\ \mathbf{u}_\alpha(t+\beta)\end{bmatrix}\begin{bmatrix}\mathbf{y}_\beta^d(t)\\ \mathbf{u}_\beta(t)\\ \mathbf{u}_\alpha(t+\beta)\end{bmatrix}^T\right\}=\underline{\mathcal{S}}\mathbf{R}_U\mathcal{S}_y^T, \tag{6.32}$$

where

$$\mathbf{R}_U=\bar{\mathrm{E}}\left\{\frac{1}{a(q^{-1})}\mathbf{u}_{n+\alpha}(t+\beta-n)\frac{1}{a(q^{-1})}\mathbf{u}_{\alpha+\beta+n}^T(t-n)\right\}.$$

The covariance matrix $\mathbf{R}_U$ is full row rank if $\mathbf{u}$ is PE($\alpha + n$). It is then clear that (6.32) is full rank since $\underline{\mathcal{S}}$ is non-singular and $\mathcal{S}_y$ is full column rank. □

Therefore, for single input systems we can relax the assumption about the input signal. The proof of Theorem 6.3 does not carry over to the multi-input case because $\mathcal{S}_y$ is not full column rank if $m > 1$ (see Appendix A.15).

Next, we give the following consistency result concerning the case when the input is a white noise process.

Theorem 6.4. *Let the input* $\mathbf{u}(t)$ *to the system in* (6.1) *be a zero-mean white sequence in the sense that* $\mathbf{r}_u(\tau) = \mathbf{r}_u(0)\delta_{\tau,0}$ *and* $\mathbf{r}(0) > \mathbf{0}$. *Assume that* ***A1-A4*** *hold, the weighting matrices* $\mathbf{W}_r$ *and* $\mathbf{W}_c$ *are positive definite, and*

$$\operatorname{rank}\left\{\begin{bmatrix}\mathcal{C}_\beta(\mathbf{A},\mathbf{B}) & \mathcal{C}_\beta(\mathbf{A},\mathbf{G})\end{bmatrix}\right\} = n. \tag{6.33}$$

Here, $\mathcal{C}_\beta(\mathbf{A},\mathbf{B})$ *is defined in* (6.27),

$$\mathcal{C}_\beta(\mathbf{A},\mathbf{G}) = \begin{bmatrix}\mathbf{A}^{\beta-1}\mathbf{G} & \mathbf{A}^{\beta-2}\mathbf{G} & \dots & \mathbf{G}\end{bmatrix},$$

and the matrix $\mathbf{G}$ *is defined as*

$$\mathbf{G} = \bar{\mathrm{E}}\{\mathbf{x}(t+1)\mathbf{y}^T(t)\}.$$

Given the above assumptions, the IV-4SID subspace estimate $\hat{\mathbf{\Gamma}}_\alpha$ *defined in* (6.11) *is consistent.*

Proof. Consider the correlation matrix in (6.23):

$$\bar{\mathrm{E}}\left\{\begin{bmatrix}\mathbf{x}(t+\beta)\\ \mathbf{u}_\alpha(t+\beta)\end{bmatrix}\begin{bmatrix}\mathbf{y}_\beta(t)\\ \mathbf{u}_\beta(t)\\ \mathbf{u}_\alpha(t+\beta)\end{bmatrix}^T\right\}$$
$$= \begin{bmatrix}\bar{\mathrm{E}}\{\mathbf{x}(t+\beta)\mathbf{y}_\beta^T(t)\} & \bar{\mathrm{E}}\{\mathbf{x}(t+\beta)\mathbf{u}_\beta^T(t)\} & \mathbf{0}\\ \mathbf{0} & \mathbf{0} & \mathbf{R}_{\mathbf{u}_\alpha}\end{bmatrix}, \tag{6.34}$$

where

$$\mathbf{R}_{\mathbf{u}_\alpha} = \bar{\mathrm{E}}\{\mathbf{u}_\alpha(t)\mathbf{u}_\alpha^T(t)\} = \mathbf{I}_\alpha \otimes \mathbf{r}_u(0).$$

The symbol $\otimes$ denotes the Kronecker product. In (6.34), we used the fact that $\bar{\mathrm{E}}\{\mathbf{x}(t)\mathbf{u}^T(t+k)\} = \mathbf{0}$ for $k \geq 0$ since $\mathbf{u}(t)$ is a white sequence.

Notice that $\mathbf{R}_{\mathbf{u}_\alpha} > \mathbf{0}$ since $\mathbf{r}_u(0) > \mathbf{0}$. Under the given assumptions it is readily proven that

$$\bar{\mathrm{E}}\{\mathbf{x}(t+\beta)\mathbf{y}_\beta^T(t)\} = \mathcal{C}_\beta(\mathbf{A}, \mathbf{G}),$$

and

$$\bar{\mathrm{E}}\{\mathbf{x}(t+\beta)\mathbf{u}_\beta^T(t)\} = \mathcal{C}_\beta(\mathbf{A}, \mathbf{B})\left(\mathbf{I}_\beta \otimes \mathbf{r}_u(0)\right).$$

We conclude that the matrix in (6.34) is full row rank under the reachability assumption given in (6.33). This concludes the proof. □

Notice that Theorem 6.4 guarantees consistency even for systems with process noise. Also observe that we here were able to relax the reachability condition on $(\mathbf{A}, \mathbf{B})$ compared to the previous theorems. Some other results for the case with a white noise input signal can be found in [Ver93].

Finally, we give a result for single input ARMA signals.

Theorem 6.5. *Assume that the scalar ($m = 1$) input $\mathbf{u}(t)$ to the system in* (6.1) *is generated by the ARMA model*

$$F(q^{-1})\mathbf{u}(t) = G(q^{-1})\varepsilon(t),$$

*where $\varepsilon(t)$ is a white noise process. Here, $F(z)$ and $G(z)$ are relatively prime polynomials of degree n_F and n_G, respectively, and they have all zeros outside the unit circle. Furthermore, assume that **A1-A4** hold, the weighting matrices $\mathbf{W}_r$ and $\mathbf{W}_c$ are positive definite, and*

1. *$(\mathbf{A}, \mathbf{B})$ is reachable.*
2. *$\beta \geq n$*
3. *$n_G \leq \beta - n$*
4. *$n_F \leq \alpha + \beta - n$*

Given the above assumptions, the IV-4SID subspace estimate $\hat{\mathbf{\Gamma}}_\alpha$ in (6.11) *is consistent.*

Proof. Study the last two block columns of (6.23). Clearly, if

$$\operatorname{rank} \bar{\mathrm{E}}\left\{ \begin{bmatrix} \mathbf{x}(t+\beta) \\ \mathbf{u}_\alpha(t+\beta) \end{bmatrix} \begin{bmatrix} \mathbf{u}_\beta(t) \\ \mathbf{u}_\alpha(t+\beta) \end{bmatrix}^T \right\} = n + \alpha m \tag{6.35}$$

holds, then so does (6.23). Using the notation introduced in (6.29), we can write the correlation matrix in (6.35) as

$$\underline{\mathcal{S}}\bar{\mathrm{E}}\left\{\left[\frac{1}{a(q^{-1})}\mathbf{u}_{n+\alpha}(t+\beta-n)\right]\mathbf{u}_{\alpha+\beta}^{T}(t)\right\}, \tag{6.36}$$

where $\underline{\mathcal{S}}$ is $(n+\alpha)\times(n+\alpha)$ and non-singular since $(\mathbf{A},\mathbf{B})$ is reachable (see Appendix A.14). Lemma A3.8 in [SS83] shows that the correlation matrix appearing in (6.36) is full row rank if

$$\max(\alpha+n+n_G, n+n_F) \leq \alpha+\beta, \tag{6.37}$$

which can be easily transformed to the conditions of the theorem. □

Notice that the theorem holds for arbitrarily colored noise as long as it is uncorrelated with the input. With some more effort the theorem can be extended to the multi-input case by modifying Lemma A3.8 in [SS83]. For example, the theorem holds if the different inputs are independent ARMA signals. The result of the theorem is very interesting since it gives a quantification of the statement that "for large enough β, the matrix in (6.25) is full rank". Also observe that an AR-input of arbitrarily high order is allowed if α is chosen large enough.

6.6 Counterexample

The purpose of this section is to present an example of a system for which the IV-4SID methods are not consistent. We have shown that a necessary condition for consistency is the validity of (6.23). In the discussion following (6.25), it was also pointed out that consistency problems may occur for systems with process noise. In this section, we give an explicit example for which the rank drops when the two terms in (6.25) are added.

Consider the cross correlation matrix appearing in (6.23) which with obvious notation, reads

$$\begin{bmatrix} \mathbf{R}_{x^d y_\beta^d} + \mathbf{R}_{x^s y_\beta^s} & \mathbf{R}_{x^d u_\beta} & \mathbf{R}_{x^d u_\alpha} \\ \mathbf{R}_{u_\alpha y_\beta^d} & \mathbf{R}_{u_\alpha u_\beta} & \mathbf{R}_{u_\alpha u_\alpha} \end{bmatrix}.$$

The construction of a system for which this matrix loses rank is divided into two major steps:

1. Find a vector $\mathbf{v}$ such that

$$\mathbf{v}^T \begin{bmatrix} \mathbf{R}_{x^d u_\beta} & \mathbf{R}_{x^d u_\alpha} \\ \mathbf{R}_{u_\alpha u_\beta} & \mathbf{R}_{u_\alpha u_\alpha} \end{bmatrix} = \mathbf{0}.$$

2. Design $\mathbf{R}_{x^s y_\beta^s}$ such that

$$\mathbf{v}^T \begin{bmatrix} \mathbf{R}_{x^d y_\beta^d} + \mathbf{R}_{x^s y_\beta^s} \\ \mathbf{R}_{u_\alpha y_\beta^d} \end{bmatrix} = \mathbf{0}. \tag{6.38}$$

The first step turns out to be similar to a construction used in the analysis of instrumental variable methods (see [SS81, SS83] and the references therein). Once a solution to the first step is found, the second step is a matter of investigating whether or not a stochastic subsystem exists, generating a valid $\mathbf{R}_{x^s y_\beta^s}$.

Let us study the first step in more detail. For notational convenience, define the covariance matrix

$$\mathcal{P}_{\eta\times\nu}(t_1, t_2) = \bar{\mathrm{E}} \left\{ \big[\frac{1}{a(q^{-1})}\mathbf{u}_\eta(t - t_1)\big]\mathbf{u}_\nu^T(t - t_2) \right\}.$$

The correlation matrix of interest in the first step can be written as

$$\begin{bmatrix} \mathbf{R}_{x^d u_\beta} & \mathbf{R}_{x^d u_\alpha} \\ \mathbf{R}_{u_\alpha u_\beta} & \mathbf{R}_{u_\alpha u_\alpha} \end{bmatrix} = \underline{\mathcal{S}}\mathcal{P}_{(\alpha+n)\times(\alpha+\beta)}(n - \beta, 0),$$

where $\underline{\mathcal{S}}$ is defined in (6.29). Here, however, it is of dimension $(n+\alpha m)\times((\alpha+n)m)$. The rank properties of $\mathcal{P}_{\eta\times\nu}(0,0)$ have been studied in [SS83]. $\mathcal{P}$ is full rank either if a is positive real and $\mathbf{u}(t)$ is persistently exciting, or if $\mathbf{u}(t)$ is an ARMA-process of sufficiently low order (e.g., white noise, cf. Theorem 6.5). Here, we consider an $a(q^{-1})$ that is not positive real to make $\mathcal{P}$ rank deficient. This implies that $n \geq 2$. Let us fix the following parameters: $n = 2$, $m = 1$, $l = 1$, $\beta = 2$ and $\alpha = 3$. If $(\mathbf{A}, \mathbf{B})$ is reachable then $\underline{\mathcal{S}}$ is non-singular (see Appendix A.14). The first step can then be solved if there exists a vector $\mathbf{g}$ such that $\mathbf{g}^T\mathcal{P}_{5\times5}(0,0) = 0$. A solution to this can be found by using the same setup as that in the counterexample ([SS83]) for an instrumental variable method. Choose a pole polynomial and an input process according to:

$$a(q^{-1}) = (1 - \gamma q^{-1})^2, \tag{6.39}$$

$$\mathbf{u}(t) = (1 - \gamma q^{-1})^2(1 + \gamma q^{-1})^2\boldsymbol{\varepsilon}(t), \tag{6.40}$$

where $\varepsilon(t)$ is a white noise process of unit variance. Notice that γ should have a modulus less than one for stability and that the input is persistently exciting to any order. Now, a straightforward calculation leads to

$$\mathcal{P}_{5\times5}(0,0) = \begin{bmatrix} 1-2\gamma^4 & -4\gamma^3 & \gamma^6-2\gamma^2 & 2\gamma^5 & \gamma^4 \\ 2\gamma & 1-2\gamma^4 & -4\gamma^3 & \gamma^6-2\gamma^2 & 2\gamma^5 \\ \gamma^2 & 2\gamma & 1-2\gamma^4 & -4\gamma^3 & \gamma^6-2\gamma^2 \\ 0 & \gamma^2 & 2\gamma & 1-2\gamma^4 & -4\gamma^3 \\ 0 & 0 & \gamma^2 & 2\gamma & 1-2\gamma^4 \end{bmatrix}.$$

This matrix is singular if γ is a solution to

$$\det(\mathcal{P}_{5\times5}(0,0)) = 1 + 4\gamma^4 + 10\gamma^8 - 8\gamma^{12} - 15\gamma^{16} - 12\gamma^{20} = 0. \quad (6.41)$$

The polynomial has two real roots for $\gamma \approx \pm 0.91837$. Choose, for example, the positive root for γ and $\mathbf{g}$ as the left eigenvector corresponding to the zero eigenvalue of $\mathcal{P}$. This provides a solution to the first step (namely, $\mathbf{v}^T = \mathbf{g}^T\underline{\mathcal{S}}^{-1}$). The solution depends on the matrix $\mathbf{B}$. Until now, we have fixed the poles of the system and a specific input process.

Remark 6.3. Observe that a subspace method that only uses the inputs $\mathbf{U}_\beta$ as instrumental variables (cf. (6.10)) is not consistent for systems satisfying the first step. In other words, the *past input MOESP* method (see [Ver94]) is not consistent if the poles and the input process are related as in (6.39)-(6.40) and if γ is a solution to (6.41). It is readily checked that the conditions of Theorem 6.5 is violated.

The free parameters in the second step are $\mathbf{B}$, $\mathbf{C}$, $\mathbf{D}$, and those specifying the stochastic subsystem, with constraints on minimality of the system description. Somewhat arbitrarily,[2] we make the choices: $\mathbf{B} = [1\ -2]^T$, $\mathbf{C} = [2\ -1]$ and $\mathbf{D} = 0$. Consider the following description of the system in state space form:

$$\mathbf{x}(t+1) = \begin{bmatrix} 2\gamma & -\gamma^2 \\ 1 & 0 \end{bmatrix}\mathbf{x}(t) + \begin{bmatrix} 1 \\ -2 \end{bmatrix}\mathbf{u}(t) + \begin{bmatrix} \mathbf{k}_1 \\ \mathbf{k}_2 \end{bmatrix}\mathbf{e}(t), \quad (6.42a)$$

$$\mathbf{y}(t) = \begin{bmatrix} 2 & -1 \end{bmatrix}\mathbf{x}(t) + \mathbf{e}(t), \quad (6.42b)$$

where the variance of the noise process $\mathbf{e}(t)$ is $\mathbf{r}_e$. With the choices made, the system is observable and reachable from $\mathbf{u}(t)$. For a given γ, (6.38)

[2] For some choices of $\mathbf{B}$, $\mathbf{C}$ and $\mathbf{D}$ we were not able to find a solution to the second step. For other choices of $\mathbf{C}$, making the system "less observable", we found solutions with lower noise variance.

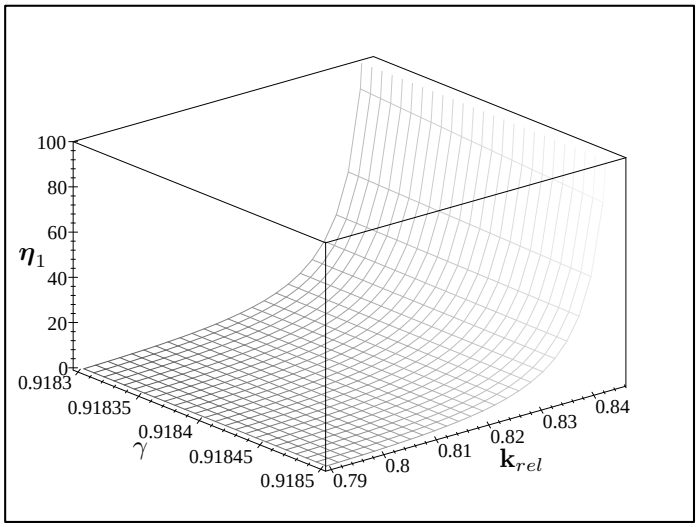

Figure 6.1: The graph shows $\boldsymbol{\eta}_1$ as a function of $\boldsymbol{\gamma}$ and $\mathbf{k}_{rel}$.

now consists of two non-linear equations in $\mathbf{k}_1$, $\mathbf{k}_2$ and $\mathbf{r}_e$. The equations are, however, linear in $\mathbf{k}_1\mathbf{r}_e$, $\mathbf{k}_2\mathbf{r}_e$, $\mathbf{k}_1^2\mathbf{r}_e$, $\mathbf{k}_2^2\mathbf{r}_e$ and $\mathbf{k}_1\mathbf{k}_2\mathbf{r}_e$. If we change variables according to:

$$\begin{aligned}\mathbf{k}_{rel} &= \frac{\mathbf{k}_1}{\mathbf{k}_2},\\ \boldsymbol{\eta}_1 &= \mathbf{k}_2^2\mathbf{r}_e,\\ \boldsymbol{\eta}_2 &= \mathbf{k}_2\mathbf{r}_e,\end{aligned}$$

then the two non-linear equations become linear in $\boldsymbol{\eta}_1$ and $\boldsymbol{\eta}_2$. Thus, given $\boldsymbol{\gamma}$ and $\mathbf{k}_{rel}$, we can easily solve for $\boldsymbol{\eta}_1$ and $\boldsymbol{\eta}_2$. Observe that $\boldsymbol{\eta}_1$ must be positive to be a valid solution. A plot of $\boldsymbol{\eta}_1$ as a function of $\boldsymbol{\gamma}$ and $\mathbf{k}_{rel}$ is shown in Figure 6.1. The solution $\boldsymbol{\eta}_1$ is positive when $\mathbf{k}_{rel}$ is between ≈ 0.7955 and $(4\boldsymbol{\gamma}^3-3\boldsymbol{\gamma}^2+1)/(2\boldsymbol{\gamma}^2-2\boldsymbol{\gamma}+2) \approx 0.8475$ ($\boldsymbol{\eta}_1$ is discontinuous at this point). Let us, for example, choose the solution corresponding to $\mathbf{k}_{rel} = 0.825$. The parameters become: $\gamma \approx 0.9184$, $\mathbf{r}_e \approx 217.1$, $\mathbf{k}_1 \approx -0.1542$ and $\mathbf{k}_2 \approx -0.1869$. Thus, feeding the system (6.42) with the input (6.40) and using $\alpha = 3$ and $\beta = 2$ will make the matrix in (6.23)

rank deficient.

We end this section with some short comments about the counterexample. Indeed, the example presented in this section is very special. However, the existence of these kind of examples indicates that the subspace methods may have a very poor performance in certain situations. As should be clear from the derivations above, the consistency of 4SID methods are related to the consistency of some instrumental variable schemes (see [SS81, SS83] and the references therein). When using 4SID methods, it is a good idea to estimate a set of models for different choices of α and β. These models should then be validated separately to see which gives the best result. This reduces the performance degradation due to a bad choice of α and β. In the counterexample presented above, such a procedure would probably have led to another choice of the dimension parameters (given that the system order is known). While this may lead to consistent estimates, the accuracy may still be poor (as indicated in the next section).

6.7 Numerical Examples

In this section, the previously obtained results are illustrated by means of numerical examples. First, the counterexample given in the previous section is simulated. Thus, identification data are generated according to (6.40) and (6.42). The extended observability matrix is estimated by (6.11) using the weighting matrices for the CVA method (see Table 6.1). Similar results are obtained with other choices of the weighting matrices. The system matrix is then estimated as

$$\hat{\mathbf{A}} = \hat{\mathbf{\Gamma}}_1^{\dagger}\hat{\mathbf{\Gamma}}_2,$$

where $(\cdot)^{\dagger}$ denotes the Moore-Penrose pseudo inverse, $\hat{\mathbf{\Gamma}}_1$ denotes the matrix made of the first $\alpha - 1$ rows and $\hat{\mathbf{\Gamma}}_2$ contains the last $\alpha - 1$ rows of $\hat{\mathbf{\Gamma}}_\alpha$. To measure the estimation accuracy we consider the estimated system poles (i.e., the eigenvalues of $\hat{\mathbf{A}}$). Recall that the system (6.42) has two poles at $\gamma = 0.9184$. Table 6.3 shows the absolute value of the bias and the standard deviation of the pole estimates. The sample statistics are based on 1000 independent trials. Each trial consists of 1000 input-output data samples. The results for two different choices of α and β are given in the table. The first corresponds to the choice made in the counterexample. It is clearly seen that the estimates are not useful. For

	$\alpha = 3,\ \beta = 2$	$\alpha = 6,\ \beta = 5$
pole 1	5.9572 (69.8826)	0.4704 (0.4806)
pole 2	2.6049 (30.9250)	0.1770 (0.3526)

Table 6.3: The figures shown in the table are the absolute values of the bias and, within brackets, the standard deviations.

	$\alpha = 3,\ \beta = 2$	$\alpha = 6,\ \beta = 5$
pole 1	0.1161 (0.2405)	0.0316 (0.0452)
pole 2	0.2266 (0.5043)	0.0282 (0.0290)

Table 6.4: Same as Table 6.3 but for the system with $\mathbf{K} = [-0.2100,\ -0.5590]^T$.

the second choice ($\alpha = 6,\ \beta = 5$), it can be shown that the algorithm is consistent. This is indicated by the much more reasonable results in Table 6.3. The accuracy, however, is still very poor since the matrix in (6.23) is nearly rank deficient.

Next, we study the influence of the stochastic sub-system on the estimation accuracy. Recall that in Section 6.6 the stochastics of the system were designed to cause a cancellation in (6.25). The zeros of the stochastic sub-system are given by the eigenvalues of $\mathbf{A} - \mathbf{KC}$ which become, approximately: $0.9791 \pm i0.1045$. In the next simulation, the locations of these zeros are changed such that they have the same distance to the unit circle, but the angle relative to the real axis is increased five times. This is accomplished by changing $\mathbf{K}$ in (6.42) to $[-0.2100,\ -0.5590]^T$. The zeros become $0.8489 \pm i0.4990$. The simulation results are presented in Table 6.4. It can be seen that the estimation accuracy is more reasonable in this case.

Finally, we change the input to be realizations of a zero-mean white noise process. The power of the white noise input is chosen to be equal to the power of the colored process (6.40). Except for the input, the parameters are the same as in the counterexample. Recall Theorem 6.4, which shows that the estimates are consistent in this case. Table 6.5 presents the result of the simulations. A comparison with the results of Table 6.3 clearly shows a great difference.

	$\alpha = 3,\ \beta = 2$	$\alpha = 6,\ \beta = 5$
pole 1	0.0464 (0.1146)	0.0184 (0.0271)
pole 2	0.0572 (0.0523)	0.0182 (0.0171)

Table 6.5: Same as Table 6.3 but with a white noise input signal.

6.8 Conclusions

Persistence of excitation conditions on the input signal have been given. These conditions ensure consistency of the subspace estimate used in subspace system identification methods. For these conditions to hold, we had to assume that the system does not contain any process noise. With process noise, a persistence of excitation condition alone is not sufficient. In fact, an example was given of a system for which subspace methods are not consistent. The system is reachable from the input and the input is persistently exciting to any order. The subspace methods fail, however, to provide a consistent model of the system transfer function. It was also shown that a white noise input (or an ARMA input signal of sufficiently low order) guarantees consistency under weak conditions. This shows that the performance of subspace methods may be very sensitive to the input excitation.

Appendix A

Proofs and Derivations

A.1 Proofs of (2.34) and (2.35)

By **R8**,

$$(\lambda_k - \sigma^2)\mathbf{B}^*\hat{\mathbf{e}}_k \simeq \mathbf{B}^*\hat{\mathbf{R}}\mathbf{e}_k, \tag{A.1}$$

where (see (2.8) and (2.13))

$$\mathbf{B}^*\hat{\mathbf{R}} = \frac{1}{2N}\mathbf{B}^* \sum_{t=1}^{N} \left[\mathbf{n}(t)\mathbf{x}^*(t) + \mathbf{J}\mathbf{n}^{\mathrm{c}}(t)\mathbf{x}^T(t)\mathbf{J}\right]. \tag{A.2}$$

Using (A.2) and the standard formula for the fourth-order moment of circular Gaussian random variables, we obtain

$$\begin{aligned}
&\mathrm{E}\left\{[\mathbf{B}^*\hat{\mathbf{R}}\mathbf{e}_i][\mathbf{B}^*\hat{\mathbf{R}}\mathbf{e}_j]^*\right\} \\
&\quad= \frac{1}{4N^2}\mathbf{B}^*\sum_{t=1}^{N}\sum_{s=1}^{N}\mathrm{E}\left[\mathbf{n}(t)\mathbf{x}^*(t)\mathbf{e}_i\mathbf{e}_j^*\mathbf{x}(s)\mathbf{n}^*(s)\right. \\
&\qquad+\mathbf{n}(t)\mathbf{x}^*(t)\mathbf{e}_i\mathbf{e}_j^*\mathbf{J}\mathbf{x}^{\mathrm{c}}(s)\mathbf{n}^T(s)\mathbf{J}+\mathbf{J}\mathbf{n}^{\mathrm{c}}(t)\mathbf{x}^T(t)\mathbf{J}\mathbf{e}_i\mathbf{e}_j^*\mathbf{x}(s)\mathbf{n}^*(s) \\
&\qquad\left.+\mathbf{J}\mathbf{n}^{\mathrm{c}}(t)\mathbf{x}^T(t)\mathbf{J}\mathbf{e}_i\mathbf{e}_j^*\mathbf{J}\mathbf{x}^{\mathrm{c}}(s)\mathbf{n}^T(s)\mathbf{J}\right]\mathbf{B} \\
&\quad= \frac{1}{4N^2}\mathbf{B}^*\left[N^2\sigma^4\mathbf{e}_i\mathbf{e}_j^*+N\sigma^2(\mathbf{e}_j^*\mathbf{R}_0\mathbf{e}_i)\mathbf{I}+\sigma^4N^2\mathbf{e}_i\mathbf{e}_j^*+\sigma^4N\mathbf{J}\mathbf{e}_j^{\mathrm{c}}\mathbf{e}_i^T\mathbf{J}\right. \\
&\qquad\left.+\sigma^4N^2\mathbf{e}_i\mathbf{e}_j^*+\sigma^4N\mathbf{J}\mathbf{e}_j^{\mathrm{c}}\mathbf{e}_i^T\mathbf{J}+N^2\sigma^4\mathbf{e}_i\mathbf{e}_j^*+\sigma^2N(\mathbf{e}_j^*\mathbf{J}\mathbf{R}_0^{\mathrm{c}}\mathbf{J}\mathbf{e}_i)\mathbf{I}\right]\mathbf{B} \\
&\quad= \frac{\sigma^2}{2N}(\mathbf{e}_j^*\mathbf{R}\mathbf{e}_i)\mathbf{B}^*\mathbf{B}=\frac{\sigma^2}{2N}\lambda_i\delta_{i,j}(\mathbf{B}^*\mathbf{B}),
\end{aligned} \tag{A.3}$$

where to derive the fourth equality use was made of the fact that $\mathbf{B}^*\mathbf{e}_i=0$ (see (2.13) and (2.22)) and that $\mathbf{B}^*\mathbf{J}\mathbf{e}_i^{\mathrm{c}}=0$ (see **R3**). The expression for $\mathrm{E}[\mathbf{z}\mathbf{z}^*]$ in (2.34) follows from (A.1) and (A.3).

Next, consider (2.35). A straightforward calculation gives

$$\begin{aligned}
&\mathrm{E}\left\{[\mathbf{B}^*\hat{\mathbf{R}}\mathbf{e}_i][\mathbf{B}^*\hat{\mathbf{R}}\mathbf{e}_j]^T\right\} \\
&\quad= \frac{1}{4N^2}\mathbf{B}^*\sum_{t=1}^{N}\sum_{s=1}^{N}\mathrm{E}\left[\mathbf{n}(t)\mathbf{x}^*(t)\mathbf{e}_i\mathbf{e}_j^T\mathbf{x}^{\mathrm{c}}(s)\mathbf{n}^T(s)\right. \\
&\qquad+\mathbf{n}(t)\mathbf{x}^*(t)\mathbf{e}_i\mathbf{e}_j^T\mathbf{J}\mathbf{x}(s)\mathbf{n}^*(s)\mathbf{J}+\mathbf{J}\mathbf{n}^{\mathrm{c}}(t)\mathbf{x}^T(t)\mathbf{J}\mathbf{e}_i\mathbf{e}_j^T\mathbf{x}^{\mathrm{c}}(s)\mathbf{n}^T(s) \\
&\qquad\left.+\mathbf{J}\mathbf{n}^{\mathrm{c}}(t)\mathbf{x}^T(t)\mathbf{J}\mathbf{e}_i\mathbf{e}_j^T\mathbf{J}\mathbf{x}(s)\mathbf{n}^*(s)\mathbf{J}\right]\mathbf{B}^{\mathrm{c}} \\
&\quad= \frac{1}{4N^2}\mathbf{B}^*\left[N^2\sigma^4\mathbf{e}_i\mathbf{e}_j^T+\sigma^4N\mathbf{e}_j\mathbf{e}_i^T+\sigma^4N^2\mathbf{e}_i\mathbf{e}_j^T+\sigma^2N\mathbf{J}(\mathbf{e}_j^T\mathbf{J}\mathbf{R}_0\mathbf{e}_i)\right. \\
&\qquad\left.+\sigma^4N^2\mathbf{e}_i\mathbf{e}_j^T+\sigma^2N\mathbf{J}(\mathbf{e}_j^T\mathbf{R}_0^{\mathrm{c}}\mathbf{J}\mathbf{e}_i)+\sigma^4N^2\mathbf{e}_i\mathbf{e}_j^T+\sigma^4N\mathbf{e}_j\mathbf{e}_i^T\right]\mathbf{B}^{\mathrm{c}} \\
&\quad= \frac{\sigma^2}{2N}(\mathbf{B}^*\mathbf{J}\mathbf{B}^{\mathrm{c}})(\mathbf{e}_j^T\mathbf{J}\mathbf{R}\mathbf{e}_i) \\
&\quad= \frac{\sigma^2}{2N}(\mathbf{B}^*\mathbf{B}\tilde{\mathbf{J}})(\mathbf{e}_j^*\mathbf{R}\mathbf{e}_i)e^{-i\psi_j} \\
&\quad= \frac{\sigma^2}{2N}(\mathbf{B}^*\mathbf{B}\tilde{\mathbf{J}})\lambda_i\delta_{i,j}\mathbf{\Gamma}_{ii}^*,
\end{aligned} \tag{A.4}$$

where the last but one equality follows from **R1** and **R3**. The expression in (2.35) for $\mathrm{E}[\mathbf{z}\mathbf{z}^T]$ follows from (A.1) and (A.4).

A.2 Asymptotic Covariance of the Residual

In order to compute the asymptotic covariance in (3.21), the first order perturbations in the residuals are related to the error in the sample covariance matrix. Since $\tilde{\mathbf{R}} = \hat{\mathbf{R}} - \mathbf{R} = O_p(1/\sqrt{N})$, it is straightforward to obtain the following first order relation from (3.4):

$$\mathbf{B}^* \hat{\mathbf{E}}_s = \mathbf{B}^* \tilde{\mathbf{R}} \mathbf{E}_s \widetilde{\mathbf{\Lambda}}^{-1} + o_p(1/\sqrt{N}), \tag{A.5}$$

where $\mathbf{B} = \mathbf{B}(\boldsymbol{\theta}_0)$ (see Section 2.3.4 or [CTO89]). Next notice that the observations are given by the model

$$\begin{aligned} \mathbf{x}(t) &= \mathbf{A}(\boldsymbol{\theta}_0, \boldsymbol{\rho})\mathbf{s}(t) + \mathbf{n}(t) \\ &= \mathbf{A}_0 \mathbf{s}(t) + \mathbf{n}(t) + \tilde{\mathbf{A}}\mathbf{s}(t), \end{aligned} \tag{A.6}$$

where $\tilde{\mathbf{A}} = \mathbf{A}(\boldsymbol{\theta}_0, \boldsymbol{\rho}) - \mathbf{A}_0$ denotes the error in the steering matrix due to $\boldsymbol{\rho}$. It is important to observe that the first two terms in (A.6) represent the observation from the nominal array, whereas the third term is due to model errors. The sample covariance matrix can be partitioned accordingly as

$$\hat{\mathbf{R}} = \frac{1}{N} \sum_{t=1}^{N} \mathbf{x}(t)\mathbf{x}^*(t) = \hat{\mathbf{R}}_{\mathrm{FS}} + \hat{\mathbf{R}}_{\mathrm{ME}}, \tag{A.7}$$

where

$$\hat{\mathbf{R}}_{\mathrm{FS}} = \frac{1}{N} \sum_{t=1}^{N} \Big(\mathbf{A}_0 \mathbf{s}(t) + \mathbf{n}(t) \Big) \Big(\mathbf{A}_0 \mathbf{s}(t) + \mathbf{n}(t) \Big)^*, \tag{A.8}$$

$$\begin{aligned} \hat{\mathbf{R}}_{\mathrm{ME}} = \frac{1}{N} \sum_{t=1}^{N} \Big[& \Big(\mathbf{A}_0 \mathbf{s}(t) + \mathbf{n}(t) \Big) \mathbf{s}^*(t) \tilde{\mathbf{A}}^* \\ & + \tilde{\mathbf{A}} \mathbf{s}(t) \Big(\mathbf{A}_0 \mathbf{s}(t) + \mathbf{n}(t) \Big)^* + \tilde{\mathbf{A}} \mathbf{s}(t) \mathbf{s}^*(t) \tilde{\mathbf{A}}^* \Big], \end{aligned} \tag{A.9}$$

and the subscripts FS and ME stand for finite sample and model error, respectively. The in-probability orders of the quantities in (A.8)-(A.9)

are

$$\begin{aligned}\tilde{\mathbf{A}} &= O_p(1/\sqrt{N}),\\ \frac{1}{N}\sum_{t=1}^{N}\mathbf{s}(t)\mathbf{s}^*(t) - \mathbf{P} &= O_p(1/\sqrt{N}),\\ \frac{1}{N}\sum_{t=1}^{N}\mathbf{s}(t)\mathbf{n}^*(t) &= O_p(1/\sqrt{N}).\end{aligned}$$

The first follows from the assumptions on $\boldsymbol{\rho}$, the second is a standard result from ergodicity theory, and the last follows from the central limit theorem (it is a sum of zero-mean independent random variables). A first order approximation of $\mathbf{B}^*\hat{\mathbf{R}}$ is then

$$\mathbf{B}^*\hat{\mathbf{R}} = \mathbf{B}^*\hat{\mathbf{R}}_{\mathrm{FS}} + \mathbf{B}^*\tilde{\mathbf{A}}\mathbf{P}\mathbf{A}_0^* + o_p(1/\sqrt{N}). \tag{A.10}$$

It is interesting to note that the residuals are, to first order, due to two independent terms. The first is the finite sample errors from the nominal array and the second is the model error contribution. Since the terms are independent, they can be considered one at a time. In view of (A.7), we denote the error in the principal eigenvectors due to finite samples and model errors by $\tilde{\mathbf{E}}_{s_{\mathrm{FS}}}$ and $\tilde{\mathbf{E}}_{s_{\mathrm{ME}}}$, respectively; that is, $\hat{\mathbf{E}}_s = \mathbf{E}_s + \tilde{\mathbf{E}}_{s_{\mathrm{FS}}} + \tilde{\mathbf{E}}_{s_{\mathrm{ME}}}$.

Let us start by deriving the part of the residual covariance matrix due to finite samples. Define $\tilde{\mathbf{R}}_{\mathrm{FS}} = \hat{\mathbf{R}}_{\mathrm{FS}} - \mathbf{R}$. By straightforward calculations it is possible to show that

$$\mathrm{E}\{\mathrm{vec}(\tilde{\mathbf{R}}_{\mathrm{FS}})\,\mathrm{vec}^*(\tilde{\mathbf{R}}_{\mathrm{FS}})\} = \frac{1}{N}\left(\mathbf{R}^T \otimes \mathbf{R}\right), \tag{A.11}$$

$$\mathrm{E}\{\mathrm{vec}(\tilde{\mathbf{R}}_{\mathrm{FS}})\,\mathrm{vec}^T(\tilde{\mathbf{R}}_{\mathrm{FS}})\} = \frac{1}{N}\left[\mathrm{vec}(\mathbf{R})\,\mathrm{vec}^T(\mathbf{R})\right]^{\mathrm{BT}}, \tag{A.12}$$

since $\{\mathbf{x}(t)\}_{t=1}^N$ is a sequence of independent circular Gaussian random vectors. Here, the notation $(\cdot)^{\mathrm{BT}}$ means that every "block" in $(\cdot)$ is transposed. (It should be clear from the context what "block" is.) Recalling

the first order equality (A.5) and making use of (A.11), we get

$$\begin{aligned}
\mathbf{C}_{\boldsymbol{\varepsilon}_{\mathrm{FS}}} &\triangleq \lim_{N\to\infty} N\ \mathrm{E}\{\mathrm{vec}(\mathbf{B}^*\tilde{\mathbf{E}}_{s_{\mathrm{FS}}})\,\mathrm{vec}^*(\mathbf{B}^*\tilde{\mathbf{E}}_{s_{\mathrm{FS}}})\} \\
&= \lim_{N\to\infty} N\ \mathrm{E}\{\mathrm{vec}(\mathbf{B}^*\tilde{\mathbf{R}}_{\mathrm{FS}}\mathbf{E}_s\widetilde{\boldsymbol{\Lambda}}^{-1})\,\mathrm{vec}^*(\mathbf{B}^*\tilde{\mathbf{R}}_{\mathrm{FS}}\mathbf{E}_s\widetilde{\boldsymbol{\Lambda}}^{-1})\} \\
&= \lim_{N\to\infty} N\ \left((\mathbf{E}_s\widetilde{\boldsymbol{\Lambda}}^{-1})^T\otimes\mathbf{B}^*\right) \\
&\qquad\qquad \times \mathrm{E}\{\mathrm{vec}(\tilde{\mathbf{R}}_{\mathrm{FS}})\,\mathrm{vec}^*(\tilde{\mathbf{R}}_{\mathrm{FS}})\}\left((\mathbf{E}_s\widetilde{\boldsymbol{\Lambda}}^{-1})^c\otimes\mathbf{B}\right) \\
&= \left((\mathbf{E}_s\widetilde{\boldsymbol{\Lambda}}^{-1})^T\otimes\mathbf{B}^*\right)(\mathbf{R}^T\otimes\mathbf{R})\left((\mathbf{E}_s\widetilde{\boldsymbol{\Lambda}}^{-1})^c\otimes\mathbf{B}\right) \\
&= \left(\widetilde{\boldsymbol{\Lambda}}^{-1}\mathbf{E}_s^T\mathbf{R}^T\mathbf{E}_s^c\widetilde{\boldsymbol{\Lambda}}^{-1}\otimes\mathbf{B}^*\mathbf{R}\mathbf{B}\right) \\
&= \left(\widetilde{\boldsymbol{\Lambda}}^{-2}\boldsymbol{\Lambda}_s\otimes\sigma^2\mathbf{B}^*\mathbf{B}\right).
\end{aligned} \tag{A.13}$$

In the third equality we used the formula in (3.8). Similarly, from (A.5) and (A.12), we have

$$\begin{aligned}
\bar{\mathbf{C}}_{\boldsymbol{\varepsilon}_{\mathrm{FS}}} &\triangleq \lim_{N\to\infty} N\ \mathrm{E}\{\mathrm{vec}(\mathbf{B}^*\tilde{\mathbf{E}}_{s_{\mathrm{FS}}})\,\mathrm{vec}^T(\mathbf{B}^*\tilde{\mathbf{E}}_{s_{\mathrm{FS}}})\} \\
&= \lim_{N\to\infty} N\ \left((\mathbf{E}_s\widetilde{\boldsymbol{\Lambda}}^{-1})^T\otimes\mathbf{B}^*\right) \\
&\qquad\qquad \times \mathrm{E}\{\mathrm{vec}(\tilde{\mathbf{R}}_{\mathrm{FS}})\,\mathrm{vec}^T(\tilde{\mathbf{R}}_{\mathrm{FS}})\}\left((\mathbf{E}_s\widetilde{\boldsymbol{\Lambda}}^{-1})\otimes\mathbf{B}^c\right) \\
&= \left((\mathbf{E}_s\widetilde{\boldsymbol{\Lambda}}^{-1})^T\otimes\mathbf{B}^*\right)\left[\mathrm{vec}(\mathbf{R})\,\mathrm{vec}^T(\mathbf{R})\right]^{\mathrm{BT}}\left((\mathbf{E}_s\widetilde{\boldsymbol{\Lambda}}^{-1})\otimes\mathbf{B}^c\right) \\
&= \left((\mathbf{E}_s\widetilde{\boldsymbol{\Lambda}}^{-1})^T\otimes\mathbf{B}^*\right)\left[\mathrm{vec}(\sigma^2\mathbf{I}_m)\,\mathrm{vec}^T(\sigma^2\mathbf{I}_m)\right]^{\mathrm{BT}}\left((\mathbf{E}_s\widetilde{\boldsymbol{\Lambda}}^{-1})\otimes\mathbf{B}^c\right) \\
&= \sigma^4\left((\mathbf{E}_s\widetilde{\boldsymbol{\Lambda}}^{-1})^T\otimes\mathbf{B}^*\right)\left(\mathbf{B}^c\otimes(\mathbf{E}_s\widetilde{\boldsymbol{\Lambda}}^{-1})\right)\left[\mathrm{vec}(\mathbf{I}_m)\,\mathrm{vec}^T(\mathbf{I}_{d'})\right]^{\mathrm{BT}} \\
&= \mathbf{0}.
\end{aligned}$$

The last two equalities follow from property 3 and property 2 of the block-transpose operation derived in Appendix A.4.

Remark A.1. The fact that $\bar{\mathbf{C}}_{\boldsymbol{\varepsilon}_{\mathrm{FS}}} = \mathbf{0}$ may be more easily realized using the asymptotic distribution of the eigenvectors (e.g. [KB86]). It is then easy to verify that $\mathrm{E}\{\mathbf{B}^*\hat{\mathbf{e}}_k\hat{\mathbf{e}}_l^T\mathbf{B}^c\} = \mathbf{0}$, where $\hat{\mathbf{e}}_k$ is column k of $\hat{\mathbf{E}}_s$.

Next, we proceed and study the model error contribution to the resid-

ual covariance matrix. Recall (A.10), (A.5), and that

$$\operatorname{vec}(\tilde{\mathbf{A}}) = \mathbf{D}_{\boldsymbol{\rho}}\tilde{\boldsymbol{\rho}} + o_p(1/\sqrt{N}).$$

We have

$$\begin{aligned}
\mathbf{C}_{\boldsymbol{\varepsilon}_{\mathrm{ME}}} &\triangleq \lim_{N\to\infty} N\ \mathrm{E}\{\operatorname{vec}(\mathbf{B}^*\tilde{\mathbf{E}}_{s_{\mathrm{ME}}})\operatorname{vec}^*(\mathbf{B}^*\tilde{\mathbf{E}}_{s_{\mathrm{ME}}})\} \\
&= \lim_{N\to\infty} N\ \mathrm{E}\{\operatorname{vec}(\mathbf{B}^*\tilde{\mathbf{A}}\mathbf{P}\mathbf{A}_0^*\mathbf{E}_s\widetilde{\boldsymbol{\Lambda}}^{-1})\operatorname{vec}^*(\mathbf{B}^*\tilde{\mathbf{A}}\mathbf{P}\mathbf{A}_0^*\mathbf{E}_s\widetilde{\boldsymbol{\Lambda}}^{-1})\} \\
&= \lim_{N\to\infty} N\ \left(\mathbf{T}^T\otimes\mathbf{B}^*\right)\mathrm{E}\{\operatorname{vec}(\tilde{\mathbf{A}})\operatorname{vec}^*(\tilde{\mathbf{A}})\}\left(\mathbf{T}^c\otimes\mathbf{B}\right) \\
&= \left(\mathbf{T}^T\otimes\mathbf{B}^*\right)\mathbf{D}_{\boldsymbol{\rho}}\bar{\boldsymbol{\Omega}}\mathbf{D}_{\boldsymbol{\rho}}^*\left(\mathbf{T}^c\otimes\mathbf{B}\right),
\end{aligned} \tag{A.14}$$

where

$$\mathbf{T} = \mathbf{A}_0^{\dagger}\mathbf{E}_s$$

and the following relation is used (cf. (3.1)):

$$\mathbf{P} = \mathbf{A}_0^{\dagger}\mathbf{E}_s\widetilde{\boldsymbol{\Lambda}}\mathbf{E}_s^*\mathbf{A}_0^{\dagger\,*}.$$

Similarly,

$$\begin{aligned}
\bar{\mathbf{C}}_{\boldsymbol{\varepsilon}_{\mathrm{ME}}} &\triangleq \lim_{N\to\infty} N\ \mathrm{E}\{\operatorname{vec}(\mathbf{B}^*\tilde{\mathbf{E}}_{s_{\mathrm{ME}}})\operatorname{vec}^T(\mathbf{B}^*\tilde{\mathbf{E}}_{s_{\mathrm{ME}}})\} \\
&= \lim_{N\to\infty} N\ \mathrm{E}\{\operatorname{vec}(\mathbf{B}^*\tilde{\mathbf{A}}\mathbf{P}\mathbf{A}_0^*\mathbf{E}_s\widetilde{\boldsymbol{\Lambda}}^{-1})\operatorname{vec}^T(\mathbf{B}^*\tilde{\mathbf{A}}\mathbf{P}\mathbf{A}_0^*\mathbf{E}_s\widetilde{\boldsymbol{\Lambda}}^{-1})\} \\
&= \lim_{N\to\infty} N\ \left(\mathbf{T}^T\otimes\mathbf{B}^*\right)\mathrm{E}\{\operatorname{vec}(\tilde{\mathbf{A}})\operatorname{vec}^T(\tilde{\mathbf{A}})\}\left(\mathbf{T}\otimes\mathbf{B}^c\right) \\
&= \left(\mathbf{T}^T\otimes\mathbf{B}^*\right)\mathbf{D}_{\boldsymbol{\rho}}\bar{\boldsymbol{\Omega}}\mathbf{D}_{\boldsymbol{\rho}}^T\left(\mathbf{T}\otimes\mathbf{B}^c\right).
\end{aligned} \tag{A.15}$$

Hence, the asymptotic covariance matrix of the residuals in (3.21) is given by

$$\mathbf{C}_{\bar{\boldsymbol{\varepsilon}}} = \begin{bmatrix} \mathbf{C}_{\boldsymbol{\varepsilon}} & \bar{\mathbf{C}}_{\boldsymbol{\varepsilon}} \\ \bar{\mathbf{C}}_{\boldsymbol{\varepsilon}}^c & \mathbf{C}_{\boldsymbol{\varepsilon}}^c \end{bmatrix},$$

with

$$\begin{aligned}
\mathbf{C}_{\boldsymbol{\varepsilon}} &= \mathbf{C}_{\boldsymbol{\varepsilon}_{\mathrm{FS}}} + \mathbf{C}_{\boldsymbol{\varepsilon}_{\mathrm{ME}}}, \\
\bar{\mathbf{C}}_{\boldsymbol{\varepsilon}} &= \bar{\mathbf{C}}_{\boldsymbol{\varepsilon}_{\mathrm{ME}}},
\end{aligned}$$

where $\mathbf{C}_{\boldsymbol{\varepsilon}_{\mathrm{FS}}}$, $\mathbf{C}_{\boldsymbol{\varepsilon}_{\mathrm{ME}}}$ and $\bar{\mathbf{C}}_{\boldsymbol{\varepsilon}_{\mathrm{ME}}}$ are given by (A.13), (A.14) and (A.15), respectively.

A.3 Proof of Theorem 3.2

Recall the expression (3.31)

$$V_i' \simeq 2\mathbf{k}_i^* \mathbf{W} \bar{\boldsymbol{\varepsilon}}.$$

Differentiating with respect to $\boldsymbol{\theta}_j$ and letting N tend to infinity leads to

$$\mathbf{H}_{ij} = 2\mathbf{k}_i^* \mathbf{W} \mathbf{k}_j.$$

Next, study the (i,j)th element of $\mathbf{Q}$ in (3.32):

$$\begin{aligned} \mathbf{Q}_{ij} &= \lim_{N\to\infty} N \, \mathrm{E}\{V_i' V_j'\} \\ &= \lim_{N\to\infty} N \, \mathrm{E}\{4\mathbf{k}_i^* \mathbf{W} \bar{\boldsymbol{\varepsilon}} \bar{\boldsymbol{\varepsilon}}^* \mathbf{W} \mathbf{k}_j\} \\ &= 4\mathbf{k}_i^* \mathbf{W} \mathbf{C}_{\bar{\boldsymbol{\varepsilon}}} \mathbf{W} \mathbf{k}_j. \end{aligned}$$

Defining the matrix

$$\mathbf{K} = \begin{bmatrix} \mathbf{k}_1 & \dots & \mathbf{k}_d \end{bmatrix},$$

the matrices $\mathbf{H}$ and $\mathbf{Q}$ can be written in compact form as

$$\mathbf{H} = 2\mathbf{K}^* \mathbf{W} \mathbf{K}, \tag{A.16}$$

$$\mathbf{Q} = 4\mathbf{K}^* \mathbf{W} \mathbf{C}_{\bar{\boldsymbol{\varepsilon}}} \mathbf{W} \mathbf{K}. \tag{A.17}$$

These expressions are valid for any $\mathbf{W}$ satisfying (3.29). It remains to prove that $\mathbf{H}^{-1}\mathbf{Q}\mathbf{H}^{-1}$ equals $N\mathbf{CRB}_{\boldsymbol{\theta}}$ for the choice $\mathbf{W} = \mathbf{W}_{\mathrm{GWSF}}$ given in (3.25). Inserting $\mathbf{W} = \mathbf{C}_{\bar{\boldsymbol{\varepsilon}}}^{-1}$ in (A.16) and (A.17) gives

$$\mathbf{H}^{-1}\mathbf{Q}\mathbf{H}^{-1} = \left(\mathbf{K}^* \mathbf{C}_{\bar{\boldsymbol{\varepsilon}}}^{-1} \mathbf{K}\right)^{-1}.$$

Next, we rewrite $\mathbf{k}_i$ as

$$\begin{aligned} \mathbf{k}_i &= \begin{bmatrix} \mathrm{vec}(\mathbf{B}_i^* \mathbf{E}_s) \\ \mathrm{vec}(\mathbf{B}_i^T \mathbf{E}_s^c) \end{bmatrix} = \begin{bmatrix} \mathrm{vec}(\mathbf{B}_i^* \mathbf{A} \mathbf{T}) \\ \mathrm{vec}(\mathbf{B}_i^T \mathbf{A}^c \mathbf{T}^c) \end{bmatrix} \\ &= -\begin{bmatrix} \mathrm{vec}(\mathbf{B}^* \mathbf{A}_i \mathbf{T}) \\ \mathrm{vec}(\mathbf{B}^T \mathbf{A}_i^c \mathbf{T}^c) \end{bmatrix} = -\begin{bmatrix} \left(\mathbf{T}^T \otimes \mathbf{B}^*\right) \mathrm{vec}(\mathbf{A}_i) \\ \left(\mathbf{T}^* \otimes \mathbf{B}^T\right) \mathrm{vec}(\mathbf{A}_i^c) \end{bmatrix}, \end{aligned} \tag{A.18}$$

and hence

$$\mathbf{K} = -\begin{bmatrix} \left(\mathbf{T}^T \otimes \mathbf{B}^*\right) \mathbf{D}_{\boldsymbol{\theta}} \\ \left(\mathbf{T}^* \otimes \mathbf{B}^T\right) \mathbf{D}_{\boldsymbol{\theta}}^c \end{bmatrix}.$$

In (A.18) we made use of the fact that $\mathbf{B}_i^*\mathbf{A} = -\mathbf{B}^*\mathbf{A}_i$, which follows from $\mathbf{B}^*\mathbf{A} = \mathbf{0}$. We also rewrite the inverse of $\mathbf{C}_{\bar{\boldsymbol{\varepsilon}}}$ using the "matrix inversion lemma":

$$\mathbf{C}_{\bar{\boldsymbol{\varepsilon}}}^{-1} = (\bar{\mathbf{L}} + \bar{\mathbf{G}}\bar{\mathbf{G}}^*)^{-1} = \bar{\mathbf{L}}^{-1} - \bar{\mathbf{L}}^{-1}\bar{\mathbf{G}}\left(\bar{\mathbf{G}}^*\bar{\mathbf{L}}^{-1}\bar{\mathbf{G}} + \mathbf{I}\right)^{-1}\bar{\mathbf{G}}^*\bar{\mathbf{L}}^{-1}. \quad \text{(A.19)}$$

In view of this, the product $\mathbf{K}^*\mathbf{C}_{\bar{\boldsymbol{\varepsilon}}}^{-1}\mathbf{K}$ contains two terms. In the sequel we consider these two separately and show that they correspond to the two terms in the expression for $\mathbf{CRB}_{\boldsymbol{\theta}}^{-1}/N$ in (3.15).

Let us first study

$$\begin{aligned}\mathbf{K}^*\bar{\mathbf{L}}^{-1}\mathbf{K} &= \begin{bmatrix}\left(\mathbf{T}^T \otimes \mathbf{B}^*\right)\mathbf{D}_{\boldsymbol{\theta}} \\ \left(\mathbf{T}^* \otimes \mathbf{B}^T\right)\mathbf{D}_{\boldsymbol{\theta}}^c\end{bmatrix}^* \begin{bmatrix}\mathbf{L}^{-1} & \mathbf{0} \\ \mathbf{0} & \mathbf{L}^{-c}\end{bmatrix} \begin{bmatrix}\left(\mathbf{T}^T \otimes \mathbf{B}^*\right)\mathbf{D}_{\boldsymbol{\theta}} \\ \left(\mathbf{T}^* \otimes \mathbf{B}^T\right)\mathbf{D}_{\boldsymbol{\theta}}^c\end{bmatrix} \\ &= 2\,\mathrm{Re}\left\{\mathbf{D}_{\boldsymbol{\theta}}^*\left(\mathbf{T}^c\sigma^{-2}\widetilde{\boldsymbol{\Lambda}}^2\boldsymbol{\Lambda}_s^{-1}\mathbf{T}^T \otimes \mathbf{B}(\mathbf{B}^*\mathbf{B})^{-1}\mathbf{B}^*\right)\mathbf{D}_{\boldsymbol{\theta}}\right\} \\ &= 2\sigma^{-2}\,\mathrm{Re}\{\mathbf{D}_{\boldsymbol{\theta}}^*\mathbf{M}\mathbf{D}_{\boldsymbol{\theta}}\} = 2\sigma^{-2}\mathbf{C}.\end{aligned} \quad \text{(A.20)}$$

Here, $\mathbf{M}$ is defined in (3.16) and we used the fact that $\mathbf{B}(\mathbf{B}^*\mathbf{B})^{-1}\mathbf{B}^* = \boldsymbol{\Pi}_{\mathbf{A}}^{\perp}$. Thus, we have shown that (A.20) equals the first term in $\mathbf{CRB}_{\boldsymbol{\theta}}^{-1}/N$.

To simplify the second term, we first need some preliminary calculations. Consider the inverse appearing in (A.19),

$$\begin{aligned}&\left(\bar{\mathbf{G}}^*\bar{\mathbf{L}}^{-1}\bar{\mathbf{G}} + \mathbf{I}\right)^{-1} \\ &= \left(\begin{bmatrix}\mathbf{G}^* & \mathbf{G}^T\end{bmatrix}\begin{bmatrix}\mathbf{L}^{-1} & \mathbf{0} \\ \mathbf{0} & \mathbf{L}^{-c}\end{bmatrix}\begin{bmatrix}\mathbf{G} \\ \mathbf{G}^c\end{bmatrix} + \mathbf{I}\right)^{-1} \\ &= \left(2\,\mathrm{Re}\{\mathbf{G}^*\mathbf{L}^{-1}\mathbf{G}\} + \mathbf{I}\right)^{-1} \\ &= \Big[2\,\mathrm{Re}\Big\{\bar{\boldsymbol{\Omega}}^{1/2}\mathbf{D}_{\boldsymbol{\rho}}^*\left(\mathbf{T}^c \otimes \mathbf{B}\right) \\ &\quad \times \left(\sigma^{-2}\widetilde{\boldsymbol{\Lambda}}^2\boldsymbol{\Lambda}_s^{-1} \otimes (\mathbf{B}^*\mathbf{B})^{-1}\right)\left(\mathbf{T}^T \otimes \mathbf{B}^*\right)\mathbf{D}_{\boldsymbol{\rho}}\bar{\boldsymbol{\Omega}}^{1/2}\Big\} + \mathbf{I}\Big]^{-1} \\ &= \frac{\sigma^2}{2}\bar{\boldsymbol{\Omega}}^{-1/2}\left(\mathrm{Re}\{\mathbf{D}_{\boldsymbol{\rho}}^*\mathbf{M}\mathbf{D}_{\boldsymbol{\rho}}\} + \frac{\sigma^2}{2}\bar{\boldsymbol{\Omega}}^{-1}\right)^{-1}\bar{\boldsymbol{\Omega}}^{-1/2} \\ &= \frac{\sigma^2}{2}\bar{\boldsymbol{\Omega}}^{-1/2}\boldsymbol{\Gamma}^{-1}\bar{\boldsymbol{\Omega}}^{-1/2},\end{aligned} \quad \text{(A.21)}$$

where $\mathbf{\Gamma}$ is defined in (3.18). We also need to compute

$$\begin{aligned}\mathbf{K}^*\bar{\mathbf{L}}^{-1}\bar{\mathbf{G}} &= -\begin{bmatrix}\left(\mathbf{T}^T \otimes \mathbf{B}^*\right)\mathbf{D}_{\boldsymbol{\theta}} \\ \left(\mathbf{T}^* \otimes \mathbf{B}^T\right)\mathbf{D}_{\boldsymbol{\theta}}^c\end{bmatrix}^* \begin{bmatrix}\mathbf{L}^{-1} & \mathbf{0} \\ \mathbf{0} & \mathbf{L}^{-c}\end{bmatrix}\begin{bmatrix}\mathbf{G} \\ \mathbf{G}^c\end{bmatrix} \\ &= -2\,\mathrm{Re}\left\{\mathbf{D}_{\boldsymbol{\theta}}^*\left(\mathbf{T}^c\sigma^{-2}\widetilde{\mathbf{\Lambda}}^2\mathbf{\Lambda}_s^{-1}\mathbf{T}^T \otimes \mathbf{B}(\mathbf{B}^*\mathbf{B})^{-1}\mathbf{B}^*\right)\mathbf{D}_{\boldsymbol{\rho}}\bar{\mathbf{\Omega}}^{1/2}\right\} \\ &= -2\sigma^{-2}\mathbf{F}_{\boldsymbol{\theta}}^T\bar{\mathbf{\Omega}}^{1/2},\end{aligned} \tag{A.22}$$

where $\mathbf{F}_{\boldsymbol{\theta}}$ is defined in (3.17). Combining (A.22), (A.21) and (A.19), we see that the second term in the product $\mathbf{K}^*\mathbf{C}_{\tilde{\boldsymbol{\varepsilon}}}^{-1}\mathbf{K}$ contributes with

$$-2\sigma^{-2}\mathbf{F}_{\boldsymbol{\theta}}^T\bar{\mathbf{\Omega}}^{1/2}\frac{\sigma^2}{2}\bar{\mathbf{\Omega}}^{-1/2}\mathbf{\Gamma}^{-1}\bar{\mathbf{\Omega}}^{-1/2}\bar{\mathbf{\Omega}}^{1/2}\mathbf{F}_{\boldsymbol{\theta}}2\sigma^{-2} = -2\sigma^{-2}\mathbf{F}_{\boldsymbol{\theta}}^T\mathbf{\Gamma}^{-1}\mathbf{F}_{\boldsymbol{\theta}}$$

which is exactly equal to the second term in $\mathbf{CRB}_{\boldsymbol{\theta}}^{-1}/N$ (see (3.15)).

A.4 Some Properties of the Block Transpose

This section contains three useful properties related to the block transpose operation. Let $\mathbf{A}_{i\times j}$ denote an arbitrary $i \times j$ matrix and define the operator

$$\mathbf{L}_{mn} = [\mathrm{vec}(\mathbf{I}_m)\,\mathrm{vec}^T(\mathbf{I}_n)]^{BT}$$

which has dimension $mn \times mn$. Observe that $\mathbf{L}_{mn} \neq \mathbf{L}_{nm}$ unless $m = n$.

Property A.1.

$$\mathbf{L}_{mn}\,\mathrm{vec}(\mathbf{A}_{m\times n}) = \mathrm{vec}(\mathbf{A}_{m\times n}^T)$$

Proof. This is easily proven by direct verification. □

Property A.2.

$$\mathbf{L}_{mn}\,(\mathbf{A}_{n\times d} \otimes \mathbf{B}_{m\times p}) = (\mathbf{B}_{m\times p} \otimes \mathbf{A}_{n\times d})\,\mathbf{L}_{pd}$$

Proof. Let $\mathbf{e}$ be an arbitrary dp-vector and let $\mathbf{E}$ be a $p \times d$ matrix defined via $\mathrm{vec}(\mathbf{E}) = \mathbf{e}$. Then

$$\begin{aligned}\mathbf{L}_{mn}\left(\mathbf{A}_{n\times d} \otimes \mathbf{B}_{m\times p}\right)\mathbf{e} &= \mathbf{L}_{mn}\,\mathrm{vec}(\mathbf{B}\mathbf{E}\mathbf{A}^T) \\ &= \mathrm{vec}(\mathbf{A}\mathbf{E}^T\mathbf{B}^T) \\ &= (\mathbf{B}\otimes\mathbf{A})\,\mathrm{vec}(\mathbf{E}^T) \\ &= (\mathbf{B}\otimes\mathbf{A})\,\mathbf{L}_{pd}\,\mathrm{vec}(\mathbf{E})\end{aligned}$$

and the result follows. □

Property A.3.

$$\begin{aligned}&\left[\mathrm{vec}(\mathbf{A}_{m\times n}\mathbf{B}_{n\times p})\,\mathrm{vec}^T(\mathbf{C}_{q\times r}\mathbf{D}_{r\times s})\right]^{BT} \\ &\qquad = (\mathbf{I}_p\otimes\mathbf{C})\left[\mathrm{vec}(\mathbf{B})\,\mathrm{vec}^T(\mathbf{D})\right]^{BT}\left(\mathbf{I}_s\otimes\mathbf{A}^T\right)\end{aligned}$$

Proof. Let $\mathbf{A}_{\bullet i}$ denote column i of $\mathbf{A}$. Consider block ij ($i = 1,\ldots,p$; $j = 1,\ldots,s$) of the left hand side:

$$\left[\mathbf{A}\mathbf{B}_{\bullet i}(\mathbf{C}\mathbf{D}_{\bullet j})^T\right]^T = \mathbf{C}(\mathbf{B}_{\bullet i}\mathbf{D}_{\bullet j}^T)^T\mathbf{A}^T$$

which is readily seen to equal block ij of the right hand side. □

A.5 Proof of Theorem 4.1

It is well known that the CRB is given by the inverse of the Fisher information matrix (FIM). Element (k,l) of the normalized FIM is given by Bangs' formula [Ban71]

$$\frac{1}{N}\mathrm{FIM}_{kl} = \mathrm{Tr}\{\mathbf{R}^{-1}\mathbf{R}_k\mathbf{R}^{-1}\mathbf{R}_l\},$$

where the notation $\mathbf{R}_k$ refers to the partial derivative of $\mathbf{R}$ with respect to the k:th parameter in $\boldsymbol{\eta}$. Using the formula $\mathrm{Tr}\{\mathbf{ABCD}\} = \mathrm{vec}^*(\mathbf{B}^*)\left(\mathbf{A}^{\mathrm{T}}\otimes\mathbf{C}\right)\mathrm{vec}(\mathbf{D})$ we get

$$\frac{1}{N}\mathrm{FIM}_{kl} = \mathrm{vec}^*(\mathbf{R}_k)\left(\mathbf{R}^{-\mathrm{T}}\otimes\mathbf{R}^{-1}\right)\mathrm{vec}(\mathbf{R}_l)\ .$$

The covariance matrix is given by

$$\mathbf{R}(\boldsymbol{\eta}) = \mathbf{A}(\boldsymbol{\theta})\mathbf{P}\mathbf{A}^*(\boldsymbol{\theta}) + \sigma^2\mathbf{I} = \sum_{i=1}^{d}\mathbf{a}(\theta_i)p_i\mathbf{a}^*(\theta_i) + \sigma^2\mathbf{I}$$

and, hence, the partial derivatives are

$$\begin{aligned}
\mathbf{R}_{\theta_i} &\triangleq \frac{\partial \mathbf{R}}{\partial \theta_i} = (\mathbf{d}_i\,\mathbf{a}_i^* + \mathbf{a}_i\,\mathbf{d}_i^*)p_i \ , \\
\mathbf{R}_{p_i} &\triangleq \frac{\partial \mathbf{R}}{\partial p_i} = \mathbf{a}_i\,\mathbf{a}_i^* \ , \\
\mathbf{R}_{\sigma^2} &\triangleq \frac{\partial \mathbf{R}}{\partial \sigma^2} = \mathbf{I} \ ,
\end{aligned}$$

where the notation $\mathbf{a}_i = \mathbf{a}(\theta_i)$ and

$$\mathbf{d}_i = \frac{\partial \mathbf{a}_i}{\partial \theta_i}$$

has been introduced. Now, define the matrices

$$\begin{aligned}
\mathbf{D}_{\boldsymbol{\theta}} &= \begin{bmatrix} \mathrm{vec}(\mathbf{R}_{\theta_1}) & \cdots & \mathrm{vec}(\mathbf{R}_{\theta_d}) \end{bmatrix} = \mathbf{DP} \ , \qquad \text{(A.23)} \\
\mathbf{D}_{\mathbf{p}} &= \begin{bmatrix} \mathrm{vec}(\mathbf{R}_{p_1}) & \cdots & \mathrm{vec}(\mathbf{R}_{p_d}) \end{bmatrix} = (\mathbf{A}^{\mathrm{c}} \circ \mathbf{A}) = \mathbf{B} \ , \\
\mathbf{D}_{\sigma^2} &= \mathrm{vec}(\mathbf{R}_{\sigma^2}) = \mathrm{vec}(\mathbf{I}) \triangleq \mathbf{i} \ , \\
\mathbf{D}_{\mathbf{n}} &= \begin{bmatrix} \mathbf{D}_{\mathbf{p}} & \mathbf{D}_{\sigma^2} \end{bmatrix} \ , \qquad \text{(A.24)}
\end{aligned}$$

and also

$$\begin{aligned}
\mathbf{W}_{\mathbf{R}} &= \left(\mathbf{R}^{-\mathrm{T}} \otimes \mathbf{R}^{-1}\right) \ , \\
\mathbf{X} &= \mathbf{D}_{\boldsymbol{\theta}}^* \mathbf{W}_{\mathbf{R}} \mathbf{D}_{\boldsymbol{\theta}} \ , \\
\mathbf{Y} &= \mathbf{D}_{\boldsymbol{\theta}}^* \mathbf{W}_{\mathbf{R}} \mathbf{D}_{\mathbf{n}} \ , \\
\mathbf{Z} &= \mathbf{D}_{\mathbf{n}}^* \mathbf{W}_{\mathbf{R}} \mathbf{D}_{\mathbf{n}} \ ,
\end{aligned}$$

where the matrix $\mathbf{D}$ in (A.23) is defined in (4.15). With the notation introduced above, note that the Fisher information matrix reads

$$\mathrm{FIM} = \begin{bmatrix} \mathbf{X} & \mathbf{Y} \\ \mathbf{Y}^* & \mathbf{Z} \end{bmatrix} \ .$$

The bound on the DOAs is given by the upper left $d \times d$ corner of the CRB matrix; that is, the upper left corner of the inverse FIM. Using the formulas for inverting partitioned matrices, the following expression is obtained

$$\begin{aligned}
\mathrm{CRB}_{\boldsymbol{\theta}}^{-1} &= \mathbf{X} - \mathbf{Y}\mathbf{Z}^{-1}\mathbf{Y}^* \\
&= \mathbf{D}_{\boldsymbol{\theta}}^* \mathbf{W}_{\mathbf{R}} \mathbf{D}_{\boldsymbol{\theta}} - \mathbf{D}_{\boldsymbol{\theta}}^* \mathbf{W}_{\mathbf{R}} \mathbf{D}_{\mathbf{n}} (\mathbf{D}_{\mathbf{n}}^* \mathbf{W}_{\mathbf{R}} \mathbf{D}_{\mathbf{n}})^{-1} \mathbf{D}_{\mathbf{n}}^* \mathbf{W}_{\mathbf{R}} \mathbf{D}_{\boldsymbol{\theta}} \\
&= \mathbf{D}_{\boldsymbol{\theta}}^* \mathbf{W}_{\mathbf{R}}^{1/2} \boldsymbol{\Pi}^{\perp}_{\mathbf{W}_{\mathbf{R}}^{1/2}\mathbf{D}_{\mathbf{n}}} \mathbf{W}_{\mathbf{R}}^{1/2} \mathbf{D}_{\boldsymbol{\theta}}. \qquad \text{(A.25)}
\end{aligned}$$

In what follows, the expression for $\mathrm{CRB}_{\boldsymbol{\theta}}^{-1}$ is rewritten in a form suitable for establishing the equality of the asymptotic estimation error covariance of the proposed estimator and $\mathrm{CRB}_{\boldsymbol{\theta}}$.

Recall from (A.24) that $\mathbf{W}_{\mathbf{R}}^{1/2}\mathbf{D}_{\mathbf{n}} = \mathbf{W}_{\mathbf{R}}^{1/2}\begin{bmatrix}\mathbf{B} & \mathbf{i}\end{bmatrix}$ and use the projection decomposition theorem to write

$$\boldsymbol{\Pi}^{\perp}_{\mathbf{W}_{\mathbf{R}}^{1/2}\mathbf{D}_{\mathbf{n}}} = \boldsymbol{\Pi}^{\perp}_{\mathbf{B}_{\mathbf{W}}} - \boldsymbol{\Pi}_{\boldsymbol{\Pi}^{\perp}_{\mathbf{B}_{\mathbf{W}}}\mathbf{i}_{\mathbf{W}}} \ , \tag{A.26}$$

where

$$\begin{aligned}\mathbf{B}_{\mathbf{W}} &= \mathbf{W}_{\mathbf{R}}^{1/2}\mathbf{B} \ , \\ \mathbf{i}_{\mathbf{W}} &= \mathbf{W}_{\mathbf{R}}^{1/2}\mathbf{i} \ .\end{aligned}$$

Let the columns of $\mathbf{G}$ form a basis for the null-space of $\mathbf{B}^*$ (this matter is further dwelled upon in Section 4.6). Observe that

$$\boldsymbol{\Pi}^{\perp}_{\mathbf{B}_{\mathbf{W}}} = \boldsymbol{\Pi}_{\mathbf{W}_{\mathbf{R}}^{-1/2}\mathbf{G}}. \tag{A.27}$$

Using (A.26) and (A.27), the expression (A.25) can be rewritten to yield

$$\begin{aligned}\mathrm{CRB}_{\boldsymbol{\theta}}^{-1} &= \mathbf{D}_{\boldsymbol{\theta}}^{*}\mathbf{W}_{\mathbf{R}}^{1/2}\left(\boldsymbol{\Pi}_{\mathbf{W}_{\mathbf{R}}^{-1/2}\mathbf{G}} - \boldsymbol{\Pi}_{\boldsymbol{\Pi}_{\mathbf{W}_{\mathbf{R}}^{-1/2}\mathbf{G}}\mathbf{i}_{\mathbf{W}}}\right)\mathbf{W}_{\mathbf{R}}^{1/2}\mathbf{D}_{\boldsymbol{\theta}} \\ &= \mathbf{D}_{\boldsymbol{\theta}}^{*}\mathbf{G}(\mathbf{G}^{*}\mathbf{W}_{\mathbf{R}}^{-1}\mathbf{G})^{-1}\mathbf{G}^{*}\mathbf{D}_{\boldsymbol{\theta}} \\ &\quad - \frac{\mathbf{D}_{\boldsymbol{\theta}}^{*}\mathbf{G}(\mathbf{G}^{*}\mathbf{W}_{\mathbf{R}}^{-1}\mathbf{G})^{-1}\mathbf{G}^{*}\mathbf{i}\mathbf{i}^{*}\mathbf{G}(\mathbf{G}^{*}\mathbf{W}_{\mathbf{R}}^{-1}\mathbf{G})^{-1}\mathbf{G}^{*}\mathbf{D}_{\boldsymbol{\theta}}}{\mathbf{i}^{*}\mathbf{G}(\mathbf{G}^{*}\mathbf{W}_{\mathbf{R}}^{-1}\mathbf{G})^{-1}\mathbf{G}^{*}\mathbf{i}} \ .\end{aligned} \tag{A.28}$$

Next it is proven that

$$\mathbf{D}_{\boldsymbol{\theta}}^{*}\mathbf{G}(\mathbf{G}^{*}\mathbf{W}_{\mathbf{R}}^{-1}\mathbf{G})^{-1}\mathbf{G}^{*}\,\mathrm{vec}(\boldsymbol{\Pi}_{\mathbf{A}}^{\perp}) = \mathbf{0} \tag{A.29}$$

and that

$$\begin{aligned}&\mathbf{i}^{*}\mathbf{G}(\mathbf{G}^{*}\mathbf{W}_{\mathbf{R}}^{-1}\mathbf{G})^{-1}\mathbf{G}^{*}\mathbf{i} \\ &\qquad = \frac{m-d}{\sigma^4} + \mathrm{vec}^{*}(\boldsymbol{\Pi}_{\mathbf{A}})\mathbf{G}(\mathbf{G}^{*}\mathbf{W}_{\mathbf{R}}^{-1}\mathbf{G})^{-1}\mathbf{G}^{*}\,\mathrm{vec}(\boldsymbol{\Pi}_{\mathbf{A}}) \ .\end{aligned} \tag{A.30}$$

Starting with (A.30):

$$\begin{aligned}\mathbf{i}^{*}\mathbf{G}(\mathbf{G}^{*}\mathbf{W}_{\mathbf{R}}^{-1}\mathbf{G})^{-1}\mathbf{G}^{*}\mathbf{i} &= \mathbf{i}^{*}\mathbf{W}_{\mathbf{R}}^{1/2}\boldsymbol{\Pi}_{\mathbf{W}_{\mathbf{R}}^{-1/2}\mathbf{G}}\mathbf{W}_{\mathbf{R}}^{1/2}\mathbf{i} \\ &= \mathbf{i}^{*}\mathbf{W}_{\mathbf{R}}^{1/2}\boldsymbol{\Pi}^{\perp}_{\mathbf{W}_{\mathbf{R}}^{1/2}\mathbf{B}}\mathbf{W}_{\mathbf{R}}^{1/2}\mathbf{i} \\ &= \mathbf{i}^{*}\mathbf{W}_{\mathbf{R}}\mathbf{i} - \mathbf{i}^{*}\mathbf{W}_{\mathbf{R}}\mathbf{B}(\mathbf{B}^{*}\mathbf{W}_{\mathbf{R}}\mathbf{B})^{-1}\mathbf{B}^{*}\mathbf{W}_{\mathbf{R}}\mathbf{i} \ .\end{aligned} \tag{A.31}$$

Observe that $\mathbf{i} = \mathrm{vec}(\mathbf{\Pi_A}) + \mathrm{vec}(\mathbf{\Pi_A^\perp})$ and

$$\begin{aligned}\mathbf{B}^*\mathbf{W_R}\,\mathrm{vec}(\mathbf{\Pi_A^\perp}) &= \mathbf{B}^*\,\mathrm{vec}(\mathbf{R}^{-1}\mathbf{\Pi_A^\perp}\mathbf{R}^{-1}) \\ &= \mathbf{L}^*\left(\mathbf{A}^{\mathrm{T}}\otimes\mathbf{A}^*\right)\mathrm{vec}(\mathbf{\Pi_A^\perp})\sigma^{-4} = \mathbf{0}\ . \quad \text{(A.32)}\end{aligned}$$

Using (A.32) in (A.31) leads to

$$\begin{aligned}&\mathbf{i}^*\mathbf{W_R}\mathbf{i} - \mathrm{vec}^*(\mathbf{\Pi_A})\mathbf{W_R}\mathbf{B}(\mathbf{B}^*\mathbf{W_R}\mathbf{B})^{-1}\mathbf{B}^*\mathbf{W_R}\,\mathrm{vec}(\mathbf{\Pi_A}) \\ &\quad= \mathbf{i}^*\mathbf{W_R}\mathbf{i} - \mathrm{vec}^*(\mathbf{\Pi_A})\mathbf{W}_\mathbf{R}^{1/2}\mathbf{\Pi}^\perp_{\mathbf{W}_\mathbf{R}^{-1/2}\mathbf{G}}\mathbf{W}_\mathbf{R}^{1/2}\,\mathrm{vec}(\mathbf{\Pi_A}) \\ &\quad= \mathbf{i}^*\mathbf{W_R}\mathbf{i} - \mathrm{vec}^*(\mathbf{\Pi_A})\mathbf{W_R}\,\mathrm{vec}(\mathbf{\Pi_A}) \\ &\qquad+ \mathrm{vec}^*(\mathbf{\Pi_A})\mathbf{G}(\mathbf{G}^*\mathbf{W}_\mathbf{R}^{-1}\mathbf{G})^{-1}\mathbf{G}^*\,\mathrm{vec}(\mathbf{\Pi_A}) \\ &\quad= \mathrm{Tr}\{\mathbf{R}^{-2} - \mathbf{R}^{-1}\mathbf{\Pi_A}\mathbf{R}^{-1}\mathbf{\Pi_A}\} \\ &\qquad+ \mathrm{vec}^*(\mathbf{\Pi_A})\mathbf{G}(\mathbf{G}^*\mathbf{W}_\mathbf{R}^{-1}\mathbf{G})^{-1}\mathbf{G}^*\,\mathrm{vec}(\mathbf{\Pi_A}) \\ &\quad= \frac{m-d}{\sigma^4} + \mathrm{vec}^*(\mathbf{\Pi_A})\mathbf{G}(\mathbf{G}^*\mathbf{W}_\mathbf{R}^{-1}\mathbf{G})^{-1}\mathbf{G}^*\,\mathrm{vec}(\mathbf{\Pi_A})\end{aligned}$$

which is (A.30). Consider next (A.29):

$$\begin{aligned}&\mathbf{D}_{\boldsymbol\theta}^*\mathbf{G}(\mathbf{G}^*\mathbf{W}_\mathbf{R}^{-1}\mathbf{G})^{-1}\mathbf{G}^*\,\mathrm{vec}(\mathbf{\Pi_A^\perp}) \\ &\quad= \mathbf{D}_{\boldsymbol\theta}^*\mathbf{W}_\mathbf{R}^{1/2}\mathbf{\Pi}^\perp_{\mathbf{B}_\mathbf{W}}\mathbf{W}_\mathbf{R}^{1/2}\,\mathrm{vec}(\mathbf{\Pi_A^\perp}) \\ &\quad= \mathbf{D}_{\boldsymbol\theta}^*\underbrace{\mathbf{W_R}\,\mathrm{vec}(\mathbf{\Pi_A^\perp})}_{\sigma^{-4}\,\mathrm{vec}(\mathbf{\Pi_A^\perp})} - \mathbf{D}_{\boldsymbol\theta}^*\mathbf{W_R}\mathbf{B}(\mathbf{B}^*\mathbf{W_R}\mathbf{B})^{-1}\underbrace{\mathbf{B}^*\mathbf{W_R}\,\mathrm{vec}(\mathbf{\Pi_A^\perp})}_{=\mathbf{0},\ \text{see (A.32)}} \\ &\quad= \sigma^{-4}\mathbf{P}\mathbf{L}^*\left[\left(\bar{\mathbf{D}}^{\mathrm{T}}\otimes\mathbf{A}^*\right) + \left(\mathbf{A}^{\mathrm{T}}\otimes\bar{\mathbf{D}}^*\right)\right]\mathrm{vec}(\mathbf{\Pi_A^\perp}) = \mathbf{0},\end{aligned}$$

where $\bar{\mathbf{D}}$ is defined in (4.16).

Making use of (A.29) and (A.30) in (A.28) yields

$$\begin{aligned}&\mathrm{CRB}_{\boldsymbol\theta}^{-1} \\ &= \mathbf{D}_{\boldsymbol\theta}^*\mathbf{G}\Bigg((\mathbf{G}^*\mathbf{W}_\mathbf{R}^{-1}\mathbf{G})^{-1} \\ &\quad- \frac{(\mathbf{G}^*\mathbf{W}_\mathbf{R}^{-1}\mathbf{G})^{-1}\mathbf{G}^*\,\mathrm{vec}(\mathbf{\Pi_A})\,\mathrm{vec}^*(\mathbf{\Pi_A})\mathbf{G}(\mathbf{G}^*\mathbf{W}_\mathbf{R}^{-1}\mathbf{G})^{-1}}{\frac{m-d}{\sigma^4} + \mathrm{vec}^*(\mathbf{\Pi_A})\mathbf{G}(\mathbf{G}^*\mathbf{W}_\mathbf{R}^{-1}\mathbf{G})^{-1}\mathbf{G}^*\,\mathrm{vec}(\mathbf{\Pi_A})}\Bigg)\mathbf{G}^*\mathbf{D}_{\boldsymbol\theta} \\ &= \mathbf{D}_{\boldsymbol\theta}^*\mathbf{G}\left(\mathbf{G}^*\mathbf{W}_\mathbf{R}^{-1}\mathbf{G} + \frac{\sigma^4}{m-d}\mathbf{G}^*\,\mathrm{vec}(\mathbf{\Pi_A})\,\mathrm{vec}^*(\mathbf{\Pi_A})\mathbf{G}\right)^{-1}\mathbf{G}^*\mathbf{D}_{\boldsymbol\theta} \\ &= \mathbf{D}_{\boldsymbol\theta}^*\mathbf{G}\left(\mathbf{G}^*\left(\mathbf{W}_\mathbf{R}^{-1} + \frac{\sigma^4}{m-d}\,\mathrm{vec}(\mathbf{\Pi_A})\,\mathrm{vec}^*(\mathbf{\Pi_A})\right)\mathbf{G}\right)^{-1}\mathbf{G}^*\mathbf{D}_{\boldsymbol\theta},\end{aligned}$$

where the matrix inversion lemma has been used to obtain the last but one equality. This concludes the proof.

A.6 Rank of $\mathbf{B}(\boldsymbol{\theta})$

In this appendix it is shown that $\text{rank}\{\mathbf{B}(\boldsymbol{\theta})\} = d$ as long as $m > d/2$. Let $\boldsymbol{\theta} = [\theta_1, \ldots, \theta_d]^{\mathrm{T}}$, and consider the following general form of the steering matrix

$$\mathbf{A}(\boldsymbol{\theta}) = \begin{bmatrix} 1 & \cdots & 1 \\ f_1(\theta_1) & & f_1(\theta_d) \\ \vdots & & \vdots \\ f_{m-1}(\theta_1) & & f_{m-1}(\theta_d) \end{bmatrix}$$

where, without loss of generality, the response from the first sensor is normalized to one. The array is assumed to be unambiguous which implies that $\mathbf{A}$ has full rank for $d = m$ and $\theta_i \neq \theta_j, i \neq j$. It follows from (4.6) that $\mathbf{B}(\boldsymbol{\theta})$ can be written as

$$\mathbf{B}(\boldsymbol{\theta}) = (\mathbf{A}^{\mathrm{c}} \circ \mathbf{A}) = \begin{bmatrix} \mathbf{A} \\ \mathbf{A}\boldsymbol{\Phi}_1 \\ \vdots \\ \mathbf{A}\boldsymbol{\Phi}_{m-1} \end{bmatrix}, \tag{A.33}$$

where $\boldsymbol{\Phi}_i = \text{diag}[f_i^{\mathrm{c}}(\theta_1) \ \ldots \ f_i^{\mathrm{c}}(\theta_d)]$. The notation $\text{diag}[\mathbf{v}]$ refers to a matrix with the entries in the vector $\mathbf{v}$ as diagonal elements. From (A.33) it is obvious that $\text{rank}\{\mathbf{B}\} = d$ if $d \leq m$ since $\mathbf{A}$ is full rank. Let us next study (non-zero) solutions $\mathbf{x} \in \mathbb{C}^{d \times 1}$ to $\mathbf{B}(\boldsymbol{\theta})\mathbf{x} = \mathbf{0}$. Any such vector must satisfy

$$\begin{aligned} \mathbf{A}\mathbf{x} &= \mathbf{0} \\ \mathbf{A}\boldsymbol{\Phi}_1\mathbf{x} &= \mathbf{0} \\ &\vdots \\ \mathbf{A}\boldsymbol{\Phi}_{m-1}\mathbf{x} &= \mathbf{0} \ . \end{aligned} \tag{A.34}$$

A necessary condition for the existence of a solution $\mathbf{x} \neq \mathbf{0}$ is $d > m$. It is also important to notice that at least $m + 1$ elements in $\mathbf{x}$ have to be different from zeros since the columns of $\mathbf{A}$ are linearly independent.

Since the dimension of the null-space of $\mathbf{A}$ is $d-m$, there are no solutions to (A.34) if

$$\operatorname{rank}\{\mathbf{x}\ \mathbf{\Phi}_1\mathbf{x}\ \cdots\ \mathbf{\Phi}_{m-1}\mathbf{x}\} > d-m\ . \tag{A.35}$$

However, it is straightforward to verify that the matrix in (A.35) can be written as $\operatorname{diag}\{\mathbf{x}\}\mathbf{A}^*$. The rank of $\operatorname{diag}\{\mathbf{x}\}\mathbf{A}^*$ is m since $d > m$ and since $\mathbf{x}$ has at least $m+1$ elements different from zero. Hence, no solution $\mathbf{x} \neq \mathbf{0}$ exists if $m > d-m$ or equivalently $m > d/2$ and we conclude that $\operatorname{rank}\{\mathbf{B}(\boldsymbol{\theta})\} = d$ if $m > d/2$.

A.7 Derivation of the Asymptotic Distribution

We will start with the derivation of $\mathbf{Q}$ defined in (4.24). From (4.19) and the fact that $\mathbf{B}^\dagger\mathbf{f} = \mathbf{p}$, we have

$$V_k' = -2\operatorname{Re}\{\mathbf{p}^*\mathbf{B}_k^*\mathbf{\Pi}_\mathbf{B}^\perp\mathbf{W}\mathbf{\Pi}_\mathbf{B}^\perp\tilde{\mathbf{f}}\} = -2\operatorname{Re}\{\mathbf{u}_k^*\tilde{\mathbf{f}}\},$$

where $\mathbf{u}_k$ is recognized as the k:th column of $\mathbf{U}$ in (4.27). From (4.24) it is evident that element (k,l) of $\mathbf{Q}$ is given by

$$\begin{aligned}\mathbf{Q}_{kl} &= \lim_{N\to\infty} 4N\,\mathrm{E}\{\operatorname{Re}\{\mathbf{u}_k^*\tilde{\mathbf{f}}\}\operatorname{Re}\{\mathbf{u}_l^*\tilde{\mathbf{f}}\}\}\\ &= \lim_{N\to\infty} 2N\,\mathrm{E}\{\operatorname{Re}\{\mathbf{u}_k^*\tilde{\mathbf{f}}\tilde{\mathbf{f}}^*\mathbf{u}_l + \mathbf{u}_k^*\tilde{\mathbf{f}}\tilde{\mathbf{f}}^{\mathrm{T}}\mathbf{u}_l^{\mathrm{c}}\}\}\\ &= 2\operatorname{Re}\{\mathbf{u}_k^*\mathbf{C}\mathbf{u}_l + \mathbf{u}_k^*\bar{\mathbf{C}}\mathbf{u}_l^{\mathrm{c}}\},\end{aligned}$$

which is element (k,l) of the expression in (4.26). Next, consider $\mathbf{H}$ as defined in (4.18). From (4.19) we get, for large N,

$$\begin{aligned}V_{kl}'' = &-2\operatorname{Re}\{\mathbf{p}^*\mathbf{B}_{kl}\mathbf{\Pi}_\mathbf{B}^\perp\mathbf{W}\mathbf{\Pi}_\mathbf{B}^\perp\hat{\mathbf{f}}\} - 2\operatorname{Re}\{\mathbf{p}^*\mathbf{B}_k^*\{\mathbf{\Pi}_\mathbf{B}^\perp\}_l\mathbf{W}\mathbf{\Pi}_\mathbf{B}^\perp\hat{\mathbf{f}}\}\\ &- 2\operatorname{Re}\{\mathbf{p}^*\mathbf{B}_k^*\mathbf{\Pi}_\mathbf{B}^\perp\mathbf{W}\{\mathbf{\Pi}_\mathbf{B}^\perp\}_l\hat{\mathbf{f}}\},\end{aligned}$$

and using (4.20) we obtain

$$\mathbf{H}_{kl} = 2\operatorname{Re}\{\mathbf{p}^*\mathbf{B}_k^*\mathbf{\Pi}_\mathbf{B}^\perp\mathbf{W}\mathbf{\Pi}_\mathbf{B}^\perp\mathbf{B}_l\,\mathbf{p}\},$$

which is element (k,l) of the matrix in (4.25).

It remains to compute the covariance matrices $\mathbf{C}$ and $\bar{\mathbf{C}}$ defined in (4.28) and (4.29), respectively. Since $\{\mathbf{x}(t)\}$ is assumed to be zero-mean

Gaussian and temporally white, it can be shown that

$$\mathrm{E}\{\hat{\mathbf{R}}_{kl}\hat{\mathbf{R}}_{pq}\} = \mathbf{R}_{kl}\mathbf{R}_{pq} + \frac{1}{N}\mathbf{R}_{kq}\mathbf{R}_{pl}. \tag{A.36}$$

From (A.36), the following two expressions are readily checked:

$$\mathrm{E}\{\mathrm{vec}(\tilde{\mathbf{R}})\,\mathrm{vec}^*(\tilde{\mathbf{R}})\} = \frac{1}{N}\left(\mathbf{R}^{\mathrm{T}} \otimes \mathbf{R}\right), \tag{A.37}$$

$$\mathrm{E}\{\mathrm{vec}(\tilde{\mathbf{R}})\,\mathrm{vec}^T(\tilde{\mathbf{R}})\} = \frac{1}{N}\left[\mathrm{vec}(\mathbf{R})\,\mathrm{vec}^T(\mathbf{R})\right]^{\mathrm{BT}}, \tag{A.38}$$

where the superscript 'BT' denotes block-transpose, which means that each $m \times m$ block is transposed. By making use of (4.23), (A.37) and (A.38), it is straightforward to derive $\mathbf{C}$ and $\bar{\mathbf{C}}$:

$$\begin{aligned}\mathbf{C} &= \lim_{N\to\infty} N\,\mathrm{E}\{\mathbf{M}\,\mathrm{vec}(\tilde{\mathbf{R}})\,\mathrm{vec}^*(\tilde{\mathbf{R}})\mathbf{M}^*\} \\ &= \mathbf{M}\left(\mathbf{R}^{\mathrm{T}} \otimes \mathbf{R}\right)\mathbf{M}^* \ , \qquad (\mathrm{A.39}) \\ \bar{\mathbf{C}} &= \lim_{N\to\infty} \mathrm{E}\{\mathbf{M}\,\mathrm{vec}(\tilde{\mathbf{R}})\,\mathrm{vec}^{\mathrm{T}}(\tilde{\mathbf{R}})\mathbf{M}^{\mathrm{T}}\} \\ &= \mathbf{M}\left[\mathrm{vec}(\mathbf{R})\,\mathrm{vec}^{\mathrm{T}}(\mathbf{R})\right]^{\mathrm{BT}}\mathbf{M}^{\mathrm{T}} \ . \qquad (\mathrm{A.40})\end{aligned}$$

Inserting the definition of $\mathbf{M}$ given in (4.23) into (A.39) leads after some tedious calculations to the following expression for $\mathbf{C}$:

$$\begin{aligned}\mathbf{C} = \left(\mathbf{R}^{\mathrm{T}} \otimes \mathbf{R}\right) - \sigma^4\left(\boldsymbol{\Pi}_{\mathbf{A}}^{\perp\mathrm{T}} \otimes \boldsymbol{\Pi}_{\mathbf{A}}^{\perp}\right) \\ + \frac{\sigma^4}{m-d}\,\mathrm{vec}(\boldsymbol{\Pi}_{\mathbf{A}})\,\mathrm{vec}^*(\boldsymbol{\Pi}_{\mathbf{A}}) \ .\end{aligned}$$

Similarly, we can obtain an expression for $\bar{\mathbf{C}}$ by inserting $\mathbf{M}$ into (A.40). Alternatively, one can use the following observation. Let $\mathbf{L}_{\mathrm{m}} = \mathbf{L}_{\mathrm{m}}^{\mathrm{T}}$ be the permutation matrix such that

$$\mathrm{vec}(\mathbf{X}^{\mathrm{T}}) = \mathbf{L}_{\mathrm{m}}\,\mathrm{vec}(\mathbf{X}) \tag{A.41}$$

for any $(m \times m)$ matrix $\mathbf{X}$ [Gra81]. It is then easy to see that $\mathbf{f}$ can be related to its conjugate $\mathbf{f}^{\mathrm{c}}$ as

$$\mathbf{f}^{\mathrm{c}} = \mathrm{vec}\big([\mathbf{E}_s\boldsymbol{\Lambda}\mathbf{E}_s^*]^{\mathrm{c}}\big) = \mathrm{vec}\big([\mathbf{E}_s\boldsymbol{\Lambda}\mathbf{E}_s^*]^{\mathrm{T}}\big) = \mathbf{L}_{\mathrm{m}}\mathbf{f}. \tag{A.42}$$

It is obvious that a similar relation holds for any vector defined as $\mathrm{vec}(\mathbf{X})$ when $\mathbf{X}$ is Hermitian. This implies that

$$\bar{\mathbf{C}} = \lim_{N\to\infty} N\,\mathrm{E}\{\tilde{\mathbf{f}}\tilde{\mathbf{f}}^{\mathrm{T}}\} = \lim_{N\to\infty} N\,\mathrm{E}\{\tilde{\mathbf{f}}\tilde{\mathbf{f}}^*\mathbf{L}_{\mathrm{m}}\} = \mathbf{C}\mathbf{L}_{\mathrm{m}}.$$

Hence, $\bar{\mathbf{C}}$ is related to $\mathbf{C}$ through a column permutation.

Remark A.2. Observe that the matrix $\mathbf{C}$ (and $\bar{\mathbf{C}}$) is singular. The null-space of $\mathbf{C}$ is spanned by the columns of $(\mathbf{E}_n^{\mathrm{c}} \otimes \mathbf{E}_n)$. The dimension of the null-space is $(m-d)^2$ and consequently the dimension of the range-space of $\mathbf{C}$ is $m^2 - (m-d)^2 = 2md - d^2$. Notice that this equals the number of real parameters in the Cholesky-factorization of $\mathbf{APA}^*$.

A.8 Proof of Theorem 4.3

Recalling the definition of $\mathbf{B}$ in (4.6) and making use of (A.41) leads to

$$\mathbf{B}^{\mathrm{c}} = \mathbf{L}_{\mathrm{m}}\mathbf{B},$$

which in turn implies that

$$\begin{aligned}
\mathbf{L}_{\mathrm{m}}\mathbf{B}_k &= \mathbf{B}_k^{\mathrm{c}} \ , \\
\mathbf{B}^{\dagger}\mathbf{L}_{\mathrm{m}} &= \mathbf{B}^{\dagger\mathrm{c}} \ , \\
\mathbf{L}_{\mathrm{m}}\mathbf{\Pi}_{\mathbf{B}}^{\perp} &= \mathbf{\Pi}_{\mathbf{B}}^{\perp\mathrm{c}}\mathbf{L}_{\mathrm{m}} = \mathbf{\Pi}_{\mathbf{B}}^{\perp\mathrm{T}}\mathbf{L}_{\mathrm{m}} \ .
\end{aligned}$$

In what follows, we will prove that the two terms in the gradient (4.19) are real valued if the weighting matrix has a special form satisfied by (4.30). Recall (A.42) and consider the first term in (4.19),

$$\hat{\mathbf{f}}^*\{\mathbf{\Pi}_{\mathbf{B}}^{\perp}\}_k\mathbf{W}\mathbf{\Pi}_{\mathbf{B}}^{\perp}\hat{\mathbf{f}} = \hat{\mathbf{f}}^{\mathrm{T}}\mathbf{L}_{\mathrm{m}}\{\mathbf{\Pi}_{\mathbf{B}}^{\perp}\}_k\mathbf{W}\mathbf{L}_{\mathrm{m}}\hat{\mathbf{f}}^{\mathrm{c}} = \hat{\mathbf{f}}^{\mathrm{T}}\{\mathbf{\Pi}_{\mathbf{B}}^{\perp}\}_k^{\mathrm{c}}\mathbf{L}_{\mathrm{m}}\mathbf{W}\mathbf{L}_{\mathrm{m}}\mathbf{\Pi}_{\mathbf{B}}^{\perp\mathrm{c}}\hat{\mathbf{f}}^{\mathrm{c}} \ .$$

If $\mathbf{L}_{\mathrm{m}}\mathbf{W}\mathbf{L}_{\mathrm{m}} = \mathbf{W}^{\mathrm{c}} = \mathbf{W}^{\mathrm{T}}$, then the two terms in (4.19) are real valued and we have

$$V_k' = 2\hat{\mathbf{f}}^*\{\mathbf{\Pi}_{\mathbf{B}}^{\perp}\}_k\mathbf{W}\mathbf{\Pi}_{\mathbf{B}}^{\perp}\hat{\mathbf{f}}.$$

This implies that

$$\mathbf{H} = 2\mathbf{P}\mathbf{D}^*\mathbf{\Pi}_{\mathbf{B}}^{\perp}\mathbf{W}\mathbf{\Pi}_{\mathbf{B}}^{\perp}\mathbf{D}\mathbf{P}, \tag{A.43}$$

$$\mathbf{Q} = 4\mathbf{U}^*\mathbf{C}\mathbf{U}, \tag{A.44}$$

where $\mathbf{U}$ is defined in (4.27). This is, as mentioned above, only valid if $\mathbf{L}_{\mathrm{m}}\mathbf{W}\mathbf{L}_{\mathrm{m}} = \mathbf{W}^{\mathrm{c}}$. We will now prove that this is true for the optimal

weighting $\mathbf{W}_{\text{opt}}$. This can be shown as follows:

$$\begin{aligned}\mathbf{L}_{\text{m}}\mathbf{W}_{\text{opt}}\mathbf{L}_{\text{m}} &= \mathbf{L}_{\text{m}}\left[\mathbf{\Pi}_{\mathbf{B}}^{\perp}\tilde{\mathbf{C}}\mathbf{\Pi}_{\mathbf{B}}^{\perp}+\mathbf{B}\mathbf{B}^{*}\right]^{-1}\mathbf{L}_{\text{m}}\\ &= \left[\mathbf{L}_{\text{m}}\left(\mathbf{\Pi}_{\mathbf{B}}^{\perp}\tilde{\mathbf{C}}\mathbf{\Pi}_{\mathbf{B}}^{\perp}+\mathbf{B}\mathbf{B}^{*}\right)\mathbf{L}_{\text{m}}\right]^{-1}\\ &= \left[\mathbf{\Pi}_{\mathbf{B}}^{\perp\text{c}}\mathbf{L}_{\text{m}}\tilde{\mathbf{C}}\mathbf{L}_{\text{m}}\mathbf{\Pi}_{\mathbf{B}}^{\perp\text{c}}\mathbf{L}_{\text{m}}+\mathbf{B}^{\text{c}}\mathbf{B}^{\text{T}}\right]^{-1}. \end{aligned} \tag{A.45}$$

It can be shown that

$$\mathbf{L}_{\text{m}}\left(\mathbf{X}\otimes\mathbf{Y}\right)=\left(\mathbf{Y}\otimes\mathbf{X}\right)\mathbf{L}_{\text{m}}$$

for any arbitrary $(m\times m)$ matrices $\mathbf{X}$ and $\mathbf{Y}$ [Gra81] (see also Section A.4). Hence, we get

$$\mathbf{L}_{\text{m}}\tilde{\mathbf{C}}\mathbf{L}_{\text{m}}=\tilde{\mathbf{C}}^{\text{c}}=\tilde{\mathbf{C}}^{\text{T}}$$

which, in view of (A.45), proves that $\mathbf{L}_{\text{m}}\mathbf{W}_{\text{opt}}\mathbf{L}_{\text{m}}=\mathbf{W}_{\text{opt}}^{\text{c}}$.

Next, we show that $\mathbf{Q}=2\mathbf{H}$ for $\mathbf{W}=\mathbf{W}_{\text{opt}}$. In order to prove this, the following calculations are needed. Let $\mathbf{G}$ be a $m^2\times(m^2-d)$ matrix whose columns span the null-space of $\mathbf{B}^*$, then (cf. Lemma 3.1)

$$\begin{aligned}\begin{bmatrix}\mathbf{G} & \mathbf{B}\end{bmatrix}^{-1} &= \begin{bmatrix}\mathbf{G} & \mathbf{B}\end{bmatrix}^{-1}\begin{bmatrix}\mathbf{G}^{*}\\ \mathbf{B}^{*}\end{bmatrix}^{-1}\begin{bmatrix}\mathbf{G}^{*}\\ \mathbf{B}^{*}\end{bmatrix}=\left(\begin{bmatrix}\mathbf{G}^{*}\\ \mathbf{B}^{*}\end{bmatrix}\begin{bmatrix}\mathbf{G} & \mathbf{B}\end{bmatrix}\right)^{-1}\begin{bmatrix}\mathbf{G}^{*}\\ \mathbf{B}^{*}\end{bmatrix}\\ &= \begin{bmatrix}(\mathbf{G}^{*}\mathbf{G})^{-1} & \mathbf{0}\\ \mathbf{0} & (\mathbf{B}^{*}\mathbf{B})^{-1}\end{bmatrix}\begin{bmatrix}\mathbf{G}^{*}\\ \mathbf{B}^{*}\end{bmatrix}=\begin{bmatrix}\mathbf{G}^{\dagger}\\ \mathbf{B}^{\dagger}\end{bmatrix}.\end{aligned}$$

Using this result in (4.30) and observing that $\mathbf{\Pi}_{\mathbf{B}}^{\perp}=\mathbf{\Pi}_{\mathbf{G}}$ gives

$$\begin{aligned}\mathbf{W}_{\text{opt}} &= \left[\mathbf{\Pi}_{\mathbf{G}}\tilde{\mathbf{C}}\mathbf{\Pi}_{\mathbf{G}}+\mathbf{B}\mathbf{B}^{*}\right]^{-1}=\left\{\begin{bmatrix}\mathbf{G} & \mathbf{B}\end{bmatrix}\begin{bmatrix}\mathbf{G}^{\dagger}\tilde{\mathbf{C}}\mathbf{G}^{\dagger *} & \mathbf{0}\\ \mathbf{0} & \mathbf{I}\end{bmatrix}\begin{bmatrix}\mathbf{G}^{*}\\ \mathbf{B}^{*}\end{bmatrix}\right\}^{-1}\\ &= \begin{bmatrix}\mathbf{G}^{\dagger *} & \mathbf{B}^{\dagger *}\end{bmatrix}\begin{bmatrix}(\mathbf{G}^{\dagger}\tilde{\mathbf{C}}\mathbf{G}^{\dagger *})^{-1} & \mathbf{0}\\ \mathbf{0} & \mathbf{I}\end{bmatrix}\begin{bmatrix}\mathbf{G}^{\dagger}\\ \mathbf{B}^{\dagger}\end{bmatrix},\end{aligned}$$

and

$$\begin{aligned}\mathbf{\Pi}_{\mathbf{B}}^{\perp}\mathbf{W}_{\text{opt}}\mathbf{\Pi}_{\mathbf{B}}^{\perp} &= \mathbf{\Pi}_{\mathbf{G}}\begin{bmatrix}\mathbf{G}^{\dagger *} & \mathbf{B}^{\dagger *}\end{bmatrix}\begin{bmatrix}(\mathbf{G}^{\dagger}\tilde{\mathbf{C}}\mathbf{G}^{\dagger *})^{-1} & \mathbf{0}\\ \mathbf{0} & \mathbf{I}\end{bmatrix}\begin{bmatrix}\mathbf{G}^{\dagger}\\ \mathbf{B}^{\dagger}\end{bmatrix}\mathbf{\Pi}_{\mathbf{G}}\\ &= \mathbf{G}^{\dagger *}(\mathbf{G}^{\dagger}\tilde{\mathbf{C}}\mathbf{G}^{\dagger *})^{-1}\mathbf{G}^{\dagger}=\mathbf{G}(\mathbf{G}^{*}\tilde{\mathbf{C}}\mathbf{G})^{-1}\mathbf{G}^{*}. \end{aligned} \tag{A.46}$$

From Remark A.2 in the end of Appendix A.7, we know that the rank of $\mathbf{C}$ is $2md-d^2$. Let the $m^2 \times (2md-d^2)$ matrix $\mathbf{T}$ be the Cholesky factor of $\mathbf{C}$ and define $\mathbf{E} = \sigma^2 \left(\mathbf{E}_n^{\mathrm{c}} \otimes \mathbf{E}_n\right)$. Recall that the columns of $\mathbf{E}$ span the null-space of $\mathbf{C}$ (see Remark A.2). Let $\mathcal{R}(\cdot)$ and $\mathcal{N}(\cdot)$ denote the range- and the null-space of a matrix, respectively. Study the decompositions

$$\mathbb{C}^{m^2} = \underbrace{\mathcal{R}(\mathbf{T})}_{2md-d^2} \oplus \underbrace{\mathcal{N}(\mathbf{T}^*)}_{(m-d)^2} = \underbrace{\mathcal{R}(\mathbf{G})}_{m^2-d} \oplus \underbrace{\mathcal{N}(\mathbf{G}^*)}_{d},$$

where the dimension of each of the subspaces is indicated, and where $\oplus$ denotes direct sum. Since it is known that $\mathcal{N}(\mathbf{T}^*) = \mathcal{N}(\mathbf{C}) = \mathcal{N}(\mathbf{E}^*) \subset \mathcal{R}(\mathbf{G})$, it follows that $\mathcal{N}(\mathbf{G}^*) \subset \mathcal{R}(\mathbf{T})$. This means that a d-dimensional subspace of $\mathcal{R}(\mathbf{T})$ forms $\mathcal{N}(\mathbf{G}^*)$. Define the $m^2 \times (2md-d^2-d)$ matrix $\bar{\mathbf{T}}$ via

$$\mathbf{G}^*\mathbf{C}\mathbf{G} = \mathbf{G}^*\mathbf{T}\mathbf{T}^*\mathbf{G} = \mathbf{G}^*\bar{\mathbf{T}}\bar{\mathbf{T}}^*\mathbf{G} \ . \tag{A.47}$$

Notice that $\tilde{\mathbf{C}} = \mathbf{C} + \mathbf{E}\mathbf{E}^*$ and, hence,

$$\mathbf{G}^*\tilde{\mathbf{C}}\mathbf{G} = \mathbf{G}^* \begin{bmatrix} \bar{\mathbf{T}} & \mathbf{E} \end{bmatrix} \begin{bmatrix} \bar{\mathbf{T}} & \mathbf{E} \end{bmatrix}^* \mathbf{G} = \mathbf{G}^* \begin{bmatrix} \bar{\mathbf{T}} & \mathbf{E} & \mathbf{B} \end{bmatrix} \begin{bmatrix} \bar{\mathbf{T}} & \mathbf{E} & \mathbf{B} \end{bmatrix}^* \mathbf{G} \ .$$

For simplicity, introduce the notation

$$\mathbf{F} = \begin{bmatrix} \bar{\mathbf{T}} & \mathbf{E} & \mathbf{B} \end{bmatrix} \ .$$

It is important to realize that the blocks in $\mathbf{F}$ are mutually orthogonal and that $\mathcal{R}(\begin{bmatrix} \bar{\mathbf{T}} & \mathbf{E} \end{bmatrix}) = \mathcal{R}(\mathbf{G})$. This implies in particular that

$$\mathbf{F}^{-1} = \begin{bmatrix} \bar{\mathbf{T}}^\dagger \\ \mathbf{E}^\dagger \\ \mathbf{B}^\dagger \end{bmatrix}$$

and

$$\mathbf{\Pi}_{\mathbf{F}^*\mathbf{G}} = \begin{bmatrix} \mathbf{I}_{2md-d^2-d} & \mathbf{0} & \mathbf{0} \\ \mathbf{0} & \mathbf{I}_{(m-d)^2} & \mathbf{0} \\ \mathbf{0} & \mathbf{0} & \mathbf{0}_{d\times d} \end{bmatrix} \ .$$

The fact that $\mathcal{R}(\begin{bmatrix} \bar{\mathbf{T}} & \mathbf{E} \end{bmatrix}) = \mathcal{R}(\mathbf{G})$ also proves that $\mathbf{G}^*\tilde{\mathbf{C}}\mathbf{G}$ is invertible.

Using the observations made above we obtain

$$\begin{aligned}
&\mathbf{D}^*\mathbf{G}(\mathbf{G}^*\tilde{\mathbf{C}}\mathbf{G})^{-1}\mathbf{G}^* \\
&\quad\overset{1}{=}\mathbf{D}^*\mathbf{F}^{-*}\mathbf{F}^*\mathbf{G}(\mathbf{G}^*\mathbf{F}\mathbf{F}^*\mathbf{G})^{-1}\mathbf{G}^*\mathbf{F}\mathbf{F}^{-1}\overset{2}{=}\mathbf{D}^*\mathbf{F}^{-*}\mathbf{\Pi}_{\mathbf{F}^*\mathbf{G}}\mathbf{F}^{-1} \\
&\quad\overset{3}{=}\mathbf{D}^*\begin{bmatrix}\bar{\mathbf{T}}^{\dagger *} & \mathbf{E}^{\dagger *} & \mathbf{B}^{\dagger *}\end{bmatrix}\begin{bmatrix}\mathbf{I}_{2md-d^2-d} & \mathbf{0} & \mathbf{0}\\ \mathbf{0} & \mathbf{I}_{(m-d)^2} & \mathbf{0}\\ \mathbf{0} & \mathbf{0} & \mathbf{0}\end{bmatrix}\begin{bmatrix}\bar{\mathbf{T}}^{\dagger}\\ \mathbf{E}^{\dagger}\\ \mathbf{B}^{\dagger}\end{bmatrix} \qquad \text{(A.48)}\\
&\quad\overset{4}{=}\mathbf{D}^*\begin{bmatrix}\bar{\mathbf{T}}^{\dagger *} & \mathbf{0} & \mathbf{B}^{\dagger *}\end{bmatrix}\begin{bmatrix}\bar{\mathbf{T}}^{\dagger}\\ \mathbf{E}^{\dagger}\\ \mathbf{0}\end{bmatrix}\overset{5}{=}\mathbf{D}^*\bar{\mathbf{T}}^{\dagger *}\bar{\mathbf{T}}^{\dagger}\overset{6}{=}\mathbf{D}^*(\bar{\mathbf{T}}\bar{\mathbf{T}}^*)^{\dagger}\ .
\end{aligned}$$

In the fourth equality, the fact that $\mathbf{D}^*\mathbf{E} = \mathbf{0}$ was used and the sixth equality follows from a property of pseudoinverses for full rank matrices (see Lemma A.1 in Appendix A.11). Now, combining (A.46), (A.47) and (A.48) in the equations (A.43) and (A.44) we get the desired result; that is,

$$\begin{aligned}
\mathbf{H} &= 2\mathbf{P}\mathbf{D}^*\mathbf{\Pi}_{\mathbf{B}}^{\perp}\mathbf{W}_{\text{opt}}\mathbf{\Pi}_{\mathbf{B}}^{\perp}\mathbf{D}\mathbf{P} \\
&= 2\mathbf{P}\mathbf{D}^*\mathbf{G}(\mathbf{G}^*\tilde{\mathbf{C}}\mathbf{G})^{-1}\mathbf{G}^*\mathbf{D}\mathbf{P}\ , \\
\mathbf{Q} &= 4\mathbf{U}^*\mathbf{C}\mathbf{U} = 4\mathbf{P}\mathbf{D}^*\mathbf{\Pi}_{\mathbf{B}}^{\perp}\mathbf{W}_{\text{opt}}\mathbf{\Pi}_{\mathbf{B}}^{\perp}\mathbf{C}\mathbf{\Pi}_{\mathbf{B}}^{\perp}\mathbf{W}_{\text{opt}}\mathbf{\Pi}_{\mathbf{B}}^{\perp}\mathbf{D}\mathbf{P} \\
&= 4\mathbf{P}\mathbf{D}^*\mathbf{G}(\mathbf{G}^*\tilde{\mathbf{C}}\mathbf{G})^{-1}\mathbf{G}^*\mathbf{C}\mathbf{G}(\mathbf{G}^*\tilde{\mathbf{C}}\mathbf{G})^{-1}\mathbf{G}^*\mathbf{D}\mathbf{P} \\
&= 4\mathbf{P}\mathbf{D}^*\mathbf{G}(\mathbf{G}^*\tilde{\mathbf{C}}\mathbf{G})^{-1}\mathbf{G}^*\bar{\mathbf{T}}\bar{\mathbf{T}}^*\mathbf{G}(\mathbf{G}^*\tilde{\mathbf{C}}\mathbf{G})^{-1}\mathbf{G}^*\mathbf{D}\mathbf{P} \\
&= 4\mathbf{P}\mathbf{D}^*(\bar{\mathbf{T}}\bar{\mathbf{T}}^*)^{\dagger}\bar{\mathbf{T}}\bar{\mathbf{T}}^*(\bar{\mathbf{T}}\bar{\mathbf{T}}^*)^{\dagger}\mathbf{D}\mathbf{P} \\
&= 4\mathbf{P}\mathbf{D}^*(\bar{\mathbf{T}}\bar{\mathbf{T}}^*)^{\dagger}\mathbf{D}\mathbf{P} \\
&= 4\mathbf{P}\mathbf{D}^*\mathbf{G}(\mathbf{G}^*\tilde{\mathbf{C}}\mathbf{G})^{-1}\mathbf{G}^*\mathbf{D}\mathbf{P}
\end{aligned}$$

and, hence, $\mathbf{Q} = 2\mathbf{H}$.

We are now ready to prove Theorem 4.3. It follows from the above that

$$\mathbf{\Gamma} = \mathbf{H}^{-1}\mathbf{Q}\mathbf{H}^{-1} = \left[\mathbf{P}\mathbf{D}^*\mathbf{G}(\mathbf{G}^*\tilde{\mathbf{C}}\mathbf{G})^{-1}\mathbf{G}^*\mathbf{D}\mathbf{P}\right]^{-1} \qquad \text{(A.49)}$$

when $\mathbf{W} = \mathbf{W}_{\text{opt}}$ is used. The expression in (A.49) is recognized as the CRB in Theorem 4.1. This concludes the proof that the weighting matrix in (4.30) gives minimum variance performance in large samples.

A.9 Proof of Expression (5.22)

In this appendix it is shown that the solution to (5.21) is given by (5.22). Inserting (5.20) in (5.21) we may equivalently write

$$\max_{\bar{\mathbf{K}}} \operatorname{Tr}\{\mathbf{W}^{1/2}\mathbf{Y}_\alpha\mathbf{\Pi}_\alpha^\perp\mathbf{P}_\beta^T\bar{\mathbf{K}}^T(\bar{\mathbf{K}}\mathbf{P}_\beta\mathbf{\Pi}_\alpha^\perp\mathbf{P}_\beta^T\bar{\mathbf{K}}^T)^{-1}\bar{\mathbf{K}}\mathbf{P}_\beta\mathbf{\Pi}_\alpha^\perp\mathbf{Y}_\alpha^T\mathbf{W}^{1/2}\}\,. \tag{A.50}$$

The trick is now to change variables. Let

$$\bar{\mathbf{K}} = \bar{\mathbf{T}}^T\mathbf{E}^T(\mathbf{P}_\beta\mathbf{\Pi}_\alpha^\perp\mathbf{P}_\beta^T)^{-1/2}, \tag{A.51}$$

where $\bar{\mathbf{T}}$ is an $n \times n$ matrix of full rank and $\mathbf{E}$ is an $(m+l)\beta \times n$ matrix with orthonormal columns. Using the SVD (5.23) and (A.51) in (A.50) we have

$$\max_{\substack{\mathbf{E}\\ \mathbf{E}^T\mathbf{E}=\mathbf{I}}} \operatorname{Tr}\{\hat{\mathbf{Q}}\hat{\mathbf{S}}\hat{\mathbf{V}}^T\mathbf{E}\mathbf{E}^T\hat{\mathbf{V}}\hat{\mathbf{S}}\hat{\mathbf{Q}}^T\} = \max_{\substack{\mathbf{E}\\ \mathbf{E}^T\mathbf{E}=\mathbf{I}}} \operatorname{Tr}\{\mathbf{E}^T\hat{\mathbf{V}}\hat{\mathbf{S}}^2\hat{\mathbf{V}}^T\mathbf{E}\}$$

which clearly is solved by $\mathbf{E} = \hat{\mathbf{V}}_s$. Inserting this solution in (A.51) gives (5.22).

A.10 Proof of Expression (5.27)

In this appendix we show that the solution to (5.25) is given by (5.27). Using (5.20), the minimization problem reads

$$\begin{aligned}
&\min_{\bar{\mathbf{K}}} \det\{\mathbf{\Theta}\} \\
&= \min_{\bar{\mathbf{K}}} \det\{\mathbf{Y}_\alpha\mathbf{\Pi}_\alpha^\perp\mathbf{Y}_\alpha^T - \mathbf{Y}_\alpha\mathbf{\Pi}_\alpha^\perp\mathbf{P}_\beta^T\bar{\mathbf{K}}^T(\bar{\mathbf{K}}\mathbf{P}_\beta\mathbf{\Pi}_\alpha^\perp\mathbf{P}_\beta^T\bar{\mathbf{K}}^T)^{-1}\bar{\mathbf{K}}\mathbf{P}_\beta\mathbf{\Pi}_\alpha^\perp\mathbf{Y}_\alpha^T\} \\
&= \min_{\bar{\mathbf{K}}} \det\{\mathbf{I} - (\mathbf{Y}_\alpha\mathbf{\Pi}_\alpha^\perp\mathbf{Y}_\alpha^T)^{-1/2}\mathbf{Y}_\alpha\mathbf{\Pi}_\alpha^\perp\mathbf{P}_\beta^T\bar{\mathbf{K}}^T(\bar{\mathbf{K}}\mathbf{P}_\beta\mathbf{\Pi}_\alpha^\perp\mathbf{P}_\beta^T\bar{\mathbf{K}}^T)^{-1} \\
&\qquad\qquad \times \bar{\mathbf{K}}\mathbf{P}_\beta\mathbf{\Pi}_\alpha^\perp\mathbf{Y}_\alpha^T(\mathbf{Y}_\alpha\mathbf{\Pi}_\alpha^\perp\mathbf{Y}_\alpha^T)^{-1/2}\} \\
&= \min_{\bar{\mathbf{K}}} \prod_{k=1}^{n}(1-\lambda_k)\,,
\end{aligned} \tag{A.52}$$

where $\{\lambda_k\}_{k=1}^n$ are the nonzero eigenvalues of

$$\begin{aligned}
\mathbf{M} = (\mathbf{Y}_\alpha\mathbf{\Pi}_\alpha^\perp\mathbf{Y}_\alpha^T)^{-1/2}\mathbf{Y}_\alpha\mathbf{\Pi}_\alpha^\perp\mathbf{P}_\beta^T\bar{\mathbf{K}}^T(\bar{\mathbf{K}}\mathbf{P}_\beta\mathbf{\Pi}_\alpha^\perp\mathbf{P}_\beta^T\bar{\mathbf{K}}^T)^{-1} \\
\times \bar{\mathbf{K}}\mathbf{P}_\beta\mathbf{\Pi}_\alpha^\perp\mathbf{Y}_\alpha^T(\mathbf{Y}_\alpha\mathbf{\Pi}_\alpha^\perp\mathbf{Y}_\alpha^T)^{-1/2}\,.
\end{aligned} \tag{A.53}$$

From the following series of implications

$$\boldsymbol{\Theta} \geq \mathbf{0} \Rightarrow \mathbf{I} - \mathbf{M} \geq \mathbf{0} \Rightarrow 1 - \lambda_k \geq 0,\ k = 1,\ \ldots,\ n,$$

it is clear that the minimum of (A.52) is attained if we can find a $\bar{\mathbf{K}}$ which maximizes all n nonzero eigenvalues of $\mathbf{M}$. Next it is shown that there indeed exists such a $\bar{\mathbf{K}}$.

If the variable $\bar{\mathbf{K}}$ is changed according to (A.51) the expression (A.53) reads

$$\begin{aligned}\mathbf{M} = (\mathbf{Y}_\alpha \boldsymbol{\Pi}_\alpha^\perp \mathbf{Y}_\alpha^T)^{-1/2} \mathbf{Y}_\alpha \boldsymbol{\Pi}_\alpha^\perp \mathbf{P}_\beta^T (\mathbf{P}_\beta \boldsymbol{\Pi}_\alpha^\perp \mathbf{P}_\beta^T)^{-1/2} \mathbf{E} \\ \times \mathbf{E}^T (\mathbf{P}_\beta \boldsymbol{\Pi}_\alpha^\perp \mathbf{P}_\beta^T)^{-1/2} \mathbf{P}_\beta \boldsymbol{\Pi}_\alpha^\perp \mathbf{Y}_\alpha^T (\mathbf{Y}_\alpha \boldsymbol{\Pi}_\alpha^\perp \mathbf{Y}_\alpha^T)^{-1/2}\,.\end{aligned}$$

The n nonzero eigenvalues of $\mathbf{M}$ are then equivalently given by the eigenvalues of

$$\begin{aligned}\mathbf{E}^T (\mathbf{P}_\beta \boldsymbol{\Pi}_\alpha^\perp \mathbf{P}_\beta^T)^{-1/2} \mathbf{P}_\beta \boldsymbol{\Pi}_\alpha^\perp \mathbf{Y}_\alpha^T \\ \times (\mathbf{Y}_\alpha \boldsymbol{\Pi}_\alpha^\perp \mathbf{Y}_\alpha^T)^{-1} (\mathbf{Y}_\alpha \boldsymbol{\Pi}_\alpha^\perp \mathbf{P}_\beta^T) (\mathbf{P}_\beta \boldsymbol{\Pi}_\alpha^\perp \mathbf{P}_\beta^T)^{-1/2} \mathbf{E}\,,\end{aligned}$$

which by Poincaré's separation theorem are bounded from above by the n largest eigenvalues of (see, e.g., [Bel70])

$$(\mathbf{P}_\beta \boldsymbol{\Pi}_\alpha^\perp \mathbf{P}_\beta^T)^{-1/2} \mathbf{P}_\beta \boldsymbol{\Pi}_\alpha^\perp \mathbf{Y}_\alpha^T (\mathbf{Y}_\alpha \boldsymbol{\Pi}_\alpha^\perp \mathbf{Y}_\alpha^T)^{-1} (\mathbf{Y}_\alpha \boldsymbol{\Pi}_\alpha^\perp \mathbf{P}_\beta^T) (\mathbf{P}_\beta \boldsymbol{\Pi}_\alpha^\perp \mathbf{P}_\beta^T)^{-1/2}. \tag{A.54}$$

The bound is attained if $\mathbf{E}$ is taken as the eigenvectors corresponding to the n largest eigenvalues of (A.54). Since $\mathbf{M}$ is positive semi definite and symmetric, the eigendecomposition of $\mathbf{M}$ is given by $\hat{\mathbf{V}}\hat{\mathbf{S}}^2\hat{\mathbf{V}}^T$ where $\hat{\mathbf{V}}$ and $\hat{\mathbf{S}}$ are defined through the SVD (5.26). Hence, the upper bound on the eigenvalues of $\mathbf{M}$ is attained if $\mathbf{E} = \hat{\mathbf{V}}_s$. The sought $\bar{\mathbf{K}}$ in (A.52) is thus given by (A.51) with $\mathbf{E} = \hat{\mathbf{V}}_s$, which is (5.27).

A.11 Proof of Theorem 5.1

Let us first introduce the following lemma.

Lemma A.1. *Let* $\mathbf{A}$ *be* $m \times r$ *and* $\mathbf{B}$ $r \times n$*, both of rank* r*, then*

$$(\mathbf{AB})^\dagger = \mathbf{B}^\dagger \mathbf{A}^\dagger\,. \tag{A.55}$$

Proof. It is straightforward to verify that the expression in (A.55) satisfies the Moore-Penrose conditions. For a reference, see [Alb72]. □

Consider the pole estimates from (5.30)-(5.31) where $\hat{\mathbf{\Gamma}}_\alpha$ is given by (5.37). Notice that the analysis below is valid even if the right hand side of (5.37) is multiplied from the right with any full rank matrix since this does not alter the pole estimates. Any such multiplication just corresponds to a similarity transformation and does not affect the eigenvalues of $\hat{\mathbf{A}}$. The error in the estimation of $\mathbf{A}$ may be written

$$\begin{aligned}\tilde{\mathbf{A}} = \hat{\mathbf{A}} - \mathbf{A} &= \left(\mathbf{J}_1\hat{\mathbf{\Gamma}}_\alpha\right)^\dagger \left(\mathbf{J}_2\hat{\mathbf{\Gamma}}_\alpha - \mathbf{J}_1\hat{\mathbf{\Gamma}}_\alpha\mathbf{A}\right) \\ &\simeq \left(\mathbf{J}_1\mathbf{\Gamma}_\alpha\right)^\dagger \left(\mathbf{J}_2\hat{\mathbf{\Gamma}}_\alpha - \mathbf{J}_1\hat{\mathbf{\Gamma}}_\alpha\mathbf{A}\right) ,\end{aligned} \tag{A.56}$$

where $\simeq$ denotes first order approximation. Assume that $\mathbf{A}$ has distinct eigenvalues and thus can be diagonalized as

$$\mathbf{A} = \mathbf{T}^{-1}\mathbf{A}_d\mathbf{T},$$

where $\mathbf{A}_d$ is a diagonal matrix with the poles, $\{\mu_k\}_{k=1}^n$, on the diagonal and $\mathbf{T}^{-1}$ contains the corresponding right eigenvectors of $\mathbf{A}$. It can be shown that errors in the system matrix transforms to first order perturbations of the eigenvalues as

$$\tilde{\mu}_k \simeq \mathbf{T}_{k\bullet}\tilde{\mathbf{A}}\mathbf{T}_{\bullet k}^{-1} ; \tag{A.57}$$

see, e.g., [Bel70]. Inserting (A.56) in (A.57) yields

$$\begin{aligned}\tilde{\mu}_k &\simeq \mathbf{T}_{k\bullet}\left(\mathbf{J}_1\mathbf{\Gamma}_\alpha\right)^\dagger \left(\mathbf{J}_2\hat{\mathbf{\Gamma}}_\alpha - \mathbf{J}_1\hat{\mathbf{\Gamma}}_\alpha\mathbf{A}\right)\mathbf{T}_{\bullet k}^{-1} \\ &= \mathbf{T}_{k\bullet}\left(\mathbf{J}_1\mathbf{\Gamma}_\alpha\right)^\dagger \left(\mathbf{J}_2 - \mathbf{J}_1\mu_k\right)\hat{\mathbf{\Gamma}}_\alpha\mathbf{T}_{\bullet k}^{-1} .\end{aligned} \tag{A.58}$$

Note that $\mathbf{\Gamma}_\alpha\mathbf{T}^{-1} = \mathbf{\Gamma}_\alpha^d$ is the extended observability matrix of the diagonal realization. Hence,

$$\mathbf{T}\left(\mathbf{J}_1\mathbf{\Gamma}_\alpha\right)^\dagger = \left(\mathbf{J}_1\mathbf{\Gamma}_\alpha\mathbf{T}^{-1}\right)^\dagger = \left(\mathbf{J}_1\mathbf{\Gamma}_\alpha^d\right)^\dagger , \tag{A.59}$$

where Lemma A.1 has been used in the first equality. Since $\mathbf{\Gamma}_\alpha = \mathbf{W}^{-1/2}\mathbf{Q}_s$, we have

$$\mathbf{W}^{-1/2}\mathbf{Q}_s\mathbf{T}^{-1} = \mathbf{\Gamma}_\alpha^d$$

which gives an expression for $\mathbf{T}^{-1}$

$$\mathbf{T}^{-1} = \mathbf{Q}_s^T \mathbf{W}^{1/2} \mathbf{\Gamma}_\alpha^d \,. \tag{A.60}$$

Using (A.59) and (A.60) in (A.58) leads to

$$\begin{aligned} \tilde{\mu}_k &\simeq \left(\mathbf{J}_1 \mathbf{\Gamma}_\alpha^d\right)_{k\bullet}^{\dagger} (\mathbf{J}_2 - \mathbf{J}_1 \mu_k)\, \hat{\mathbf{\Gamma}}_\alpha \mathbf{Q}_s^T \mathbf{W}^{1/2} (\mathbf{\Gamma}_\alpha^d)_{\bullet k} \\ &= \mathbf{f}_k^* \mathbf{W}^{-1/2} \hat{\mathbf{Q}}_s \mathbf{Q}_s^T \mathbf{W}^{1/2} (\mathbf{\Gamma}_\alpha^d)_{\bullet k}, \end{aligned} \tag{A.61}$$

where $\mathbf{f}_k^*$ is defined in (5.44). Observe that

$$\begin{aligned} \mathbf{f}_k^* \mathbf{\Gamma}_\alpha^d &= \left(\mathbf{J}_1 \mathbf{\Gamma}_\alpha^d\right)_{k\bullet}^{\dagger} \left(\mathbf{J}_2 \mathbf{\Gamma}_\alpha^d - \mathbf{J}_1 \mathbf{\Gamma}_\alpha^d \mu_k\right) \\ &= \left(\mathbf{J}_1 \mathbf{\Gamma}_\alpha^d\right)_{k\bullet}^{\dagger} \left(\mathbf{J}_1 \mathbf{\Gamma}_\alpha^d \mathbf{A}_d - \mathbf{J}_1 \mathbf{\Gamma}_\alpha^d \mu_k\right) = \mathbf{0} \,. \end{aligned}$$

Thus, $\mathbf{f}_k^*$ is orthogonal to $\mathbf{\Gamma}_\alpha^d$, $\mathbf{\Gamma}_\alpha$ and $\mathbf{W}^{-1/2}\mathbf{Q}_s$. Viberg, Ottersten, Wahlberg and Ljung (see [VWO97] and also [VOWL91, VOWL93]) have shown that $\sqrt{N}\mathbf{f}_k^* \mathbf{W}^{-1/2} \hat{\mathbf{Q}}_s$ has a limiting zero-mean Gaussian distribution with covariances[1]

$$\begin{aligned} \lim_{N\to\infty} N\, \mathrm{E}\big\{ (\mathbf{f}_k^* \mathbf{W}^{-1/2} \hat{\mathbf{Q}}_s)^T (\mathbf{f}_l^* \mathbf{W}^{-1/2} \hat{\mathbf{Q}}_s) \big\} \\ = \sum_{|\tau|<\alpha} \mathbf{H}^T \mathbf{R}_{\boldsymbol{\zeta}}(\tau) \mathbf{H} \mathbf{f}_k^* \mathbf{R}_{\mathbf{n}_\alpha}(\tau) \mathbf{f}_l^c \,, \end{aligned} \tag{A.62a}$$

$$\begin{aligned} \lim_{N\to\infty} N\, \mathrm{E}\big\{ (\mathbf{f}_k^* \mathbf{W}^{-1/2} \hat{\mathbf{Q}}_s)^T (\mathbf{f}_l^* \mathbf{W}^{-1/2} \hat{\mathbf{Q}}_s)^c \big\} \\ = \sum_{|\tau|<\alpha} \mathbf{H}^T \mathbf{R}_{\boldsymbol{\zeta}}(\tau) \mathbf{H} \mathbf{f}_k^* \mathbf{R}_{\mathbf{n}_\alpha}(\tau) \mathbf{f}_l \,, \end{aligned} \tag{A.62b}$$

where $\mathbf{H}$ is defined as (cf. (5.50))

$$\mathbf{H} = \mathbf{R}_H \mathbf{V}_s \mathbf{S}_s^{-1} \,. \tag{A.63}$$

The asymptotic normality of $\mathbf{f}_k^* \mathbf{W}^{-1/2} \hat{\mathbf{Q}}_s$ implies that of $\tilde{\mu}_k$ (by the relation (A.61)). From (A.62) and (A.61) we readily obtain

$$\begin{aligned} \lim_{N\to\infty} N\, \mathrm{E}\{\tilde{\mu}_k \tilde{\mu}_l^c\} &= \sum_{|\tau|<\alpha} \mathbf{b}_k^T \mathbf{R}_{\boldsymbol{\zeta}}(\tau) \mathbf{b}_l^c \mathbf{f}_k^* \mathbf{R}_{\mathbf{n}_\alpha}(\tau) \mathbf{f}_l \,, \\ \lim_{N\to\infty} N\, \mathrm{E}\{\tilde{\mu}_k \tilde{\mu}_l\} &= \sum_{|\tau|<\alpha} \mathbf{b}_k^T \mathbf{R}_{\boldsymbol{\zeta}}(\tau) \mathbf{b}_l \mathbf{f}_k^* \mathbf{R}_{\mathbf{n}_\alpha}(\tau) \mathbf{f}_l^c \,, \end{aligned}$$

[1] Modified to the situation considered here.

where

$$\mathbf{b}_k = \mathbf{H}\mathbf{Q}_s^T\mathbf{W}^{1/2}(\mathbf{\Gamma}_\alpha^d)_{\bullet k}\,. \tag{A.64}$$

Inserting the definition of $\mathbf{H}$ (A.63) in (A.64) gives

$$\mathbf{b}_k = \mathbf{R}_H\mathbf{V}_s\mathbf{S}_s^{-1}\mathbf{Q}_s^T\mathbf{W}^{1/2}(\mathbf{\Gamma}_\alpha^d)_{\bullet k}\,. \tag{A.65}$$

Next, recall that $\mathbf{Q}_s\mathbf{S}_s\mathbf{V}_s^T = \lim_{N\to\infty}\hat{\mathbf{Q}}\hat{\mathbf{S}}\hat{\mathbf{V}}^T$ is given by the limit in (5.42). This implies that

$$\mathbf{V}_s\mathbf{S}_s^{-1}\mathbf{Q}_s^T = \left(\mathbf{W}^{1/2}\mathbf{\Gamma}_\alpha^d\mathbf{R}^d\right)^\dagger = \mathbf{R}^{d\dagger}\left(\mathbf{W}^{1/2}\mathbf{\Gamma}_\alpha^d\right)^\dagger\,, \tag{A.66}$$

where Lemma A.1 has been used in the last equality. Inserting (A.66) in (A.65) gives

$$\mathbf{b}_k = \mathbf{R}_H\mathbf{R}^{d\dagger}\left(\mathbf{W}^{1/2}\mathbf{\Gamma}_\alpha^d\right)^\dagger\mathbf{W}^{1/2}(\mathbf{\Gamma}_\alpha^d)_{\bullet k} = \mathbf{R}_H\mathbf{R}^{d\dagger}_{\bullet k} \tag{A.67}$$

which is exactly equal to $(\mathbf{\Omega}_d)_{\bullet k}$ as defined in (5.45). We have thus proven Theorem 5.1.

A.12 Proof of Theorem 5.3

The proof of Theorem 5.3 is divided into three parts. In part one we prove (5.51). In part two we show that (5.52) is the optimal choice of the weighting $\mathbf{\Lambda}$. Finally, in part three the calculations leading to (5.53) are given.

Part 1: For convenience, introduce the notation

$$\mathbf{F} = \mathbf{F}(\boldsymbol{\theta}) = \mathbf{W}^{1/2}\mathbf{\Gamma}_\alpha(\boldsymbol{\theta})\,, \tag{A.68}$$

$$\mathbf{\Pi}^\perp = \mathbf{\Pi}^\perp_{\mathbf{W}^{1/2}\mathbf{\Gamma}_\alpha}(\boldsymbol{\theta}) = \mathbf{\Pi}^\perp_{\mathbf{F}} = \mathbf{I} - \mathbf{F}\left(\mathbf{F}^*\mathbf{F}\right)^{-1}\mathbf{F}^*\,. \tag{A.69}$$

The cost-function considered, (5.35), now reads

$$V(\boldsymbol{\theta}) = \mathrm{vec}^T(\mathbf{\Pi}^\perp\hat{\mathbf{Q}}_s)\mathbf{\Lambda}\,\mathrm{vec}(\mathbf{\Pi}^\perp\hat{\mathbf{Q}}_s)\,. \tag{A.70}$$

Since $\hat{\boldsymbol{\theta}}$ minimizes $V(\boldsymbol{\theta})$ a first order Taylor expansion of the gradient, $V'(\boldsymbol{\theta})$, around the true value, $\boldsymbol{\theta}_0$, leads to

$$(\hat{\boldsymbol{\theta}} - \boldsymbol{\theta}_0) = -[\bar{V}'']^{-1}V'(\boldsymbol{\theta}_0) + \mathrm{o}(V'(\boldsymbol{\theta}_0)) \tag{A.71}$$

where the limiting Hessian

$$\bar{V}'' = \lim_{N\to\infty} V''(\boldsymbol{\theta}_0) \tag{A.72}$$

is assumed to be invertible[2]. As shown below, $\sqrt{N}V'(\boldsymbol{\theta})$ is asymptotically Gaussian. Thus, the normalized parameter estimation error is also asymptotically Gaussian distributed,

$$\sqrt{N}(\hat{\boldsymbol{\theta}} - \boldsymbol{\theta}_0) \in \mathrm{AsN}(\mathbf{0}, \boldsymbol{\Xi}),$$

where

$$\boldsymbol{\Xi} = [\bar{V}'']^{-1}\boldsymbol{\Upsilon}[\bar{V}'']^{-1},$$

and where $\boldsymbol{\Upsilon}$ is

$$\boldsymbol{\Upsilon} = \lim_{N\to\infty} N\,\mathrm{E}\left\{[V'(\boldsymbol{\theta}_0)]\,[V'(\boldsymbol{\theta}_0)]^T\right\}\,. \tag{A.73}$$

Next we derive expressions for the matrices $\bar{V}''$ and $\boldsymbol{\Upsilon}$. In the following let a subscript i denote partial derivative with respect to $\boldsymbol{\theta}_i$. The partial derivative of (A.69) is given by

$$\boldsymbol{\Pi}_i^{\perp} = -\boldsymbol{\Pi}^{\perp}\mathbf{F}_i\mathbf{F}^{\dagger} - \mathbf{F}^{*^{\dagger}}\mathbf{F}_i^{*}\boldsymbol{\Pi}^{\perp}. \tag{A.74}$$

This gives for (A.70)

$$\begin{aligned} V_i &= -2\,\mathrm{vec}^T(\boldsymbol{\Pi}^{\perp}\mathbf{F}_i\mathbf{F}^{\dagger}\hat{\mathbf{Q}}_s + \mathbf{F}^{\dagger^*}\mathbf{F}_i^{*}\boldsymbol{\Pi}^{\perp}\hat{\mathbf{Q}}_s)\boldsymbol{\Lambda}\,\mathrm{vec}(\boldsymbol{\Pi}^{\perp}\hat{\mathbf{Q}}_s) \\ &\simeq -2\,\mathrm{vec}^T(\boldsymbol{\Pi}^{\perp}\mathbf{F}_i\mathbf{F}^{\dagger}\mathbf{Q}_s)\boldsymbol{\Lambda}\,\mathrm{vec}(\boldsymbol{\Pi}^{\perp}\hat{\mathbf{Q}}_s), \end{aligned}$$

where $\simeq$ denotes first order approximation (around $\boldsymbol{\theta}_0$). Next, a result from [OV94] will be used, modified to the situation in this chapter. The elements of $\sqrt{N}\,\mathrm{vec}(\boldsymbol{\Pi}^{\perp}\hat{\mathbf{Q}}_s)$ have a limiting zero-mean Gaussian distribution with asymptotic covariance

$$\begin{aligned} \boldsymbol{\Sigma} &= \lim_{N\to\infty} N\,\mathrm{E}\left\{\mathrm{vec}(\boldsymbol{\Pi}^{\perp}\hat{\mathbf{Q}}_s)\,\mathrm{vec}^T(\boldsymbol{\Pi}^{\perp}\hat{\mathbf{Q}}_s)\right\} \\ &= \sum_{|\tau|<\alpha} \left(\mathbf{H}^T\mathbf{R}_{\zeta}(\tau)\mathbf{H}\right) \otimes \left(\boldsymbol{\Pi}^{\perp}\mathbf{W}^{1/2}\mathbf{R}_{n_\alpha}(\tau)\mathbf{W}^{1/2}\boldsymbol{\Pi}^{\perp}\right), \end{aligned} \tag{A.75}$$

where the various expressions have been defined previously and should be evaluated in $\boldsymbol{\theta}_0$ (cf. (5.48)). Since (A.75) involves projected errors, $\boldsymbol{\Sigma}$

[2] A property that in general is valid if the parameters are identifiable.

is singular with a null space of dimension n^2 (the null space of $\mathbf{I}_n \otimes \mathbf{\Pi}^\perp$) and it has a rank equal to $n(\alpha l - n)$ (the dimension of the space onto which $\mathbf{I}_n \otimes \mathbf{\Pi}^\perp$ projects)[3]. Inserting this in (A.73), the (i,j)th element of $\mathbf{\Upsilon}$ is given by

$$\begin{aligned}\mathbf{\Upsilon}_{(ij)} &= \lim_{N\to\infty} N \, \mathrm{E}\{V_i V_j\} \\ &= 4\,\mathrm{vec}^T(\mathbf{\Pi}^\perp \mathbf{F}_i \mathbf{F}^\dagger \mathbf{Q}_s)\mathbf{\Lambda}\mathbf{\Sigma}\mathbf{\Lambda}\,\mathrm{vec}(\mathbf{\Pi}^\perp \mathbf{F}_j \mathbf{F}^\dagger \mathbf{Q}_s)\,.\end{aligned}$$

Since the second partial derivative of (A.70) reads

$$V_{ij} = 2\,\mathrm{vec}^T(\mathbf{\Pi}_{ij}^\perp \hat{\mathbf{Q}}_s)\mathbf{\Lambda}\,\mathrm{vec}(\mathbf{\Pi}^\perp \hat{\mathbf{Q}}_s) + 2\,\mathrm{vec}^T(\mathbf{\Pi}_i^\perp \hat{\mathbf{Q}}_s)\mathbf{\Lambda}\,\mathrm{vec}(\mathbf{\Pi}_j^\perp \hat{\mathbf{Q}}_s)$$

and that $\hat{\mathbf{Q}}_s \to \mathbf{Q}_s$ w.p.1 [4], the (i,j)th element of the limiting Hessian (A.72) is given by

$$\begin{aligned}\bar{V}''_{(ij)} &= \lim_{N\to\infty} V_{ij} = 2\,\mathrm{vec}^T(\mathbf{\Pi}_i^\perp \mathbf{Q}_s)\mathbf{\Lambda}\,\mathrm{vec}(\mathbf{\Pi}_j^\perp \mathbf{Q}_s) = \\ &= 2\,\mathrm{vec}^T(\mathbf{\Pi}^\perp \mathbf{F}_i \mathbf{F}^\dagger \mathbf{Q}_s)\mathbf{\Lambda}\,\mathrm{vec}(\mathbf{\Pi}^\perp \mathbf{F}_j \mathbf{F}^\dagger \mathbf{Q}_s)\,.\end{aligned}$$

Introduce a matrix $\mathbf{G}$ whose ith column is given by

$$\mathbf{G}_{\bullet i} = \mathrm{vec}(\mathbf{\Pi}^\perp \mathbf{F}_i \mathbf{F}^\dagger \mathbf{Q}_s) = \mathrm{vec}\big(\mathbf{\Pi}^\perp_{\mathbf{W}^{1/2}\mathbf{\Gamma}_\alpha} \mathbf{W}^{1/2} \mathbf{\Gamma}_{\alpha_i} (\mathbf{W}^{1/2}\mathbf{\Gamma}_\alpha)^\dagger \mathbf{Q}_s\big),$$

where all expressions should be evaluated in $\boldsymbol{\theta}_0$. Using the identity

$$\mathrm{vec}(\mathbf{ABC}) = (\mathbf{C}^T \otimes \mathbf{A})\,\mathrm{vec}(\mathbf{B}) \tag{A.76}$$

for matrices with compatible dimensions, $\mathbf{G}$ can be written

$$\begin{aligned}\mathbf{G} = \Big\{\Big[(\mathbf{W}^{1/2}\mathbf{\Gamma}_\alpha)^\dagger \mathbf{Q}_s\Big]^T \otimes \mathbf{\Pi}^\perp_{\mathbf{W}^{1/2}\mathbf{\Gamma}_\alpha} \mathbf{W}^{1/2}\Big\} \\ \times \big[\mathrm{vec}(\mathbf{\Gamma}_{\alpha_1})\ \mathrm{vec}(\mathbf{\Gamma}_{\alpha_2})\ \ldots\ \mathrm{vec}(\mathbf{\Gamma}_{\alpha_d})\big],\end{aligned} \tag{A.77}$$

[3] We have no proof of the exact rank of $\mathbf{\Sigma}$. In other words, we do know that the rank is no more than $n(\alpha l - n)$ but we can not state (useful) conditions on the data and on the system for the rank to be equal to $n(\alpha l - n)$. However in all numerical examples we have performed, the rank was $n(\alpha l - n)$.

[4] It should be noted that possible non-uniqueness of the SVD components may affect "local" results in this chapter, however, in all final results only unique parts appear. $\mathbf{Q}_s$ is for example not unique if several singular values in $\mathbf{S}_s$ are equal.

which is (5.47). Remember that d is the number of parameters in $\boldsymbol{\theta}$. If $\boldsymbol{\Gamma}_\alpha(\boldsymbol{\theta})$ is properly parameterized the matrix $\mathbf{G}$ will have full rank. With this notation, the matrices $\boldsymbol{\Upsilon}$ and $\bar{V}''$ may be written in the following compact form

$$\begin{aligned}\boldsymbol{\Upsilon} &= 4\mathbf{G}^T\boldsymbol{\Lambda}\boldsymbol{\Sigma}\boldsymbol{\Lambda}\mathbf{G} \\ \bar{V}'' &= 2\mathbf{G}^T\boldsymbol{\Lambda}\mathbf{G}\,.\end{aligned}$$

The asymptotic covariance matrix is thus given by

$$\boldsymbol{\Xi} = [\bar{V}'']^{-1}\boldsymbol{\Upsilon}[\bar{V}'']^{-1} = (\mathbf{G}^T\boldsymbol{\Lambda}\mathbf{G})^{-1}(\mathbf{G}^T\boldsymbol{\Lambda}\boldsymbol{\Sigma}\boldsymbol{\Lambda}\mathbf{G})(\mathbf{G}^T\boldsymbol{\Lambda}\mathbf{G})^{-1}$$

which is (5.51).

Part 2: In this part we show that the covariance matrix (5.51) as a function of the weighting matrix $\boldsymbol{\Lambda}$ has a lower bound, and that this bound is attained for the choice made in (5.52). The rank of $\boldsymbol{\Sigma}$ is $n(\alpha l - n)$ which is equal to the rank of $\mathbf{I} \otimes \boldsymbol{\Pi}^{\perp}_{\mathbf{W}^{1/2}\boldsymbol{\Gamma}_\alpha}$. Studying the expression for $\boldsymbol{\Sigma}$ in (A.75), it is seen that the range space of $\boldsymbol{\Sigma}$ is given by the range space of $\mathbf{I} \otimes \boldsymbol{\Pi}^{\perp}_{\mathbf{W}^{1/2}\boldsymbol{\Gamma}_\alpha}$. Similarly, it can be seen from (A.77) that the range space of $\mathbf{G}$ lies in the range space of $\mathbf{I} \otimes \boldsymbol{\Pi}^{\perp}_{\mathbf{W}^{1/2}\boldsymbol{\Gamma}_\alpha}$, i.e., in the range space of $\boldsymbol{\Sigma}$. Hence, the projector on the range space of $\boldsymbol{\Sigma}$ has no effect when operating on $\mathbf{G}$, i.e., $\boldsymbol{\Sigma}\boldsymbol{\Sigma}^\dagger\mathbf{G} = \mathbf{G}$.

Next we show that $\mathbf{G}^T\boldsymbol{\Sigma}^\dagger\mathbf{G}$ is positive definite. This can be proven by using the orthogonal decomposition of the Euclidean space

$$\mathbb{R}^{n\alpha l} = \mathcal{R}(\boldsymbol{\Sigma}) \oplus \mathcal{N}(\boldsymbol{\Sigma}^T)\,,$$

where $\mathcal{N}(\cdot)$ denotes the null space of $(\cdot)$ and $\oplus$ denotes direct sum; see e.g. [SS89]. Since, for any $\mathbf{x}$, $\mathbf{G}\mathbf{x}$ is in $\mathcal{R}(\boldsymbol{\Sigma})$ it can not be in $\mathcal{N}(\boldsymbol{\Sigma}^T) = \mathcal{N}(\boldsymbol{\Sigma}) = \mathcal{N}(\boldsymbol{\Sigma}^\dagger)$ and thus $\mathbf{G}^T\boldsymbol{\Sigma}^\dagger\mathbf{G} > \mathbf{0}$.

Study the following matrix

$$\begin{aligned}\begin{bmatrix}\mathbf{G}^T\boldsymbol{\Lambda}\boldsymbol{\Sigma}\boldsymbol{\Lambda}\mathbf{G} & \mathbf{G}^T\boldsymbol{\Lambda}\mathbf{G} \\ \mathbf{G}^T\boldsymbol{\Lambda}\mathbf{G} & \mathbf{G}^T\boldsymbol{\Sigma}^\dagger\mathbf{G}\end{bmatrix} &= \begin{bmatrix}\mathbf{G}^T\boldsymbol{\Lambda}\boldsymbol{\Sigma}\boldsymbol{\Lambda}\mathbf{G} & \mathbf{G}^T\boldsymbol{\Lambda}\boldsymbol{\Sigma}\boldsymbol{\Sigma}^\dagger\mathbf{G} \\ \mathbf{G}^T\boldsymbol{\Sigma}^\dagger\boldsymbol{\Sigma}\boldsymbol{\Lambda}\mathbf{G} & \mathbf{G}^T\boldsymbol{\Sigma}^\dagger\boldsymbol{\Sigma}\boldsymbol{\Sigma}^\dagger\mathbf{G}\end{bmatrix} \\ &= \begin{bmatrix}\mathbf{G}^T\boldsymbol{\Lambda} \\ \mathbf{G}^T\boldsymbol{\Sigma}^\dagger\end{bmatrix}\boldsymbol{\Sigma}\begin{bmatrix}\boldsymbol{\Lambda}\mathbf{G} & \boldsymbol{\Sigma}^\dagger\mathbf{G}\end{bmatrix} \geq \mathbf{0}\end{aligned} \tag{A.78}$$

where the last inequality follows since $\boldsymbol{\Sigma} \geq \mathbf{0}$. The matrix inequality should be interpreted as that the matrix is positive semi-definite. Since

the matrix (A.78) is positive semi-definite, the same holds for the Schur complement to $\mathbf{G}^T\boldsymbol{\Sigma}^\dagger\mathbf{G}$ [SS89], i.e.,

$$\mathbf{G}^T\boldsymbol{\Lambda}\boldsymbol{\Sigma}\boldsymbol{\Lambda}\mathbf{G} - \mathbf{G}^T\boldsymbol{\Lambda}\mathbf{G}(\mathbf{G}^T\boldsymbol{\Sigma}^\dagger\mathbf{G})^{-1}\mathbf{G}^T\boldsymbol{\Lambda}\mathbf{G} \geq \mathbf{0}\,. \tag{A.79}$$

The matrix $\mathbf{G}^T\boldsymbol{\Lambda}\mathbf{G}$ was in part one of this appendix shown to be the limiting Hessian of the cost-function (5.34). We have previously assumed it to be invertible for the analysis to hold. This sets some constraint on the choice of the weighting $\boldsymbol{\Lambda}$ but is needed for parameter identifiability. Multiplying (A.79) from left and right with $(\mathbf{G}^T\boldsymbol{\Lambda}\mathbf{G})^{-1}$ gives the desired result

$$(\mathbf{G}^T\boldsymbol{\Sigma}^\dagger\mathbf{G})^{-1} \leq (\mathbf{G}^T\boldsymbol{\Lambda}\mathbf{G})^{-1}(\mathbf{G}^T\boldsymbol{\Lambda}\boldsymbol{\Sigma}\boldsymbol{\Lambda}\mathbf{G})(\mathbf{G}^T\boldsymbol{\Lambda}\mathbf{G})^{-1}\,.$$

Thus, the weighting matrix in (5.52) gives a lower bound on the asymptotic covariance matrix.

Part 3: In this part the expression (5.53) is derived. The first equality in (5.53) follows trivially from (5.51) and (5.52) since $\boldsymbol{\Sigma}^\dagger\boldsymbol{\Sigma}\boldsymbol{\Sigma}^\dagger = \boldsymbol{\Sigma}^\dagger$. The remainder of this appendix proves the second equality in (5.53) (and thus Corollary 5.4).

First, note that

$$(\mathbf{W}^{1/2}\boldsymbol{\Gamma}_\alpha)^\dagger\mathbf{Q}_s = (\mathbf{Q}_s\mathbf{T}^{-1})^\dagger\mathbf{Q}_s = \mathbf{T}\mathbf{Q}_s^T\mathbf{Q}_s = \mathbf{T}\,, \tag{A.80}$$

where $\mathbf{T}$ is the similarity transformation matrix describing the fact that the limiting estimate of the observability matrix may correspond to a different realization than the one corresponding to $\boldsymbol{\Gamma}_\alpha$. Remember that $\boldsymbol{\Gamma}_\alpha$ is the parameterized extended observability matrix of some realization. Here, $\hat{\mathbf{Q}}_s \to \mathbf{Q}_s = \mathbf{W}^{1/2}\boldsymbol{\Gamma}_\alpha\mathbf{T}$ as N tends to infinity. The matrix $\mathbf{T}$ depends on $\mathbf{W}$. Let

$$\boldsymbol{\Pi}^\perp_{\mathbf{W}^{1/2}\boldsymbol{\Gamma}_\alpha} = \mathbf{E}\mathbf{E}^T \tag{A.81}$$

be an orthonormal factorization, i.e., $\mathbf{E}$ is $\alpha l \times (\alpha l - n)$ and $\mathbf{E}^T\mathbf{E} = \mathbf{I}$. Such a factorization is possible since a projection matrix is symmetric and has eigenvalues equal to one or zero. Observe that this implies that $\mathbf{E}^\dagger = \mathbf{E}^T$. In the following we make extensive use of the following rules for Kronecker products

$$\begin{aligned}(\mathbf{A}\otimes\mathbf{B})(\mathbf{C}\otimes\mathbf{D}) &= \mathbf{A}\mathbf{C}\otimes\mathbf{B}\mathbf{D}\,,\\ (\mathbf{A}\otimes\mathbf{B})^T &= \mathbf{A}^T\otimes\mathbf{B}^T\,,\\ (\mathbf{A}\otimes\mathbf{B})^\dagger &= \mathbf{A}^\dagger\otimes\mathbf{B}^\dagger\,.\end{aligned}$$

Rewrite (5.48) as

$$\boldsymbol{\Sigma} = (\mathbf{I}_n \otimes \mathbf{E}) \times \left(\sum_{|\tau|<\alpha} (\mathbf{H}^T \mathbf{R}_{\boldsymbol{\zeta}}(\tau)\mathbf{H}) \otimes \mathbf{E}^T \mathbf{W}^{1/2} \mathbf{R}_{\mathbf{n}_\alpha}(\tau) \mathbf{W}^{1/2} \mathbf{E} \right) \times \left(\mathbf{I}_n \otimes \mathbf{E}^T\right) .$$

The pseudo-inverse of $\boldsymbol{\Sigma}$ now takes the form

$$\boldsymbol{\Sigma}^\dagger = (\mathbf{I}_n \otimes \mathbf{E}) \times \left(\sum_{|\tau|<\alpha} (\mathbf{H}^T \mathbf{R}_{\boldsymbol{\zeta}}(\tau)\mathbf{H}) \otimes \mathbf{E}^T \mathbf{W}^{1/2} \mathbf{R}_{\mathbf{n}_\alpha}(\tau) \mathbf{W}^{1/2} \mathbf{E} \right)^{-1} \times \left(\mathbf{I}_n \otimes \mathbf{E}^T\right), \quad \text{(A.82)}$$

where Lemma A.1 has been used. Combining (5.47) and (A.82), with (A.81), the following is obtained:

$$\begin{aligned} \mathbf{G}^T \boldsymbol{\Sigma}^\dagger \mathbf{G} = {} & [\mathrm{vec}(\boldsymbol{\Gamma}_{\alpha_1}) \ \mathrm{vec}(\boldsymbol{\Gamma}_{\alpha_2}) \ \cdots \ \mathrm{vec}(\boldsymbol{\Gamma}_{\alpha_d})]^T \left(\mathbf{T} \otimes \mathbf{W}^{1/2}\mathbf{E}\right) \\ & \times \left(\sum_{|\tau|<\alpha} (\mathbf{H}^T \mathbf{R}_{\boldsymbol{\zeta}}(\tau)\mathbf{H}) \otimes \mathbf{E}^T \mathbf{W}^{1/2} \mathbf{R}_{\mathbf{n}_\alpha}(\tau) \mathbf{W}^{1/2} \mathbf{E} \right)^{-1} \\ & \times \left(\mathbf{T}^T \otimes \mathbf{E}^T\mathbf{W}^{1/2}\right) [\mathrm{vec}(\boldsymbol{\Gamma}_{\alpha_1}) \ \mathrm{vec}(\boldsymbol{\Gamma}_{\alpha_2}) \ \cdots \ \mathrm{vec}(\boldsymbol{\Gamma}_{\alpha_d})] . \end{aligned} \quad \text{(A.83)}$$

Proceeding with the interesting part in the middle gives

$$\left(\sum_{|\tau|<\alpha} (\mathbf{T}^{-T} \mathbf{H}^T \mathbf{R}_{\boldsymbol{\zeta}}(\tau) \mathbf{H} \mathbf{T}^{-1}) \otimes (\mathbf{E}^T\mathbf{W}^{1/2})^\dagger \mathbf{E}^T \mathbf{W}^{1/2} \mathbf{R}_{\mathbf{n}_\alpha}(\tau) \mathbf{W}^{1/2} \mathbf{E} (\mathbf{W}^{1/2}\mathbf{E})^\dagger \right)^\dagger \quad \text{(A.84)}$$

where, again, Lemma A.1 has been used. Consider $\mathbf{H}$, given in (5.50),

$$\begin{aligned} \mathbf{H} = \mathbf{R}_H \mathbf{V}_s \mathbf{S}_s^{-1} &= \mathbf{R}_H \mathbf{V}_s \mathbf{S}_s^{-1} \mathbf{Q}_s^T \mathbf{Q}_s = \mathbf{R}_H \left(\mathbf{W}^{1/2} \boldsymbol{\Gamma}_\alpha \mathbf{R}^{\boldsymbol{\theta}_0}\right)^\dagger \mathbf{Q}_s \\ &= \mathbf{R}_H \mathbf{R}^{\boldsymbol{\theta}_0 \dagger} \left(\mathbf{W}^{1/2} \boldsymbol{\Gamma}_\alpha\right)^\dagger \mathbf{Q}_s = \mathbf{R}_H \mathbf{R}^{\boldsymbol{\theta}_0 \dagger} \mathbf{T} , \end{aligned}$$

where (A.80), (A.66) and Lemma A.1 have been used. Hence, $\mathbf{H}\mathbf{T}^{-1}$ is equal to $\mathbf{\Omega}_{\boldsymbol{\theta}_0}$ defined in (5.49). Finally, the factor $\mathbf{W}^{1/2}\mathbf{E}(\mathbf{W}^{1/2}\mathbf{E})^\dagger$ in (A.84) is a projection matrix on $\mathcal{R}[\mathbf{W}^{1/2}\mathbf{E}]$. Now, the columns in $\mathbf{E}$ form a basis for the null-space of $\mathbf{\Gamma}_\alpha^*\mathbf{W}^{1/2}$, denoted as $\mathcal{N}[\mathbf{\Gamma}_\alpha^*\mathbf{W}^{1/2}]$. This implies that the columns in $\mathbf{W}^{1/2}\mathbf{E}$ form a basis for $\mathcal{N}[\mathbf{\Gamma}_\alpha^*]$. Thus, a projector projecting on $\mathcal{R}[\mathbf{W}^{1/2}\mathbf{E}]$, in fact projects on $\mathcal{N}[\mathbf{\Gamma}_\alpha^*]$. To conclude, the projector $\mathbf{W}^{1/2}\mathbf{E}(\mathbf{W}^{1/2}\mathbf{E})^\dagger$ can be written as

$$\mathbf{\Pi}_{\mathbf{\Gamma}_\alpha}^\perp = \mathbf{I} - \mathbf{\Gamma}_\alpha \left(\mathbf{\Gamma}_\alpha^*\mathbf{\Gamma}_\alpha\right)^{-1}\mathbf{\Gamma}_\alpha^*$$

and the expression (A.83) simplifies to (5.53) which was set to prove.

A.13 Proof of Theorem 5.5

In this appendix it is shown that (5.55) and (5.56) are asymptotically equivalent estimators. Let

$$\begin{aligned}\hat{\mathbf{R}} &= \mathbf{W}^{1/2}\mathbf{Y}_\alpha\mathbf{\Pi}_\alpha^\perp\mathbf{P}_\beta^T(\mathbf{P}_\beta\mathbf{\Pi}_\alpha^\perp\mathbf{P}_\beta^T)^{-1}\mathbf{P}_\beta\mathbf{\Pi}_\alpha^\perp\mathbf{Y}_\alpha^T\mathbf{W}^{1/2}\\ &= \hat{\mathbf{Q}}_s\hat{\mathbf{S}}_s^2\hat{\mathbf{Q}}_s^T + \hat{\mathbf{Q}}_n\hat{\mathbf{S}}_n^2\hat{\mathbf{Q}}_n^T\end{aligned}$$

and let $\mathbf{F}$ be as in (A.68). Also recall the expression (A.69) and the corresponding derivative (A.74). Introduce the two cost-functions

$$V(\boldsymbol{\theta}) = \mathrm{Tr}\left\{\mathbf{\Pi}_{\mathbf{F}}^\perp\hat{\mathbf{R}}\right\}\,, \tag{A.85}$$

$$J(\boldsymbol{\theta}) = \mathrm{Tr}\left\{\mathbf{\Pi}_{\mathbf{F}}^\perp\hat{\mathbf{Q}}_s\mathbf{S}_s^2\hat{\mathbf{Q}}_s^T\right\}\,. \tag{A.86}$$

Observe that $\hat{\mathbf{R}}$ is real and thus there exists real singular vectors, $\mathbf{F}$ may on the other hand be complex-valued. Since the minimizers of (A.85) and (A.86) are consistent estimates of the true parameters it suffices, under mild conditions, to show that [Lju87, SS89]

$$V_i = J_i + \mathrm{o}_p(1/\sqrt{N})\,, \tag{A.87}$$

$$V_{ij} = J_{ij} + \mathrm{o}_p(1)\,, \tag{A.88}$$

where V_i denotes the partial derivative with respect to $\boldsymbol{\theta}_i$ and similarly V_{ij} denotes the second partial derivative (cf. (A.71)). The notation $\mathrm{o}_p(\cdot)$ means the probability version of the corresponding deterministic notation[5]. Perturbation theory of subspaces gives

$$\mathbf{\Pi}_{\mathbf{F}}^\perp\hat{\mathbf{R}}\mathbf{Q}_s = \mathbf{\Pi}_{\mathbf{F}}^\perp\hat{\mathbf{Q}}_s\mathbf{S}_s^2 + \mathrm{o}_p(1/\sqrt{N})\,;$$

[5] A sequence, x_N, of random variables is $\mathrm{o}_p(a_N)$ if the probability limit of $a_N^{-1}x_N$ is zero.

see Section 2.3.4 or [CTO89]. The following holds for the limiting principal singular vectors

$$\mathbf{Q}_s\mathbf{T} = \mathbf{F}$$

for some full rank $\mathbf{T}$. The scene is now settled to verify (A.87) and (A.88) by straightforward calculations. Consider (A.87)

$$\begin{aligned}
V_i &= \operatorname{Tr}\left\{\mathbf{\Pi}_{\mathbf{F}}^{\perp}{}_i\hat{\mathbf{R}}\right\} \\
&= -2\ \operatorname{Re}\ \operatorname{Tr}\left\{\mathbf{\Pi}_{\mathbf{F}}^{\perp}\mathbf{F}_i(\mathbf{F}^*\mathbf{F})^{-1}\mathbf{F}^*\hat{\mathbf{R}}\right\} \\
&= -2\ \operatorname{Re}\ \operatorname{Tr}\left\{\mathbf{F}_i(\mathbf{F}^*\mathbf{F})^{-1}\mathbf{T}^*\mathbf{Q}_s^*\hat{\mathbf{R}}\mathbf{\Pi}_{\mathbf{F}}^{\perp}\right\} \\
&= -2\ \operatorname{Re}\ \operatorname{Tr}\left\{\mathbf{F}_i(\mathbf{F}^*\mathbf{F})^{-1}\mathbf{T}^*\mathbf{S}_s^2\hat{\mathbf{Q}}_s^T\mathbf{\Pi}_{\mathbf{F}}^{\perp}\right\} + \mathrm{o}_p(1/\sqrt{N})\,,
\end{aligned}$$

$$\begin{aligned}
J_i &= \operatorname{Tr}\left\{\mathbf{\Pi}_{\mathbf{F}}^{\perp}{}_i\hat{\mathbf{Q}}_s\mathbf{S}_s^2\hat{\mathbf{Q}}_s^T\right\} \\
&= -2\ \operatorname{Re}\ \operatorname{Tr}\left\{\mathbf{\Pi}_{\mathbf{F}}^{\perp}\mathbf{F}_i(\mathbf{F}^*\mathbf{F})^{-1}\mathbf{F}^*\hat{\mathbf{Q}}_s\mathbf{S}_s^2\hat{\mathbf{Q}}_s^T\right\} \\
&= -2\ \operatorname{Re}\ \operatorname{Tr}\left\{\mathbf{\Pi}_{\mathbf{F}}^{\perp}\mathbf{F}_i(\mathbf{F}^*\mathbf{F})^{-1}(\mathbf{Q}_s\mathbf{T})^*\mathbf{Q}_s\mathbf{S}_s^2\hat{\mathbf{Q}}_s^T\right\} + \mathrm{o}_p(1/\sqrt{N}) \\
&= -2\ \operatorname{Re}\ \operatorname{Tr}\left\{\mathbf{F}_i(\mathbf{F}^*\mathbf{F})^{-1}\mathbf{T}^*\mathbf{S}_s^2\hat{\mathbf{Q}}_s^T\mathbf{\Pi}_{\mathbf{F}}^{\perp}\right\} + \mathrm{o}_p(1/\sqrt{N})\,.
\end{aligned}$$

Hence, (A.87) holds true. Now turn to (A.88). Since

$$\hat{\mathbf{R}} = \mathbf{R} + \mathrm{o}_p(1) = \mathbf{Q}_s\mathbf{S}_s^2\mathbf{Q}_s^T + \mathrm{o}_p(1)\,,$$

the result is immediate.

A.14 Rank of Coefficient Matrix

Lemma A.2. *Let* $\mathbf{A}$ *be an* $n \times n$ *matrix with all eigenvalues inside the unit circle and let* $\mathbf{B}$ *be an* $n \times m$ *matrix. Define the matrix polynomial* $\mathbf{F}^u(q^{-1})$ *as in* (6.17)*. The coefficient matrix is, then;*

$$\begin{bmatrix}\mathbf{F}_n^u & \dots & \mathbf{F}_1^u\end{bmatrix},$$

and it has the same rank as the reachability matrix of $(\mathbf{A}, \mathbf{B})$.

Proof. The result follows from a simple construction. Let $a(q^{-1})$ be as in (6.18); then,

$$\begin{aligned}\mathbf{F}^u(q^{-1}) &= \frac{\mathrm{Adj}\{q\mathbf{I}-\mathbf{A}\}\mathbf{B}}{q^n}\\ &= a(q^{-1})\big(q\mathbf{I}-\mathbf{A}\big)^{-1}\mathbf{B}\\ &= (a_0 + a_1q^{-1} + \cdots + a_nq^{-n})\\ &\quad \times q^{-1}(\mathbf{I} + q^{-1}\mathbf{A} + q^{-2}\mathbf{A}^2 + \dots)\mathbf{B}.\end{aligned}$$

Comparison of coefficients leads to

$$\begin{bmatrix}\mathbf{F}_n^u & \dots & \mathbf{F}_1^u\end{bmatrix} = \begin{bmatrix}\mathbf{A}^{n-1}\mathbf{B} & \mathbf{A}^{n-2}\mathbf{B} & \dots & \mathbf{B}\end{bmatrix} \times \begin{bmatrix} a_0\mathbf{I}_m & \mathbf{0} & \mathbf{0} & \dots & \mathbf{0}\\ a_1\mathbf{I}_m & a_0\mathbf{I}_m & \mathbf{0} & & \\ \vdots & & \ddots & & \vdots \\ a_{n-1}\mathbf{I}_m & a_{n-2}\mathbf{I}_m & \dots & & a_0\mathbf{I}_m\end{bmatrix},$$

where $\mathbf{I}_m$ is a $m \times m$ identity matrix. The last factor is clearly non-singular (since $a_0 = 1$), so the lemma is proven. □

The lemma shows that the first block row of $\mathcal{S}$ as defined in (6.19) has full row rank if $(\mathbf{A},\ [\mathbf{B}\ \mathbf{K}])$ is reachable. This implies that $\mathcal{S}$ has full row rank (since $a_0 = 1$).

A.15 Rank of Sylvester Matrix

Consider the Sylvester matrix $\mathcal{S}_y$ in (6.31) generalized to the multi-input case. This means that every a_i is replaced by $a_i\mathbf{I}_m$ and that every $\mathbf{F}_i^y$ is now a matrix of dimension $l \times m$. The dimension of $\mathcal{S}_y$ becomes $((\alpha+\beta)m+\beta l)\times((\alpha+\beta+n)m)$. Observe that the relation (6.30) holds. Define

$$\mathbf{z} = \begin{bmatrix}\mathbf{y}_\beta^d(t)\\ \mathbf{u}_\beta(t)\\ \mathbf{u}_\alpha(t+\beta)\end{bmatrix}$$

and express $\mathbf{z}$ in the following two equivalent ways:

$$\mathbf{z} = \mathcal{S}_y\frac{1}{a(q^{-1})}\mathbf{u}_{\alpha+\beta+n}(t-n)$$

and

$$\mathbf{z} = \begin{bmatrix} \mathbf{\Gamma}_\beta & \mathbf{\Phi}_\beta & \mathbf{0} \\ \mathbf{0} & \mathbf{I}_{\beta m} & \mathbf{0} \\ \mathbf{0} & \mathbf{0} & \mathbf{I}_{\alpha m} \end{bmatrix} \begin{bmatrix} \mathbf{x}^d(t) \\ \mathbf{u}_\beta(t) \\ \mathbf{u}_\alpha(t+\beta) \end{bmatrix} \triangleq \mathbf{\Xi} \begin{bmatrix} \mathbf{x}^d(t) \\ \mathbf{u}_\beta(t) \\ \mathbf{u}_\alpha(t+\beta) \end{bmatrix}.$$

Next, study

$$\bar{\mathrm{E}}\{\mathbf{z}\mathbf{z}^T\} = \mathcal{S}_y \bar{\mathrm{E}} \left\{ \frac{1}{a(q^{-1})} \mathbf{u}_{\alpha+\beta+n}(t-n) \frac{1}{a(q^{-1})} \mathbf{u}^T_{\alpha+\beta+n}(t-n) \right\} \mathcal{S}_y^T \tag{A.89}$$

$$= \mathbf{\Xi}\, \bar{\mathrm{E}} \left\{ \begin{bmatrix} \mathbf{x}^d(t) \\ \mathbf{u}_\beta(t) \\ \mathbf{u}_\alpha(t+\beta) \end{bmatrix} \begin{bmatrix} \mathbf{x}^d(t) \\ \mathbf{u}_\beta(t) \\ \mathbf{u}_\alpha(t+\beta) \end{bmatrix}^T \right\} \mathbf{\Xi}^T. \tag{A.90}$$

From the proof of Theorem 6.2 we know that the covariance matrix in the middle of (A.90) is positive definite if $\mathbf{u}(t)$ is at least $\mathrm{PE}(\alpha+\beta+n)$ and if $(\mathbf{A}, \mathbf{B})$ is reachable. If $\operatorname{rank}\{\mathbf{\Gamma}_\beta\} = n$, then $\mathbf{\Xi}$ is full column rank and it follows that

$$\operatorname{rank}\left\{\bar{\mathrm{E}}\{\mathbf{z}\mathbf{z}^T\}\right\} = n + (\alpha+\beta)m. \tag{A.91}$$

Furthermore, if $\mathbf{u}(t)$ is $\mathrm{PE}(\alpha+\beta+n)$ then

$$\bar{\mathrm{E}} \left\{ \frac{1}{a(q^{-1})} \mathbf{u}_{\alpha+\beta+n}(t-n) \frac{1}{a(q^{-1})} \mathbf{u}^T_{\alpha+\beta+n}(t-n) \right\}$$

is positive definite [SS83]. Notice that we assume that the system is stable. This assumption implies that $a(z)$ has all roots outside the unit circle. Comparing (A.91) and (A.89), it can be concluded that,

$$\operatorname{rank}\{\mathcal{S}_y\} = n + (\alpha+\beta)m.$$

This result holds if $(\mathbf{A}, \mathbf{B})$ is reachable, if $(\mathbf{A}, \mathbf{C})$ is observable, and if β is greater than or equal to the observability index. The observability and reachability assumptions are equivalent to requiring that the polynomials $\mathbf{F}^y(z)$ and $a(z)$ do not share any common zeros.

Appendix B

Notations

In general, boldface uppercase letters are used for matrices and boldface lowercase letters denote vectors. Scalars are set in normal typeface.

$\mathbb{R}$, $\mathbb{C}$	The set of real and complex numbers, respectively.
$m \times n$	The dimension of a matrix with m rows and n columns.
$\mathbf{X} \in \mathbb{R}^{m \times n}$	$\mathbf{X}$ is an $m \times n$ matrix of real numbers.
$\mathbf{X} \in \mathbb{C}^{m \times n}$	$\mathbf{X}$ is an $m \times n$ matrix of complex numbers.
$\mathbf{A}_{ij}$	The (i,j)th element of the matrix $\mathbf{A}$.
$\boldsymbol{\theta}_k$	The kth element of the vector $\boldsymbol{\theta}$.
$\mathbf{A}_{\bullet k}$	The kth column of $\mathbf{A}$.
$\mathbf{A}_{k\bullet}$	The kth row of $\mathbf{A}$.
$\mathbf{A}^T, \mathbf{A}^*, \mathbf{A}^c$	The transpose, complex conjugate transpose and complex conjugate of the matrix $\mathbf{A}$, respectively.
$\mathbf{A}^{-T}$	The transpose of the inverse of $\mathbf{A}$. That is, $\mathbf{A}^{-T} = (\mathbf{A}^{-1})^T$.
$\mathbf{A}^\dagger$	The Moore-Penrose pseudo inverse of $\mathbf{A}$.
$\mathrm{Tr}\{\mathbf{A}\}$	The trace operator [Gra81].
$\|\mathbf{x}\|_2$	The 2-norm of the vector $\mathbf{x}$ ($\|\mathbf{x}\|_2^2 = \mathbf{x}^*\mathbf{x}$).

$\|\mathbf{A}\|_F$	The Frobenius norm of the matrix $\mathbf{A}$.
$\text{vec}\{\mathbf{A}\}$	The vectorization operator [Gra81].
$\otimes$	Kronecker product [Gra81, Bre78].
$\odot$	The Hadamard or Schur product (elementwize multiplication).
$\circ$	The Khatri-Rao product (columnwize Kronecker product) [Bre78].
$\mathbf{I}_n$	The $n \times n$ identity matrix. The subscript is often omitted.
$\mathbf{0}_{m\times n}$	An $m \times n$ matrix of zeros. The subscript is typically omitted.
$\text{diag}\{\mathbf{x}\}$	A diagonal matrix with the elements of the vector $\mathbf{x}$ on the diagonal.
$\text{Re}\{\mathbf{A}\}, \text{Im}\{\mathbf{A}\}$	The real and imaginary part of $\mathbf{A}$, respectively.
$\mathbf{A} > \mathbf{0}$ $(\mathbf{A} \geq \mathbf{0})$	The Hermitian matrix $\mathbf{A} = \mathbf{A}^*$ is positive definite (positive semidefinite). For two Hermitian matrices $\mathbf{A}$ and $\mathbf{B}$, the notation $\mathbf{A} > \mathbf{B}$ $(\mathbf{A} \geq \mathbf{B})$ means that $\mathbf{A} - \mathbf{B}$ is positive definite (positive semidefinite).
$\text{rank}(\mathbf{A})$	The rank of the matrix $\mathbf{A}$.
$\mathcal{N}\{\mathbf{A}\}$	The null-space of the matrix $\mathbf{A}$.
$\mathcal{R}\{\mathbf{A}\}$	The range-space of $\mathbf{A}$.
$\oplus$	Direct orthogonal sum of vector spaces.
$\arg\min_x f(x)$	The value of x that minimizes $f(x)$.
$\hat{\boldsymbol{\theta}}$	An estimate of the quantity $\boldsymbol{\theta}$.
$O(x)$	An arbitrary function such that $\|O(x)/x\| \leq c < \infty$ as $x \to 0$.
$o(x)$	An arbitrary function such that $\|o(x)/x\| \to 0$ as $x \to 0$.

$O_p(x)$, $o_p(x)$	The in-probability versions of $O(x)$ and $o(x)$, respectively [MKB79].
$\delta_{i,j}$	Kronecker's delta function ($\delta_{i,j} = 1$ if $i = j$ and zero otherwise.)
$\lfloor k \rfloor$	The largest integer less than or equal to $k \in \mathbb{R}$.
$s \in (r, t]$	Half-open interval, $r < s \leq t$.
q, q^{-1}	The forward and backward unit shift operators, respectively ($q\mathbf{u}(t) = \mathbf{u}(t+1)$ and $q^{-1}\mathbf{u}(t) = \mathbf{u}(t-1)$).
$\log\{\cdot\}$	The natural logarithm.
$\det\{\cdot\}$	The determinant function.
$\mathrm{E}\{\cdot\}$	Mathematical expectation.
$\bar{\mathrm{E}}\{x(t)\}$	$\lim_{N\to\infty} \frac{1}{N} \sum_{t=1}^{N} \mathrm{E}\{x(t)\}$
$\mathbf{x} \in \mathrm{N}(\mathbf{m}, \mathbf{P})$	The vector $\mathbf{x}$ is (complex) Gaussian distributed with mean $\mathbf{m}$ and covariance $\mathbf{P}$.
$\mathbf{x} \in \mathrm{AsN}(\mathbf{m}, \mathbf{P})$	The vector $\mathbf{x}$ is asymptotically (complex) Gaussian distributed with mean $\mathbf{m}$ and covariance $\mathbf{P}$.

Appendix C

Abbreviations and Acronyms

4SID	State-space subspace system identification
ABC	Asymptotically best consistent
AR	Autoregressive
ARMA	Autoregressive moving average
ARX	Autoregressive model with exogenous inputs
CRB	Cramér Rao lower bound
CVA	Canonical variate analysis
DEUCE	Direction estimator for uncorrelated emitters
DOA	Direction of arrival
ESPRIT	Estimation of signal parameters by rotational invariance techniques
EVD	Eigenvalue decomposition
FB	Forward backward
FS	Finite samples

GWSF	Generalized weighted subspace fitting
IV	Instrumental variable
ME	Model errors
ML	Maximum likelihood
MLE	Maximum likelihood estimate
MODE	Method of direction estimation
MOESP	Multi-input multi-output output error state-space model realization
MUSIC	Multiple signal classification
N4SID	Numerical algorithms for subspace state space system identification
PEM	Prediction error method
SNR	Signal to noise ratio
SVD	Singular value decomposition
ULA	Uniform linear array
w.p.1	With probability one
WSF	Weighted subspace fitting

Bibliography

[AJ76] B. D. O. Anderson and E. I. Jury. "Generalized Bezoutian and Sylvester Matrices in Multivariable Linear Control". *IEEE Transactions on Automatic Control*, AC-21:551–556, Aug. 1976.

[AK90] K. S. Arun and S. Y. Kung. "Balanced Approximation of Stochastic Systems". *SIAM J. Matrix Analysis and Applications*, 11:42–68, 1990.

[Aka74a] H. Akaike. "A New Look at the Statistical Model Identification". *IEEE Trans. Automat. Contr.*, AC-19:716–723, Dec. 1974.

[Aka74b] H. Akaike. "Stochastic Theory of Minimal Realization". *IEEE Trans. Automat. Contr.*, AC-19(6):667–674, Dec. 1974.

[Aka75] H. Akaike. "Markovian Representation of Stochastic Processes by Canonical Variables". *SIAM Journal on Control*, 13(1):162–173, 1975.

[Alb72] A. Albert. *Regression and the Moore-Penrose Pseudoinverse.* Academic Press, New York, 1972.

[And84] T.W. Anderson. *"An Introduction to Multivariate Statistical Analysis,* 2^{nd} *edition".* John Wiley & Sons, New York, 1984.

[Aok87] M. Aoki. *State Space Modeling of Time Series.* Springer Verlag, Berlin, 1987.

[Ban71] W. J. Bangs. *Array Processing with Generalized Beamformers.* PhD thesis, Yale University, New Haven, CT, 1971.

[Bar83] A.J. Barabell. "Improving the Resolution Performance of Eigenstructure-Based Direction-Finding Algorithms". In *Proc. ICASSP 83*, pages 336–339, Boston, MA, 1983.

[Bay92] D. Bayard. "An Algorithm for State-space Frequency Domain Identification Without Windowing Distortions". In *Proc. 31st IEEE Conf. on Decision and Control*, pages 1707–1712, Tucson, AZ, 1992.

[BDS97] D. Bauer, M. Deistler, and W. Scherrer. "The Analysis of the Asymptotic Variance of Subspace Algorithms". In *Proc. 11th IFAC Symposium on System Identification*, pages 1087–1091, Fukuoka, Japan, 1997.

[Bel70] R. Bellman. *Introduction to Matrix Analysis,* 2^{nd} *edition.* McGraw-Hill, New York, 1970.

[Bie79] G. Bienvenue. "Influence of the Spatial Coherence of the Background Noise on High Resolution Passive Methods". In *Proc. ICASSP'79*, pages 306–309, Washington, DC, 1979.

[BKAK78] R. R. Bitmead, S. Y. Kung, B. D. O. Anderson, and T. Kailath. "Greatest Common Divisors via Generalized Sylvester and Bezout Matrices". *IEEE Transactions on Automatic Control*, 23(6):1043–1047, Dec. 1978.

[BM86] Y. Bresler and A. Macovski. "Exact Maximum Likelihood Parameter Estimation of Superimposed Exponential Signals in Noise". *IEEE Trans. ASSP*, ASSP-34:1081–1089, Oct. 1986.

[Böh86] J.F. Böhme. "Estimation of Spectral Parameters of Correlated Signals in Wavefields". *Signal Processing*, 10:329–337, 1986.

[Boh91] T. Bohlin. *"Interactive System Identification: Prospects and Pitfalls"*. Springer-Verlag, 1991.

[Bre78] J. W. Brewer. "Kronecker Products and Matrix Calculus in System Theory". *IEEE Trans. on Circuits and Systems*, CAS-25(9):772–781, September 1978.

[CK95] Y.M. Cho and T. Kailath. "Fast Subspace-based System Identification: An Instrumental Variable Approach". *Automatica*, 31(6):903–905, 1995.

[Com82] R. T. Compton. "The Effect of Random Steering Vector Errors in the Applebaum Adaptive Array". *IEEE Trans. on Aero. and Elec. Sys.*, AES-18(5):392–400, Sept. 1982.

[Cra46] H. Cramér. *Mathematical Methods of Statistics*. Princeton University Press, 1946.

[CS96] M. Cedervall and P. Stoica. "System Identification from Noisy Measurements by Using Instrumental Variables and Subspace Fitting". *Circuits, Systems and Signal Processing*, 15(2):275–290, 1996.

[CTO89] H. Clergeot, S. Tressens, and A. Ouamri. "Performance of High Resolution Frequencies Estimation Methods Compared to the Cramér-Rao Bounds". *IEEE Trans. ASSP*, 37(11):1703–1720, November 1989.

[CXK94] Y.M. Cho, G. Xu, and T. Kailath. "Fast Recursive Identification of State Space Models via Exploitation of Displacement Structure". *Automatica, Special Issue on Statistical Signal Processing and Control*, 30(1):45–59, Jan. 1994.

[De 88] B. De Moor. *Mathematical Concepts and Techniques for Modeling of Static and Dynamic Systems*. PhD thesis, Kath. Universiteit Leuven, Heverlee, Belgium, 1988.

[DPS95] M. Deistler, K. Peternell, and W. Scherrer. "Consistency and Relative Efficiency of Subspace Methods". *Automatica, special issue on trends in system identification*, 31(12):1865–1875, Dec. 1995.

[DVVM88] B. De Moor, J. Vandewalle, L. Vandenberghe, and P. Van Mieghem. "A Geometrical Strategy for the Identification of State Space Models of Linear Multivariable Systems with Singular Value Decomposition". In *Proc. IFAC 88*, pages 700–704, Beijing, China, 1988.

[Eyk74] P. Eykhoff. *"System Identification, Parameter and State Estimation"*. Wiley, 1974.

[Fau76] P.L. Faurre. Stochastic realization algorithms. In R.K. Mehra and D.G. Lainiotis, editors, *System Identification: Advances and Case Studies*. Academic Press, NY, 1976.

[FFLC95] A. Flieller, A. Ferreol, P. Larzabal, and H. Clergeot. "Robust Bearing Estimation in the Presence of Direction-Dependent Modelling Errors: Identifiability and Treatment". In *Proc. ICASSP*, pages 1884–1887, Detroit, MI, 1995.

[Fri90a] B. Friedlander. "A Sensitivity Analysis of the MUSIC Algorithm". *IEEE Trans. on ASSP*, 38(10):1740–1751, October 1990.

[Fri90b] B. Friedlander. "Sensitivity of the Maximum Likelihood Direction Finding Algorithm". *IEEE Trans. on AES*, 26(6):953–968, November 1990.

[Fuc92] J.J. Fuchs. "Estimation of the Number of Signals in the Presence of Unknown Correlated Sensor Noise". *IEEE Trans. on Signal Processing*, SP-40(5):1053–1061, May 1992.

[FW94] B. Friedlander and A.J. Weiss. "Effects of Model Errors on Waveform Estimation Using the MUSIC Algorithm". *IEEE Trans. onSP*, SP-42(1):147–155, Jan. 1994.

[GJO96] B. Göransson, M. Jansson, and B. Ottersten. "Spatial and Temporal Frequency Estimation of Uncorrelated Signals Using Subspace Fitting". In *Proceedings of 8th IEEE Signal Processing Workshop on Statistical Signal and Array Processing*, pages 94–96, Corfu, Greece, June 1996.

[GO97] B. Göransson and B. Ottersten. "Efficient Direction Estimation of Uncorrelated Sources Using Polynomial Rooting". In *Proc. 13th Intl. Conf. DSP'97*, pages 935–938, Santorini, Greece, 1997.

[Goo63] N.R. Goodman. "Statistical Analysis Based on a Certain Multivariate Complex Gaussian Distribution (An Introduction)". *Annals Math. Stat.*, Vol. 34:152–176, 1963.

[Gop69] B. Gopinath. "On the Identification of Linear Time-Invariant Systems from Input-Output Data". *The Bell System Technical Journal*, Vol. 48(5):1101–1113, 1969.

[Gor97] A. Gorokhov. *"Blind Separation of Convolutive Mixtures: Second Order Methods"*. PhD thesis, Ecole Nationale Superieure des Telecommunications (ENST), Paris, 1997.

[GP77] G. C. Goodwin and R. L. Payne. *"Dynamic System Identification: Experiment Design and Data Analysis"*, volume 136 of *Mathematics in Science and Engineering Series*. Academic Press, 1977.

[Gra81] A. Graham. *Kronecker Products and Matrix Calculus with Applications*. Ellis Horwood Ltd, Chichester, UK, 1981.

[Gus97] T. Gustafsson. "System Identification Using Subspace-based Instrumental Variable Methods". In *Proc. 11th IFAC Symposium on System Identification*, pages 1119–1124, Fukuoka, Japan, 1997.

[GV96] G.H. Golub and C.F. Van Loan. *Matrix Computations, third edition*. Johns Hopkins University Press, Baltimore, MD., 1996.

[GW74] K. Glover and J. C. Willems. "Parameterizations of Linear Dynamical Systems: Canonical Forms and Identifiability". *IEEE Trans. on Automatic Control*, AC-19(6):640–646, Dec. 1974.

[GW84] M. Gevers and V. Wertz. "Uniquely Identifiable State-space and ARMA Parameterizations for Multivariable Linear Systems". *Automatica*, 20(3):333–347, 1984.

[Haa97a] M. Haardt. *"Efficient One-, Two-, and Multidimensional High-Resolution Array Signal Processing"*. PhD thesis, Technical University of Munich, Shaker Verlag, 1997.

[Haa97b] M. Haardt. "Structured Least Squares to Improve the Performance of ESPRIT-Type Algorithms". *IEEE Trans. Signal Processing*, 45(3):792–799, Mar. 1997.

[Hay91] S. Haykin. *Advances in Spectrum Analysis and Array Processing, edited by S. Haykin*, volume 2. Prentice-Hall, Englewood Cliffs, NJ, 1991.

[HD88] E. J. Hannan and M. Deistler. *The Statistical Theory of Linear Systems*. J. Wiley & Sons, N. Y., 1988.

[HK66] B.L. Ho and R.E. Kalman. "Efficient Construction of Linear State Variable Models from Input/Output Functions". *Regelungstechnik*, 14:545–548, 1966.

[Hot33] H. Hotelling. "Analysis of a Complex of Statistical Variables into Principal Components". *J. Educ. Psych.*, 24:417–441,498–520, 1933.

[Jaf88] A. G. Jaffer. "Maximum Likelihood Direction Finding of Stochastic Sources: A Separable Solution". In *Proc. ICASSP 88*, volume 5, pages 2893–2896, New York, April 1988.

[Jan95] M. Jansson. "On Performance Analysis of Subspace Methods in System Identification and Sensor Array Processing". Technical Report TRITA-REG-9503, ISSN 0347-1071, Automatic Control, Signals, Sensors & Systems, KTH, Stockholm, June 1995. Licentiate Thesis.

[JD93] D.H. Johnson and D.E. Dudgeon. *Array Signal Processing – Concepts and Techniques*. Prentice-Hall, Englewood Cliffs, NJ, 1993.

[JGO97a] M. Jansson, B. Göransson, and B. Ottersten. "A Subspace Method for Direction of Arrival Estimation of Uncorrelated Emitter Signals". Submitted to IEEE Trans. on Signal Processing, Aug. 1997.

[JGO97b] M. Jansson, B. Göransson, and B. Ottersten. "Analysis of a Subspace-Based Spatial Frequency Estimator". In *Proceedings of ICASSP'97*, pages 4001–4004, München, Germany, April 1997.

[JO95] M. Jansson and B. Ottersten. "Covariance Preprocessing in Weighted Subspace Fitting". In *IEEE/IEE workshop on signal processing methods in multipath environments*, pages 23–32, Glasgow, Scotland, 1995.

[Joh93] R. Johansson. *"System Modeling and Identification"*. Information and System Sciences Series. Prentice Hall, 1993.

[JP85] J.N. Juang and R.S. Pappa. "An Eigensystem Realization Algorithm for Modal Parameter Identification and Model Reduction". *J. Guidance, Control and Dynamics*, 8(5):620–627, 1985.

[JSO97] M. Jansson, A. L. Swindlehurst, and B. Ottersten. "Weighted Subspace Fitting for General Array Error Models". Submitted to IEEE Trans. on Signal Processing, Jul. 1997.

[JW95] M. Jansson and B. Wahlberg. "On Weighting in State-Space Subspace System Identification". In *Proc. European Control Conference, ECC'95*, pages 435–440, Roma, Italy, 1995.

[JW96a] M. Jansson and B. Wahlberg. "A Linear Regression Approach to State-Space Subspace System Identification". *Signal Processing (EURASIP), Special Issue on Subspace Methods, Part II: System Identification*, 52(2):103–129, July 1996.

[JW96b] M. Jansson and B. Wahlberg. "On Consistency of Subspace System Identification Methods". In *Preprints of 13th IFAC World Congress*, pages 181–186, San Francisco, California, 1996.

[JW97a] M. Jansson and B. Wahlberg. "Counterexample to General Consistency of Subspace System Identification Methods". In *11th IFAC Symposium on System Identification*, pages 1677–1682, Fukuoka, Japan, 1997.

[JW97b] M. Jansson and B. Wahlberg. "On Consistency of Subspace Methods for System Identification". Submitted to Automatica, Jun. 1997.

[KAB83] S. Y. Kung, K. S. Arun, and D. V. BhaskarRao. "State-Space Singular Value Decomposition Based Method for the Harmonic Retrieval Problem". *J. Opt. Soc. Amer.*, 73:1799–1811, Dec. 1983.

[KB86] M. Kaveh and A. J. Barabell. "The Statistical Performance of the MUSIC and the Minimum-Norm Algorithms in Resolving Plane Waves in Noise". *IEEE Trans. ASSP*, ASSP-34(2):331–341, April 1986. Correction in ASSP-34(3), June 1986, p. 633.

[KDS88] A.M. King, U.B. Desai, and R.E. Skelton. "A Generalized Approach to q-Markov Covariance Equivalent Realizations of Discrete Systems". *Automatica*, 24(4):507–515, 1988.

[KF93] M. Koerber and D. Fuhrmann. "Array Calibration by Fourier Series Parameterization: Scaled Principle Components Method". In *Proc. ICASSP*, pages IV340–IV343, Minneapolis, Minn., 1993.

[KP89] B. H. Kwon and S. U. Pillai. "A Self Inversive Array Processing Scheme for Angle-of-Arrival Estimation". *Signal Processing*, 17(3):259–277, Jul. 1989.

[KSS94] A. Kangas, P. Stoica, and T. Söderström. "Finite Sample and Modeling Error Effects on ESPRIT and MUSIC Direction Estimators". *IEE Proc. Radar, Sonar, & Navig.*, 141:249–255, 1994.

[KSS96] A. Kangas, P. Stoica, and T. Söderström. "Large Sample Analysis of MUSIC and Min-Norm Direction Estimators in the Presence of Model Errors". *Circ., Sys., and Sig. Proc.*, 15:377–393, 1996.

[Kun78] S.Y. Kung. "A New Identification and Model Reduction Algorithm via Singular Value Decomposition". In *Proc. 12th Asilomar Conf. on Circuits, Systems and Computers*, pages 705–714, Pacific Grove, CA, November 1978.

[Kun81] S. Y. Kung. "A Toeplitz Approximation Method and Some Applications". In *Proc. Int. Symp. Mathematical Theory of Networks and Systems*, pages 262–266, Santa Monica, CA., Aug. 1981.

[KV96] H. Krim and M. Viberg. "Two Decades of Array Signal Processing Research: The Parametric Approach". *IEEE Signal Processing Magazine*, 13(4):67–94, Jul. 1996.

[Lar83] W. E. Larimore. "System Identification, Reduced-Order Filtering and Modeling via Canonical Variate Analysis". In *Proc. ACC*, pages 445–451, June 1983.

[Lar90] W. E. Larimore. "Canonical Variate Analysis in Identification, Filtering and Adaptive Control". In *Proc. 29th CDC*, pages 596–604, Honolulu, Hawaii, December 1990.

[Lar94] W. E. Larimore. "The Optimality of Canonical Variate Identification by Example". In *Proc. 10th IFAC Symp. on Syst. Id.*, volume 2, pages 151–156, Copenhagen, Denmark, 1994.

[Law40] D. N. Lawley. The estimation of factor loadings by the method of maximum likelihood. In *Proceedings of the Royal Society of Edinburgh, Sec. A.*, volume 60, pages 64–82, 1940.

[Liu92] K. Liu. "Identification of Multi-Input and Multi-Output Systems by Observability Range Space Extraction". In *Proc. CDC*, pages 915–920, Tucson, AZ, 1992.

[Lju87] L. Ljung. *System Identification: Theory for the User*. Prentice-Hall, Englewood Cliffs, NJ, 1987.

[Lju91] L. Ljung. "A Simple Start-up Procedure for Canonical Form State Space Identification, Based on Subspace Approximation". In *Proc. 30th IEEE Conf. on Decision and Control*, pages 1333–1336, Brighton, U.K., 1991.

[LM87] J. Lo and S. Marple. "Eigenstructure Methods for Array Sensor Localization". In *Proc. ICASSP*, pages 2260–2263, Dallas, TX, 1987.

[LS91] K. Liu and R. E. Skelton. "Identification and Control of NASA's ACES Structure". In *Proc. American Control Conference*, pages 3000–3006, Boston, MA, 1991.

[LV92] F. Li and R. Vaccaro. "Sensitivity Analysis of DOA Estimation Algorithms to Sensor Errors". *IEEE Trans. AES*, AES-28(3):708–717, July 1992.

[McK94a] T. McKelvey. "Fully Parametrized State-Space Models in System Identification". In *Proc. 10th IFAC Symp. on Syst. Id.*, volume 2, pages 373–378, Copenhagen, Denmark, 1994.

[McK94b] T. McKelvey. On state-space models in system identification. Technical Report LiU-TEK-LIC-1994:33, Linköping University, May 1994. Licentiate Thesis.

[MDVV89] M. Moonen, B. De Moor, L. Vandenberghe, and J. Vandewalle. "On- and off-line identification of linear state-space models". *Int. J. Control*, 49(1):219–232, 1989.

[MKB79] K.V. Mardia, J.T. Kent, and J.M. Bibby. *Multivariate Analysis*. Academic Press, London, 1979.

[MR94] D. McArthur and J. Reilly. "A Computationally Efficient Self-Calibrating Direction of Arrival Estimator". In *Proc. ICASSP*, pages IV–201 – IV–205, Adelaide, Australia, 1994.

[NK94] V. Nagesha and S. Kay. "On Frequency Estimation with the IQML Algorithm". *IEEE Trans. on Signal Processing*, 42(9):2509–2513, Sep. 1994.

[NN93] B. Ng and A. Nehorai. "Active Array Sensor Location Calibration". In *Proc. ICASSP*, pages IV21–IV24, Minneapolis, Minn., 1993.

[OAKP97] B. Ottersten, D. Asztély, M. Kristensson, and S. Parkvall. "A Statistical Approach to Subspace Based Estimation with Applications in Telecommunications". In S. Van Huffel, editor, *2nd International Workshop on TLS and Errors-in-Variables Modeling*, pages 285–294, Leuven, Belgium, 1997. SIAM.

[ORK89] B. Ottersten, R. Roy, and T. Kailath. "Signal Waveform Estimation in Sensor Array Processing". In *Proc.* 23^{rd} *Asilomar Conf. Sig., Syst.,Comput.*, pages 787–791, Nov. 1989.

[Ott89] B. Ottersten. *Parametric Subspace Fitting Methods for Array Signal Processing*. PhD thesis, Stanford University, Stanford, CA, Dec. 1989.

[OV94] B. Ottersten and M. Viberg. "A Subspace-Based Instrumental Variable Method for State-Space System Identification". In *Proc.* 10*th IFAC Symp. on Syst. Id.*, volume 2, pages 139–144, Copenhagen, Denmark, 1994.

[OVK90] B. Ottersten, M. Viberg, and T. Kailath. "Asymptotic Robustness of Sensor Array Processing Methods". In *Proc. ICASSP 90 Conf*, pages 2635–2638, Albuquerque, NM, April 1990.

[OVSN93] B. Ottersten, M. Viberg, P. Stoica, and A. Nehorai. "Exact and Large Sample ML Techniques for Parameter Estimation and Detection in Array Processing". In Haykin, Litva, and Shepherd, editors, *Radar Array Processing*, pages 99–151. Springer-Verlag, Berlin, 1993.

[Pil89] S. U. Pillai. *"Array Signal Processing"*. New York: Springer-Verlag, 1989.

[Pis73] V.F. Pisarenko. "The Retrieval of Harmonics from a Covariance Function". *Geophys. J. Roy. Astron. Soc.*, 33:347–366, 1973.

[PK85] A. Paulraj and T. Kailath. "Direction-of-Arrival Estimation by Eigenstructure Methods with Unknown Sensor Gain and Phase". In *Proc. IEEE ICASSP*, pages 17.7.1–17.7.4, Tampa, Fla., March 1985.

[PK89] S. U. Pillai and B. H. Kwon. "Performance Analysis of MUSIC-Type High Resolution Estimators for Direction Finding in Correlated and Coherent Scenes". *IEEE Trans. on ASSP*, 37(8):1176–1189, Aug. 1989.

[PPL90] D. Pearson, S.U. Pillai, and Y. Lee. "An Algorithm for Near-Optimal Placements of Sensor Elements". *IEEE Transactions on Information Theory*, 36(6):1280–1284, Nov. 1990.

[PRK86] A. Paulraj, R. Roy, and T. Kailath. "A Subspace Rotation Approach to Signal Parameter Estimation". *Proceedings of the IEEE*, pages 1044–1045, July 1986.

[PSD95] K. Peternell, W. Scherrer, and M. Deistler. "Statistical Analysis of Subspace Identification Methods". In *Proc. European Control Conference, ECC'95*, pages 1342–1347, Roma, Italy, 1995.

[PSD96] K. Peternell, W. Scherrer, and M. Deistler. "Statistical Analysis of Novel Subspace Identification Methods". *Signal Processing (EURASIP), Special Issue on Subspace Methods, Part II: System Identification*, 52(2):161–177, July 1996.

[Qua82] A. H. Quazi. "Array Beam Response in the Presence of Amplitude and Phase Fluctuations". *J. Acoust. Soc. Amer.*, 72(1):171–180, July 1982.

[Qua84] N. Quang. "On the Uniqueness of the Maximum-Likelihood Estimate of Structured Covariance Matrices". *IEEE Trans. on Acoustics, Speech, and Signal Processing*, ASSP-32(6):1249–1251, Dec. 1984.

[RA92] B.D. Rao and K.S. Arun. "Model Based Processing of Signals: A State Space Approach". *Proceedings of the IEEE*, 80(2):283–309, Feb. 1992.

[RH80] D. J. Ramsdale and R. A. Howerton. "Effect of Element Failure and Random Errors in Amplitude and Phase on the

Sidelobe Level Attainable with a Linear Array". *J. Acoust. Soc. Amer.*, 68(3):901–906, Sept. 1980.

[RH89] B. D. Rao and K. V. S. Hari. "Performance Analysis of ESPRIT and TAM in Determining the Direction of Arrival of Plane Waves in Noise". *IEEE Trans. ASSP*, ASSP-37(12):1990–1995, Dec. 1989.

[RH93] B. D. Rao and K. V. S. Hari. "Weighted Subspace Methods and Spatial Smoothing: Analysis and Comparison". *IEEE Trans. ASSP*, 41(2):788–803, Feb. 1993.

[RK89] R. Roy and T. Kailath. "ESPRIT–Estimation of Signal Parameters Via Rotational Invariance Techniques". *IEEE Trans. ASSP*, ASSP-37(7):984–995, Jul. 1989.

[RPK86] R. Roy, A. Paulraj, and T. Kailath. "ESPRIT – A Subspace Rotation Approach to Estimation of Parameters of Cisoids in Noise". *IEEE Trans. on ASSP*, ASSP-34(4):1340–1342, October 1986.

[RS87a] Y. Rockah and P. M. Schultheiss. "Array Shape Calibration Using Sources in Unknown Locations – Part I: Far-Field Sources". *IEEE Trans. on ASSP*, 35:286–299, March 1987.

[RS87b] Y. Rockah and P. M. Schultheiss. "Array Shape Calibration Using Sources in Unknown Locations – Part II: Near-Field Sources and Estimator Implementation". *IEEE Trans. on ASSP*, 35:724–735, June 1987.

[SCE95] P. Stoica, M. Cedervall, and A. Eriksson. "Combined Instrumental Variable and Subspace Fitting Approach to Parameter Estimation of Noisy Input-Output Systems". *IEEE Trans. on Signal Processing*, 43(10):2386–97, Oct. 1995.

[Sch79] R.O. Schmidt. "Multiple Emitter Location and Signal Parameter Estimation". In *Proc. RADC Spectrum Estimation Workshop*, pages 243–258, Rome, NY, 1979.

[Sch81] R. O. Schmidt. *A Signal Subspace Approach to Multiple Emitter Location and Spectral Estimation*. PhD thesis, Stanford Univ., Stanford, CA, Nov. 1981.

[SH92] V. C. Soon and Y. F. Huang. "An Analysis of ESPRIT Under Random Sensor Uncertainties". *IEEE Trans. on Sig. Proc.*, SP-40(9):2353–2358, 1992.

[SJ97] P. Stoica and M. Jansson. "On Forward-Backward MODE for Array Signal Processing". *Digital Signal Processing – A Review Journal*, 1997. Accepted.

[SK90] A. Swindlehurst and T. Kailath. "On the Sensitivity of the ESPRIT Algorithm to Non-Identical Subarrays". *Sādhanā, Academy Proc. in Eng. Sciences*, 15(3):197–212, November 1990.

[SK92] A. Swindlehurst and T. Kailath. "A Performance Analysis of Subspace-Based Methods in the Presence of Model Errors – Part 1: The MUSIC Algorithm". *IEEE Trans. on Sig. Proc.*, 40(7):1758–1774, July 1992.

[SK93] A. Swindlehurst and T. Kailath. "A Performance Analysis of Subspace-Based Methods in the Presence of Model Errors – Part 2: Multidimensional Algorithms". *IEEE Trans. on Sig. Proc.*, 41(9):2882–2890, Sept. 1993.

[SM97] P. Stoica and R. Moses. *"Introduction to Spectral Analysis"*. Prentice Hall, Upper Saddle River, New Jersey, 1997.

[SN89a] P. Stoica and A. Nehorai. "MUSIC, Maximum Likelihood and Cramér-Rao Bound". *IEEE Trans. ASSP*, ASSP-37:720–741, May 1989.

[SN89b] P. Stoica and A. Nehorai. "MUSIC, Maximum Likelihood and Cramér-Rao Bound: Further Results and Comparisons". In *ICASSP'89*, 1989.

[SN90] P. Stoica and A. Nehorai. "Performance Study of Conditional and Unconditional Direction-of-Arrival Estimation". *IEEE Trans. ASSP*, ASSP-38:1783–1795, October 1990.

[SROK95] A.L. Swindlehurst, R. Roy, B. Ottersten, and T. Kailath. "A Subspace Fitting Method for Identification of Linear State Space Models". *IEEE Trans. Autom. Control*, 40(2):311–316, Feb. 1995.

[SS81] T. Söderström and P. Stoica. "Comparison of Some Instrumental Variable Methods – Consistency and Accuracy Aspects". *Automatica*, 17(1):101–115, 1981.

[SS83] T. Söderström and P. G. Stoica. *Instrumental Variable Methods for System Identification*. Springer-Verlag, Berlin, 1983.

[SS89] T. Söderström and P. Stoica. *System Identification*. Prentice-Hall International, Hemel Hempstead, UK, 1989.

[SS90a] P. Stoica and K. Sharman. "Maximum Likelihood Methods for Direction-of-Arrival Estimation". *IEEE Trans. ASSP*, ASSP-38:1132–1143, July 1990.

[SS90b] P. Stoica and K. Sharman. "Novel Eigenanalysis Method for Direction Estimation". *IEE Proc. Part F*, 137(1):19–26, Feb 1990.

[SS91] P. Stoica and T. Söderström. "Statistical Analysis of MUSIC and Subspace Rotation Estimates of Sinusoidal Frequencies". *IEEE Trans. ASSP*, ASSP-39:1836–1847, Aug. 1991.

[SV95] P. Stoica and M. Viberg. "Maximum-Likelihood Parameter and Rank Estimation in Reduced-Rank Multivariate Linear Regressions". Technical Report CTH-TE-31, Chalmers University of Technology, Gothenburg, Sweden, July 1995. Submitted to IEEE Trans SP.

[SV96] P. Stoica and M. Viberg. "Maximum-Likelihood Parameter and Rank Estimation in Reduced-Rank Multivariate Linear Regressions". *IEEE Trans. on Signal Processing*, 44(12):3069–3078, Dec. 1996.

[Swi96] A. Swindlehurst. "A Maximum a Posteriori Approach to Beamforming in the Presence of Calibration Errors". In *Proc. 8th Workshop on Stat. Sig. and Array Proc.*, Corfu, Greece, June 1996.

[TO96] T. Trump and B. Ottersten. "Estimation of Nominal Direction of Arrival and Angular Spread Using an Array of Sensors". *Signal Processing*, 50(1-2):57–69, Apr. 1996.

[Tre71] H.L. Van Trees. *Detection, Estimation and Modulation Theory*, volume III. Wiley, New York, 1971.

[Van95] P. Van Overschee. *Subspace Identification: Theory - Implementation - Application*. PhD thesis, Katholieke Universiteit Leuven, Belgium, Feb. 1995.

[VB88] B.D. Van Veen and K.M. Buckley. "Beamforming: A Versatile Approach to Spatial Filtering". *Signal Processing Magazine*, pages 4–24, Apr. 1988.

[VD91] M. Verhaegen and E. Deprettere. "A Fast Subspace, Recursive MIMO State-space Model Identification Algorithm". In *Proc. 30th IEEE Conf. on Decision and Control*, pages 1349–1354, Brighton, U.K., 1991.

[VD92] M. Verhaegen and P. Dewilde. "Subspace Model Identification. Part I: The Output-Error State-Space Model Identification Class of Algorithms". *Int. J. Control*, 56:1187–1210, 1992.

[VD93] P. Van Overschee and B. De Moor. "Subspace Algorithms for the Stochastic Identification Problem". *Automatica*, 29(3):649–660, 1993.

[VD94a] P. Van Overschee and B. De Moor. "A Unifying Theorem for three Subspace System Identification Algorithms". In *Proc. 10th IFAC Symp. on Syst. Id.*, Copenhagen, Denmark, 1994.

[VD94b] P. Van Overschee and B. De Moor. "N4SID: Subspace Algorithms for the Identification of Combined Deterministic-Stochastic Systems". *Automatica, Special Issue on Statistical Signal Processing and Control*, 30(1):75–93, Jan. 1994.

[VD95a] P. Van Overschee and B. De Moor. "About the choice of State Space Basis in Combined Deterministic-Stochastic Subspace Identification". *Accepted for publication in Automatica*, 1995.

[VD95b] P. Van Overschee and B. De Moor. Choice of state-space basis in combined deterministic-stochastic subspace identification. *Automatica, Special issue on trends in system identification*, 31(12):1877–1883, Dec. 1995.

[VD95c] P. Van Overschee and B. De Moor. A unifying theorem for three subspace system identification algorithms. *Automatica, Special issue on trends in system identification*, 31(12):1853–1864, Dec. 1995.

[VD96] P. Van Overschee and B. De Moor. *Subspace Identification for Linear Systems: Theory–Implementation–Applications*. Kluwer Academic Publishers, 1996.

[VDS93] A.-J. Van Der Veen, E.F. Deprettere, and A.L. Swindlehurst. "Subspace-Based Signal Analysis Using Singular Value Decomposition". *Proceedings of the IEEE*, 81(9):1277–1308, Sept. 1993.

[Ver91] M. Verhaegen. "A Novel Non-iterative MIMO State Space Model Identification Technique". In *Proc. 9th IFAC/IFORS Symp. on Identification and System Parameter Estimation*, pages 1453–1458, Budapest, 1991.

[Ver93] M. Verhaegen. "Subspace Model Identification. Part III: analysis of the ordinary output-error state space model identification algorithm". *Int. J. Control*, 58:555–586, 1993.

[Ver94] M. Verhaegen. "Identification of the Deterministic Part of MIMO State Space Models given in Innovations Form from Input-Output Data". *Automatica, Special Issue on Statistical Signal Processing and Control*, 30(1):61–74, Jan. 1994.

[Vib89] M. Viberg. *Subspace Fitting Concepts in Sensor Array Processing*. PhD thesis, Linköping University, Linköping, Sweden, Oct. 1989.

[Vib94] M. Viberg. "Subspace Methods in System Identification". In *Proc. 10th IFAC Symp. on Syst. Id.*, volume 1, pages 1–12, Copenhagen, Denmark, 1994.

[Vib95] M. Viberg. "Subspace-based Methods for the Identification of Linear Time-invariant Systems". *Automatica, Special issue on trends in system identification*, 31(12):1835–1851, Dec. 1995.

[VL82] A.J.M. Van Overbeek and L. Ljung. "On-line Structure Selection for Multivariable State-space Models". *Automatica*, 18(5):529–543, 1982.

[VO91] M. Viberg and B. Ottersten. "Sensor Array Processing Based on Subspace Fitting". *IEEE Trans. SP*, SP-39(5):1110–1121, May 1991.

[VOK91a] M. Viberg, B. Ottersten, and T. Kailath. "Detection and Estimation in Sensor Arrays Using Weighted Subspace Fitting". *IEEE Trans. SP*, SP-39(11):2436–2449, Nov. 1991.

[VOK91b] M. Viberg, B. Ottersten, and T. Kailath. "Subspace Based Detection for Linear Structural Relations". *J. of Combinatorics, Information,& Systems Sciences*, 16(2-3):170–189, 1991.

[VOWL91] M. Viberg, B. Ottersten, B. Wahlberg, and L. Ljung. "A Statistical Perspective on State-Space Modeling Using Subspace Methods". In *Proc.* 30^{th} *IEEE Conf. on Decision & Control*, pages 1337–1342, Brighton, England, Dec. 1991.

[VOWL93] M. Viberg, B. Ottersten, B. Wahlberg, and L. Ljung. "Performance of Subspace-Based System Identification Methods". In *Proc. IFAC 93*, Sydney, Australia, July 1993.

[VS94a] M. Viberg and A. L. Swindlehurst. "A Bayesian Approach to Auto-Calibration for Parametric Array Signal Processing". *IEEE Trans. on Sig. Proc.*, 42(12):3495–3507, Dec. 1994.

[VS94b] M. Viberg and A. L. Swindlehurst. "Analysis of the Combined Effects of Finite Samples and Model Errors on Array Processing Performance". *IEEE Trans. on Sig. Proc.*, 42(11):3073–3083, Nov. 1994.

[VWO97] M. Viberg, B. Wahlberg, and B. Ottersten. "Analysis of State Space System Identification Methods Based on Instrumental Variables and Subspace Fitting". *Automatica*, 1997. Accepted.

[Wax91] M. Wax. "Detection and Localization of Multiple Sources via the Stochastic Signals Model". *IEEE Trans. on SP*, 39(11):2450–2456, Nov. 1991.

[Wax92] M. Wax. "Detection and Localization of Multiple Sources in Noise with Unknown Covariance". *IEEE Trans. on Signal Processing*, SP-40(1):245–249, Jan. 1992.

[WF89] A. J. Weiss and B. Friedlander. "Array Shape Calibration Using Sources in Unknown Locations - A Maximum Likelihood Approach". *IEEE Trans. on ASSP*, 37(12):1958–1966, Dec. 1989.

[WJ94] B. Wahlberg and M. Jansson. "4SID Linear Regression". In *Proc. IEEE 33rd Conf. on Decision and Control*, pages 2858–2863, Orlando, USA, December 1994.

[WOV91] B. Wahlberg, B. Ottersten, and M. Viberg. "Robust Signal Parameter Estimation in the Presence of Array Perturbations". In *Proc. IEEE ICASSP*, pages 3277–3280, Toronto, Canada, 1991.

[WRM94] M. Wylie, S. Roy, and H. Messer. "Joint DOA Estimation and Phase Calibration of Linear Equispaced (LES) Arrays". *IEEE Trans. on Sig. Proc.*, 42(12):3449–3459, Dec. 1994.

[WSW95] M. Wax, J. Sheinvald, and A. J. Weiss. "Localization of Correlated and Uncorrelated Signals in Colored Noise via Generalized Least Squares". In *Proc. ICASSP 95*, pages 2104–2107, Detroit, MI, 1995. IEEE.

[WWN88] K. M. Wong, R. S. Walker, and G. Niezgoda. "Effects of Random Sensor Motion on Bearing Estimation by the MUSIC Algorithm". *IEE Proceedings*, 135, Pt. F(3):233–250, June 1988.

[WZ89] M. Wax and I. Ziskind. "On Unique Localization of Multiple Sources by Passive Sensor Arrays". *IEEE Trans. on ASSP*, ASSP-37(7):996–1000, July 1989.

[YS95] J. Yang and A. Swindlehurst. "The Effects of Array Calibration Errors on DF-Based Signal Copy Performance". *IEEE Trans. on Sig. Proc.*, 43(11):2724–2732, November 1995.

[YZ95] P. Yip and Y. Zhou. "A Self-Calibration Algorithm for Cyclostationary Signals and its Uniqueness Analysis". In *Proc. ICASSP*, pages 1892–1895, Detroit, MI, 1995.

[ZM74] H.P. Zeiger and A.J. McEwen. "Approximate Linear Realizations of Given Dimension via Ho's Algorithm". *IEEE Trans. AC*, AC-19:153, April 1974.

[ZW88] J. X. Zhu and H. Wang. "Effects of Sensor Position and Pattern Perturbations on CRLB for Direction Finding of Multiple Narrowband Sources". In *Proc.* 4^{th} *ASSP Workshop on Spectral Estimation and Modeling*, pages 98–102, Minneapolis, MN, August 1988.